THE UNIVERSITY OF MANCHESTER - APPROVED ELECTRONICALLY GENERATED THESIS/DISSERTATION COVER-PAGE

The Regulation of Endothelial Cell Activation by the Extracellular Matrix after Acute Brain Injury

A thesis submitted to the University of Manchester for the degree of
Doctor of Philosophy
in the Faculty of Medical and Human Sciences

2014

Korakoch Kangwantas

Manchester School of Pharmacy

Table of content

(Total word count: 57,276)

Abstract

Inflammation or injury of the central nervous system generally results in the activation of brain endothelial cells and a change in the composition and expression of the extracellular matrix (ECM) network of the basal lamina of the brain vasculature. The main contributors to brain damage are interleukin (IL)-1-mediated inflammatory processes. The main aim of this project is to investigate whether the ECM associated with brain endothelial cells is modified in response to ischaemic injury *in vitro*, and to test the hypothesis that alteration of ECM composition following injury is a critical regulator of IL-1-induced endothelial cell activation. The *in vitro* blood-brain barrier model used in this thesis was composed of brain endothelial cells and astrocytes and this model displayed classic BBB characteristics. Oxygen-glucose deprivation (OGD) for 2.5 hours followed by 4 hours of reperfusion ± 10 ng/ml IL-1β induced changes in rat brain endothelial cell (rBEC) morphology, occludin and ZO-1 distribution and cytokine-induced neutrophil chemoattractant (CINC)-1 release. Immunohistochemistry on brain sections from animals subjected to middle cerebral artery occlusion (MCAO) demonstrated upregulation of laminin α4 protein following 48 hours and 6 days of reperfusion. Fibronectin expression was also increased in the brain vessels of animals subjected to MCAO following 48 hours of reperfusion. Similarly, 2.5 hours OGD and 2 hours reperfusion ±IL-1β induced changes in laminin α4, β1 and γ1, type IV collagen α1 chain and fibronectin mRNA expression *in vitro*. ECM molecules also influenced rBEC morphology, adhesion, proliferation, organisation and TEER. Integrin β1 mediated rBEC adhesion to type I collagen, type IV collagen and cellular fibronectin but not laminin-511 and the combination of laminin-411 and -511. Laminin-511 and the combination of laminin-411 and -511 significantly increased CINC-1 release compared to type I collagen. Laminin-411 and -511 also upregulated occludin protein expression and maintained occludin distribution following IL-1β treatment in rBECs. To conclude, ECM associated with brain endothelial cells was modified in response to ischaemic injury ±IL-1β *in vitro*, and vascular ECM proteins altered rBEC activation in response to IL-1β. Therefore, a change in ECM composition following injury is a critical regulator of IL-1-induced endothelial cell activation.

Declaration

No portion of the work referred to in the thesis has been submitted in support of an application for another degree or qualification of this or any other university or other institute of learning

Copyright statement

List of tables and figures

List of tables

List of figures

List of abbreviations

BBB: blood-brain barrier

BrdU: Bromodeoxyuridine

BSA: bovine serum albumin

c/m: the ratio of the mean cytoplasmic intensity to the mean membranous intensity

CPT-cAMP: 8-(4-chlorophenylthio) adenosine 3′,5′-cyclic monophosphate sodium salt

CINC: cytokine-induced neutrophil chemoattractant

CNS: central nervous system

DIV: day *in vitro*

DMEM: Dulbecco's Modified Eagle's Medium

EAE: experimental autoimmune encephalomyelitis,

ECM: extracellular matrix

EDTA: Ethylenediaminetetraacetic acid

ELISA: Enzyme-linked immunosorbent assay

FAK: Focal adhesion kinase

FBS: heat inactivated foetal bovine serum

GFAP: glial fibrillary acidic protein

GK: guanylate kinase

HRP: horseradish peroxidase

HSPG: heparan sulfate proteoglycan

HUVEC: human umbilical vein endothelial cell

ICAM: intercellular cell adhesion molecule

IL: interleukin

IL-1RA: interleukin-1 receptor antagonist

IL-1RAcP: interleukin-1 receptor accessory protein

IL-1RI: interleukin-1 receptor type I

IL-1RII: interleukin-1 receptor type I

ILK: Integrin-linked kinase

IRAK: interleukin-1 receptor associated kinase

JAM: junction adhesion molecule

JNK: c-Jun N-terminal kinase

MAGUK: membrane-associated guanylate kinases

MAPK: mitogen activated protein kinase

MCAO: middle cerebral artery occlusion

MMP: matrix metalloproteinase

NF-κB: nuclear factor κB

OGD: Oxygen-glucose deprivation

pBEC: porcine brain endothelial cells

PBS: phosphate buffered saline

PBST: 0.05% (v/v) Tween-20 in phosphate buffered saline

PDZ: post synaptic density, disc-large, zonula occludens domains

PINCH: particularly interesting Cys-His-rich protein

RT-PCR: reverse-transcriptase polymerase chain reaction

PCR: polymerase chain reaction

PDL: poly-D-lysine

PDS: plasma-derived serum

PECAM: platelet endothelial cell adhesion molecule

P-gp: P-glycoprotein

PVDF: polyvinylidene fluoride

rBEC: rat brain endothelial cell

SD: standard deviation

SDS: sodium dodecyl sulfate

SDS-PAGE: sodium dodecyl sulfate-polyacrylamide gel electrophoresis

SH3: Src-homology-3

TAE: Tris-Acetate-EDTA

TEER: transendothelial electrical resistance

TNF: tumour necrosis factor

TRAF6: tumour necrosis factor receptor-associated factor 6

U: unique

VCAM: vascular cell adhesion molecule

vWF: von Willebrand factor

ZO: zonula occludens

ZONAB: ZO-1-associated nucleic acid-binding protein

Chapter 1 General introduction

1.1. Neuroinflammation in acute brain injury

Cerebral ischaemia is the temporary or permanent disruption of blood supply in brain caused by occlusion of cerebral blood vessels or brain haemorrhage. This condition occurs generally in stroke, traumatic brain injury and subarachnoid haemorrhage, which are the major causes of death and long-term disabilities in the United Kingdom and worldwide.

A key step in brain damage induced by acute brain injury is the development of a potent inflammatory response, a host innate defence mechanism to tissue injury, infection and ischaemia. Pathogens, or danger associated molecular pattern molecules expressed or released by pathogens or damaged cells, are recognised by resident macrophages, microglial cells (main immune cells of the central nervous system, CNS) and neutrophils which in turn become activated. These activated effector cells engulf pathogens and remove dead cells and debris. They also release many inflammatory mediators including proinflammatory cytokines, vasoactive molecules, eicosanoids and cytotoxic substances. This leads to the leakage of plasma proteins from vessels, an increase in immune cells transmigration into the site of inflammation and cell death. This mechanism generally resolves the damage and allows tissues to recover and regain homeostasis in the periphery (Janeway, 2001). However, in the case of the CNS in which parenchymal cells have limited capacity to regenerate and are very sensitive to blood-borne molecules, the inflammatory process might be considered as a detrimental reaction rather than a beneficial mechanism.

The brain is very sensitive to oxygen and glucose levels. Once there is a clot or haemorrhage in the brain blocking blood flow an ischaemic condition, in which the brain tissue lacks oxygen and vital nutrients, occurs. Prolonged infarction leads to irreversible tissue damage called the infarct core. A large volume around the infarct core, termed the penumbra, is the area where cells survive and have a potential to regain their functions (Amantea et al., 2009). Therefore, current therapeutic strategies for the treatment of cerebral ischaemia mainly aim at rescuing the penumbra from further damage caused by impaired blood circulation, brain oedema

and inflammation which usually occurs hours or days after the ischaemic attack. Accumulative evidence indicates that the main contributors to brain damage are proinflammatory cytokine-mediated inflammatory processes. The main events indicating that inflammation does occur in cerebral ischemia are the rapid up-regulation of inflammatory mediators, the activation of glial cells, brain oedema and infiltration of peripheral inflammatory cells (Lucas et al., 2006). Ischaemia leads to loss of ion and chemical homeostasis, excitotoxicity and an increase in free radical generation (Sandoval and Witt, 2008). In the case of brain haemorrhage, exposure of the brain parenchyma to the blood also results in brain tissue damage by blood toxicity (Greve and Zink, 2009). Activation of CNS cells and nearby macrophages stimulates the production of inflammatory mediators, such as interleukin (IL)-1, IL-6, nitric oxide, proteases and tumour necrosis factor (TNF)-α. Microglial cells are the first cell type activated by injury, with subsequent inflammatory mediators produced by astrocytes, endothelial cells and neurones (Vogt et al., 2008, Pearson et al., 1999). Inflammatory cytokines and vasoactive molecules released after brain ischaemia lead to the loss of cerebral vascular permeability and peripheral cell transmigration which usually leads to additional brain damage (Stanimirovic and Satoh, 2000, Sandoval and Witt, 2008).

1.2. Proinflammatory cytokine: interleukin-1

Cytokines are small proteins which are synthesised and released by all nucleated cells. Proinflammatory cytokines are those cytokines that promote inflammation, and although these are beneficial in physiological conditions, pathogen clearance and tissue recovery, they may be detrimental to tissues during the course of inflammation (Dinarello, 2000).

IL-1 is a multifunctional proinflammatory cytokine produced mainly by immune cells such as macrophages, dendritic cells and microglia in response to injury or infection. IL-1 induces cells to display inflammatory phenotypes and influences the expression of about a hundred genes involved in an inflammatory processes such as expression of cytokines and their receptors, adhesion molecules and extracellular matrix (ECM) components. IL-1 acts on most cell types throughout the body including cells located within the brain (Pinteaux et al., 2002, Zhang et al., 1999,

O'Neill and Greene, 1998, Lee et al., 1993, Kusano et al., 1998, Kimura et al., 2009, Huang et al., 2006, Himi et al., 1997, Hess et al., 1994a, Chaitanya et al., 2012). IL-1 is constitutively expressed in some areas of the normal brain and plays regulatory roles in some physiological functions in the brain such as sleep, food intake and body temperature (Simi et al., 2007). On the other hand, IL-1 has been considered as a key contributor to brain damage after acute brain injury. It is rapidly upregulated in response to stroke and brain trauma. It acts as the initiator of many inflammatory events which, in most cases, worsen the damage.

There are only a few drugs available for stroke patients. Most of the drugs are preventive and currently there is only one therapeutic agent, tissue plasminogen activator, approved for stroke treatment. However, this medicine provides long-term benefits only when administered within three hours after an ischaemic attack has taken place but its use potentially increases the risk of haemorrhage which may worsen the brain injury and can be fatal (CAEP, 2001, NINDS, 1995). Therefore, more than 95% of patients cannot receive this treatment (CAEP, 2001, Adibhatla and Hatcher, 2008). So far, it is still unclear whether the benefits outweigh the side-effects. From the limited efficacy of tissue plasminogen activator in stroke treatment, it appears that reperfusion of the occluded vessel does not sufficiently correct the actual cause of brain damage (Amantea et al., 2009). It has been demonstrated that neuroinflammation happens following cerebral ischaemia and that IL-1 is the major contributor to brain damage. Therefore, blockage of IL-1 action is a potential therapeutic approach for acute brain injury.

1.2.1 The interleukin-1 ligands and receptors

Classic IL-1 ligands in the brain include two agonists, IL-1α and IL-1β, and one antagonist, IL-1 receptor antagonist (IL-1RA). IL-1α and IL-1RA are synthesised in active pro-forms, whereas pro-IL-1β is inactive and requires a proteolytic enzyme known as caspase-1 or IL-1 converting enzyme to cleave it into an active isoform (Barksby et al., 2007). It was accepted that IL-1α and IL-1β exhibit an identical potency, exert the same functions and transduce the same signalling pathway. However, many recent studies suggest that IL-1α and IL-1β activities are different depending on cell-type and concentration (see (Pinteaux et al., 2009) for review).

IL-1 receptor type I (IL-1RI) and type II (IL-1RII) are the main IL-1 receptors expressed by brain tissue. Structurally, IL-1RI is composed of three extracellular immunoglobulin-like domains, which constitute the ligand-binding sites, and an intracellular Toll-IL-1 receptor domain (Subramaniam et al., 2004). IL-1RI coupling with IL-1 receptor accessory protein (IL-1RAcP) complex is necessary for IL-1α or IL-1β to exert its activity (Sims et al., 1993, Wesche et al., 1997). IL-1RII possesses a similar structure to that of IL-1RI but it is regarded as a decoy receptor due to lack of intracellular domain which is normally required for signal transduction. IL-1RII and IL-1RA play a regulatory role in IL-1 actions. Soluble IL-1RII sequesters IL-1RAcP, IL-1α and IL-1β, but binds to IL-1RA with a relatively lower affinity, resulting in inhibition of IL-1 activities (Subramaniam et al., 2004). IL-1RA binds to IL-1RI and blocks all known activity of IL-1 (Dinarello, 1994).

1.2.2 Interleukin-1 signalling pathway

The IL-1 signalling pathway has been widely studied due to its central role in inflammatory process and its effect on a large amount of genes (O'Neill and Greene, 1998). IL-1 exerts its actions through the transcription factor, nuclear factor-kappa B (NF-κB) and mitogen-activated protein kinases (MAPKs). After the ligand-receptor complex is formed, a cytosolic adaptor protein, MyD88, is recruited to the intracellular domain of IL-1R1. MyD88, in turn, recruits the IL-1 receptor associated kinase (IRAK) which interacts with IL-1RAcP and TNF receptor-associated factor 6 (TRAF6). TRAF6 activates NFκB-inducing kinase and IκB kinases leading to the phosphorylation of IκB, an inhibitory protein that retains NF-κB in the cytoplasm. NF-κB is freed and able to translocate into the nucleus and initiate expressions of many pro-inflammatory proteins (O'Neill and Greene, 1998, Janeway, 2001).

IRAK and TRAF6 also activate signalling molecules in the MAPK pathway leading to gene expression via the transcription factor, activator protein 1. MAPK signalling molecules involved include c-jun N-terminal kinase (JNK) (or known as stress-activated protein kinase), p38 and p42/p44 MAPK (known as extracellular signal regulated kinase) (O'Neill and Greene, 1998).

1.2.3 Evidence of interleukin-1 involvement in brain damage

IL-1 has been considered as an early mediator of brain tissue damage. Many studies have clearly demonstrated IL-1 as a key contributor to the brain damage after acute brain injury. IL-1 is constitutively expressed at very low level in healthy individuals and exogenous IL-1 does not affect or cause any harm to a normal brain (Simi et al., 2007). IL-1 expression is rapidly and markedly up-regulated in experimental models of acute brain injury (Minami et al., 1992, Legos et al., 2000). Moreover, administration of exogenous IL-1 exacerbate the brain damage in experimental models, whereas blockage of IL-1, for instance, by *IL-1* gene deletion (Boutin et al., 2001), administration of anti-IL-1 antibody (Yamasaki et al., 1995) or administration of IL-1RA (Relton and Rothwell, 1992) reduces injury. Furthermore, mice deficient in the *IL-1RA* gene have increased brain damage as well as mortality rates (Pinteaux et al., 2006).

1.3. The blood-brain barrier: the interface of the blood and the brain

The brain is very sensitive to changes in the microenvironment. In normal physiological conditions the brain is securely protected from the blood by the blood-brain barrier (BBB), a highly restrictive cellular structure that regulates the passage of blood-borne substances into the brain. Cerebral injuries are usually followed by disruption of this barrier which results in leakage of blood-borne neurotoxic substances and loss of the brain microenvironmental homeostasis. An understanding of the BBB structure and function in physiological and pathological conditions is crucial not only for understanding the mechanisms of neurodegenerative disorders, but also to help develop new neurologic drugs and drug delivery systems.

1.3.1 Cellular structure of the blood-brain barrier

The BBB is the specialised cellular structure of the cerebral blood vessels. It is comprised of endothelial cells, pericytes and astrocyte endfeet processes (Figure 1.1A), which are all attached onto the basal lamina (or basement membrane). The brain endothelial cells are one of the main cellular components that establish BBB integrity. One endothelial cell can form the circumference of a capillary but several endothelial cells are required to generate a large vessel (Wolburg et al., 2009). Basal

lamina completely covers and separates the brain endothelial layer from astrocyte endfeet. Unlike other endothelial cells, cerebral endothelial cells have a low rate of transcytosis, high numbers of specific transporters, no fenestrae, high numbers of mitochondria and continuous basal lamina (Petty and Lo, 2002, de Boer and Gaillard, 2006). Brain endothelial cells also have highly restrictive intercellular tight junctions which contribute to a transendothelial electrical resistance (TEER) above 1500 $\Omega.cm^2$ compared to a TEER lower than $50\Omega.cm^2$ in other barriers (de Boer and Gaillard, 2006, Stamatovic et al., 2008). The main function of the BBB is to maintain brain homeostasis by limiting the entry of blood-borne substances whilst providing vital nutrients and ions to the brain.

Figure 1.1 Components of the blood-brain barrier and junction complexes

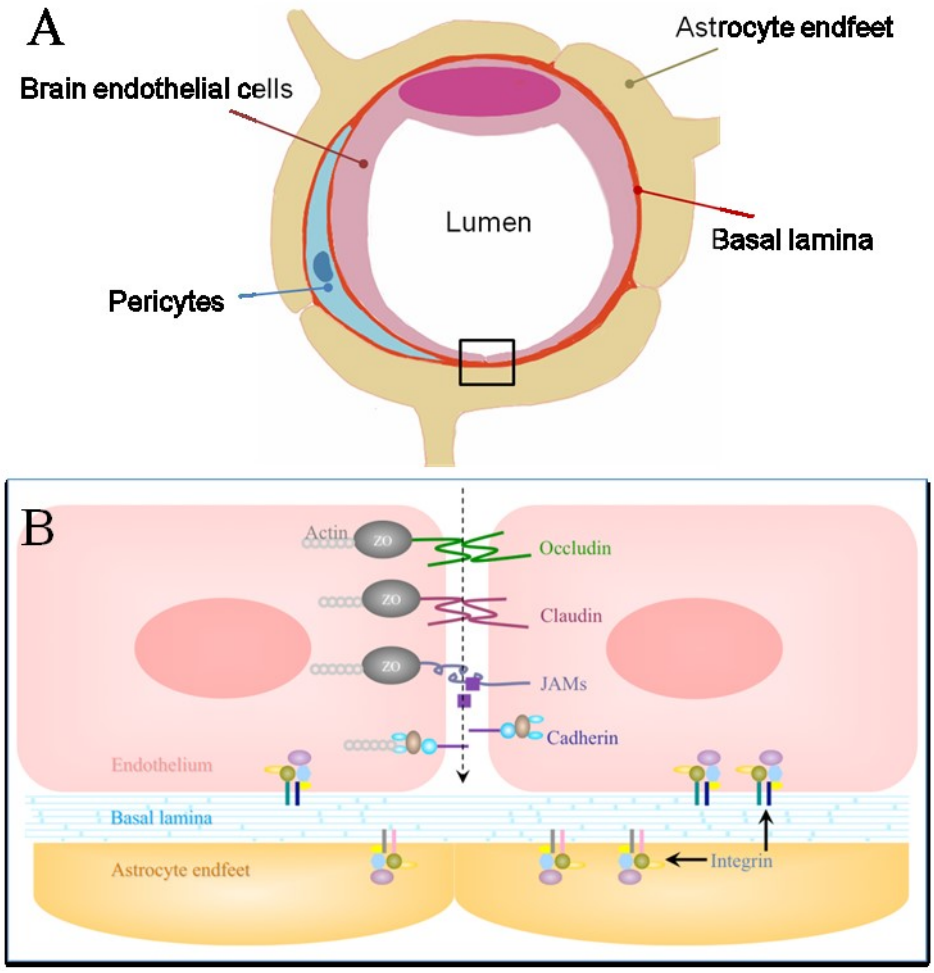

A The BBB is composed of endothelial cells, pericytes and astrocyte endfeet processes which cover the ECM-containing basal lamina.

B The brain endothelial cells are connected by transcellular and cytoplasmic protein structures known as tight junction and adherens junction. The tight junction complex including membranous occludin, claudin and junction adhesion molecules (JAMs), and intracellular zonula occludens (ZO) is located on the apical side of brain endothelial cells whereas adherens junction complex composed of cadherin and catenin is at the basal side. (Adapted from (Abbott et al., 2010, Wolburg et al., 2009, Stamatovic et al., 2008))

1.3.2 Junction complexes

1.3.2.1 Tight junctions

The apical side of the brain endothelium contains tight junctions (Figure 1.1B); these structures not only connect the endothelium, but also play a crucial role by restricting the entry of substances into the brain through a paracellular pathway. Molecules of tight junctions include transmembrane proteins (claudin, occludin and JAMs) and cytoplasmic accessory proteins (ZO, 7H6 and cingulin).

Claudin is a superfamily of more than twenty small trans-membrane proteins of 20-22 kDa. A claudin molecule typically contains four trans-membrane domains and two extracellular loops which form homodimers with a claudin molecule of the adjacent endothelial cell to seal the tight junction. Among the different members, claudin-5 is abundantly expressed on the brain endothelial cell-cell junctions (Ohtsuki et al., 2008, Morita et al., 1999). However, loss of claudin-5 expression does not affect tight junction formation (Stamatovic et al., 2008). Claudin-5 plays a role in regulation of BBB permeability to small molecules (Nitta et al., 2003, Ohtsuki et al., 2007). Another trans-membrane tight junction protein, occludin, is a 60 kDa molecule that has a similar basic structure to that of claudin with four trans-membrane domains and two extracellular loops (Furuse et al., 1993). However, there is no gene sequence homology between the two molecules. Occludin is highly expressed in the brain vasculature (Hirase et al., 1997, Furuse et al., 1993). The third type of transmembrane proteins found in tight junctions is JAMs. JAMs, including JAM-A, B and C, contain one trans-membrane domain and two extracellular immunoglobulin-like loops (Martin-Padura et al., 1998) (Petty and Lo, 2002). Their cytoplasmic tails contain a PDZ binding site which can be recognised by cytoplasmic accessory proteins (Stamatovic et al., 2008).

Cytoplasmic accessory proteins form a linkage between trans-membrane proteins and the actin cytoskeleton. ZO, consisting of three structurally-related proteins, ZO-1, ZO-2 and ZO-3, are a major component of intercellular tight junction protein complexes located in the cytoplasmic regions of epithelial and endothelial cells. ZO-1, a 225 kDa multidomain protein was first identified in mammal epithelia and endothelia by Stevenson et al. (Stevenson et al., 1986). It is a member of membrane-

associated guanylate kinases (MAGUK). ZO proteins contain three post synaptic density, disc-large, zonula occludens domains (PDZ) namely PDZ-1, PDZ-2 and PDZ-3, followed by one Src-homology-3 (SH3) domain and one guanylate kinase (GK) domain. Each domain is separated by Unique (U) domains, U1-U6. ZO-1 and ZO-2 are essential *in vivo* as ZO-1 and ZO-2 knockout cause embryonic lethality in mice (Xu et al., 2008, Katsuno et al., 2008). ZO-3 is specifically expressed by epithelial cells. ZO-3-gene knockout mice did not show any phenotypic abnormality (Xu et al., 2008). Domains at the N-terminal of ZO interact with many transmembrane and cytosolic tight junction proteins (Haskins et al., 1998, Furuse et al., 1994). The COOH terminal end of most claudins contains Tyr and Val which binds to the PDZ-1 domains of ZO (Itoh et al., 1999). Occludin, another key tight junction protein, also interacts with the GK domain of ZO via its C-terminal coiled coil domain (Muller et al., 2005). The PDZ-3 domain of ZO interacts with JAM proteins (Ebnet et al., 2000) whilst the C-terminal of this protein interacts with F-actin. Therefore, ZO acts as a direct or indirect linker between transmembrane tight junction protein and actin cytoskeleton. Moreover, adherens junction proteins such as α-catenin and AF6 have also been reported to bind to ZO-1 and ZO-2 (Itoh et al., 1997, Yamamoto et al., 1997).

Apart from connecting transmembrane and cytoplasmic tight junction proteins, ZO plays a significant role in tight junction formation. ZO-1 and ZO-2 are necessary for tight junction formation, as depleting both ZO-1 and ZO-2 completely abolished tight junction assembly in epithelial cells (Tsukita et al., 2009). Reduction or depletion of ZO-1 expression alone caused the delay of tight junction protein assembly in epithelial cells (McNeil et al., 2006, Umeda et al., 2004). There was also a significant delay in the recruitment occludin and claudin to the junction in ZO-1 knockout cells (Umeda et al., 2006). This suggests that ZO-1 acts as tight junction organiser recruiting other associated proteins to the junction. ZO-2 gene knockdown cells did not exhibit any abnormality in tight junction formation. Moreover, ZO proteins are involved in gene regulation. ZO-1 interacts with the transcription factor ZO-1-associated nucleic acid-binding protein (ZONAB) which can regulate barrier permeability, cell differentiation and proliferation (Balda et al., 2003, Balda and Matter, 2000, Lima et al., 2010, Pannequin et al., 2007, Umeda et al., 2006).

Other proteins, which lack a PDZ domain such as Cingulin and 7H6 antigen, are considered as scaffold phosphoproteins, and their amino-terminal can interact with other accessory proteins such as ZO and AF6 as well as actin-myosin cytoskeletons (Petty and Lo, 2002, Stamatovic et al., 2008).

1.3.2.2 Adherens junctions

Another type of junctional complex is the adherens junction located on the basal region of the brain endothelium (Figure 1.1B). The main function of this structure is to stabilise the vascular structures by joining adjacent brain endothelial cells (Sandoval and Witt, 2008). Adherens junctions are composed of calcium-dependent glycoproteins of the cadherins superfamily linked to scaffold proteins, catenins. A homodimerised cadherin forms a head-to-head contact with another molecule from the adjacent cell. Cytoplasmic tails of cadherins are recognised by the catenins (β, γ and $p120^{ctn}$). β- and γ-catenins bind to α-catenin which is linked to actin. p120 catenin binds with a high affinity to vascular endothelium cadherin but its function is still unknown (Stamatovic et al., 2008).

Phosphorylation is an important regulatory mechanism of the BBB junction complexes. Tight junction proteins contain many putative phosphorylation sites and therefore maybe potential substrates of kinases. Many studies demonstrated the role of protein kinases, particularly protein kinase C, as main regulators of endothelial tight junctions and BBB permeability. Protein tyrosine kinases also play a role in BBB permeability. Reactive oxygen species induce production of matrix metalloproteinases (MMPs) and phosphorylation of tight junction molecules via a protein tyrosine kinase-dependent mechanism (Haorah et al., 2007). In addition, tight junction molecules are also affected by the MAPK pathway. HIV-1 Tat protein decreases expression of brain endothelial claudin-5 and inhibition of MAPKs reverses this effect (Andras et al., 2005).

Brain endothelium also expresses the homophillic adhesion molecule, platelet endothelial cell adhesion molecule (PECAM)-1. PECAM-1 or CD31 is a well-studied intercellular junction molecule belonging to the immunoglobulin family. It is found not only at the endothelial cell-cell junction but also found in leukocytes and

platelets. In immunohistochemistry, PECAM-1 is widely used as an endothelial cell marker in tissue sections (Fawcett et al., 1995, Albelda et al., 1991).

1.3.3 The blood-brain barrier after cerebral ischaemia

The BBB is the interface between the blood and the brain. Therefore, brain endothelial cells are the first cellular component of the brain which undergone ischemia. Brain endothelial cells are also an important brain cellular compartment that plays a key role in the initiation and regulation of neuroinflammation. Pathological conditions of the brain are usually accompanied with BBB disruption which then leads to brain oedema, leukocyte recruitment and subsequently, secondary brain damage (Sandoval and Witt, 2008).

Brain endothelial cells are regarded as the main source of inflammatory mediators after cerebral ischaemia and play a key role in BBB disruption and leukocyte recruitment. Cerebral vessels rapidly express IL-1 in response to focal ischaemia (Zhang et al., 1998). This can also be seen *in vitro* after lipopolysaccharide treatment and oxygen-glucose deprivation (OGD) (Fabry et al., 1993, Zhang et al., 2000, Stanimirovic and Satoh, 2000). Brain endothelial cells constitutively express IL-1RI (Van Dam et al., 1996) suggesting that endothelial IL-1 may have an autocrine effect (Stanimirovic and Satoh, 2000).

The loss of BBB integrity is mostly due to an increase in paracellular permeability. However, an increase in transcytosis rate can be observed in neuroinflammatory conditions (Stamatovic et al., 2008) which suggests that BBB leakage can be attributed by both paracellular and transcellular pathways. Several mediators including growth factors (Nitz et al., 2003, Murakami et al., 2009), cytokines (Royall et al., 1989, Martin et al., 1988), MMPs (Yang and Rosenberg, 2011, Yang et al., 2007, Rosenberg et al., 1998, Liu et al., 2012a), free radicals (Lochhead et al., 2010) can induce BBB disruption. Proinflammatory cytokines induce activation of endothelial cells which, in turn, express adhesion molecules (Frijns and Kappelle, 2002, Wong and Dorovini-Zis, 1992, Stins et al., 1997, Stanimirovic et al., 1997) and alter BBB permeability and functions (Blamire et al., 2000, Royall et al., 1989, Martin et al., 1988).

Leukocyte infiltration is attributed to secondary brain damage. Peripheral leukocytes are attracted to the site of inflammation by chemokine gradients. They then recognise adhesion molecules on endothelial cells where they adhere, roll and transmigrate to the site of inflammation. *In vitro* ischaemia or IL-1 treatment can induce endothelial and astrocytic production of neutrophil attractants such as monocyte chemotactic protein-1 (Zhang et al., 1999). Up-regulation of adhesion molecules on brain endothelial cells can be detected after neuroinflammation. Three classes of adhesion molecules, selectins, integrins and immunoglobulins are up-regulated during neuroinflammation and are involved in leukocyte infiltration. Brain endothelial cells express E-selectin which is important for leukocyte adhesion to the brain vascular endothelial cells and rolling in response to focal brain ischaemia (Okada et al., 1994, Haring et al., 1996). Endothelial cells also express cell adhesion molecules such as intercellular cell adhesion molecule (ICAM)-1 (Wang et al., 1994, Okada et al., 1994) and vascular cell adhesion molecule (VCAM)-1 (Stins et al., 1997). They are members of the immunoglobulin superfamily which are receptors of LFA-1 (CD11b/CD18) and very late antigen-4 (or α4β1), respectively, expressed on leukocytes. They are responsible for firm attachment of leukocytes to the endothelium (Huang et al., 2006).

1.4. Basal lamina and the extracellular matrix

Under the endothelial layer is found the basal lamina onto which astrocyte endfeet and pericytes are attached (Wolburg et al., 2009). This membrane is composed of a network of ECM molecules which are collagens, non-collagenous glycoproteins and proteoglycans. They are widely distributed throughout the brain but their compositions are varied depending on the brain area and age (Venstrom and Reichardt, 1993). Type IV collagen and laminins are the major component of the basal lamina. Other ECM molecules including fibronectin, nidogens, entacin, thrombospondin and heparan sulfate proteoglycan (HSPG) are also found in the cerebral vasculature.

1.4.1 The structures and functions of extracellular matrix molecules

1.4.1.1 Laminins

Laminins are a family of ECM molecules that are major components of the basal lamina in the brain. Laminins are expressed abundantly in the basal lamina and their expression is highly organised. In cerebral vessels, laminin-α4 and -α5 are located on the endothelial basement membrane whereas laminin-α1 and -α2 are expressed on the side of the astrocyte-endfeet. In the brain, the basal lamina of capillaries is composed of laminin-α4, -α5 and -α2 (Sixt et al., 2001). Laminin is composed of three different domains, α, β, and γ, forming a cross-shape structure (Figure 1.2). Each domain contains globular domains (IVa, IVb and VI), multiple epidermal growth factor (EGF)-like repeats (IIIa, IIIb and V) and an α-helical region (I and II) where α, β, and γ chains form a triple helix. There are at least 5α, 4β, and 3γ subunit isoforms forming 15 different laminin chains (see (Hallmann et al., 2005) for review). Laminin-111 (or laminin-1) is the prototype composed of α1, β1, and γ1 chains. Laminin-111, laminin-211 (α2β1γ1 or laminin-2), laminin-411 (α4β1γ1 or laminin-8) and laminin-511 (α5β1γ1 or laminin-10) are the main forms expressed in the brain vasculature (Sixt et al., 2001). They possess distinct α chains but share β1 and γ1 chains. Laminin α1, α2 and α5 chains similarly have three globular domains, three rod-like domains, α helix and a G region. Laminin α4 has similar α helix and a G region. However, it only has one rod-like domain containing three EGF-like repeats and one flanking incomplete repeat in the short arm (Iivanainen et al., 1995, Miner et al., 1995). Laminins are recognised by α1β1, α2β1, α3β1, α6β1, α7β1, αvβ3 and α6β4 integrins (Table 1.1).

Laminin contains different integrins and other ECM binding sites. The main integrin-recognition site of laminin is the long arm (E8) which can be bound by α3β1, α6β1, α7β1, α6β4 (Taniguchi et al., 2009, Lee et al., 1992, Sonnenberg et al., 1990, Ido et al., 2004). The short arm of laminin (E1′) is recognised by integrin α1β1, α2β1 (Colognato et al., 1997, Desban et al., 2006, Colognato-Pyke et al., 1995). G4-5 (E8) in the G region of laminin is recognised by α dystroglycan (Ido et al., 2004). Laminin also possesses binding sites for laminin (self assembly) (Hussain et al., 2011, Yurchenco et al., 1985) and other ECM molecules including collagen, heparin

and nidogen (Gersdorff et al., 2005a, Colognato-Pyke et al., 1995, Chen et al., 1999, Gersdorff et al., 2005b).

Figure 1.2 Structure of laminins

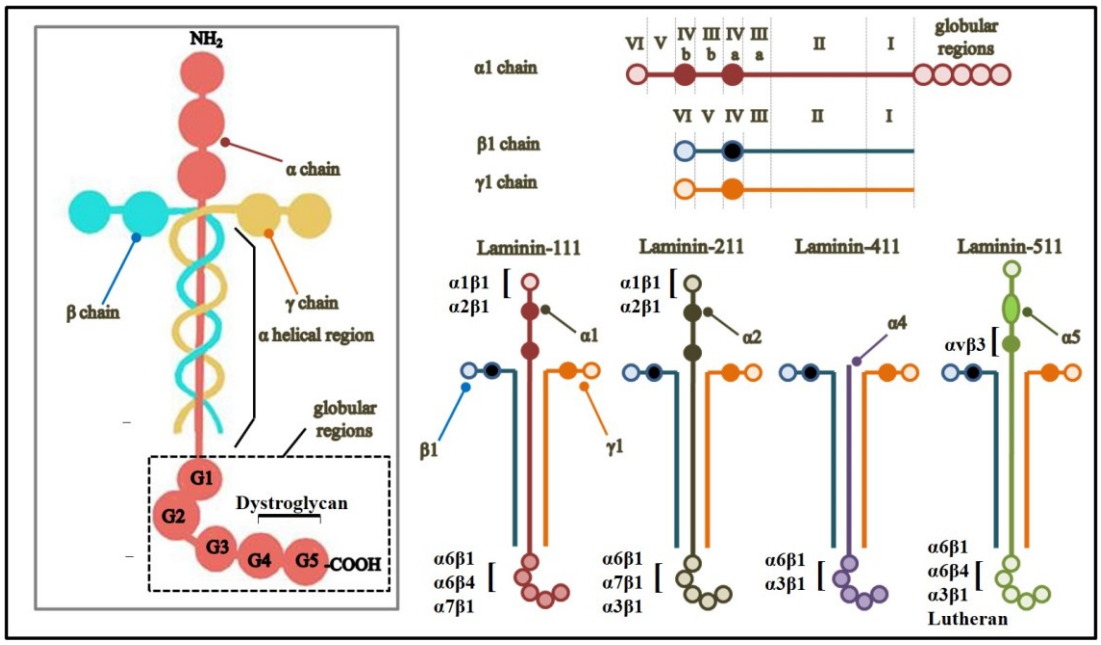

Schematic representation of classic laminin-111 and cerebral vascular laminin isoforms, laminin-211, laminin-411 and laminin-511. Laminin is composed of three subunits, α, β and γ, which form a cross-shaped heterotrimeric structure. Each chain contains globular (VI and IV) and rod-like (V and III) in the short arms domains. The long arms (I and II) of α, β and γ chains form a coil, so called α helical region. Distinctively from β and γ, the α chain has an extra globular region containing five homologous repeats. (Adapted from (Colognato and Yurchenco, 2000, Miner et al., 1995, Beck et al., 1990))

1.4.1.1 Collagens

Collagens are a family of proteins found most abundantly throughout the body in mammals. They are major structural ECM proteins formed by triple helix fibres. Collagen I is the most abundant type of collagen in the bones, tendons and blood vessels. It absorbs tension, and strengthens and stabilises blood vessels. Collagen IV is widely distributed throughout the developing brain basal lamina and is the major component in mature cerebral vessels (Kleppel et al., 1989, Venstrom and Reichardt, 1993). Structurally, all collagens contain three α-chains, 300-400nm in length polypeptide consisting of glycine-X-Y repeats (X and Y often are proline and 4-hydroxyproline, respectively).

Biosynthesis of collagens, like usual proteins, involves many steps including transcription, translation and post-translation modification. Transcription and translation of genes encoding individual α chains yields the prepro-α chain polypeptide which is then cleaved in the rough endoplasmic reticulum to produce a pro-α chain. Proline and lysine residues are then hydroxylated and glycosylated. Three pro α chains subsequently assemble to form triple helices, now called procollagen. Procollagen molecules are then secreted from the Golgi to the extracellular space. The N- and C- terminals of the procollagen are cleaved by procollagen peptidases and the end product is called tropocollagen. This molecule assembles in parallel to form fibrils (Harvey and Ferrier, 2011).

The structure of type IV collagen is different from that of classic type I collagen. Type IV collagen contains a cysteine-glycine rich N-terminal, namely 7S, Gly-X-Y repeats and a globular C-terminal, namely NC1 (Figure 1.3). The biosynthesis of type IV collagen, similar to other collagens, involves many post-translational modifications including hydroxylation, glycosylation, the addition of oligosaccharide and the formation of disulphide bridges in the NC domain. The assembly of type IV collagen molecules is head to head rather than in parallel as is observed with type I collagen. Also type IV collagen contains 21 for α1 and 23 for α2 interruptions in the Gly-X-Y repeats, thus creating a loose and flexible collagen network. With these distinct features, type IV collagen is categorised as network forming collagen, unlike

type I collagen which is a fibril-forming one (Leitinger and Hohenester, 2007, Khoshnoodi et al., 2008).

There are 6 different collagen IV monomers, α1(IV) to α6(IV). Collagen IV consists of two α1(IV) and one α2(IV) is the most common type expressed in the BM including of the brain whereas the expression of α3(IV) to α6(IV) is very limit to some organs such as kidney, lung and oesophagus. The C4 triple helix self-assembles which is mainly mediated by NC domain to form a collagen network in the basal lamina (Kühn, 1995). Cells can recognise the ECM molecules via cellular receptors called integrins (see Section 1.4.2). Collagens are recognised by α1β1, α2β1 and α3β1 integrins (Gehlsen et al., 1989, Pfaff et al., 1994) (Table 1.1).

Figure 1.3 Structure of type IV collagen

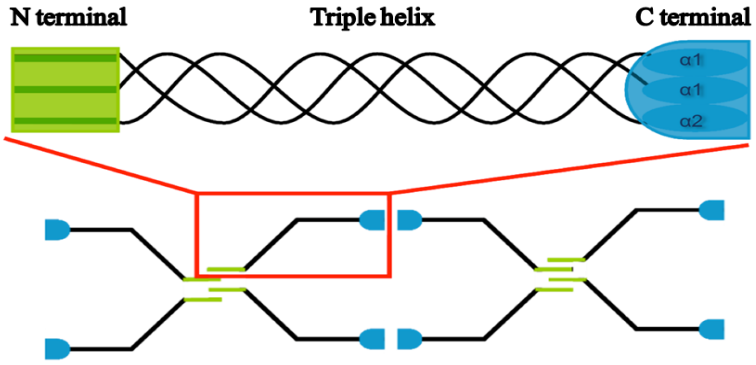

Type IV collagen is one of the main vascular ECM molecules. It is a right-handed triple helix formed by three monomers termed α chain. Each α chain consists of an amino-terminal, triple helix region and carboxy-terminal. Type IV collagen self-assembles to form net-work mediated by its N- and C termini. (Adapted from (Kühn, 1995))

1.4.1.2 Fibronectin

Fibronectin is a long glycoprotein composed of two 250 kDa monomers linked with two disulfide bonds at the C-terminus (Figure 1.4). Each fibronectin monomer contains three repeated subunits, type I, type II and type III (Reichardt and Tomaselli, 1991). The 10th type III subunit contains one arginine-glycine-aspartic acid sequence (RGD) which is involved in integrin recognition. Fibronectin is encoded by a single gene and alternative splicing of a single mRNA yields approximately twenty forms of fibronectin in human (Pankov and Yamada, 2002). There are two types of fibronectin, soluble and insoluble fibronectin. Soluble or plasma fibronectin is produced by hepatocytes and found abundantly as a protein component in the blood. The insoluble or membrane-bound fibronectin is secreted by many cell types and incorporated into the matrix as a part of basal lamina (Pankov and Yamada, 2002). Fibronectin is expressed by cerebral blood vessels in developing brain but its expression is decreased in adult brain.

It has been long known that fibronectin plays a role in cell development, adhesion and migration (Pankov and Yamada, 2002). Several studies suggested a role of fibronectin in angiogenesis in both developing and injured brain. Fibronectin is expressed on developing (angiogenic) cerebral vessels (Milner and Campbell, 2002). Fibronectin promotes proliferation and survival of brain capillary endothelial cells *in vitro* (Wang and Milner, 2006). Fibronectin exerts its activity via binding to the cellular integrin receptors α5β1, αvβ3, α3β1 and αvβ6 (Venstrom and Reichardt, 1993) (Table 1.1).

Figure 1.4 Structure of fibronectin

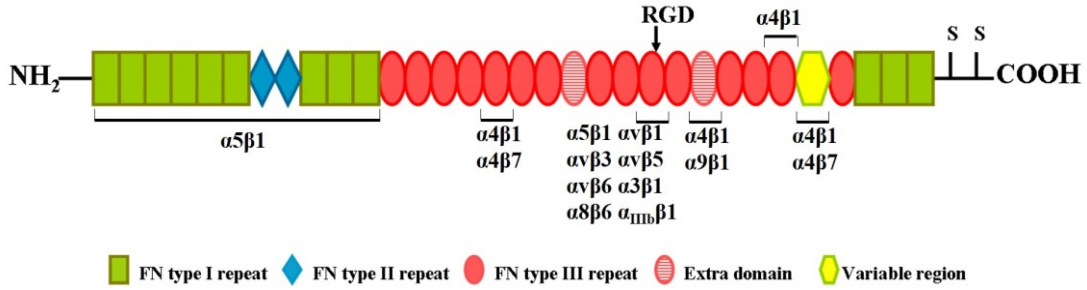

Fibronectin monomer is composed of three repeated domain, fibronectin type I, type II and type III. A single fibronectin chain possesses several binding sites for cells and other ECM molecules such as collagen and heparin. Within the 10th fibronectin type III repeats contains RGD motifs which are the main binding sites for integrins. (Adapted from (Pankov and Yamada, 2002))

4.1.1.2 Other ECM molecules

Heparan sulfate proteoglycans are a common component of vascular ECMs. Perlecan is a major HSPG found in the endothelial basement membrane and is mainly produced by endothelial cells (Wang and Shuaib, 2007). Perlecan is composed of a protein core and three heparan sulphate chains. Another HSPG, the syndecans, have been shown to be expressed on the cerebral endothelium. Syndecan-2 is expressed on brain endothelial cells of all blood vessels whereas syndecan-1 and -3 expression is restricted to large vessels of the brain (Floris et al., 2003). HPSGs possess anionic properties which play a role in molecular impermeability of the basal lamina (Garcia de Yebenes et al., 1999). HSPGs interact with several ligands including chemokines, adhesion molecules and other ECMs. Moreover, HSPGs bind to several growth factors and act as a mechanism of growth factor storage (see (Taipale and Keski-Oja, 1997) for review). They recognise adhesion molecules, e.g. Mac-1, expressed on leukocytes (Diamond et al., 1995). It has been shown that addition of heparin, the polysulphated form of heparan sulphate, reduces monocyte transmigration across non-activated brain endothelial cells *in vitro* (Floris et al., 2003).

Fibrillin is a major component of vascular microfibrils surrounding the amorphous elastin core in the vascular medial layer. To date, 3 members of fibrillin have been discovered. Fibrillin-1 and 2 are widely distributed throughout the body (Kielty et al., 2005). Fibrillin-3, which shares 61% and 68% homology with fibrillin-1 and -2, respectively, is expressed mainly in foetal brain (Nagase et al., 2001, Corson et al., 2004). However, little is known about its function and distribution in the brain. Fibrillin-1 is a large glycoprotein containing forty seven EGF-like domains, seven 8-cysteine domains (also known as TB motifs), two hybrid domains (similar to both EGF-like and TB motifs) and a proline-rich region. Forty three EGF-like domains are calcium-binding motifs (cbEGF), which is the factor determining fibrillin folding and molecular function. TB motifs are interspersed among the EGF-like domains. Within the fourth TB motif of fibrillin-1, there is one RGD motif which is required for α5β1 and αvβ3 integrin recognitions. Fibrillin enhances cell attachment via recognition of α5β1 and αvβ3 (Bax et al., 2003). Fibrilin-3 has similar structure to

fibrillin-1 which is composed of multiple cbEGF, TB domains and hybrid modules. Unlike fibrilin-1 and 2, fibrillin-3 contains proline and glycine-rich residue. In addition to conserved RGD motifs at the fourth TB module, fibrillin-3 also contains the other RGD sequence located within the 19th cbEGF (Corson et al., 2004).

1.4.2 Integrins: the extracellular matrix receptors

Regulation of cell behaviour by the ECM is mediated through the main cellular ECM receptors, integrins. Integrins are a family of adhesive molecules composed of α and β heterodimers. Eighteen α chains and eight β chains have been discovered so far. A combination of α and β integrin subunits forms a specific receptor to a particular matrix molecule; for instance, α1β1 and α6β1 integrin subunits are the main laminin receptor, on the other hand fibronectin is recognised by α5β1 (Venstrom and Reichardt, 1993).

Expression of integrins in the brain is well-established (Table 1.2). In postnatal brain, there is high expression of α4β1 and α5β1 integrins which is associated with expression of their ligand, fibronectin. However, during development, their expression is reduced and replaced by α1β1 (laminin and collagen type IV receptor), α6β1 (laminin receptor) and α4β6 (laminin-5 receptor) whose ligands are highly expressed in adult brain (Tagaya et al., 2001, Milner and Campbell, 2002).

Integrins not only attach cells to the matrix but also regulate cell behaviour. Integrins can regulate cell behaviour by binding to ECM and transducing intracellular signalling events (Wang and Milner, 2006). Binding between ECM molecules and integrins can induce an intercellular signalling which triggers the formation of focal adhesions, points of attachment of cells to the surrounding ECM. Unbound integrins are uniformly expressed as an inactive form. Intracellular signalling activates integrins which, in turn, increases their binding affinity to the ECM. Binding of ECM-integrin induces clustering of integrins and initiates many intracellular events which involve several kinases and phosphatases including focal adhesion kinase. These activate and recruit actin cytoskeletons leading to actin assembly as well as modulating intracellular signals (Legate et al., 2006).

Signalling between cell and extracellular matrix, via integrin, is bidirectional. Binding of the integrin to its extracellular ligand transduces signals into cells. This is

known as “outside-in” signalling. There is also “inside-out” signalling in which inactive integrin is activated (significantly increasing ligand affinity) in response to cellular stimulation, e.g. cellular stimulation by cytokine. The transmembrane domains of the integrin α subunit determine the ligand specificity whereas the cytoplasmic tail of the integrin β chain is involved in signal transduction and cytoskeleton connection. The key protein necessary for integrin activation is an adapter protein called talin. Binding of talin to the cytoplasmic tail of the integrin β subunit alters the interaction between the ectodomains of integrin α and β subunits (Wegener et al., 2007) leading to a conformation change of the integrin receptors and an increase in the affinity of the integrin for its substrates (Ginsberg et al., 2005, Ratnikov et al., 2005, Luo et al., 2007, Wegener et al., 2007). Talin also interacts with the cytoplasmic domain of vinculin, an actin-binding protein (Bois et al., 2006) and to focal adhesion kinase (FAK) (Chen et al., 1995). Binding of clustered integrins to their substrates results in assembly of multiple protein complexes at the ECM-integrin cytoplasmic sites. These protein complexes connect the activated integrins to cytoskeletal proteins and to signalling molecules (Critchley and Gingras, 2008). FAK was the first integrin signalling protein discovered. FAK is a cytoplasmic, non-receptor, tyrosine kinase. Autophosphorylation of FAK allows FAK to bind to SH2-containing proteins (Schaller et al., 1994), for example, members of the Src- kinase family. Src kinases, in turn, phosphorylate FAK and activate many downstream signalling proteins and adaptors (Giannone and Sheetz, 2006, Ginsberg et al., 2005). Paxillin, another essential signalling scaffold protein localises at the integrin adhesion site early on in the process of protein complex formation. Paxillin binds directly to the cytoplasmic tail of integrin receptors and FAK. Paxillin also interacts with many proteins including kinases, cytoskeletal proteins and regulators of the Rho family of small GTPase (See (Deakin and Turner, 2008, Schaller, 2001) for review). Integrin-linked kinase (ILK) is one of many proteins recruited to the focal adhesion. Rather than functioning as a kinase, ILK acts as a key scaffold proteins in cell-ECM adhesion (Wickstrom et al., 2010). Kindlin-2 (Montanez et al., 2008), α-parvin (Fukuda et al., 2009) and Paxillin (Nikolopoulos and Turner, 2001) are required for ILK localisation to the focal adhesion. ILK forms a proteolytic resistant heterotrimetric complex with particularly interesting Cys-His-

rich protein (PINCH, of which there are two isoforms PINCH-1 and 2) and parvin (actin and vinculin binding proteins). ILK directly binds to the cytoplasmic tail of the integrin receptor (Hannigan et al., 1996; Pasquet et al., 2002; Yamaji et al., 2002) and indirectly connects to the actin cytoskeleton via parvin. ILK also interacts with paxillin which binds to actin or vinculin. Distinct signalling outcomes are created depending on the precise ILK-PINCH-parvin combination. i.e. the ILK-PINCH-parvin complex formed by one ILK, with one of the two PINCH isoforms and with one of the three parvin isoforms (α, β and γ-parvin). PINCH-1, but not PINCH-2, interacts with Ras suppressor 1, an upstream effector of JNK signalling pathway (Dougherty et al., 2005; Gonzalez-Nieves et al., 2013). PINCH-1 also interacts with a cytoplasmic adaptor protein, NCK2 (Tu et al., 1998). α-Parvin directly binds to F-actin or indirectly interacts with paxillin (Nikolopoulos and Turner,2000). It also binds to testis-specific protein kinase 1 which can phosphorylates cofilin (LaLonde et al., 2005). β-parvin binds to actin, α-actinin (Yamaji et al., 2004) and Rac/Cdc42 guanine nucleotide exchange factor 6 (namely ARHGEF6 or α-PIX) (Rosenberger et al., 2003). Apart from regulating Ras-like family of Rho proteins, ARHGEF 6 also interacts with calpain-4 which can cleave talin (Rosenberger et al., 2005; Franco et al., 2004).

Table 1.1 Extracellular matrix molecules and their integrin receptors

	α1β1	α2β1	α3β1	α5β1	α6β1	α7β1	αvβ3	α6β4	Reference
Fibronectin			+/-	++[1]	-				(Nishiuchi et al., 2003, Gehlsen et al., 1989)
Collagen IV	++	++[2]	+						(Gehlsen et al., 1989, Pfaff et al., 1994, Knight et al., 2000, Hall et al., 1990)
Laminins									
111	+	+	+/-	-	+	+	+[1]	+	(Nishiuchi et al., 2003, Nomizu et al., 1995, Yao et al., 1996, Ignatius et al., 1990, Delwel et al., 1994, Elices and Hemler, 1989, Gehlsen et al., 1989, Sonnenberg et al., 1988, Lee et al., 1992, Yu and Talts, 2003, Genersch et al., 2003a, Chang et al., 1995)
211/221	-	-	+/-	-	+	+		+	(Nishiuchi et al., 2003, Kikkawa et al., 2004, Yao et al., 1996, Genersch et al., 2003a, Pfaff et al., 1994, Chang et al., 1995)
411			-		+			+	(Nishiuchi et al., 2003, Kortesmaa et al., 2000)
511/521			++	+[1]	++		+[1]	+	(Kikkawa et al., 2004, Nishiuchi et al., 2003, Pouliot et al., 2000, Kikkawa et al., 2000, Kikkawa et al., 1998, Genersch et al., 2003a)

(Note: interaction is mediated by 1= RGD; 2=GFOGER)

Table 1.2 Expression of integrins by cerebral endothelial cells *in vivo*

α1	α2	α3	α4	α5	α6	α7	αv	β1	β3	β4	Reference
++								++			(Tagaya et al., 2001)
	+	+	-	+	++		-	++	+	++	(Paulus et al., 1993)
++				-	++			++			(Milner and Campbell, 2006)
				+	++			++	-		(Li et al., 2012)
										+	(Welser-Alves et al., 2013)
++	-	-			++		+	++			(Sobel et al., 1998)
		-			++	-		++		-	(Sixt et al., 2001)

1.4.3 Changes in extracellular matrix and integrin expression after acute brain injury

Change in the brain ECM composition and expression of ECM proteins observed after acute brain injury is generally accompanied by loss of BBB integrity and the development of a potent inflammatory response. ECM molecules are easily degraded by protease enzymes, expression of the latter being induced early after ischemic insult. Evidence suggests that MMP-2 and -9 (Fukuda et al., 2004), plasminogen-plasmin enzymes (Yepes et al., 2003) and neutrophil elastase (Stowe et al., 2009) are involved in matrix degradation during cerebral ischaemia. Changes in expression of ECM proteins in the brain vasculature following brain injury are shown in Table 1.3. Expression of collagens, laminins and fibronectin is diminished as early as 2 hours after cerebral ischaemia (Hamann et al., 1995). Reduction in perlecan is also demonstrated in middle cerebral artery occlusion (MCAO) model (Fukuda et al., 2004). Type VI collagen (C6) and pro-collagen III are only expressed in the adventitia layer of small arteries in the meninges. However, increases in expression of these molecules in the intima layer and capillaries was observed in human ischemic brains (Roggendorf et al., 1988). Expression of endostatin, a naturally-occurring 20-kDa C-terminal fragment of type XVIII collagen, is upregulated very early and prolonged (at least 48 hours), following ischemic insult in MCAO models (Tian et al., 2007). Degradation of matrix molecules can be detected within hours but re-expression of ECM proteins is believed to occur days after the onset of injury (Milner et al., 2008).

Expression of integrins is closely regulated by cytokines (Milner and Campbell, 2003, Wang and Milner, 2006). Proinflammatory cytokines such as TNF-α and IL-1β can induce downregulation of integrin expression on human endothelial cells (Defilippi et al., 1992). Loss of integrin expression, including α1β1, α3β1 and α6β1, is accompanied with detachment of astrocyte endfeet following MCAO (Tagaya et al., 2001)

Table 1.3 Changes in vascular extracellular matrix in an *in vivo* model of brain injury

Brain injury	Changes in ECM molecules	References
MCAO	↓ collagen ↓ laminin ↓ fibronectin	(Hamann et al., 1995)
	↓ laminin	(Liu et al., 2012b)
	↑ laminin	(Ji and Tsirka, 2012)
Kainic acid	↑ laminin	(Sarkar and Schmued, 2010, Sarkar et al., 2012, Gualtieri et al., 2012)
Hypoperfusion	↑ laminin	(Wappler et al., 2011)
Stab wound	↑ laminin	(Szabo and Kalman, 2008)
	↑ laminin ↑ fibronectin	(Krum et al., 1991)
Experimental autoimmune encephalomyelitis,(EAE)	↑ laminin-411 ↓ laminin-511	(Sixt et al., 2001)

1.4.4 Regulation of cellular responses to inflammatory mediators by the extracellular matrix

Binding of ECM molecules to integrin receptors induces changes in intracellular activities. Cell-matrix interaction induces the activation of signalling molecules including NF-κB and JNK (Zhu et al., 1998, Wang and Milner, 2006). Many studies have demonstrated the regulation of expression of inflammatory mediators by the ECM; for instance, collagen, laminins and fibronectin influence expression of inflammatory mediators including IL-1β, IL-1RA, IL-6, TNF-α and MMP-9 by monocytes (Chana et al., 2003, Graves and Roman, 1996). In addition, an RGD-containing fibrillin-1 recombinant fragment modulates MMP-1 and -3 expression in human dermal fibroblasts (Booms et al., 2005).

1.5. Aim of the study

Mechanisms of brain endothelial cell activation and inflammation in response to acute brain injury are quite well established. Regulation of IL-1 action in peripheral and central immune cells by the ECM has been widely demonstrated. However, the regulatory roles of ECM molecules on brain endothelial cell activation after acute brain injury are still unknown. The ECM can modulate the IL-1 signalling pathway and actions of the cytokine through the MAPK signalling pathway. On the other hand, endothelial cells attached to ECM molecules, which are mediated through focal adhesion kinase, may affect distribution of junctional complex proteins and BBB integrity (Sandoval and Witt, 2008). Therefore, the overall aim of this research is to investigate the regulatory effect of ECM molecules on primary brain endothelial cells in culture after OGD or IL-1β treatment (OGD/IL-1β). The specific objectives are:

1) To investigate the expression of brain endothelial ECM following ischemic injury.

2) To investigate the effects of different ECM molecules on brain endothelial cell behaviours (namely cell adhesion, proliferation, organisation and TEER).

3) To investigate the effects of different ECM molecules on brain endothelial cell function (namely production of cytokines, expression of junction complex proteins and TEER) following OGD/IL-1β treatment.

Chapter 2 Materials and methods

Cell culture plates and Transwell® inserts were purchased from BD Falcon, UK. All reagents were obtained from Sigma-Aldrich UK unless stated otherwise.

2.1 Plate coating

Solutions of rat tail collagen type I and type IV (BD Biosciences, UK) were diluted in 1 mM acetic acid to the required concentration. Human plasma fibronectin (Chemicon, UK), cellular fibronectin, laminin-511 and laminin-411 were diluted in Dulbecco's phosphate buffered saline (PBS) to the required concentrations. Plates were treated with ECM solution for either 2 hours at 37˚C or overnight at 4˚C. For type I collagen and fibronectin coating, surfaces were treated with type I collagen for 2 hours at 37˚C followed by incubation with 10 μg/ml plasma fibronectin overnight at 4˚C. The volume of ECM solution added was as recommended by the supplier (Table 2.1). Following treatment of culture surfaces with ECM, ECM solution was removed and replaced with heat-denatured (85˚C 10 minutes) 1% (w/v) bovine serum albumin (BSA) in PBS (sterilised by filtration through a 0.22 μm pore size syringe filter) for 1 hour in order to block any nonspecific cell-binding sites. All treated surfaces were then washed with PBS twice prior to cell seeding.

Poly-D-lysine (PDL) solution was diluted with sterile dH_2O to 1 mg/ml and was added to each well of 12-well plates. Plates were incubated for 1 hour at room temperature. The solution was then aspirated and plates were allowed to dry for at least 1 hour before cell seeding.

Table 2.1 Volume of extracellular matrix solution for Transwell® insert coating

	Surface area (cm^2)	Coating volume (µl)
T25 flask	25	1500
6-well plate	9.6	500
24-well plate	1.9	200
96-well plate	0.3	50
Insert fitted to 6-well plate	4.2	300
Insert fitted to 12-well plate	0.9	150
Insert fitted to 24-well plate	0.3	50

2.2 Isolation of primary cells and cell culture

2.2.1 Isolation and culture of rat brain endothelial cells

Rat brain endothelial cells (rBECs) were isolated as previously reported (Abbott et al., 2012) with slight modification. Six 2-3 months old Sprague-Dawley rats (approximately 250 g in weight) were sacrificed by cervical dislocation. Each rat was individually decapitated. Skin was cut vertically from the neck to the nose and pulled to the side to reveal the skull. The skull was cut along the temporal ridges with bone scissors. The rear of the skull was removed with pliers in a lifting motion. Parietal bones and parts of the frontal bones were removed with pliers to reveal the whole brain. The brain was removed and placed on ice-cold Hanks' balanced salt solution, without calcium and magnesium ions, supplemented with 10 mM HEPES, 0.5% (w/v) BSA, 100 units/ml penicillin and 0.1 mg/ml streptomycin, so called Buffer A. These steps were repeated for all animals. In a laminar airflow hood, the cerebellum was removed and each brain was cut longitudinally into two halves with a scalpel. Hemispheres were maintained in ice-cold Buffer A during dissection. Each hemisphere was rolled on a dry sterile filter paper to remove surface blood vessels. White matter and optic nerves were carefully removed using forceps and the hemispheres were then transferred to a new Falcon tube containing fresh ice-cold Buffer A. These steps were repeated for all hemispheres. Brain tissue was chopped into 2-3 mm sized pieces using a scalpel and the tube was centrifuged at 380 x g at 4 ˚C for 5 minutes. The supernatant was removed and 15 ml Buffer A containing 1 mg/ml collagenase/dispase (Roche Applied Science, UK), 0.147 ng/ml Tosyllysine Chloromethyl Ketone and 0.2 U/ml deoxyribonuclease I, so called Enzyme solution, was added to the pellet. Tissues were briefly triturated with a 5 ml stripette, placed in an orbital shaker and agitated at 200 rpm at 37˚C for 1 hour.

After digestion, the suspension was triturated with a rounded sterile Pasteur pipette (the tip of the pipette was smoothed by putting over a flame for 2 seconds) for 2 minutes and with a narrowed sterile Pasteur pipette (the tip of the pipette was heated for 5 seconds to narrow the orifice) for another 2 minutes. The suspension was then centrifuged at 380 x g at 4 ˚C for 5 minutes. The supernatant was removed and 30 ml 18% (w/v) dextran in Buffer A was added. Pellets were triturated and the suspension

was centrifuged at 2500 x g at 4 ˚C for 15 minutes. Following centrifugation, the tube was gently rolled to loosen the myelin plug and the myelin plug along with the supernatant was poured into a new Falcon tube. The myelin plug and supernatant were resuspended and centrifuged as above to recover any additional capillaries.

Capillary pellets were resuspended in Buffer A and the suspension was centrifuged at 380 x g at 4 ˚C for 5 minutes. The resulting pellets were resuspended in 5 ml Enzyme solution and the capillaries were incubated at 37 ˚C for 3 hours on an orbital shaker at 200 rpm.

Two centrifuge tubes were filled with 8 ml 50% (v/v) Percoll pH 7.3 and centrifuged at 25000 x g at 4 ˚C for 1 hour to generate a gradient. After the second enzyme digestion, the suspension was drawn into rounded Pasteur pipettes and the pipettes were held horizontally for approximately 10 seconds until debris adhered to the glass, after which capillaries in suspension were expelled. This suspension was centrifuged at 380 x g at 4 ˚C for 5 minutes. The supernatant was aspirated, the pellets resuspended in 1 ml Buffer A and the sample was gently loaded onto the top of the Percoll gradient. Tubes were centrifuged at 2500 x g at 4 ˚C for 20 minutes.

Approximately 1.5 ml of frosty layer just above the layer of red blood cells was collected using a Pasteur pipette and the cell suspension centrifuged at 550 x g at 4 ˚C for 5 minutes. Pellets were resuspended in 5 ml Buffer A and 5 ml Dulbecco's Modified Eagle's Medium (DMEM) and centrifuged at 380 x g, 4 ˚C for 5 minutes. Cells were finally resuspended in 3 ml per brain of DMEM supplemented with 16.7% (v/v) plasma-derived serum (PDS), 2 mM glutamine, 80 μg/ml heparin, 4 μg/ml puromycin, 100 units/ml penicillin, 0.1 mg/ml streptomycin and 1% (v/v) rBEC supplement (to a final concentration of 5 μg/ml ascorbic acid, 5 μg/ml insulin, 5 μg/ml transferrin, 5 ng/ml sodium selenite and 325 μg/ml glutathione), and seeded at 3 ml per T25 flask (pre-coated with 100 μg/ml rat tail type I collagen in 2 mM acetic acid treated at 37˚C for 3 h). Cells were maintained in 5% CO_2 in a humidified incubator for 2 days after which medium was replaced by 4 ml per flask of Growth medium: DMEM supplemented with 16.7% (v/v) PDS, 2 mM glutamine, 80 μg/ml heparin, 0.5 μg/ml basic fibroblast growth factor, 1% (v/v) rBEC supplement, 100 units/ml penicillin and 0.1 mg/ml streptomycin.

When cells had reached 70% confluency (usually between 4-7 days), cells were washed with warm PBS, and then were briefly washed again with 1 ml 0.25% (w/v) trypsin in PBS. This wash was discarded, 1 ml 0.25% (w/v) trypsin was added to each flask and cells were incubated for 2-5 minutes until cells had detached. Growth medium, 2 ml, was added to each flask to neutralise trypsin activity. The cell suspension was added onto an appropriate culture surface at a required cell density.

2.2.2 Isolation and culture of primary rat astrocytes

Zero- to three-day-old rat pups were sacrificed by dislocation of the neck and decapitation. Heads were collected, and the skin and skull were cut longitudinally with fine scissors and pinned to the side to reveal the brain. Brains were removed with forceps and maintained in warm DMEM containing 4500 mg/L glucose and sodium pyruvate supplemented with 9.09% (v/v) heat inactivated foetal bovine serum (FBS, Lonza Sales AG), 100 units/ml penicillin and 0.1 mg/ml streptomycin. Brains were halved and each hemisphere was rolled on sterile filter paper to remove the meninges and associated capillaries. Brains were homogenised in growth medium by trituration and was filtered through 60 μm nylon meshes.

The homogenate was centrifuged at 400 x g for 5 minutes. The supernatant was aspirated and the pellet was resuspended in a volume of n-1 ml fresh growth medium where n = number of pups. Cell suspension, 1 ml, was added to each T75 flask containing 9 ml of fresh growth medium. Cells were maintained in a 5% CO_2 humidified incubator at 37 ˚C. The medium was changed 5 days after seeding. When cells were confluent, flasks were agitated on an orbital shaker at 37 ˚C for 2 hours. The medium was removed (or kept for microglial cells) and cells washed twice with warm PBS. Cells were then incubated with 3 ml per flask of 0.25% (v/v) trypsin at 37 ˚C for approximately 5 minutes until the majority of cells detached. Trypsin activity was neutralised with 6 ml of growth medium. Cells were counted using a haemocytometer. The cell suspension was centrifuged and the cell pellet resuspended in FBS containing 10% (v/v) dimethylsulfoxide at a density of 1 x 10^6 cells/ml. When required, cells were thawed and added to growth medium. Cells, at a density of 10,000 cells/cm^2, were plated onto PDL-coated tissue culture plates and maintained in a 5% CO_2 humidified incubator at 37 ˚C. The medium was changed on

the day 1 and every 2-3 days. Cells were grown for three days before being co-cultured with rBECs.

2.2.3 Generation of the rat *in vitro* blood-brain barrier model

Illustration of the rat *in vitro* BBB model generation is shown in Figure 2.1. Astrocyte growth medium was completely removed from primary rat astrocytes which had been grown on the surface of the lower chamber for 3 days and was replaced with rBEC growth medium. Transwell® inserts (0.4 µm pore size polyester membrane) were then transferred into the appropriate well. Then rBECs were seeded at a density of 75,000 cells/cm^2 onto ECM-coated Transwell® inserts. The rat BBB model was maintained in a 5% CO_2 humidified incubator at 37 ˚C. The medium was changed 24 hours post seeding and on alternate days. The volume of culture medium to be added to each compartment of the Transwell® insert system is shown in Table 2.2.

Figure 2.1 Timeline for generation of the *in vitro* rat blood-brain barrier model

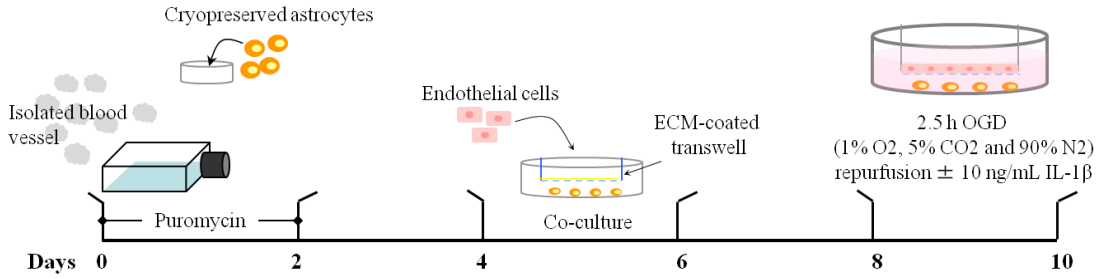

Table 2.2 Volume of cell culture medium added to apical and basolateral compartments of the *in vitro* blood-brain barrier model

	Volume (ml)	
	Apical	Basolateral
6-well plate	1.5	3.0
12-well plate	0.5	1.5
24-well plate	0.25	0.75

2.3 Measurement of transendothelial electrical resistance

An EVOM™ epithelial voltohmmeter and chopstick electrodes (World Precision Instruments, UK) was used for the measurement of the electrical resistance of brain endothelial cell monolayers grown on Transwell® inserts. Each value was corrected for the value obtained from filters that did not contain endothelial cells and normalised for surface area of insert.

2.4 Immunocytochemical detection of protein expression

Rat brain endothelial cells were grown on precoated Transwell® inserts or coverslips in 24-well plates. Rat brain endothelial cells were characterised by determining expression of von Willebrand factor (vWF). Expression of the tight junction proteins occludin and ZO-1 were also assessed. Medium was aspirated and cells were fixed by incubating with 4% (w/v) paraformaldehyde and 4% (w/v) sucrose in PBS for 15 minutes. For Transwell® inserts, the polyester membranes were cut out of the insert cases with a scalpel. The cells were then rinsed three times with PBS and permeabilised by treatment with primary diluent (0.1% (v/v) Triton-X 100 and 1.5 mM sodium azide in PBS) for 10 minutes at room temperature. Transwell® inserts or coverslips were rinsed once with PBS and cells incubated with 0.25% (w/v) NH_4Cl in PBS for 5 minutes. After three washings with PBS, cells were incubated with 1% (v/v) donkey serum in primary diluent (500 µL/well) for 1 hour in order to block all non-specific binding sites. Cells were subsequently incubated with primary antibodies (rabbit anti-human ZO-1 antibody (Invitrogen, UK) at a final concentration of 0.25 µg/ml, mouse anti-human occludin antibody (Invitrogen, UK) at a final concentration of 0.25 µg/ml, rabbit anti-human vWF at the working dilution of 1:200, rabbit anti-glial fibrillary acidic protein (GFAP) antibody (Dako, UK) at the working dilution of 1:500 or mouse anti-human cellular fibronectin (Abcam, UK) at the working dilution of 1:500). Coverslips were rinsed with PBS three times and then incubated for 1 hour with Alexa Flour® 594 conjugated donkey anti-mouse IgG antibodies (Invitrogen, UK) and Alexa Flour® 488 conjugated donkey anti-rabbit IgG antibodies (Invitrogen, UK) both at the working dilution of 1:1000.

To identify focal adhesions, cells were fixed by incubating with 4% (w/v) paraformaldehyde and 4% (w/v) sucrose in PBS for 9 minutes. The cells were then rinsed three times with PBS and permeabilised by treatment with primary diluent (0.1% (v/v) Triton-X 100 and 1.5 mM sodium azide in PBS) for 10 minutes at room temperature. Transwell® inserts or coverslips were rinsed once with PBS and subsequently incubated for 1 hour with mouse anti-human vinculin antibody (Abcam, UK) diluted in PBS at the working dilution of 1:400. Cells were rinsed with PBS three times and then incubated for 1 hour with Alexa Flour® 488 conjugated donkey anti-mouse IgG antibodies (Invitrogen, UK) at the working dilution of 1:1000 and Texas red-conjugated phalloidin (Invitrogen, UK) at the working dilution of 1:400. Coverslips were washed three times with PBS, twice with water and excess water remove by touching the side onto a clean tissue before mounting with Prolong® gold anti-fade reagent containing DAPI (Invitrogen, UK). For polyester Transwell® membranes, membranes were placed onto a glass slide and allowed to dry for 10 minutes prior to mounting. The cells were analysed through an Olympus BX51 upright microscope using 10x/ 0.30 UPlan Fln, 20x/ 0.50 UPlan Fln, 40x/ 0.75 UPlan Fln and 60x/ 0.65-1.25 UPlan Fln (Ph 3) objectives and captured using a Coolsnap EZ camera (Photometrics) through MetaVue Software (Molecular Devices). Specific band pass filter sets for DAPI, FITC and Texas red were used to prevent bleed through from one channel to the next. Images were then processed and analysed using ImageJ (http://rsb.info.nih.gov/ij). The mean intensity, circularity and the ratio of the mean intensity cytoplasmic intensity to the mean membranous intensity were calculated and statistically analysed using GraphPad Prism version 5 and shown as mean ± standard deviation (SD). Circularity of cells was calculated automatically by the ImageJ software using the formula:

$$\textbf{Circularity} = 4\P(\text{area}/\text{perimeter}^2).$$

The circularity value of 1.0 indicates perfect circle. The value of 0.0 indicates an elongated shape. T-test, one-way ANOVA or two-way ANOVA with Bonferroni post-hoc tests were applied to compare all data obtained from at least 3 independent cultures. All analysed data were considered statistically significant when $p<0.05$.

2.5 Oxygen glucose deprivation and interleukin-1β treatment

In order to assess the response of the *in vitro* BBB model following *in vitro* simulation of acute brain injury (OGD), rBEC-astrocytic co-cultures were placed in an airtight hypoxic glove box. Nitrogen gas was used to purge other gases from the hypoxic glove box and the box was incubated in an air-tight chamber at 37 ˚C with CO_2 and O_2 levels set at 5% and 1%, respectively.

The original glucose-containing medium was removed and wells were washed once with glucose-free DMEM before addition of glucose-free DMEM medium to each well. Cultures were exposed to OGD for 2.5 hours. The OGD condition was terminated and the reperfusion condition was simulated by adding glucose and PDS back to the culture medium to the final concentration of 1000 mg/L and 16.7% (v/v), respectively. The control culture was maintained in serum free DMEM containing glucose for 2.5 hours. IL-1β dissolved in 1% (w/v) low endotoxin BSA in 0.9% (w/v) sodium chloride, so called vehicle was added to the cells in the Transwell® insert compartment at a final concentration of 10 ng/ml at the beginning of reperfusion condition.

2.6 Enzyme-linked immunosorbent assay (ELISA)

To assess the effect of IL-1β on endothelial cell CINC-1 production, CINC-1 levels were measured using Rat CXCL1/CINC-1 DuoSet (R&D systems, UK). Wash buffer (0.05% (v/v) Tween-20 in PBS) and reagent diluent (1% w/v BSA in PBS) were prepared according to the manufacturer's instructions. Following treatment of endothelial cells with IL-1β, culture medium was collected and stored at -20 ˚C until used in ELISA. Wells of a 96-well ELISA plate were treated overnight at room temperature with 50 µL per well of 0.4 µg/ml goat anti-rat CINC-1 prepared in PBS. The solution was then aspirated, wells washed four times with wash buffer and wells treated with reagent diluent for at least 1 hour in order to block non-specific binding sites. A standard curve, ranging from 3.9 to 1000 pg/ml for CINC-1 was prepared in either growth medium or cell lysate solution (without protease inhibitor cocktail) depending on samples. Standard CINC-1 solutions, 50 µL, (in duplicate) were added into appropriate wells of the ELISA plate. The blank condition (in triplicate) contained either growth medium or cell lysate solution depending on samples. Cell

culture medium was tested in duplicate. After 2-hour incubation at room temperature, the solutions were aspirated and the plate washed four times with wash buffer prior to addition of 50 µL per well of 50 ng/ml biotinylated goat anti-rat CINC-1 prepared in reagent diluent. The solutions were then aspirated and the plate washed four times with wash buffer.

Fifty microlitres of 0.5% horseradish peroxidase (HRP)-conjugated Streptavidin, prepared in reagent diluent, were then added to each well and the plate incubated for 20 minutes at room temperature. The antibody solution was aspirated and wells washed four times with wash buffer. Fifty microlitres of 1:1 hydrogen peroxide:tetramethylbenzidine were then added to each well and the plate incubated at room temperature in a light-protected container for 20 minutes. Twently five microlitres of 2N H_2SO_4 were added to each well to stop the reaction. The optical density at 450 nm minus the optical density of 540 nm was measured using a Biotek plate reader. A standard curve was generated by plotting log concentration of standard solution versus log optical density. The CINC-1 concentrations of cell culture medium samples were calculated and statistically analysed using GraphPad Prism version 5 and shown as mean ± SD. Two-way ANOVA and Bonferroni post-hoc tests were applied to compare all CINC-1 concentration data obtained from at least 3 independent cultures. All analysed data were considered statistically significant when $p<0.05$.

Chapter 3 Characterisation of the *in vitro* blood-brain barrier model

3.1 Introduction

The BBB is a specialised vascular structure composed of several cellular components including brain endothelial cells forming vessel tubes on the basal lamina, pericytes embedding in the matrix of the basal lamina and astrocytes of which endfeet completely covering the whole cerebral blood vessels separating the vasculature and the parenchyma. Brain endothelial cells and its basal lamina are in close interaction in physiological state. ECM regulates cell behaviour such as cell adhesion (Tilling et al., 2002, Pedraza et al., 2000, Sixt et al., 2001), proliferation (Form et al., 1986, Cybulsky and McTavish, 1997, Wang and Milner, 2006) and survival (Finlay et al., 2000, Wang and Milner, 2006). Furthermore, the ECM can modulate cell response to inflammation (Summers et al., 2009, Vaday et al., 2001, Summers et al., 2010, Milner and Campbell, 2003, Floris et al., 2003, Borgquist et al., 2002). Under acute and chronic pathological circumstances, changes in the basal lamina ECM proteins (Sixt et al., 2001, De-Carvalho et al., 1999, Fukuda et al., 2004, Ji and Tsirka, 2012, Liu et al., 2012b, Tian et al., 2007, Li et al., 2010) and disappearance of integrin (ECM receptor) expression (Tagaya et al., 2001, Li et al., 2010, Milner et al., 2008) of brain endothelial cells are observed. To investigate the effect of acute brain injury on brain endothelial ECM expression and the effect of ECM proteins on brain endothelial cell activation, we selected an *in vitro* model that allow us to determine the molecular and cellular responses as required. The *in vitro* BBB model composed of brain endothelial cells grown on Transwell® inserts co-cultured with astrocytes has been long and widely used for physiological and pharmaceutical experiments (Didier et al., 2003, Krizanac-Bengez et al., 2003, Miller et al., 2005, Skinner et al., 2009) and seems to be a suitable model for our study. A number of BBB model from varied species have been developed (Abbott et al., 1992, Bowman et al., 1983, Weidenfeller et al., 2005, Song and Pachter, 2003, Siddharthan et al., 2007, Rubin et al., 1991, Roux and Couraud, 2005). Mammalian sources such as bovine and porcine provided barrier properties comparable to those *in vivo* and closely related to human whilst brain endothelial cells isolated from rodents such as rat and mouse are widely used due to their connection with animal

models. Neighbouring cells are an important component for BBB maintenance and co-culturing with other brain resident cells or astrocyte-conditioned medium induces and maintains BBB phenotype of primary brain endothelial cell culture (Schiera et al., 2003, Nakagawa et al., 2009, Haseloff et al., 2005, Arthur et al., 1987, Cantrill et al., 2012). Serum removal (Nitz et al., 2003, Hoheisel et al., 1998) and supplementation of cell culture medium with hydrocortisone (Hoheisel et al., 1998, Forster et al., 2005, Weidenfeller et al., 2005, Perriere et al., 2005) or cyclic adenosine monophosphate agonists, 8-(4-chlorophenylthio) adenosine 3′,5′-cyclic monophosphate sodium salt (CPT-cAMP) and phosphodiesterase inhibitor, RO 20-1724 (Rubin et al., 1991, Wolburg et al., 1994, Cantrill et al., 2012) have also been reported to maintain barrier integrity. Isolation of brain endothelial cells involving tissue dissection, mechanical disintegration, enzyme digestion and centrifugation can cause cell damage and loss some *in vivo* properties. Therefore, it requires validation following cell isolation in order to confirm that cells obtained by a particular method retain their properties as they express *in vivo*, including cellular morphology, cell organisation and expression of marker proteins markers. The condition of *in vitro* acute brain injury also required validation. Oxygen-glucose deprivation and treatment with inflammatory mediators have been widely applied to investigate the effect of acute brain injury *in vitro* (Liu et al., 2012a, An and Xue, 2009, Stanimirovic et al., 1997, Ji and Tsirka, 2012), whilst studies report pro-inflammatory IL-1 mediated hypoxia-induced change in BBB permeability *in vitro* (Yamagata et al., 2004, Argaw et al., 2006). However, the conditions such as time courses, cytokine concentration or medium component are slightly different from experiment to experiment. Here we have characterised the culture composed in the *in vitro* BBB model by observing cell morphology under a light microscope, ECM production by mass spectrometry and immunocytochemistry probed for specific cellular markers. We have also investigated the localisation of two key tight junction proteins, occludin and ZO-1 by immunocytochemistry and quantified CINC-1 release by ELISA in order to validate the optimal conditions to produce an *in vitro* model of acute brain injury using OGD/IL-1β.

3.2 Materials and methods

3.2.1 Establishment of the porcine *in vitro* blood-brain barrier model

3.2.1.1 Isolation and culture of porcine brain endothelial cells

The protocol for pBEC isolation was previously described by Cantrill et al. (Cantrill et al., 2012). Routinely, 10-12 adult porcine brains were kept in DMEM containing 4500 mg/L glucose and sodium pyruvate supplemented with 100 units/ml penicillin and 0.1 mg/ml streptomycin on ice whilst transporting from abattoir to the laboratory. The brain hemispheres were washed in ice-cold PBS and meninges were removed with watchmaker's forceps. After the white matter was removed, the brains were cut into small pieces with sterile scissors in a sterile beaker containing DMEM with 4500 mg/L glucose and sodium pyruvate supplemented with 1M HEPES (Fisher scientific, UK), 10% (v/v) FBS, 100 units/ml penicillin and 0.1 mg/ml streptomycin. Samples were then initially homogenised by passage through a 50 mL syringe into a sterile container.

Crude brain homogenates, 15 ml, were sequentially homogenised using loose (Dounce Homogeniser, Jencons, UK; 89-127 μm clearance) and then tight pestles (25-76 μm clearance) for 17 strokes each. The homogenate was then filtered through a sterile 150 μm pore size mesh and then through a 60 μm pore size mesh. The 60 μm meshes on which the capillaries were retained were then treated with M199 containing 210 U/ml collagenase (Worthington Lorne Lab, UK), 114 U/ml deoxyribonuclease I (Worthington Lorne Lab, UK), 91 U/ml trypsin (Worthington Lorne Lab, UK), 10% (v/v) FBS, 100 units/ml penicillin and 0.1 mg/ml streptomycin. Meshes were incubated for 1 hour at 37˚C and then, material retained on meshes was flushed off using stripettes. The suspension was centrifuged at 400 x g for 5 minutes. The capillary pellet was resuspended in DMEM and the suspension centrifuged as described above. This washing step was repeated. Capillaries were then resuspended in 90% (v/v) FBS and 10% (v/v) dimethylsulfoxide and stored at -80˚C until use.

Cryopreserved pBECs were thawed in a water bath at 37˚C and then seeded onto 6-well plates pre-coated with type I collagen solution (as described above). Cells were maintained in pBEC growth medium: DMEM containing 1000 mg/L glucose and sodium bicarbonate supplemented with 10% (v/v) PDS, 2 mM glutamine, 125 µg/ml heparin, 100 units/ml penicillin and 0.1 mg/ml streptomycin at 37˚C with 5% CO_2 in a humidified incubator. Twenty four hours post plating, the medium was aspirated and replaced with fresh growth medium containing 3 µg/ml puromycin. Following puromycin treatment for four days, cells were routinely maintained in a medium comprised of 50% (v/v) pBEC growth medium and 50% (v/v) astrocyte-conditioned medium. To produce astrocyte-conditioned medium, the CTX-TNA2 rat astrocyte cell line was maintained in pBEC growth medium for 2 days. This astrocyte-conditioned medium was removed from the CTX-TNA2 cells and retained at 4˚C until use. Porcine brain endothelial cells were maintained in the 6-well plates until confluent.

To transfer pBECs from 6-well plates to Transwell® inserts, culture medium was removed and cells were washed twice with warm PBS. Three hundred microlitres of 0.25% (w/v) trypsin in PBS was added into each well and plates incubated at the 37˚C with occasional taps until all the cells had detached from the surface. The cell suspension was transferred to a universal tube and centrifuged at 400 x g for 5 minutes. The supernatant was removed and the cell pellet was resuspended in 1 ml growth medium. Cells were then counted by using a haemocytometer and the cell suspension diluted with 50% (v/v) pBEC growth medium and 50% (v/v) astrocyte conditioned medium. Cells were seeded at a density of 75,000 cells/cm^2 onto the Transwell® insert. The upper chamber of the Transwell® system contained 0.5 ml growth medium whilst the lower chamber contained 1.5 ml medium. The medium was changed twenty four hours post seeding and on alternate days. After 3 days in the Transwell® system, Transwell® inserts were transferred into a 12-well plate containing CTX-TNA2 cells on the surface of the lower chamber. Porcine brain endothelial cells on Transwell® inserts were co-cultured with the rat astrocyte cell line for four days prior to use.

3.2.1.2 Culture of the CTX-TNA2 cell line and the porcine in vitro BBB model

Cryopreserved CTX-TNA2 cells were thawed in a 37˚C water bath and maintained in DMEM containing 4500 mg/L glucose and sodium pyruvate supplemented with 9.09% (v/v) FBS (50 ml FBS to 500 ml DMEM), 100 units/ml penicillin and 0.1 mg/ml streptomycin. Cells were grown in an atmosphere of 5% CO_2 in a humidified incubator at 37˚C. Medium was changed 24 hours post seeding and every 3 days. When confluent, cells were detached using 0.25% (w/v) trypsin in PBS and transferred onto either uncoated or ECM-coated plates as required at the density of 10,000 cells/cm^2.

3.2.2 Establishment of the rat *in vitro* blood-brain barrier model

Isolation and culture of primary rBECs and primary rat astrocytes is described in details in section 2.2.1 and 2.2.2, respectively. Rat brain endothelial cells were trypsinised from flasks and transferred to Transwell® inserts coated with 10 μg/ml rat tail collagen (See section 2.1 for plate coating protocol) at a cell density of 75,000 cells/cm^2. The medium in which astrocytes had been growing for three days prior to coculture was completely removed and replaced by rBEC growth medium. The Tranwell® inserts were placed onto wells with growing astrocytes and maintained in a 5% CO_2 humidified incubator at 37 ˚C. Medium was changed on day 1 and every 2 days.

3.2.3 Measurement of transendothelial electrical resistance

For pBECs, cerebromicrovascular endothelial cells were grown on ECM-coated Transwell® inserts at 75,000 cells/cm^2 and were maintained in growth medium. Growth medium was replaced with serum-free medium containing 312.5 mM RO 20-1724 (Merck Biosciences) and 17.5 mM CPT-cAMP. After 24 hours TEER was measured as described in section 2.3. For rBECs, cells were maintained in growth medium supplemented with 180 ng/ml hydrocortisone (rBECs) as required.

3.2.4 Polyacrylamide gel electrophoresis and Western blotting

The sodium dodecyl sulfate-polyacrylamide gel electrophoresis (SDS-PAGE) method used was that of Laemmli (1970) using a Mini-PROTEAN II Cell system

(Bio-Rad Laboratories Ltd., UK). Resolving gels containing 10% acrylamide, and 5% stacking gels were employed. Protein samples were loaded into wells and subjected to electrophoresis at 80 V for 20 minutes and 120 V for 60 minutes using running buffer containing 0.025 M Tris base (Fisher Scientific, UK), 0.192 M glycine (Fisher Scientific, UK) and 1% (w/v) sodium dodecyl sulfate (SDS) in dH_2O. Proteins were then electrotransferred from the gel to polyvinylidene fluoride (PVDF; GE Healthcare, UK) membrane for western blotting. PVDF membrane was activated by soaking in methanol for 1 minute. The membrane was then rinsed twice with dH_2O. Sponges, filters, PVDF membrane and gel were soaked in ice-cold transfer buffer containing 48 mM Tris base, 39 mM glycine and 0.025% (v/v) SDS in dH_2O for 30 minutes prior to use. The gel and the membrane were sandwiched between filter papers and sponges in a transfer cassette, immersed in ice-cold transfer buffer and electrotransfer of proteins carried out at 4˚C, 100 V for 60 minutes. After transfer, the membrane was incubated with 5% (w/v) skimmed milk in 0.05% (v/v) Tween-20 in PBS (PBST) for 1 hour at room temperature to block non-specific protein binding sites. The membrane was then washed for 4 x 5 minutes (20 minutes in total) with PBST and incubated with mouse anti-cellular fibronectin antibody at 1:1000 (Abcam, UK) diluted in 1% (w/v) BSA in PBST at 4˚C overnight. The membrane was then washed with PBST for 4 x 5 minutes and incubated with HRP-conjugated rabbit anti-mouse IgG secondary antibody (Dako, UK) in 5% w/v skimmed dry milk in PBST for 1 hour at room temperature. The membrane was washed as described above, placed onto a clear plastic sheet and 0.5 ml Amersham™ ECL™ Plus (GE Healthcare, UK) was added. The membrane was visualised using GE health care ImageQuant™.

3.2.5 Sample preparation for mass spectrometry analysis

The cell detachment method employed in this thesis was adapted from Turoverova et al. (Turoverova et al., 2009). Porcine brain endothelial cells were grown on uncoated plastic 6-well plates for 7 days. Cells were treated with 2 mM Ethylenediaminetetraacetic acid (EDTA) in PBS and plates placed on a shaker for 10 minutes at 37 ˚C. Cell monolayers were then gently rinsed with 2 mM EDTA in PBS to help remove any remaining cells. This step was repeated until all cells had

completely detached. The well surface was washed again with the same solution and 200 µL Laemmli's 6x sample buffer was added to 3 wells of a 6-well plate. The surface of the wells was scraped thoroughly to remove ECM proteins. Samples was collected and kept in -20 ˚C until use.

ECM sample was run on a 10% resolving and 5% stacking SDS-PAGE gel for 15 minutes or until all sample had migrated approximately 0.5 cm into the gel. The gel was stained with Coomassie blue by placing the gel in a tray and incubating with 0.2% (w/v) Coomassie blue in 45% (v/v) methanol and 10% (v/v) glacial acetic acid in dH_2O for 1 hour. The tray was gently agitated on a rocker at room temperature. To destain the gel the Coomassie blue solution was replaced by 45% (v/v) methanol and 10% (v/v) glacial acetic acid in dH_2O and the tray was gently agitated for 1 hour at room temperature. The gel was then immediately sent to Mass spectrometry facility for analysis.

High throughput protein identification protocol using Liquid chromatography-tandem mass spectrometry was adapted from Humphries et al. (2009) (Humphries et al., 2009). Briefly, the stained band was cut from the gel, placed into a well of a 96-well plate, 50 µl acetonitrile added and the sample incubated for 5 minutes. The plate was centrifuged for 1 minute at 300 x g using a 96-well plate rotor. The acetonitrile was removed and the gel was dried in a vacuum centrifuge for 15 minutes. 10 mM DTT in 25 mM NH_4HCO_3 was added to reduce the proteins and the sample incubated at 56°C for 1 hour. The plate was placed at room temperature to cool and then centrifuged for 1 minute at 300 x g. The DTT solution was removed. 55 mM iodoacetamide in 25 mM NH_4CO_3 was added to the gel and the sample incubated for 45 minutes at room temperature in the dark. The plate was centrifuged for 1 minute at 300 x g, the iodoacetamide solution removed and the gel was washed with 50-100 µl 25 mM NH_4HCO_3 for 10 minutes. The gel was then washed with 50-100 µl acetonitrile for 5 minutes before the plate was centrifuged as described above. The acetonitrile was removed, 25 mM NH_4HCO_3 was added and the gel incubated for 5 minutes. The plate was centrifuged as described above and the 25 mM NH_4HCO_3 solution. The gel was washed again with acetonitrile for 5 minutes before the solvent was removed and the gel completely dried in a vacuum centrifuge for 15 minutes.

Five microlitres of 12.5 pg/ml trypsin solution and 45 µl 25 mM NH_4CO_3 were added and the sample placed on ice for 45 minutes. The plate was incubated overnight at 37 °C in a humidified container and subsequently the peptides were extracted from the gel by treating with 50 µl 20 mM NH_4HCO_3 for 20 minutes. The plate was centrifuged as described above, the solvent removed and the extraction was repeated twice with 5% (v/v) formic acid in 50% (v/v) acetonitrile. The solvent fractions from all three extractions were pooled and the solvent was evaporated down to a volume of 20 µl in a vacuum centrifuge. Samples were stored in -20 °C freezer until analysis.

Samples were analysed by mass spectrometry and results obtained were identified using the search engine software, Mascot, and the UNIPROT_mammalian database.

3.2.6 Immunocytochemical detection of protein expression

The primary rat BBB model composed of rBECs grown on type I collagen-coated Transwell® inserts was obtained as described in Section 3.2.2. Astrocytes (see Section 2.2) were grown on glass coverslips to 100% confluency. Primary microglial cells were obtained from confluent mixed glial culture medium following 2-hour culture flask agitation. Mixed glial medium was collected and centrifuged at 400 x g for 5 minutes. Supernatant was discarded and cell pellet was resuspended in growth medium. Microglial cells were seeded onto glass coverslips at the cell density of $1x10^6$ cells/ml and ready to use on the next day. Prior to cell fixation, isolectin GS-IB_4 from *Griffonia simplicifolia*, Alexa Fluor® 594 conjugate (Invitrogen, UK) was added to the culture medium to the final concentration of 2.5 µg/ml and cells was incubated for 30 minutes at 37 °C in a humidified incubator. Astrocytes, rBECs and microglia were fixed and stained as described in section 2.4.

To obtain the mean cytoplasmic intensity and the mean membranous intensity using ImageJ software, membranous and cytoplasmic regions were identified (based on tight junction staining) on appropriate immunocytochemical images of ZO-1 and occludin. Regions of interest in membranous and cytoplasmic areas were selected using the “free hand line” tool of ImageJ software and the intensity of fluorescence in the selected areas was measured using “measure” tool of ImageJ software. The

ratio of the intensity between the cytoplasmic and membranous areas was calculated and analysed as described in section 2.4.

3.2.7 Oxygen glucose deprivation and interleukin-1β treatment

The primary rat BBB model was obtained as described in Section 3.2.2. The model was then exposed to OGD and IL-1β treatment as described in Section 2.5.

3.2.8 Enzyme-linked immunosorbent assay

Following OGD/IL-1β treatment, cell culture medium was collected on ice and kept in Eppendorf tubes at -20°C until use. Samples were thawed on ice for approximately one hour and were briefly mixed before ELISA. See section 2.6 for ELISA protocol.

3.3 Results

3.3.1 Morphology of porcine brain endothelial cells in culture

The *in vitro* model of the BBB comprising a co-culture of primary brain endothelial cells and the CTX-TNA2 astrocyte cell line is a suitable model for our research project. Although the cell isolation and co-culture procedures used in this project have been applied routinely in our laboratory as a model to study drug transport and drug delivery at the BBB, the initial studies contained in this thesis sought to characterise the model prior to further studies investigating the role of ECM in endothelial cell activation.

Porcine brain capillary fragments were seeded onto collagen-coated plates. Images were taken immediately after plating (Figure 3.1A). Capillary fragments in tubular shapes, varied in size (from <50 μm to >1 mm), and were dispersed throughout the growth medium. Capillaries adhered to the wells and tapered-shaped cells started to grow from capillaries on day *in vitro* (DIV) 1 (Figure 3.1B). Image was taken on DIV 2 following puromycin removal which non-adherent cells were removed (Figure 3.1C). Porcine brain endothelial cells displayed long and pointed at both end. Nuclei were oval-shaped and phase dark. Cells were tightly apposed and grew in many separate small groups which met at later stage of culture growth and combine into a large cell monolayer. Cells continuously proliferated and were 80% confluent on DIV 5 (Figure 3.1D). Cells were transferred to rat tail type I collagen-coated Transwell® inserts and reach confluency on DIV10 (Figure 3.1E).

A low TEER of a monolayer reflects a potentially "leaky" barrier, i.e. a cell barrier with a high permeability; whereas a high TEER reflects a more highly restrictive, less permeable barrier. A highly restrictive barrier is important for studies investigating transport of small molecules, though the absolute restrictive nature of the barrier is less important when using the model to investigate non-transport related studies. The TEER values obtained in the present study reflect a tightly formed cell monolayer, a property of the BBB *in vivo*. TEER measurement was carried out every day for 7 days since cells were grown on Transwell® inserts

(Figure 3.2). TEER was at approximately 68.8 ± 27.5 $\Omega.cm^2$ on the first day. TEER of the cell monolayer increased slightly on the 2nd and 3rd day on Transwell® inserts. On DIV 4 on Transwell® inserts, TEER dramatically increased after cells reached confluency and pBECs were co-cultured with astrocytes. TEER of the porcine BBB model was significantly higher on the 7th day on Transwell® inserts, reaching 204 ± 24.1 $\Omega.cm^2$.

Figure 3.1 Porcine brain endothelial cell culture under phase-contrast microscopy

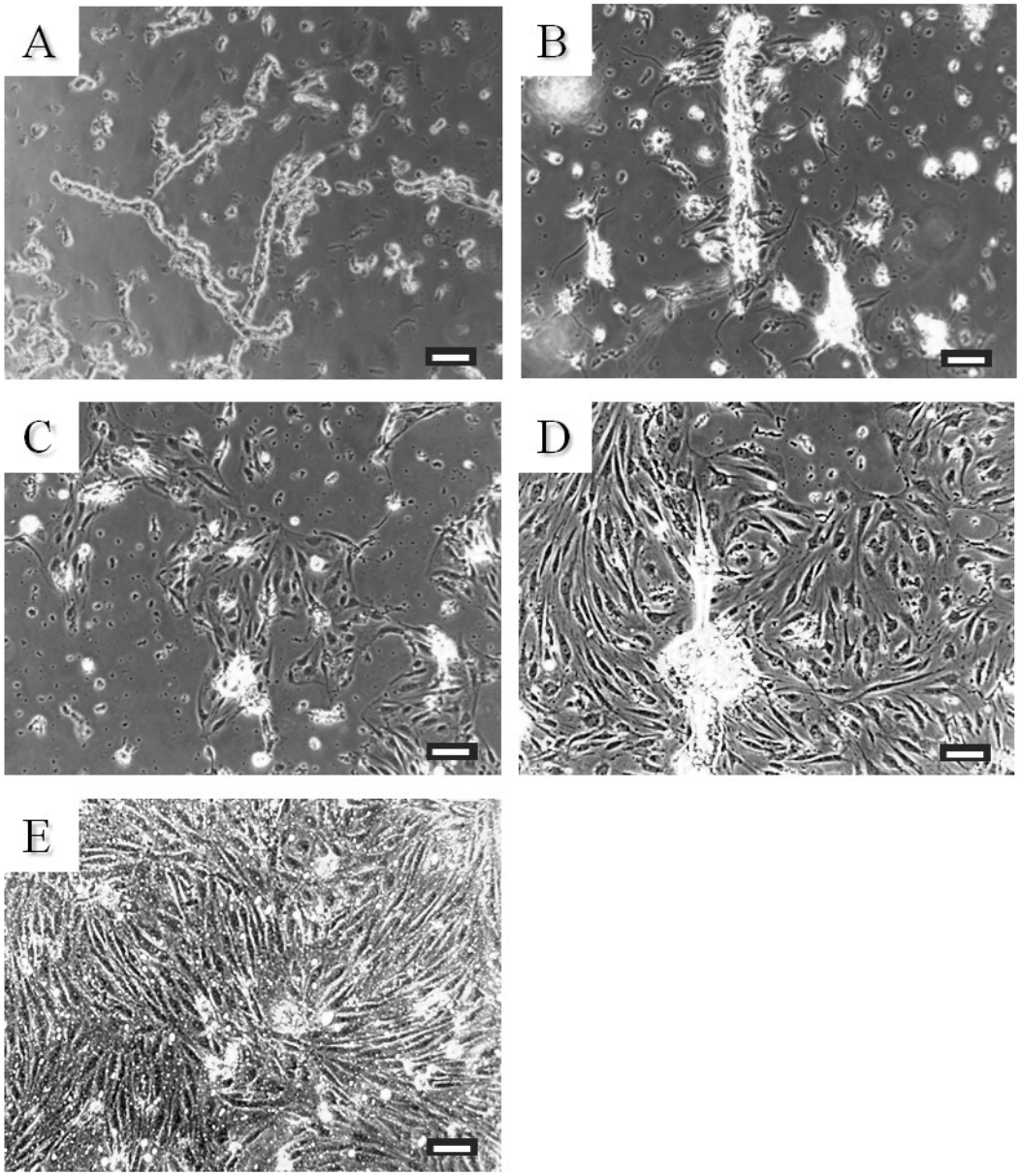

(A) Porcine cerebral vessels on DIV0. (B) On DIV1, cells started to grow out from the attached vessels. (C) On DIV2, more cells were observed compared to DIV1. (D) At DIV5 pBECs began to form a discernable monolayer (~80% confluent). (E) At DIV10, pBEC monolayers on a Transwell® insert (0.4 μm pore size) reached confluency. Scale bar represents 100 μm (200x magnification).

Figure 3.2 Transendothelial electrical resistance of primary porcine brain endothelial cells monolayer on rat tail collagen-coated Transwell® inserts

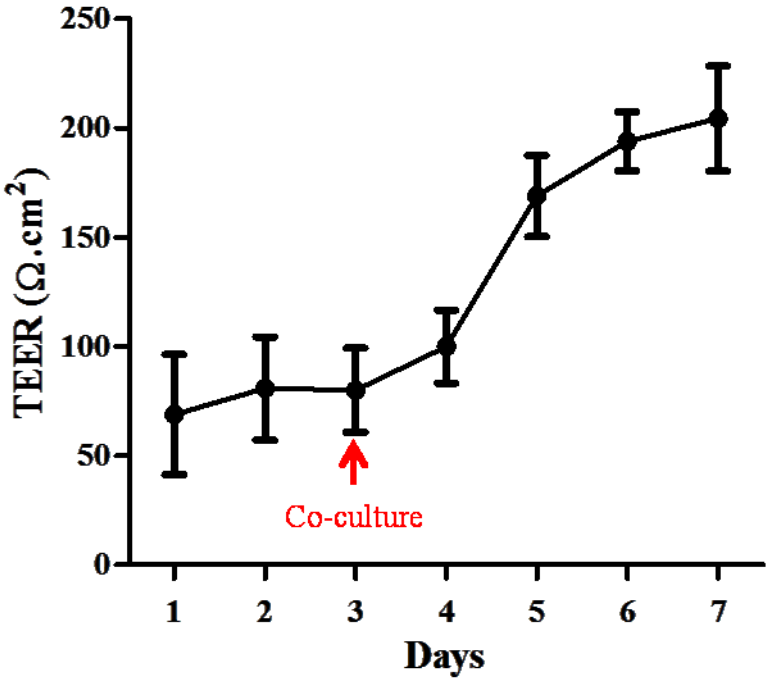

pBECs were grown on Type I collagen-coated Transwell® inserts for 3 days before co-cultured with the CTX-TNA2 rat astrocyte cell line. TEER measurements were performed daily using EVOM Epithelium Voltohmmeter electrodes for 7 days. Data are shown as means ± SD. TEER data were obtained from six Transwell® inserts from a single pBEC culture.

ECM in the basal lamina of the brain capillaries is produced by cells including endothelial cells, pericytes and astrocytes. ECM proteins in the basal lamina of the brain vessels are found to be cell-specific. For example, the ECM proteins underlying brain endothelial cells are laminin α4 and α5 isoforms whereas those associated with astrocytes are laminin α1 and α2 isoforms (Sixt et al., 2001).

Consequently, it is interesting to investigate which ECM proteins (and isoforms) are produced by the brain endothelial cells *in vitro*. ECM proteins will be isolated from *in vitro* cultures and identified by mass spectroscopic proteomic analysis. This will allow comparison of ECM proteins produced *in vitro* to ECM proteins which are known to be expressed *in vivo* (this approach also can potentially identify new ECM proteins which have not been reported).

Our preliminary data suggested that porcine brain endothelial cells in culture produced basal lamina (Cantrill et al., 2012). The confluent brain endothelial cells were detached via the method of Turoverova et al. and theorectically left the basal lamina on the culture plate. The ECM proteins were then extracted, the protein sample was subjected to electrophoresis. The gel was subsequently stained with Coomassie blue to establish if the proteins has been successfully isolated (Figure 3.3A) and western blotting to detect cellular fibronectin (Figure 3.3B) was also carried out.

There were at least 15 major bands of proteins observable following Coomassie blue staining (Figure 3.3A). The western blot for cellular fibronectin revealed a faintly cross reactive band above 250 kDa (Figure 3.3B). Together, these findings suggested that the method used for isolation of ECM was valid.

Part of the same sample that was analysed by western blotting was subjected to SDS-PAGE gel for 10 minutes and the gel was stained by Coomassie blue. The stained band was excised and sent to mass spectrometry facility for protein identification. Mass spectrometry results showed 16 and 19 proteins were identified from SWISSPROT database and UNIPROT database, respectively (Table 3.1). The majority of proteins detected by mass spectrometry were non-ECM proteins, namely keratin, cytoskeleton proteins (myosin, actin, tubulin and filamin) and serum components (albumin). Two ECM proteins, fibronectin and vitronectin, were

detected. However, no major vascular ECM molecules such as type IV collagen or laminins were detected.

With the second repeat, 70 proteins were detected (Table 3.2). Most of the proteins detected on the first repeat were also appeared on the second time of mass spectrometry. Sample was identified as from many species including human (*Homo sapiens*), cow (*Bos taurus*) pig (*sus scrofa*), sheep (*Ovis aries*), mouse (*Mus musculus*), dog (*Canis familiaris*), fruit fly (*Drosophila*), blood fluke (*Schistosoma mansoni*), atlantic white-sided dolphin (*Lagenorhynchus acutus*), baboon (*Papio anubis*), chimpanzee (*Pan troglodytes verus*), monkey (*Aotus trivirgatus*), horse (*Equus caballus*), marmoset (*Callithrix jacchus*) and rat (*Rattus norvegicus*). The ECM molecules detected including human collagen alpha I chain, bovine vitronectin, bovine fibronectin, mouse type VI collagen alpha 3 subunit, type VI collagen alpha-2 chain (fragment), bovine collagen alpha-2(I) chain and rat col1a1 protein (Procollagen, type 1, alpha 1). There was still no major vascular ECM molecules detected

Figure 3.3 Production of extracellular matrix proteins in porcine brain endothelial cell cultures

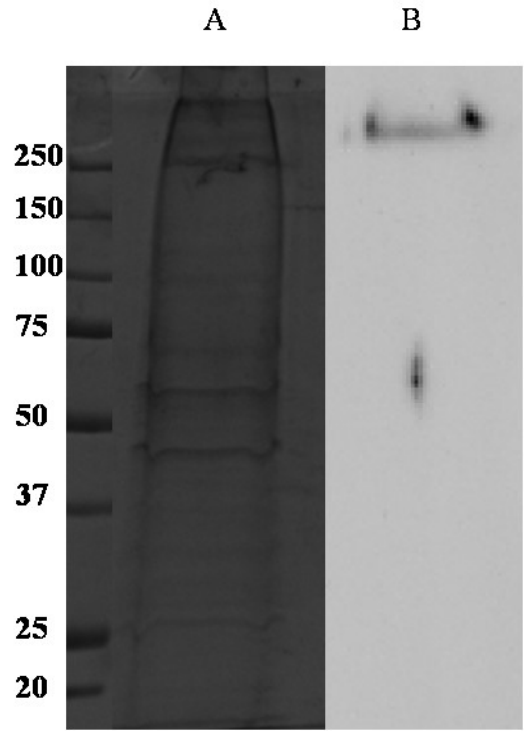

ECM proteins produced *in vitro* by rBECs were extracted and analysed by SDS-PAGE gels. Gels were stained by Coomassie blue (A) or were subjected to western blot analysis for cellular fibronectin (B). Samples were obtained from a single pBEC culture.

Table 3.1 Lists of proteins detected by mass spectrometry from SWISSPROT (A) and UNIPROT (B)

#	**A) Identified Proteins (16) SWISSPROT**	**Species**	**MW (kDa)**	**KK 1**
1	Keratin, type II cytoskeletal 1	*Homo sapiens*	66	18
2	Keratin, type I cytoskeletal 10	*Homo sapiens*	60	14
3	Myosin-9	*Canis familiaris*	226	17
4	Vimentin	*Homo sapiens*	54	8
5	Serum albumin precursor	*Bos taurus*	69	9
6	Actin-5C	*Drosophila melanogaster*	42	6
7	Keratin, type I cytoskeletal 9	*Homo sapiens*	62	5
8	Keratin, type II cytoskeletal 2 epidermal	*Homo sapiens*	66	5
9	Keratin, type II cytoskeletal 4	*Homo sapiens*	57	5
10	Tubulin beta-5 chain	*Bos taurus*	50	4
11	Keratin, type I cytoskeletal 13	*Homo sapiens*	50	3
12	Tubulin alpha-1B chain	*Sus scrofa*	50	3
13	Actin-1	*Schistosoma mansoni*	42	2
14	Vitronectin precursor	*Homo sapiens*	54	2
15	Filamin-A	*Homo sapiens*	281	2
16	Vinculin	*Homo sapiens*	124	2
#	B) Identified Proteins (19) UNIPROT Mammalian		MW (kDa)	KK
1	Myosin-9	*Canis familiaris*	226	22
2	Keratin, type II cytoskeletal 1	*Homo sapiens*	66	16
3	Keratin, type I cytoskeletal 10	*Homo sapiens*	60	17
4	Vimentin	*Homo sapiens*	54	11
5	A2M protein	*Bos taurus*	167	10
6	Beta-actin	*Lagenorhynchus acutus*	41	8
7	Keratin, type I cytoskeletal 9	*Homo sapiens*	62	9
8	Serum albumin precursor	*Bos taurus*	69	9

9	Keratin, type II cytoskeletal 4	*Homo sapiens*	57	5
10	Vitronectin	*Bos taurus*	54	5
11	Keratin 2A	*Pan troglodytes verus*	66	4
12	LOC539882 protein	*Bos taurus*	50	4
13	Tubulin beta chain	*Sus scrofa*	50	4
14	Keratin 13	*Homo sapiens*	50	3
15	Filamin-A	*Homo sapiens*	281	2
16	Keratin, type I cytoskeletal 15	*Ovis aries*	49	2
17	Vinculin	*Homo sapiens*	124	2
18	IGHM protein	*Bos taurus*	66	2
19	B6-derived CD11 +ve dendritic cells cDNA, RIKEN full-length enriched library, clone:F730215J21 product:heat shock protein 8, full insert sequence.	*Mus musculus*	50	2

Table 3.2 Lists of proteins detected by mass spectrometry from UNIPROT mammal database

#	Identified Proteins (70)	Species	MW (kDa)	KK1
1	Myosin-9	*Canis familiaris*	226	22
2	Vimentin variant 1 (Vimentin variant 2)	*Homo sapiens*	54	22
3	Keratin, type I cytoskeletal 10	*Homo sapiens*	60	15
4	cDNA FLJ78508	*Homo sapiens*	42	16
5	Filamin B	*Homo sapiens*	282	13
6	Keratin, type II cytoskeletal 1	*Homo sapiens*	66	13
7	Keratin, type II cytoskeletal 2 epidermal	*Homo sapiens*	66	13
8	Filamin A, alpha (Predicted)	*Papio anubis*	280	14
9	Neuroblast differentiation-associated protein AHNAK	*Homo sapiens*	629	9
10	Serum albumin	*Bos taurus*	69	9
11	Vinculin	*Sus scrofa*	124	9
12	Talin 1	*Mus musculus*	270	6
13	Trypsin	*Sus scrofa*	24	4
14	A2M protein	*Bos taurus*	168	6
15	Keratin, type I cytoskeletal 9	*Homo sapiens*	62	6
16	Keratin, type II cytoskeletal 5	*Homo sapiens*	62	6
17	Tubulin, beta 5	*Mus musculus*	50	5
18	Heterogeneous nuclear ribonucleoprotein B1	*Rattus norvegicus*	37	4
19	Putative uncharacterized protein	*Homo sapiens*	11	6
20	Spectrin, beta, non-erythrocytic 1 (Spectrin, beta, non-erythrocytic 1, isoform CRA_h)	*Homo sapiens*	251	6
21	Keratin 6A	*Homo sapiens*	60	5
22	Keratin, type I cytoskeletal 14	*Homo sapiens*	52	5
23	Annexin A2	*Sus scrofa*	39	4

24	Glyceraldehyde 3-phosphate dehydrogenase	*Mus musculus*	36	3
25	Uncharacterized protein SPTAN1	*Homo sapiens*	285	4
26	Inducible heat shock protein 70	*Mus musculus*	70	4
27	Heat shock 70kD protein 5 (Glucose-regulated protein)	*Mus musculus*	72	4
28	Myosin-9	*Rattus norvegicus*	226	4
29	TIB-55 BB88 cDNA, RIKEN full-length enriched library, clone:I730039G24 product:transgelin 2, full insert sequence	*Mus musculus*	22	4
30	Lamin A/C, transcript variant 1	*Pan troglodytes verus*	74	4
31	Collagen alpha-1(I) chain	*Homo sapiens*	139	2
32	PDIA3 protein	*Bos taurus*	57	3
33	HIST1H1C protein	*Bos taurus*	21	3
34	Myosin light chain 6 (Fragment)	*Ovis aries*	16	2
35	Vitronectin	*Bos taurus*	54	2
36	H2B histone family, member S	*Homo sapiens*	14	2
37	Complement C3	*Bos taurus*	187	2
38	TUBA1B protein	*Bos taurus*	50	2
39	Fibronectin	*Bos taurus*	250	3
40	Heterogeneous nuclear ribonucleoprotein M	*Homo sapiens*	78	3
41	Inter-alpha-trypsin inhibitor heavy chain H4	*Bos taurus*	102	3
42	Type VI collagen alpha 3 subunit	*Mus musculus*	287	3
43	Plectin-1	*Mus musculus*	534	3
44	LIM and SH3 domain protein 1	*Rattus norvegicus*	30	3
45	Gelsolin	*Bos taurus*	81	3
46	Alpha-2-HS-glycoprotein	*Bos taurus*	38	3
47	Type VI collagen alpha-2 chain (Fragment)	*Sus scrofa*	27	3
48	IGHM protein	*Bos taurus*	66	2
49	Ubiquitin B	*Sus scrofa*	24	2

50	Peptidyl-prolyl cis-trans isomerase A	*Aotus trivirgatus*	18	2
51	Collagen alpha-2(I) chain	*Bos taurus*	129	2
52	Elongation factor 1-alpha	*Homo sapiens*	50	2
53	ATP synthase subunit beta	*Homo sapiens*	57	2
54	Histone H2A (Fragment)	*Mus musculus*	14	2
55	Uncharacterized protein MSN (Fragment)	*Homo sapiens*	68	2
56	Col1a1 protein (Procollagen, type 1, alpha 1, isoform CRA_b)	*Rattus norvegicus*	138	2
57	MGC140363 protein (Similar to myosin:SUBUNIT=regulatory light chain)	*Bos taurus*	20	2
58	Mx1 protein	*Sus scrofa*	78	2
59	Transgelin	*Equus caballus*	23	2
60	ATP synthase subunit alpha	*Homo sapiens*	54	2
61	cDNA FLJ75925, highly similar to Homo sapiens keratin 16 (focal non-epidermolytic palmoplantar keratoderma) (KRT16), mRNA (Keratin 16) (Focal non-epidermolytic palmoplantar keratoderma)	*Homo sapiens*	51	2
62	Alpha-actinin-4	*Bos taurus*	105	2
63	Cofilin 1 (Non-muscle)	*Bos taurus*	19	2
64	cDNA, FLJ92534, highly similar to Homo sapiens heat shock 60kDa protein 1 (chaperonin) (HSPD1), mRNA	*Homo sapiens*	61	2
65	Conglutinin	*Bos taurus*	38	2
66	Actin, alpha cardiac muscle 1	*Bos taurus*	42	2
67	Junction plakoglobin	*Mus musculus*	82	2
68	Malate dehydrogenase (Fragment)	*Callithrix jacchus*	20	2
69	RRBP1 protein	*Homo sapiens*	103	2
70	Sodium/potassium-transporting ATPase subunit alpha-1	*Bos taurus*	113	2

3.3.2 Morphology of rat brain endothelial cell monolayer under a light microscope

Analysing cell morphology is useful since it can indicate cell type and condition of cells. The process of obtaining brain endothelial cells initially results in isolation of capillary fragments which attach to plastic or adhesive substrates and display a spindle-shaped morphology or sometimes a cobblestone-like morphology. To confirm that the isolated cells we obtained were brain endothelial cells, we firstly analysed the cellular morphology using light microscopy.

After seeding on type I collagen-coated plates, digested rat brain capillary fragments, approximately 50-200 μm in length, were clusters of round endothelial cells in a beads-on-a-string like structure (Figure 3.4A). The capillaries were occasionally branched. The next day, cells could be seen to grow out around brain endothelial cell clusters (Figure 3.4B). On DIV 2, cells grew out along the periphery of cell clusters and displayed a slender-shaped morphology (Figure 3.4C). They were approximately 10 μm in width and 100 μm in length with phase-dark appearance at the centre and transparent cell bodies. They were also tightly apposed. They continuously proliferated (Figure 3.4D) and an 80% confluent uniform monolayer without overlapping was formed 4 days after isolation (Figure 3.4E). Cells were grown in swirling patterns tightly against each other leaving gaps in the culture. After trypsinisation and transferring to Transwell® inserts, rBECs appeared as small clusters of 3-5 phase-bright round cells (Figure 3.4F) on the day of seeding and began to display endothelial cell morphology on the following day. Cells were confluent on Transwell® inserts on around 10 days after isolation (Figure 3.4G). Primary rat astrocytes displayed a phase-dark irregular morphology and were varied in size ranging from 100-500 μm (Figure 3.4H). Most of astrocytes in culture display several short processes.

Figure 3.4 Phase contrast micrographs of primary rat brain endothelial cell cultures and rat astrocytes

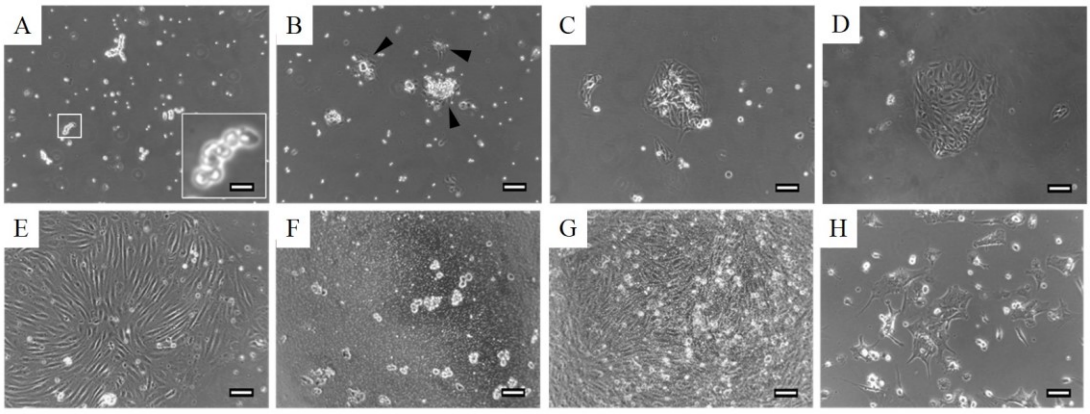

(A) Short fragments of rat brain microvessels immediately after plating. Inset in (A) is a close-up of a short capillary fragment which showed cluster of round cells. (B) Cells grew out (arrow heads) from attached cell clusters the day after seeding. (C) Slender-shaped cells observed 2 days following seeding. (D) A group of attached cells 3 days after seeding. The majority of cells were elongated in shape and clear cell alignment can be seen. (E) Cells reached 80% confluency. (F) Cells immediately after trypsinisation and transfering onto ECM-coated Transwell® inserts. Small bright dots in the background were pores of the Transwell® insert membrane. (G) Confluent rBEC monolayer on Transwell® inserts. (H) Primary rat astrocytes. Scale bar represents 100 μm (100x magnification).

3.3.3 Characterisation of rat primary brain endothelial cell culture

In addition to analysing cellular morphology, another method used to characterise the brain endothelial cells in culture is immunological detection of cell marker proteins specific to the cell of interest (and which are not expressed by other cell types). In addition to characterisation of marker protein expression, immunocytochemistry is useful for investigating the purity of brain endothelial cell cultures. The purity of brain endothelial cells in culture can determine the restrictive nature of the barrier *in vitro* since endothelial cells do not form highly restrictive tight junctions with non-endothelial cell types. In addition, there is more confidence in data obtained from pure endothelial cells in culture compared to cultures containing a combination of endothelial and non-endothelial cells, i.e. that the responses observed are from the cell type of interest and not the contaminating cells.

Rat brain endothelial cells formed monolayers in culture maintained on Transwell® inserts. More than 99% of rBECs were stained positive for vWF, a specific endothelial cell marker (Figure 3.5). This suggested that they retained their endothelial cell phenotypes *in vitro*. Expression of vWF antigen appeared punctate and was localised within the cell body and also in the perinuclear zone. The presence of tight junction proteins including occludin and ZO-1 were also shown by immunofluorescence staining. Rat brain endothelial cells appeared positive in occludin (Figure 3.6) and ZO-1 (Figure 3.7). Distributions of both occludin and ZO-1 were continuous along the cell-cell contact zones.

Purity of primary rat astrocyte culture was determined by immunocytochemistry for GFAP. More than 90% of cells in the culture were positively stained for GFAP (Figure 3.8). GFAP staining showed fibrous-like appearance throughout the cell bodies and processes but negative staining at the cell centre where nuclei are located. Cells were also cross-stained with isolectin GS-IB_4 which specifically bound to microglia. 5-7% of cells in culture were isolectin GS-IB_4 positive. DAPI nuclei staining of isolectin GS-IB4 positive cells were small and dense compared to those of GFAP positive cells. Normal rabbit IgG showed unspecific binding faintly to nuclei of rBEC monolayer and primary rat astrocytes.

Figure 3.5 Immunocytochemistry of rat brain endothelial cells for von willebrand factor

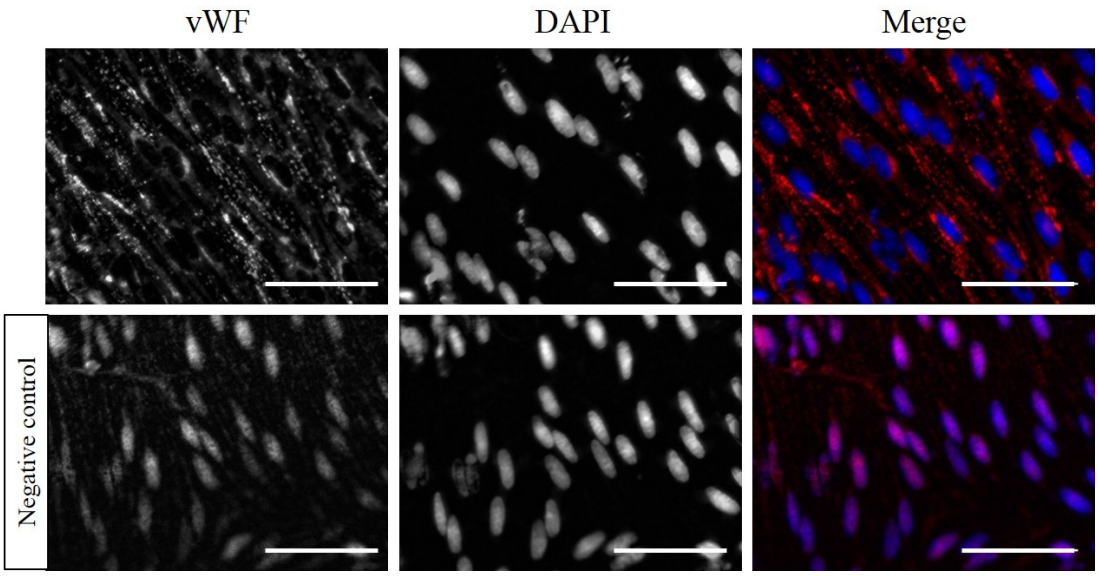

Primary cultures of rBECs on type I collagen-coated Transwell® inserts were used after being cultured for 8-10 days. Cells were fixed with 4% (w/v) paraformaldehyde and 4% (w/v) sucrose in PBS and were permeablised with 0.1% Triton®-X 100 prior to applications of antibodies. Rat brain endothelial cell monolayers were probed for vWF (red) and DAPI nuclei stain (blue). Negative control; rabbit IgG was added instead of anti-vWF antibodies. Digital pictures were taken with a Coolsnap ES camera through MetaVue software following visualization with an Olympus BX51 microscope. Nearly 100% of cells were vWF-positive. Scale bars represent 50 μm (600x magnification).

Figure 3.6 Immunocytochemistry of rat brain endothelial cells for occludin expression

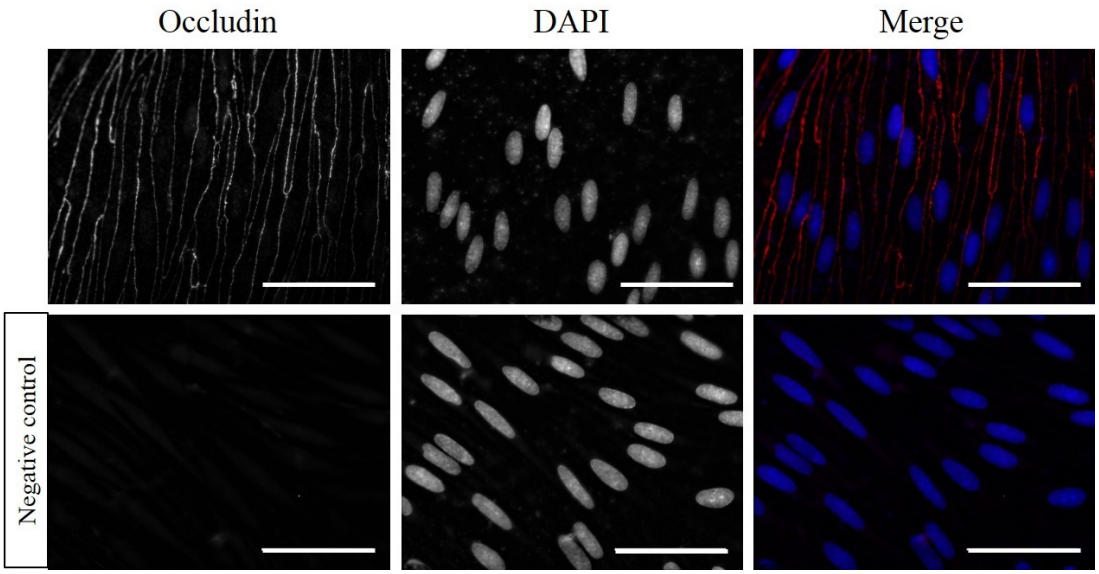

Primary culture of rBECs on type I collagen-coated Transwell® insert was used after being cultured for 8-10 days. Cells were fixed with 4% (w/v) paraformaldehyde and 4% (w/v) sucrose in PBS and were permeablised with 0.1% (w/v) Triton®-X 100 prior applications of antibodies. Rat brain endothelial cell monolayers were probed for occludin (red) and DAPI nuclei stain (blue). The monolayer was stained as a negative control for mouse IgG (red) and DAPI nuclei stain (blue). Digital pictures were taken with a Coolsnap ES camera through MetaVue software following visualization with an Olympus BX51 microscope. Scale bars represent 50 μm (600x magnification).

Figure 3.7 Immunocytochemistry of rat brain endothelial cells for ZO-1 expression

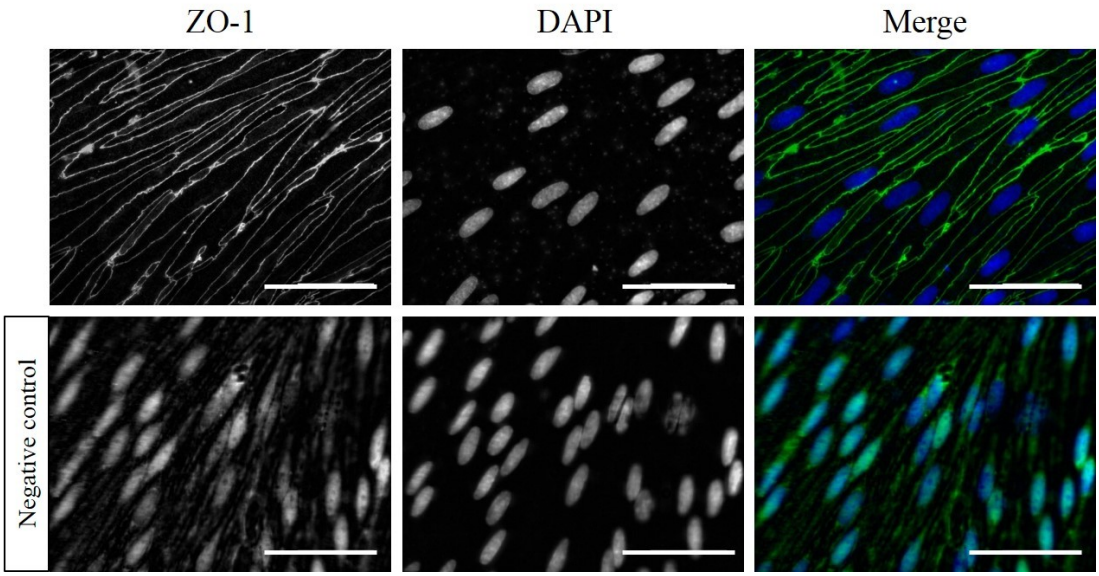

Primary culture of rBECs on type I collagen-coated Transwell® insert was used after being cultured for 8-10 days. Cells were fixed with 4% (w/v) paraformaldehyde and 4% (w/v) sucrose in PBS and were permeablised with 0.1% Triton®-X 100 prior applications of antibodies. Rat brain endothelial cell monolayers were probed for ZO-1 (green) and DAPI nuclei stain (blue). The monolayer was also stained as a negative control for rabbit IgG (green) and DAPI nuclei stain (blue). Digital pictures were taken with a Coolsnap ES camera through MetaVue software following visualization with an Olympus BX51 microscope. Scale bars represent 50 μm (600x magnification).

Figure 3.8 Immunocytochemistry of primary rat astrocytes

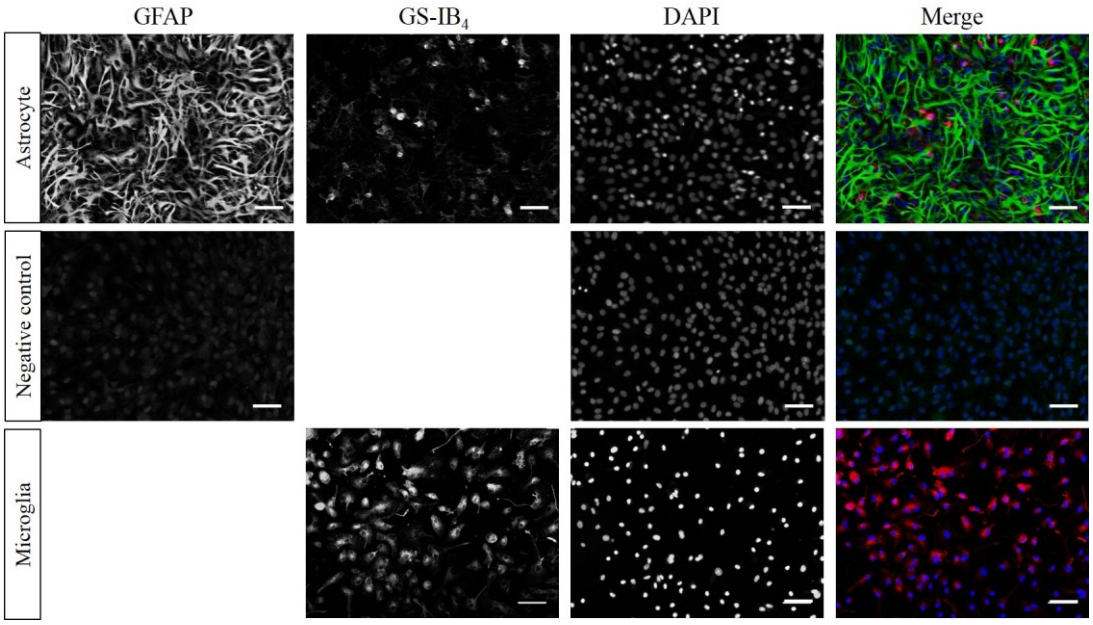

Cryopreserved rat astrocytes were seeded onto coverslips and were grown to confluent for 5 days. Cells were fixed with 4% (w/v) paraformaldehyde and 4% (w/v) sucrose in PBS and were permeablised with 0.1% (v/v) Triton®-X 100 prior applications of antibodies. Culture of rat astrocytes was triple-stained for GFAP (green), isolectin GS-IB_4 (red) and DAPI nuclei stain (blue). Images in the second row represent negative control for GFAP staining; rabbit IgG (green) and DAPI (blue). Images in the third row represent microglia culture stained for isolectin GS-IB_4 (red) and DAPI (blue). Digital pictures were taken with a Coolsnap ES camera through MetaVue software following visualization with an Olympus BX51 microscope. Scale bars represent 50 μm (200x magnification).

3.3.4 Transendothelial electrical resistance measurement of the rat *in vitro* blood-brain barrier model

The transendothelial electrical resistance is a reflection of the integrity of the brain endothelial cell monolayers and, unlike the others methods outlined above, the process of TEER measurement is simple and can be done on live cells. On day 0, the TEER of rBECs freshly plated on Transwell® inserts was 0 $\Omega \cdot cm^2$, the same level as empty inserts, i.e. inserts conatining no cells (Figure 3.9). Rat brain monolayers gradually developed TEER over time, with TEER reaching a peak on DIV4 of 75.5 ± 3.4 $\Omega \cdot cm^2$ diminishing to 43.7 ± 5.8 $\Omega \cdot cm^2$ at DIV 5.

Methods to increase TEER such as serum removal, addition of CPT-cAMP and RO 20-1724 and addition of hydrocortisone were tested with this model (Figure 3.10). Serum removal resulted in detachment of rBECs from Transwell® inserts. Cell monolayers grown in medium containing 180 μg/ml hydrocortisone had a significantly higher TEER (82.7 ± 6.8 $\Omega \cdot cm^2$) than cell monolayers grown in hydrocortisone-free medium (55.1 ± 3.3 $\Omega \cdot cm^2$). Addition of 250 μM CPT-cAMP and 17.5 μM RO-201724 to growth medium did not significantly increase the TEER (62.0 ± 0.01 $\Omega \cdot cm^2$).

Besides increasing TEER, hydrocortisone is a well-known steroid hormone which has anti-inflammatory effects. To test whether hydrocortisone has any effect on IL-1β-induced CINC-1 release, different concentration of IL-1β were added to rBECs grown on type I collagen coated 96-well plates in growth media with or without hydrocortisone. The results showed that hydrocortisone (at both 180 and 500 ng/ml did not dramatically modify CINC-1 release (Figure 3.11).

Figure 3.9 Transendothelial electrical resistance of primary rat brain endothelial cell monolayer grown on rat tail collagen-coated Transwell® inserts

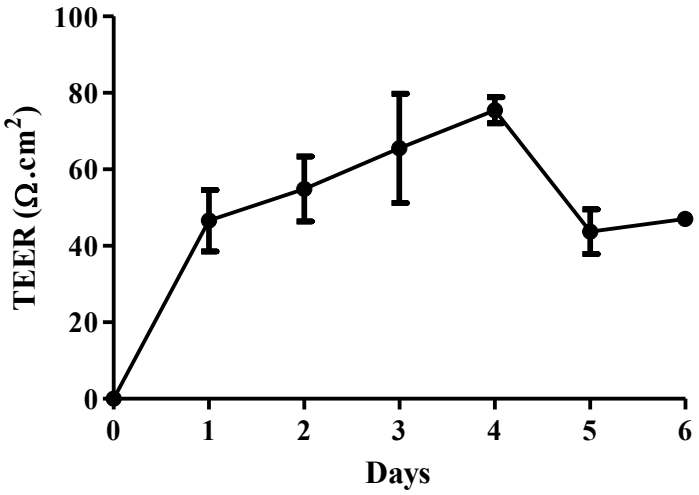

TEER measurement was performed daily using EVOM Epithelium Voltohmmeter electrodes for 6 days. TEER of rBEC monolayer increase until reaching a peak on day 4. Data are shown as mean ± SD. TEER data were obtained from three individual rBEC cultures.

Figure 3.10 Transendothelial electrical resistance of the rat *in vitro* blood-brain barrier model maintained in growth medium supplemented with CPT-cAMP and RO 20-1724 or hydrocortisone

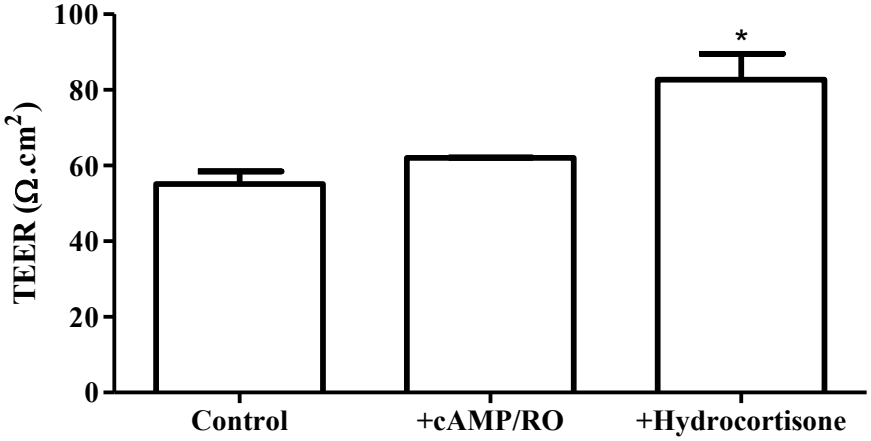

Cells were maintained in growth medium (Control) or growth medium supplemented with 180 mg/ml hydrocortisone (+Hydrocortisone) until confluent. CPT-cAMP and RO 20-1724 (+cAMP/RO) were added to the medium and cells incubated for at least 24 hours. TEER measurement was performed using EVOM Epithelium Voltohmmeter electrodes on day 8. TEER data were obtained from two independent rBEC cultures. Data were statistically analysed using Prism version 5 and are shown as mean ± SD. One-way ANOVA and Bonferroni post-hoc tests were applied to compare all data with control. All analysed data were considered statistically significant when $p<0.05$ (*=$p<0.05$).

Figure 3.11 Hydrocortisone did not alter interleukin-1β-induced cytokine-induced neutrophil chemoattractant-1 release

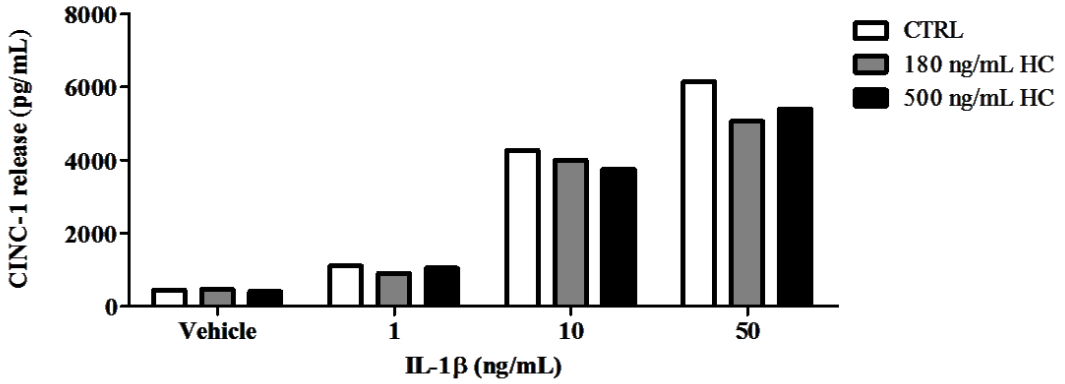

Rat brain endothelial cells were grown on rat tail type I collagen coated 96-well plates. Cells were treated with different dose of IL-1β (1, 10 and 50 ng/ml) or vehicle. The concentration of CINC-1 in cell culture medium was measured using ELISA. Data were obtained from a single culture.

3.3.5 Cytokine-induced neutrophil chemoattractant-1 release following oxygen glucose deprivation and interleukin-1β treatment

The brain requires a constant supply of oxygen and glucose to maintain its normal functions and remain viable. Restriction of the supply of oxygen and glucose, characteristics associated with stroke, induces a cascade of events which lead to neuronal cell death. Inflammation in the brain, also associated with stroke, is one of the main factors that induces brain damage in many *in vivo* models of acute brain injury. The proinflammatory cytokine, IL-1β is a key contributor to the brain damage following acute brain injury and release of IL-1β can induce brain endothelial cell activation i.e. release of chemoattractant proteins and expression of cell adhesion molecules. Therefore, it is extremely important to establish the effects of OGD and IL-1β on the activation of the endothelial cells of our *in vitro* rat BBB model. In initial studies we first measured the level of CINC-1, a chemoattractant protein know to be released by brain endothelial cells following OGD and IL-1β treatment.

The *in vitro* BBB model was treated with vehicle, 1, 10, 50 and 100 ng/ml IL-1β. Following 4 and 18 hours IL-1β treatment, the media from apical and basolateral side of Transwell® inserts were collected and analysed for CINC-1 concentration. The results showed CINC-1 release was increased significantly in response to 10, 50 and 100 ng/ml IL-1β compared to vehicle-treated control at both 4 hours (Figure 3.12A) and 18 hours time points (Figure 3.12B). At 4 hours, CINC-1 concentration in response to IL-1β reached a plateau at 50 ng/mL. At 18 hours following IL-1β treatment, CINC-1 release was increased in an IL-1β concentration-dependent manner. The concentration of 10 ng/ml of IL-1β was applied throughout the experiments.

The effect of OGD/IL-1β on CINC-1 release has also been assessed. Both IL-1β treatment (229.7 ± 39.0 pg/ml) and the combination of OGD and IL-1β (309.2 ± 78.5 pg/ml) significantly increased CINC-1 release compared to vehicle control (46.4 ± 26.9 pg/ml). There was no such effect observed with OGD alone (96.0 ± 65.7 pg/ml) (Figure 3.13).

Figure 3.12 Cytokine-induced neutrophil chemoattractant-1 release by the *in vitro* blood-brain barrier model following interleukin-1β treatment

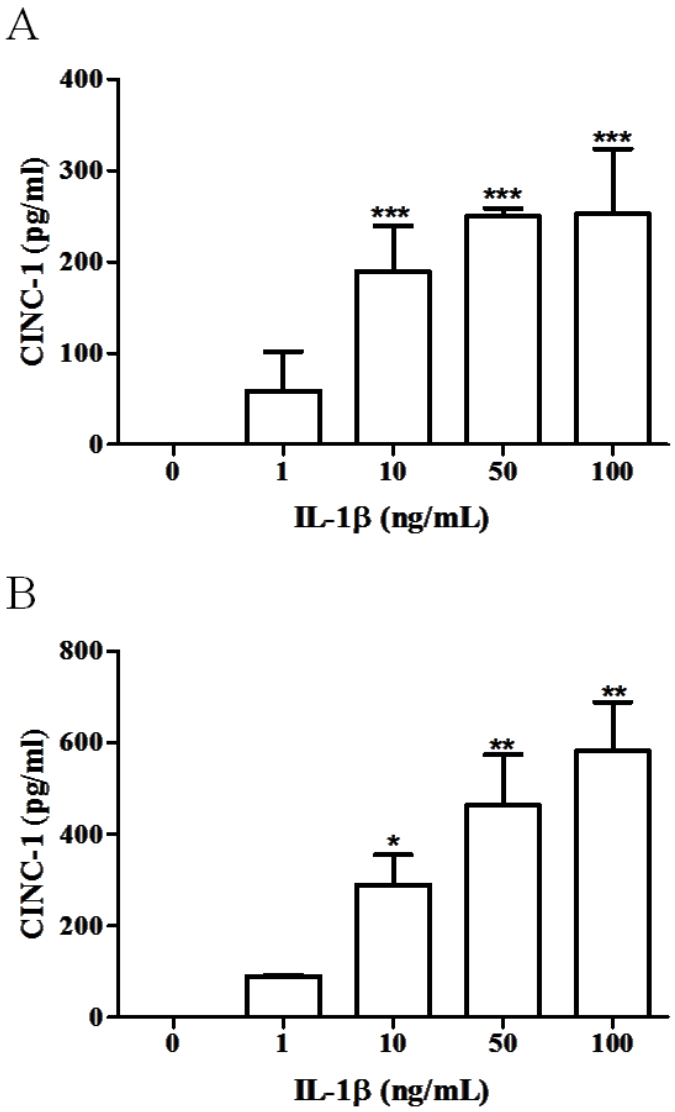

rBECs were grown on Transwell® inserts until confluent. Cells were treated with IL-1β at 1, 10, 50 and 100 ng/ml for 4 hours (A) and 18 hours (B). The concentration of CINC-1 in cell culture medium was measured using ELISA. Data are shown as mean ± SD. Data were obtained from three independent cultures. One-way ANOVA and Bonferroni post-hoc tests were applied to compare all data with vehicle control (IL-1β at 0 ng/ml). All analysed data were considered statistically significant when $p<0.05$ (*=$p<0.05$; **=$p<0.01$; ***=$p<0.001$).

Figure 3.13 Cytokine-induced neutrophil chemoattractant-1 release by the *in vitro* blood-brain barrier model following oxygen-glucose deprivation and 18 hours reperfusion with or without interleukin-1β treatment.

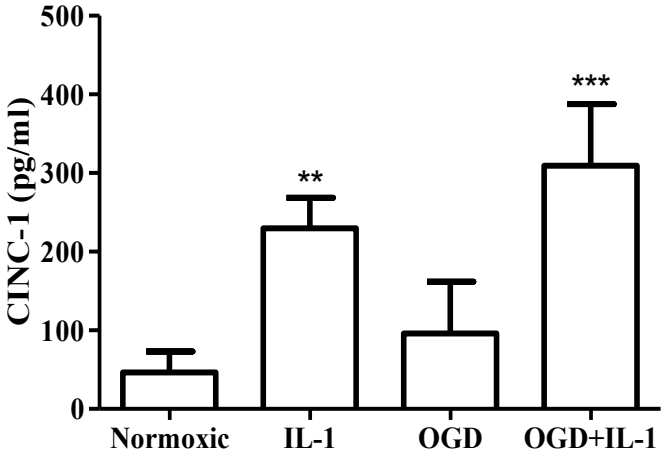

Culture supernatants were collected from the *in vitro* model of BBB following normoxia (normoxic), 18 hours IL-1β treatment (IL-1), 2.5 hours OGD and 18 hours reperfusion (OGD) and 2.5 hours OGD followed by 18 hours reperfusion and IL-1β treatment (OGD+IL-1). The concentration of CINC-1 in cell culture medium was measured using ELISA. Data are shown as mean ± SD from three independent cultures. One-way ANOVA and Bonferroni post-hoc tests were applied to compare all data with normoxic control. All analysed data were considered statistically significant when $p<0.05$.(**=$p<0.01$; ***=$p<0.001$).

3.3.6 Effects of oxygen glucose deprivation and interleukin-1 on expression and localisation of tight junction proteins

Under normal physiological conditions, brain endothelial cells express high levels of tight junction proteins including, occludin, claudin-5 and ZO-1, at their apical side. Tight junction proteins seal the inter-cell junction and prevent, or restrict, the passage of substances between blood and brain compartments. Loss of the expression or change in localisation (from plasma membrane to cytoplasm) of the endothelial cell tight junction proteins has been reported following acute injury *in vivo* and OGD or inflammatory conditions *in vitro*. Such changes are associated with a breakdown in the highly restrictive nature of the BBB and could therefore have serious consequences in terms of protection of the central nervous system. Here we investigate the effects of OGD and the proinflammatory cytokine IL-1β on expression of key tight junction proteins in our *in vitro* rat BBB model.

Expression and localisation of the tight junction proteins, occludin and ZO-1 following IL-1β/OGD were determined using immunocytochemistry. The cells were observed:

i) immediately following 2.5 hours OGD (2.5+0)

ii) following 2.5 hours OGD and 4 hours reperfusion (2.5+4)

iii) following 2.5 hours OGD and 18 hours reperfusion (2.5+18)

Immediately after 2.5 hours OGD (Figure 3.14 and 3.15), cells did not significantly display any differences compared to normoxic control in term of cell circularity and levels and localisations of occludin and ZO-1.

However, following 2.5 hours OGD and 4 hours reperfusion (2.5+4), occludin in vehicle-treated rBECs localised along the cell-cell contact zone, whereas in cells that underwent IL-1β treatment, OGD and OGD with IL-1β treatment, occludin localised throughout the cell cytoplasm and membrane (Figure 3.16). Discontinuous distribution of occludin at the cell-cell contacts could also be observed following IL-

1β treatment, OGD and OGD with IL-1β treatment. Cells that underwent IL-1β treatment, OGD and OGD with IL-1β treatment displayed ZO-1 at the cell membrane and cytoplasm (Figure 3.17). Following 4 hours IL-1β treatment and 2.5 hours OGD and 4 hours reperfusion, cells became rounder compared to normoxic vehicle-treated control (Figure 3.18A). The intensity of occludin (Figure 3.18B) and ZO-1 (Figure 3.18C) fluorescence in rBECs was not significantly different from fluorescence in cells exposed to vehicle, IL-1β, OGD and OGD with IL-1β. To assess the localisation shift of occludin and ZO-1 from plasma membrane to cytoplasm, the ratio of the mean cytoplasmic intensity to the mean membranous intensity (c/m) was calculated. The result showed that c/m of ZO-1 in cells subjected to IL-1β treatment and OGD with IL-1β treatment was higher than vehicle control (Figure 3.18D). In addition, c/m of occludin in culture exposed to IL-1, OGD and OGD with IL-1β was higher than cells exposed to vehicle (Figure 3.18E).

Following 2.5 hours of OGD and 18 hours of reperfusion (Figure 3.19, 3.20 and 3.21), cells did not display any differences compared to normoxic control in term of cell circularity and levels and localisations of occludin and ZO-1.

Figure 3.14 Immunocytochemistry of occludin and ZO-1 in rat brain endothelial cell monolayers following 2.5 hours of oxygen-glucose deprivation.

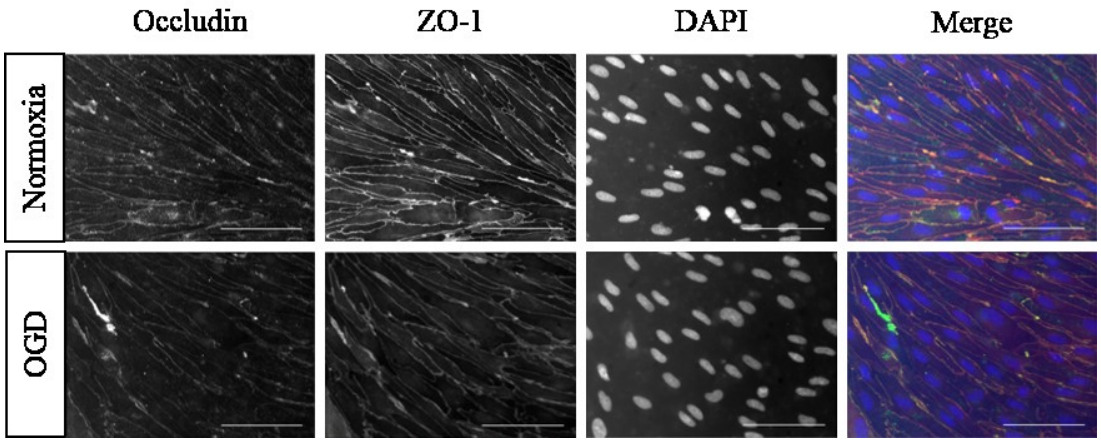

Primary cultures of rBECs on type I collagen-coated Transwell® inserts were used after 2.5 hours OGD. Cells were fixed with 4% (w/v) paraformaldehyde and 4% (w/v) sucrose in PBS and were permeablised with 0.1% (v/v) Triton®-X 100 prior applications of antibodies. Rat brain endothelial cell monolayers were probed for occludin (green), ZO-1 (red) DAPI nuclei stain (blue). Digital pictures were taken with a Coolsnap ES camera through MetaVue software following visualization with an Olympus BX51 microscope. Scale bars represent 50 μm (600x magnification).

Figure 3.15 Rat brain endothelial cell monolayers following 2.5 hours oxygen-glucose deprivation

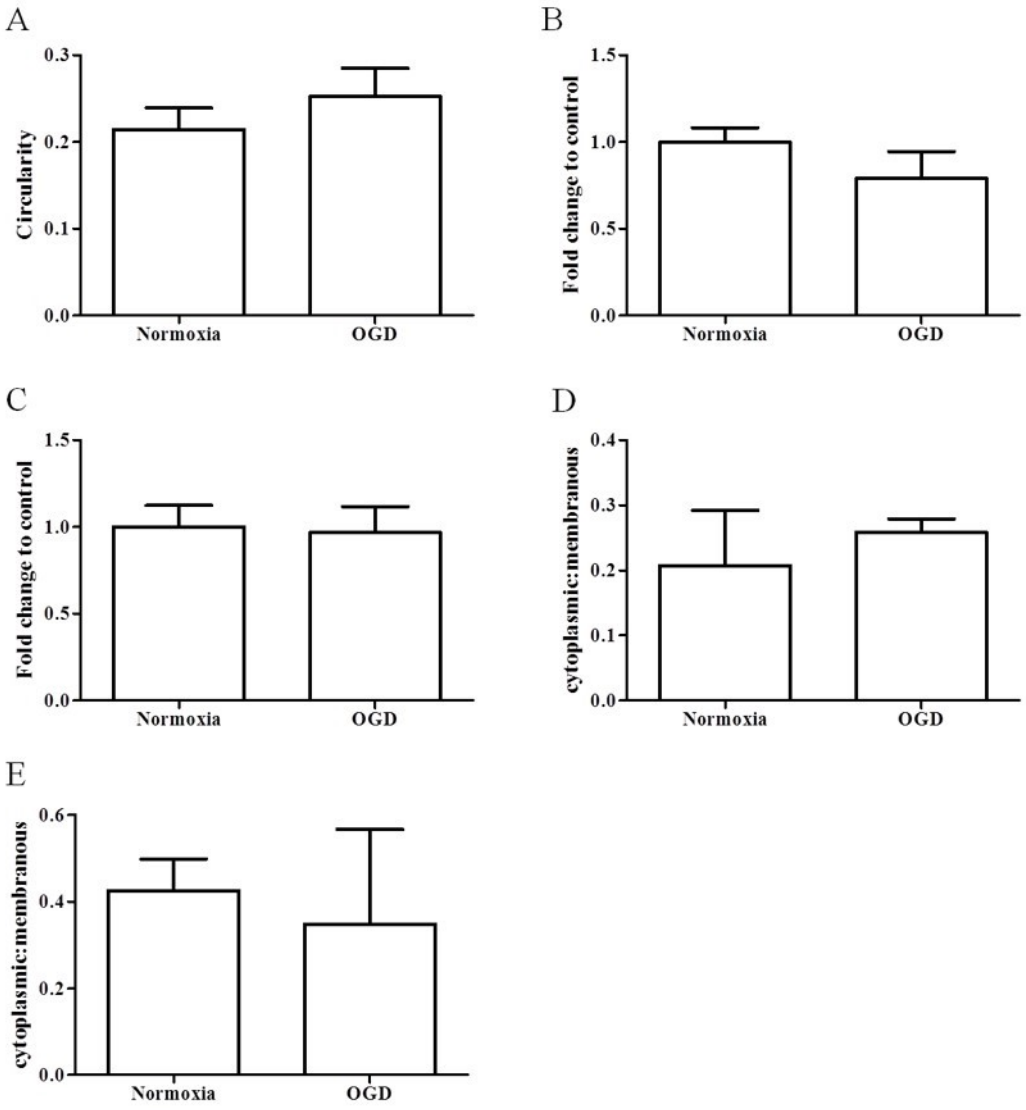

Primary culture of rBECs on type I collagen-coated Transwell® inserts was used after 2.5 hours OGD. Immunocytochemical images were analysed with ImageJ. Circularity (A), intensity of ZO-1 (B), intensity of occludin (C), ratio of mean cytoplasmic intensity to mean membranous intensity of ZO-1 (D) and occludin (E) were shown as mean ± SD from three independent cultures. Unpaired t-test was applied to compare all data with normoxic control. All analysed data were considered statistically significant when $p<0.05$.

Figure 3.16 Localisation of occludin in rat brain endothelial cell monolayer following 2.5 hours of oxygen-glucose deprivation and 4 hours reperfusion with or without interleukin-1β treatment

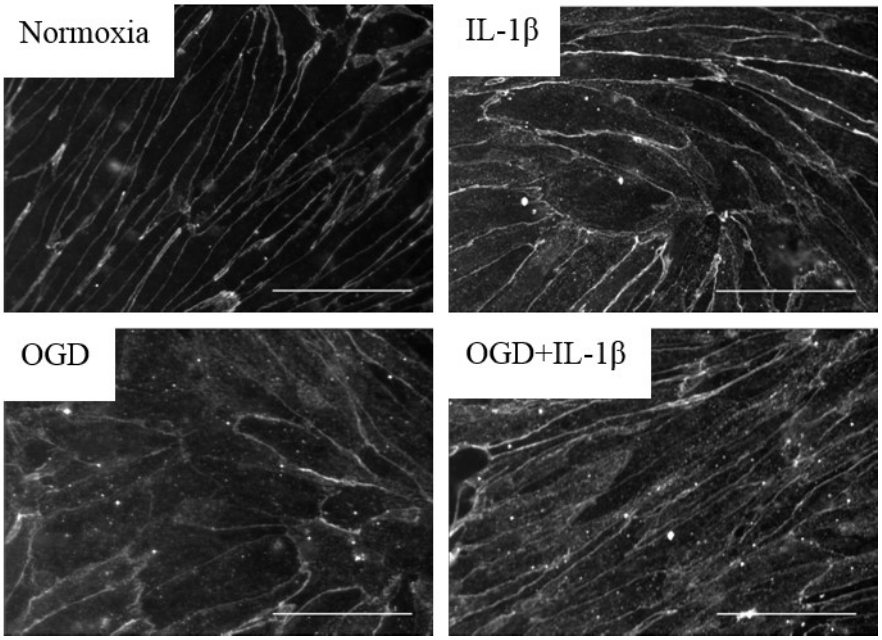

Primary culture of rBECs on type I collagen-coated Transwell® inserts was used after 2.5 hours OGD and 4 hours repurfusion with or without IL-1β treatment. Cells were fixed with 4% (w/v) paraformaldehyde and 4% (w/v) sucrose in PBS and were permeablised with 0.1% (v/v) Triton®-X 100 prior to applications of mouse anti-occludin antibody. Digital pictures were taken with a Coolsnap ES camera through MetaVue software following visualization with an Olympus BX51 microscope. Immunofluorescence microscopy images showed rBECs undergone normoxia, IL-1β for 4 hours (IL-1β), 2.5 hours OGD and 4 hours reperfusion (OGD), 2.5 hours OGD and 4 hours reperfusion with IL-1β (OGD+IL-1β). Scale bar represents 100 μm (600x magnification).

Figure 3.17 Localisation of ZO-1 on rat brain endothelial cell monolayer following 2.5 hours of oxygen-glucose deprivation and 4 hours reperfusion with or without interleukin-1β treatment.

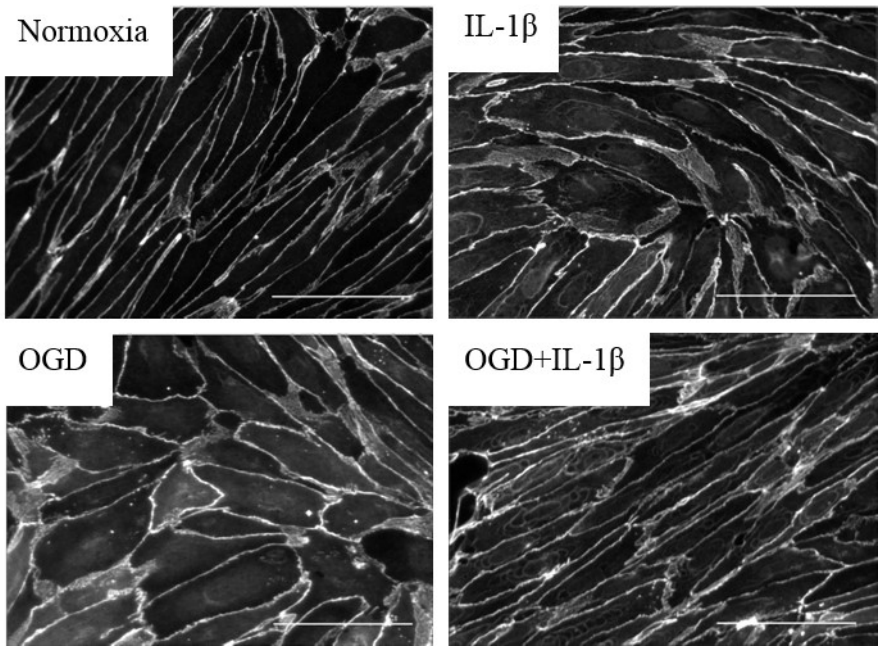

Primary culture of rBECs on type I collagen-coated Transwell® inserts was used after 2.5 hours OGD and 4 hours repurfusion with or without IL-1β treatment. Cells were fixed with 4% (w/v) paraformaldehyde and 4% (w/v) sucrose in PBS and were permeablised with 0.1% Triton®-X 100 prior to applications of rabbit anti-ZO-1 antibody. Digital pictures were taken with a Coolsnap ES camera through MetaVue software following visualization with an Olympus BX51 microscope. Immunofluorescence microscopy images of ZO-1 expression in rBECs subjected to normoxic condition, IL-1β for 4 hours (IL-1β), 2.5 hours OGD and 4 hours reperfusion (OGD) and 2.5 hours OGD and 4 hours reperfusion with IL-1β (OGD+ IL-1β). Scale bar represents 100 μm (600x magnification).

Figure 3.18 Rat brain endothelial cell monolayer following 2.5 hours oxygen-glucose deprivation and 4 hours reperfusion with or without interleukin-1β treatment

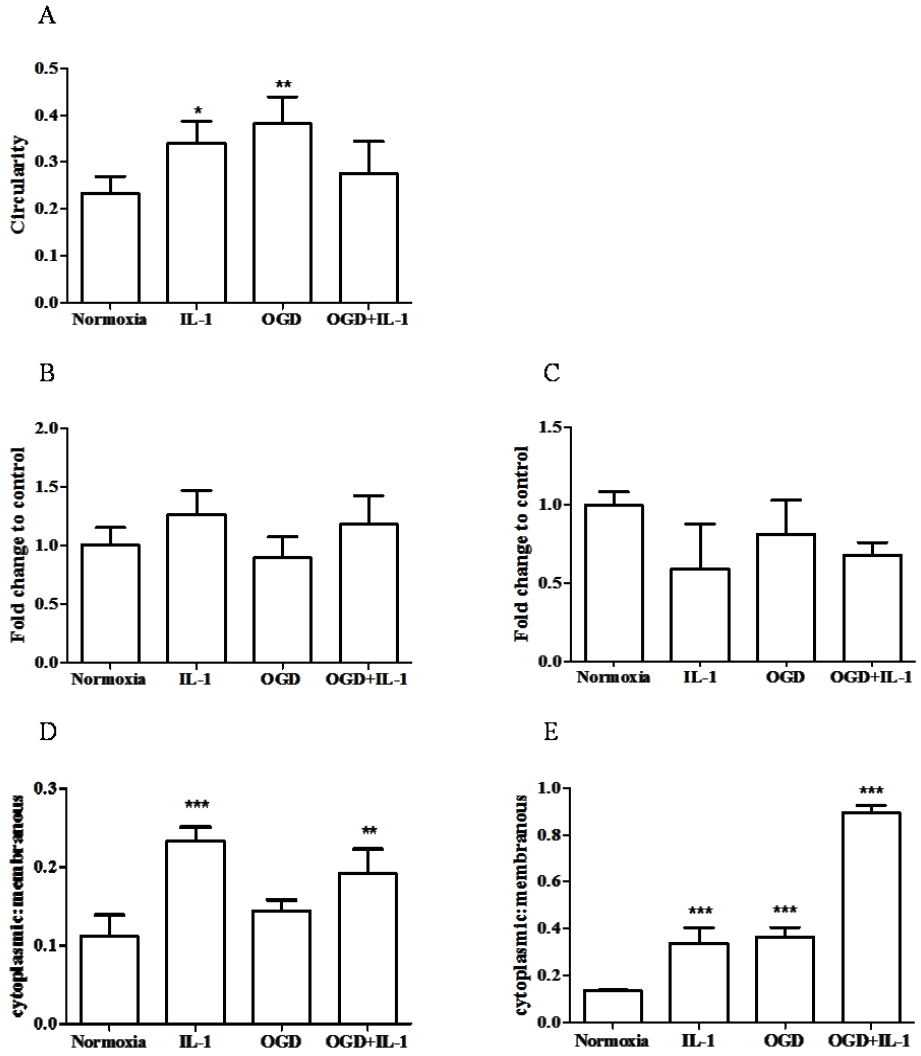

Primary culture of rBECs on type I collagen-coated Transwell® inserts subjected to normoxia, IL-1β, OGD and OGD+IL-1 at 2.5+4 time point. Immunocytochemical images for tight junction proteins were analysed with ImageJ. Circularity (A), intensity of ZO-1 fluorescence (B) and intensity of occludin fluorescence (C) ratio of mean cytoplasmic intensity to mean membranous intensity of ZO-1 (D) and occludin (E). Data are shown as mean ± SD. from three independent cultures. Data were statistically analysed using one-way ANOVA and Bonferroni post-hoc tests compared to normoxic control. All analysed data were considered statistically significant when $p<0.05$ (*=$p<0.05$; **=$p<0.01$; ***=$p<0.001$).

Figure 3.19 Localisation of occludin in rat brain endothelial cell monolayer following 2.5 hours of oxygen-glucose deprivation and 18 hours reperfusion with or without IL-1β treatment

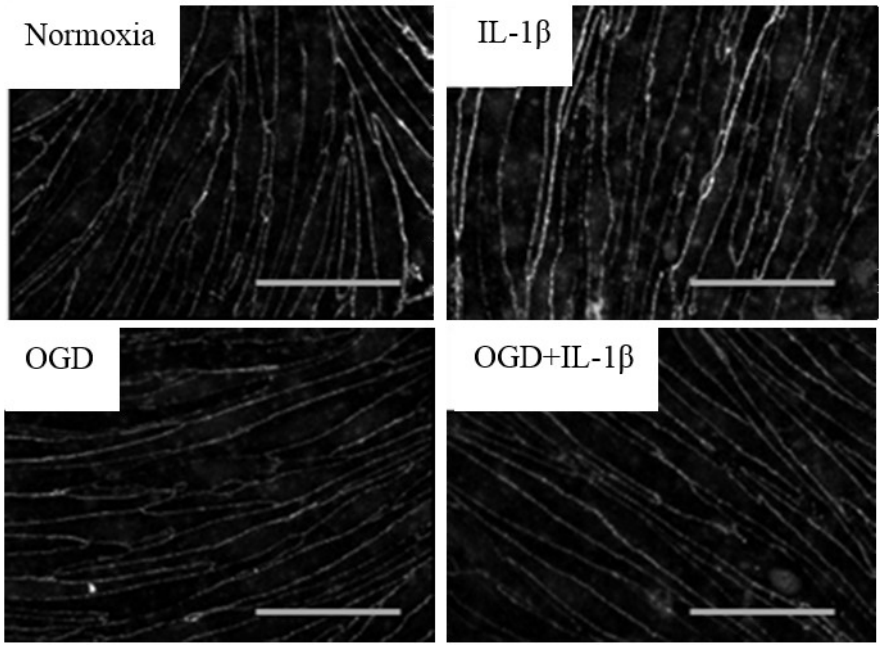

Primary cultures of rBECs on type I collagen-coated Transwell® inserts were used after 2.5 hours OGD and 18 hours repurfusion with or without IL-1β treatment. Cells were fixed with 4% (w/v) paraformaldehyde and 4% (w/v) sucrose in PBS and were permeablised with 0.1% Triton®-X 100 prior to applications of mouse anti-occludin antibody. Digital pictures were taken with a Coolsnap ES camera through MetaVue software following visualization with an Olympus BX51 microscope. Immunofluorescence microscopy images of occludin expression in rBECs subjected to normoxia, IL-1β for 18 hours (IL-1β), 2.5 hours OGD and 18 hours reperfusion (OGD), 2.5 hours OGD and 18 hours reperfusion with IL-1β (OGD+ IL-1β). Scale bar represents 100 μm (600x magnification).

Figure 3.20 Localisation of ZO-1 of rat brain endothelial cell monolayer following 2.5 hours of oxygen-glucose deprivation and 18 hours reperfusion

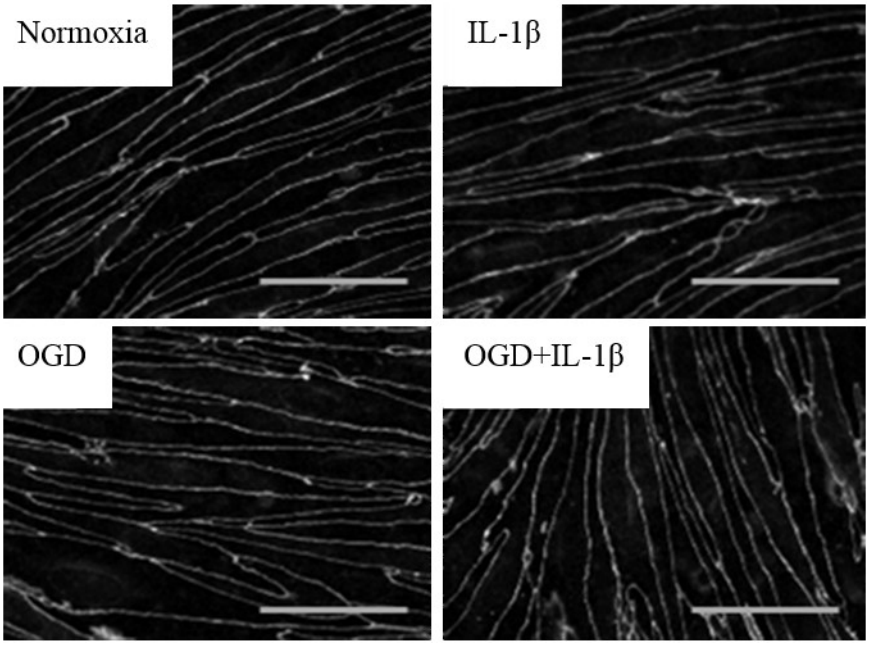

Primary cultures of rBECs on type I collagen-coated Transwell® inserts were used after 2.5 hours OGD and 18 hours repurfusion with or without IL-1β treatment. Cells were fixed with 4% (w/v) paraformaldehyde and 4% (w/v) sucrose in PBS and were permeablised with 0.1% (v/v) Triton®-X 100 prior to applications of rabbit anti-ZO-1 antibody. Digital pictures were taken with a Coolsnap ES camera through MetaVue software following visualization with an Olympus BX51 microscope. Immunofluorescence microscopy images of ZO-1 expression in rBECs subjected to normoxia, IL-1β for 18 hours, 2.5 hours OGD (IL-1β) and 18 hours reperfusion (OGD), 2.5 hours OGD and 18 hours reperfusion with IL-1β (OGD+IL-1β). Scale bar represents 100 μm (600x magnification).

Figure 3.21 Rat brain endothelial cell monolayer following 2.5 hours oxygen-glucose deprivation and 18 hours reperfusion

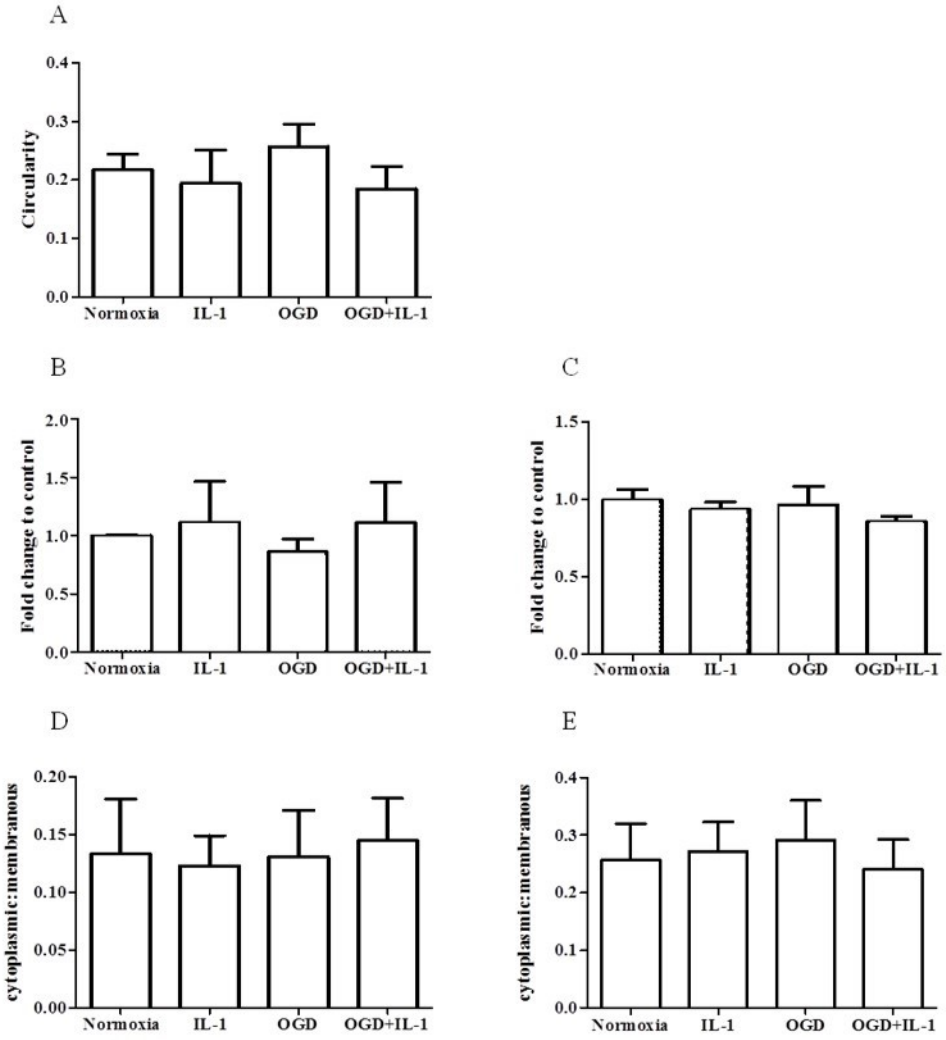

Primary culture of rBECs on type I collagen-coated Transwell® inserts underwent normoxic (Normoxia), IL-1β for 18 hours (IL-1), 2.5 hours OGD and 18 hours reperfusion (OGD) and 2.5 hours OGD and 18 hours reperfusion with IL-1β (OGD+IL-1). Immunocytochemical images for tight junction proteins were analysed with ImageJ. Circularity (A), intensity of ZO-1 (B) and intensity of occludin (C) ratio of mean cytoplasmic intensity to mean membranous intensity of ZO-1 (D) and occludin (E) were shown as mean ± SD from three independent cultures. Data were statistically analysed using one-way ANOVA and Bonferroni post-hoc tests All analysed data were considered statistically significant when $p<0.05$ (*=$p<0.05$; **=$p<0.01$; ***=$p<0.001$).

3.4 Discussion

The aim of this thesis was to investigate the effect of conditions that resemble acute brain injury on brain endothelial cell ECM protein expression *in vitro*, thus initially establishing a suitable model for the whole project was necessary. The *in vitro* system which contains selected cell types allows us to manipulate factors of interest, to study the effect of changing the environment and to investigate cellular responses to such environmental changes. When establishing an *in vitro* BBB model to be used to study the effects of OGD and IL-1β (associated with acute brain injury *in vivo*), we had to consider whether the model could maintain BBB properties and also show signs of damage or inflammation following OGD or IL-1β treatment. An *in vitro* 2D BBB model composed of brain endothelial cells grown on Transwell® inserts and glial cells grown on the well surface is suitable for investigating the effects of various treatments on brain endothelial cell activation and response. The *in vitro* BBB model is commonly acquired from primary mouse (Weidenfeller et al., 2005, Song and Pachter, 2003, Ohtsuki et al., 2008), rat (Perriere et al., 2005, Abbott et al., 1992, Arthur et al., 1987, Calabria et al., 2006, Nakagawa et al., 2009, Ohtsuki et al., 2007), pig (Nitz et al., 2003, Cantrill et al., 2012, Jeliazkova-Mecheva and Bobilya, 2003, Rubin et al., 1991) and cow (Bowman et al., 1983, Deli et al., 1995, Gaillard et al., 2001) tissues. Our laboratory has an access to porcine, rat and mouse BBB models. Isolation of pBECs gave a higher cell yield and was also less expensive compared to rBECs mainly because a pig brain is larger than a rat brain. Also the TEER of the *in vitro* porcine BBB (~2000 $\Omega \cdot cm^2$) (Cantrill et al., 2012) is comparable to TEER of the BBB *in vivo* whereas the rodent BBB models generally demonstrate relatively lower TEER (~400 $\Omega \cdot cm^2$) (Nakagawa et al., 2009). The advantages of rodent models are that they are well-characterised and most of the specific antibodies and reagents are commercially available. Moreover, genetically engineered animals can be generated for further experiments. The BBB model from human tissue is also in use nowadays (Siddharthan et al., 2007, Pardridge et al., 1985, Cordon-Cardo et al., 1989). However, human brain tissue is obtained from surgical material thus availability is very restricted. There is also a risk of human-to-human infection when using human brain tissue.

The process of endothelial cell isolation involves enzyme digestion and mechanical disintegration of brain tissue can and may cause cell damage and a change in cellular properties. Therefore, we first investigated whether cells obtained using the cell isolation method maintained their brain endothelial cell and astrocytic phenotypes. First, we set up the *in vitro* model of the BBB composed of pBECs and an astrocytic cell line. Initially, we obtained capillary fragments which later attached to type I collagen coated plates. Cells growing from the capillary fragments displayed a tapered-shape with pointed ends indicating endothelial morphology (Cantrill et al., 2012, Abbott et al., 1992). For rBECs, the initial capillary fragments had a beads-on-a-string like appearance. Cells then grew out from them, proliferated and occupied the empty space on the culture plates. Rat brain endothelial cells also displayed a spindle-shaped morphology. Immunocytochemistry revealed that more than 99% of rBECs in the culture were positive for vWF, a specific endothelial cell marker. This indicated that the rBEC culture was of a high purity. Since the meninges were totally removed during the dissection step, we obtained endothelial cells derived from brain microvessels that form the BBB. Brain endothelial cells express the P-glycoprotein (P-gp) efflux transporter at high levels whereas the expression of this transporter in common contaminating cells is relatively low (Jette et al., 1993, Cordon-Cardo et al., 1989, Beaulieu et al., 1997). Many cytotoxic P-gp substrates have been tested for culture purification purpose since brain endothelial cells should theorectically be more resistant to toxicity of P-gp substrates than other contaminating cells (Perriere et al., 2005). Adding puromycin, which is a cytotoxic P-gp substrate, to brain endothelial cells in culture has been shown to effectively remove contaminating cells (Perriere et al., 2005, Calabria et al., 2006) and this approach was used in this thesis. Primary rat brain endothelial cells expressed the tight junction proteins, occludin and ZO-1 at the cell margin where cells contacted their neighbours. This indicated that cells retained one of the most important *in vivo* BBB phenotypes. For pBECs, we did not validate the model by immunostaining. However, validation of the model we used has been published by our group (Cantrill et al., 2012). Endothelial cell isolations obtained by our method had high purity and maintained endothelial cells their BBB properties such as spindle-shaped morphology, expression of many endothelial cell markers and barrier integrity comparable to that *in vivo*.

Many factors such as the source of endothelial cells, purity of brain endothelial cells, cellular components, medium supplementation, etc. can affect the TEER of the BBB model. As mentioned above, cerebral endothelial cell monolayer generated from porcine and bovine sources demonstrate relatively high TEER compared to those from rodents. Adding puromycin alone or in conjunction with other supplements to the culture has been reported to improve barrier properties of *in vitro* BBB models (Cantrill et al., 2012, Perriere et al., 2005, Calabria et al., 2006). Supplementation with hydrocortisone (Forster et al., 2008, Weidenfeller et al., 2005, Perrière et al., 2007) or CPT-cAMP and RO 20-1724 (Cantrill et al., 2012, Perrière et al., 2007) has also been reported to raise TEER. In the literature, the TEER of pBEC monolayers co-cultured with astrocytes range from approximately 100 to 400 $\Omega.cm^2$ without hydrocortisone, CPT-cAMP and RO 20-1724 supplementation or serum depletion (Rubin et al., 1991, Franke et al., 2000, Jeliazkova-Mecheva and Bobilya, 2003). The TEER of our *in vitro* porcine BBB model was approximately 200 $\Omega.cm^2$ which was moderate compared to the TEER reported by other laboratories. The TEER of our rat model was comparable to rat BBB model reported by others (Nakagawa et al., 2009, Perriere et al., 2005, Wilhelm et al.)

The main reason we initially choose a porcine model to study ECM protein production by cerebral endothelial cells in culture was that the electron microscopy images of pBECs showed cell monolayers on a thin sheet-like structure, probably basal lamina (Cantrill et al., 2012). Therefore, we investigated whether pBECs produced basal lamina ECM molecules *in vitro*. By western blotting, we showed pBECs produced cellular fibronectin, which is one of the endothelial ECM components in the basal lamina. Mass spectrometry analysis revealed the presence of keratins (from human) and serum albumin (from cell culture medium) which were common contaminants which could not be eliminated. Other proteins detected were mainly cytoskeletal proteins including myosin, beta actin, keratin, tubulin, vimentin and filamin probably debris from dead/detached cells or were attached to ECM molecules. Mass spectrometry detected fibronectin and vitronectin which were either ECM proteins from the basal lamina or from bovine serum in the cell culture medium. Fibronectin has been found to be expressed in the brain vasculature *in vivo*

(Hamann et al., 1995, Krum et al., 1991). The findings that fibronectin was produced by pBECs in culture is important since it confirms the pBECs used in our *in vitro* BBB model retain characteristics of brain endothelial cells *in vivo*. This finding is also consistent with previous studies reporting expression and production of fibronectin by cerebral endothelial cell culture *in vitro* (Tilling et al., 2002, Webersinke et al., 1992). Laminins and type IV collagen are known to be major components of brain capillary ECM *in vivo* (Krum et al., 1991, Kleppel et al., 1989, Venstrom and Reichardt, 1993, Sixt et al., 2001, Hallmann et al., 2005, Tilling et al., 2002, Kühn, 1995, Hamann et al., 1995). Type IV collagen, and laminin were also reported to be expressed and produced by brain endothelial cell culture *in vitro* (Tilling et al., 2002, Webersinke et al., 1992, Abbott et al., 1992). No main basal lamina components such as laminins or type IV collagen were detected reflecting that this method required development.

Tight junction proteins play a crucial role in maintaining BBB integrity and degradation of these proteins is a hallmark of BBB breakdown in many pathological states. OGD has been widely employed to induce *in vitro* injury to endothelial cells in culture. OGD has been reported to induce morphological changes (Xu et al., 2000), death (Keep et al., 2005, An and Xue, 2009, Lee et al., 2007, Yin et al., 2002), altered gene/protein expression (Xu et al., 2000) and loss of barrier integrity *in vitro* (Zehendner et al., 2012, Zhu et al., 2010). Many studies have linked the alteration of expression of tight junction protein with loss of BBB integrity (An and Xue, 2009, Andras et al., 2005, Bolton et al., 1998, Fischer et al., 2002, Forster et al., 2008, Hawkins et al., 2004, Hirase et al., 1997, Xu et al., 2012). However, the recent study by Krueger et al. (2013) challenged this idea. They found that expression of tight junction proteins did not correlate with BBB breakdown in an embolic stroke model (Krueger et al., 2013). Also, Weidenfeller et al. reported that morphology rather than expression of tight junction in brain endothelial cells influenced barrier properties of a mouse BBB model (Weidenfeller et al., 2005). In this thesis, morphological changes observed in rBECs following OGD/IL-1β treatment are consistent with what has been reported by other laboratories (Zehendner et al., 2012, Xu et al., 2000) suggesting an alteration of the barrier function. Our study also showed that OGD

and/or IL-1β treatment slightly reduced, but not significantly, the expression of occludin protein following 2.5 hours OGD and 4 hours reperfusion. Expression of ZO-1 following 4 hour IL-1β treatment was increased, but not significantly. Disappearance or diffused expression of ZO-1 protein (An and Xue, 2009, Zhu et al., 2010, Zehendner et al., 2012) and occludin (Liu et al., 2012a) at the cell-cell contact zone of the brain endothelial cells subjected to OGD has been reported previously. We did not find downregulation of occludin and ZO-1 proteins as reported by others. Instead, the localisation of occludin and ZO-1 in rBECs was changed from membranous to cytoplasm following OGD/IL-1β. This could possibly be due to intracellular transfer of proteins from the membrane and/or turnover of membrane protein and synthesis of new proteins.

A study by Zhang et al demonstrated that IL-1β activated human brain endothelial cells in culture and induced chemokine expression including CINC-1 (Zhang et al., 1999). Our findings also demonstrated treatment of rBECs in culture with IL-1β resulted in CINC-1 release from endothelial cells. Expression of chemokines was also reported to be induced by OGD (Zhang et al., 1999). However, in our studies, 2.5 hours of OGD and 4 or 18 hours of repurfusion did not significantly induce release of CINC-1 compared to control cells. A study by Chaitanya et al. demonstrated hypoxia upregulated VCAM-1 and E-selectin but not ICAM-1 and PECAM-1 *in vitro* (Chaitanya et al., 2012). Induction of monocyte chemoattractant protein-1 in a mouse BBB model by OGD and reperfusion is time-dependent (Leow-Dyke, 2012). These results suggest that OGD selectively and time-dependently induced expression of proteins by the BBB model. Activation of rBECs can be investigated further at different timepoints of OGD and reperfusion. Also, the expression of other chemokines such as IL-8 or adhesion molecules such as ICAM-1, VCAM-1 and PECAM in the rBECs subjected to OGD would be interesting.

Chapter 4 Changes in brain endothelial extracellular matrix expression following injury

4.1 Introduction

In normal physiological conditions brain endothelial basal lamina is mainly composed of type IV collagen (Muellner et al., 2003, Uspenskaia et al., 2004) and laminins (Ji and Tsirka, 2012, Sixt et al., 2001) connected by entactin (Schittny and Yurchenco, 1989). Type IV collagen expressed by brain endothelial cells is trimeric, being composed of two type IV collagen α1 chains and one type IV collagen α2 chain. Laminin isoforms expressed by cerebral endothelial cells are mainly laminin-411 and laminin-511 (Sixt et al., 2001). In addition, fibronectin (Milner et al., 2008), thrombospondin (Webersinke et al., 1992) and proteoglycans (Garcia de Yebenes et al., 1999, Stone and Nikolics, 1995) are also associated with the brain vasculature. In pathological and inflammatory states of the brain there are changes in expression of ECM molecules in the basal lamina of the brain vasculature, including loss of laminin α4 in the inflamed capillaries with transmigrated leukocytes observed between endothelial and astrocytic basal lamina in EAE mice (Sixt et al., 2001). Loss of brain vessel-associated type IV collagen has been reported following traumatic brain injury (Muellner et al., 2003). and altered fibronectin protein expression was observed in the brains of mice that underwent hyperbaric hypoxia treatment (Milner et al., 2008). Changes in expression of ECM molecules have also been reported in *in vitro* experiments. Human intestinal epithelial cells in culture treated with inflammatory mediators, such as TNF-α and Interferon-γ, showed increased expression of several laminin mRNAs (Francoeur et al., 2004). Also, IL-6 has been shown to induce changes in expression of α1 collagen III, fibronectin and laminin mRNAs in bovine mesangial cells *in vitro* (Zoja et al., 1993).

In the previous chapter, we have shown that an *in vitro* rat BBB model comprising rBECs, grown on type I collagen-coated Transwell® inserts, and primary rat astrocytes in a non-contact co-culture manner displayed BBB properties and produced a network of cellular fibronectin. Abbott et al. (1992) demonstrated that rBECs also produced laminin in culture. To determine whether acute brain injury has any effect on expression of ECM components of the basal lamina in the brain

vasculature, we have investigated the expression of laminin α4 chain and cellular fibronectin in the brain of mice subjected to MCAO. We also investigated the effect of acute brain injury *in vitro* (represented by OGD/IL-1β treatment) on rBEC expression of ECM genes.

4.2 Materials and Methods

4.2.1 Cell culture

4.2.1.1 The rat blood-brain barrier model

Rat brain endothelial cells were isolated from rat brains as described in Section 2.2.1. Following cell detachment, rBECs were transferred to uncoated 6-well tissue-culture plastic plates. Primary rat astrocytes were isolated and cultured as described in Section 2.2.2. Primary rat astrocytes were grown on PDL-coated Transwell® inserts. The Transwell® inserts were then transferred into 6-well plates containing rBEC monolayers. Plates were maintained in a 5% CO_2 humidified incubator at 37 ˚C for 5 days before OGD/IL-1β treatment.

4.2.1.2 Primary rat skin fibroblasts

One- to three-day-old rat pups were sacrificed by cervical dislocation and decapitation. Skin was cleaned with 70% (v/v) ethanol. Limps were amputated and skin was cut longitudinally from the tail to the neck. Skin was peeled laterally and incubated with 0.25% (w/v) trypsin in Hanks' balanced salt solution without calcium and magnesium at 4 ˚C overnight. Dermis was separated from epidermis using forceps. Tissue was cut into 2 mm x 2 mm using surgical blade and placed onto Petri dishes with 1 cm gap between each piece of skin. In order to fix the tissue with the plastic surface, skin was left to dry in a laminar airflow hood for 1 hour. Tissue was maintained in DMEM supplemented with 9.09% (v/v) FBS, 100 units/ml Penicillin, 0.1 mg/ml Streptomycin in a 5 % CO_2 humidified incubator at 37 ˚C.

4.2.2 Immunohistochemistry

The methods of MCAO in the animal model of brain injury, brain collection and preparation of brain sections were adapted from Rodriguez-Grande et al. (2012). Sections of brains from mice that underwent 45 minutes of MCAO followed by either 48 hours or 6 days of reperfusion and the photographs of brain slides stained with cresyl violet were kindly provided by B. Rodriguez-Grande. Coronal brain sections were maintained at -20 °C in an antifreeze solution (30% (v/v) ethylene glycol and 20% (v/v) glycerol (Fisher Scientific, Loughborough, UK) in PBS) in a

24-well plate. Antifreeze solution was carefully removed and coronal sections of the brain were rinsed thoroughly with PBS. Brain sections were then incubated in 2% (v/v) normal donkey serum in primary diluent (0.3% (v/v) Triton-X-100 in PBS) for 1 hour at room temperature. The solution was carefully removed and primary antibodies (rabbit anti-mouse PECAM-1 antibody (Abcam, UK) at working concentration of 1:50, mouse anti-human cellular fibronectin (Abcam, UK) at the working dilution of 1:500 and rabbit anti-human laminin alpha 4 (Abcam, UK) at the working of 1:200) diluted in primary diluent were added to the brain slides and samples incubated overnight at 4 ˚C on an orbital shaker (60 rpm). Brains sections were then rinsed with PBS three times and incubated for 2 hour with Alexa Flour® 594 conjugated donkey anti-mouse IgG antibodies (Invitrogen, UK) and Alexa Flour® 488 conjugated donkey anti-rabbit IgG antibodies (Invitrogen, UK) both at the working dilution of 1:500 at room temperature. The solution was carefully removed and the sections were then washed with PBS three times. The brain sections were transferred onto glass slides and mounted using Prolong Gold antifade reagent with DAPI (Invitrogen, UK). The sections were analysed with an Olympus BX51 upright microscope using 10x/ 0.30 UPlan Fln, 20x/ 0.50 UPlan Fln, 40x/ 0.75 UPlan Fln and 60x/ 0.65-1.25 UPlan Fln (Ph 3) objectives and images captured using a Coolsnap EZ camera (Photometrics) through MetaVue Software (Molecular Devices). Specific band pass filter sets for DAPI, FITC and Texas Red were used to prevent bleed through from one channel to the next. Images were then processed and analysed using ImageJ (http://rsb.info.nih.gov/ij). The background intensity was subtracted in all studies. Five random areas of capillaries were selected and the mean fluorescence intensity was measured. Intensity data were statistically analysed using GraphPad Prism version 5 and are shown as mean ± SD. Student t-test was applied to compare all data obtained from at least 3 independent brains. All analysed data were considered statistically significant when $p<0.05$.

4.2.3 Immunocytochemistry

Rat brain endothelial cells grown on Transwell® inserts were fixed and stained as described in Section 2.4. The primary antibody used was mouse anti-human cellular fibronectin (Abcam, UK) at 1:200 dilution.

4.2.4 Reverse-transcriptase polymerase chain reaction (RT-PCR)

4.2.4.1 Isolation of total RNA and cDNA synthesis

rBECs were initially grown on type I collagen-coated tissue culture treated 6-well plates and then co-cultured with primary rat astrocytes grown on Transwell® inserts (rBECs were seeded onto the basolateral compartment instead of the apical compartment in order to increase cell growth area). RNA was isolated from rBECs using the ISOLATE RNA mini kit (Bioline, UK). The procedure was carried out at room temperature unless stated otherwise. Briefly, growth medium was aspirated from Transwell® inserts, 450 µl lysis buffer added and cells incubated for 3 minutes. The reagent was transferred to an Eppendorf tube and the tube centrifuged at 12000 x g for 1 minute. The supernatant was carefully transferred to an R1 spin column and the column centrifuged at 10000 x g for 1 minute at room temperature. The spin column was discarded and 450 µl 70% (v/v) ethanol was added to the filtrate. The solution was transferred to an R2 spin column housed in a new collection tube and centrifuged at 10000 x g for 2 minutes at room temperature. The filtrate was discarded. AR wash buffer, 500 µl, was added to the column and the tube centrifuged at 10000 x g for 1 minute at room temperature. The filtrate was discarded and 700 µl BR wash buffer added to the column. The tube was centrifuged at 10000 x g for 1 minute at room temperature. The spin column was transferred to a new collection tube and the tube was centrifuged at 10000 x g for 2 minutes at room temperature. The column was transferred into an elution tube, 30 µl RNase-free water was added to the column with incubation for 1 minute at room temperature. The tube was then centrifuged at 6000 x g. The isolated RNA was maintained on ice. The concentration and purity of RNA were determined by measuring the A260nm and A260nm/280nm ratio, respectively using Nanodrop (Thermo Scientific, UK). mRNA was reverse transcribed to cDNA using the cDNA synthesis kit (Bioline, UK). Total RNA, 0.5 µg,

was diluted with nuclease-free water to a volume of 12.5 µl. Oligo dT_{18}, 1 µl, was added to the total RNA and the sample incubated at 70 °C for 2 minutes. 5x reaction buffer, 4 µl, 1 µl dNTP mix, 0.5 µl ribonuclease inhibitor and 1 µl of Maloney murine leukaemia virus reverse transcriptase was added to the tube (final volume was 20 µl) and the tube incubated at 42 °C for 1 hour then 94 °C for 5 minutes. The cDNA-containing sample was diluted with nuclease-free water to 100 µl and kept at -70 °C until use.

4.2.4.2 Polymerase chain reaction (PCR)

The PCR primers were designed using PRIMER3 software (http://biotools.umassmed.edu/bioapps/primer3_www.cgi). The PCR reactions were carried out in a GeneAmp® PCR system 9700 in a final volume of 50 µl. Mytaq red mix was purchased from Bioline, UK. Primers were purchased from Eurofins MWG operon, UK. Each reaction contained 5 µl Mytaq red mix, 200 nM forward primer, 200 nM reverse primer (primer sequences are listed in Table 4.1), 1 µl cDNA and RNase-free water to 10 µl. The following protocol was used: 1 minute at 95 °C [15 seconds at 95 °C, 15 seconds at annealing temperature (T_a), 10 seconds at 72 °C] for 18-38 cycles. Ta for each pair of primers and size of the PCR-amplified product are listed in Table 4.1.

Table 4.1 List of forward primers and reverse primers

CDS	Primer forward	Primer reverse	Size (bp)	T_a (°C)
COL4A1	aaaggagagcgaggctacc	gtccaacttcgcctgtcaa	349	51
LAMA5	gactcgcctcatgtctgtca	tgcactggcctgactctg	424	53
LAMC1	gcagccttcttgaccgacta	gccttccttccagagttgaa	379	53
RPL13A	gagggcatcaacatttctgg	gcctgtttccttagcctcaa	428	55
LAMA4	agaatgttcgccctgtgact	ccaggagcacatctttcaca	437	53
FN	cacatggagcaagaaggaca	aggtgaacgggagaacacag	257	53
LAMB1	tcctgacagccatctcattg	aagcaggatctaaggcacga	371	53

4.2.4.3 DNA agarose gel electrophoresis

Agarose gel 1.2% (w/v) was prepared by adding 1.2 g of agarose powder to 100 ml Tris-Acetate-EDTA (TAE) 1x buffer (40 mM of Tris acetate and 1 mM EDTA in dH_2O). The mixture was heated in a microwave oven for 2-3 minutes, with heating periodically stopped to allowing manual mixing and to avoid overflow, until the agarose had completed dissolved. The agarose solution was left to cool for 10 minutes at room temperature before ethidium bromide was added to a final concentration of 0.5 μg/ml. The solution was poured carefully, to avoid air bubbles, into a gel tray with a well comb already attached. The gel was then left to set for 20 minutes before transferring the gel tray to an electrophoresis tank filled with TAE 1x buffer. PCR-amplified samples were mixed with DNA loading dye 5x (Biorad, UK). Samples and DNA ladder (Hyperladder IV, Bioline, UK) were then loaded to appropriate wells. The gel was subjected to electrophoresis at 100 V for approximately 45-60 minutes or until the dye line had travelled 80-90% of the gel length. Then the gel was visualised and photographed under UV using GE healthcare ImageQuant™. The band intensity was measured with ImageJ software. Intensity data were statistically analysed using GraphPad Prism version 5 and are shown as mean ± SD. One-way ANOVA and Bonferroni post-hoc tests were applied to compare all data obtained from at least 3 independent cultures. All analysed data were considered statistically significant when $p<0.05$.

4.2.5 Western blotting

Rat brain endothelial cells were maintained in co-culture with astrocytes for 4 days prior to the experiment. Primary rat skin fibroblasts were grown for 7 days. Culture medium was aspirated and cells were lysed with ice-cold 1% (v/v) Triton-X 100 in PBS. Cell lysates were initially kept on ice and then transferred to -20 ºC until use. Boiled 6x Laemmli sample buffer was then added to the culture plates of the rBECs and fibroblasts. Plates were scraped thoroughly and the ECM sample was collected into an Eppendorf tube and kept in -20 ºC freezer until use. Lysates were mixed with 6x Laemmli sample buffer. Lysate and ECM sample were then heated at 70 ºC for 5

minutes. SDS-PAGE and western blotting were carried out as described in Section 3.2.4.

4.3 Results

4.3.1 Upregulation of extracellular matrix protein in mouse brain following middle cerebral artery occlusion

Expression of ECM proteins can be modulated by several factors including hormones, injury and inflammation and many studies have investigated the effect of brain injury on the expression of ECM components in the basal lamina of the cerebral vasculature. However, most of the studies have focused on the early events (hours rather than days) following injury and there is still a lack of information on the effects of inflammation on ECM protein expression in the basal lamina of the brain vasculature days following injury. In terms of physiological events, we would expect de-novo production of basal lamina ECM proteins in the brain vasculature as a sign of the active tissue repairing process.

Here, we investigated the effect of MCAO followed by 48 hours or 6 days reperfusion on the expression of two endothelial basal lamina components, laminin α4 chain protein and fibronectin. Immunohistochemical detection of laminin α4 chain and cellular fibronectin in the brain sections revealed changes in expression of these basal lamina components in some areas of the brain.

In the contralateral side of the brain of mice subjected to MCAO and 48 hours reperfusion, there is positive expression of laminin α4 chain along the brain vessels (Figure 4.1A). Following MCAO and 48 hours reperfusion, there was a dramatic increase in the expression of laminin α4 chain in the vasculature of the ipsilateral cortical area (infarct area) (Figure 4.1C) compared with the same area in the contralateral side (Figure 4.1A). Immunocytochemical detection of laminin α4 chain in the contralateral side of the brain of mice subjected to MCAO and 6 days reperfusion was undetectable (Figure 4.1D). Upregulation of laminin α4 chain in the vasculature was also found in the ipsilateral infarct area of the brain of mice subjected to MCAO following 6 days reperfusion (Figure 4.1F).

The area in the brain including cortex (Figure 4.2 A-D) and striatum (Figure 4.2 E and F) in which the upregulation of laminin α4 was observed had a clear border that resembled the border of infarct area seen in cresyl violet staining of the brain slice from the adjacent section.

Expression of fibronectin in mouse brains subjected to MCAO followed by 48 hours reperfusion was also investigated. Similar to expression of laminin α4 chain, there was an increase in the expression of fibronectin in the basal lamina of the infarct area compared with the same area in the contralateral side (Figure 4.3A-C). The brain section was also probed for PECAM, endothelial cell marker. The localisation of fibronectin was in close proximity to the PECAM positive staining (Figure 4.3D-F) suggesting that endothelial cells were adjacent to the staining. Fibronectin staining was partly co-localised with laminin α4 (yellow in Figure 4.3I).

Figure 4.1 Immunohistochemical detection of laminin α4 chain expression in mouse brain following middle cerebral artery occlusion

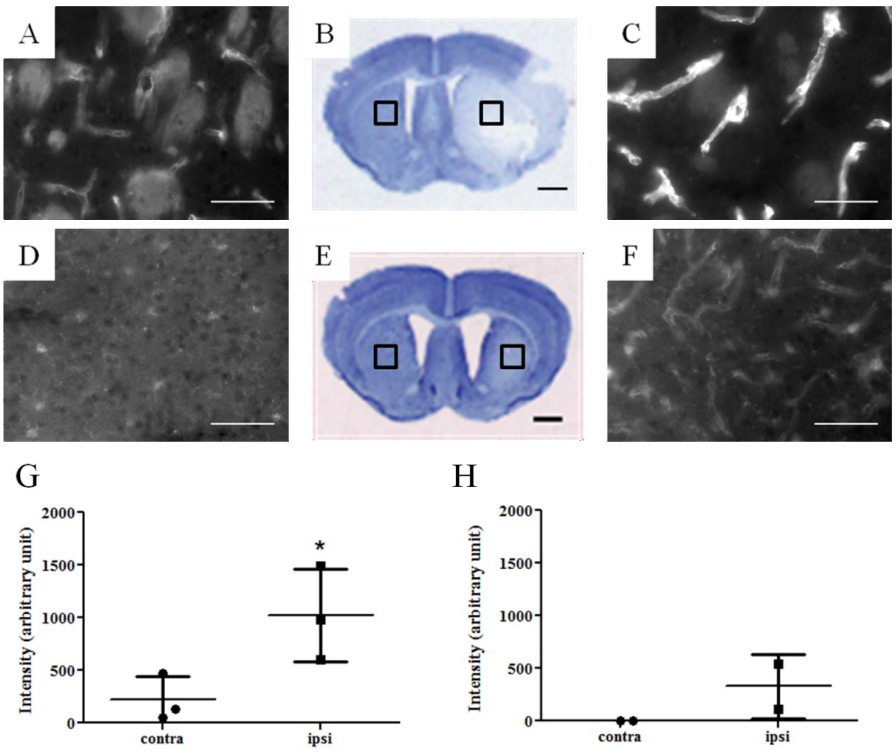

Mice underwent 45 minutes of MCAO followed by either 48 hours reperfusion (A-C) or 6 days reperfusion (D-F). Coronal brain sections were stained for laminin α4 chain. Panels A and D are images of the contralateral side of the brain. Panels C and F are images of the ipsilateral side of the brain. Fluorescent images were taken from the areas of the brain sections indicated by the square in the cresyl violet stained panels (B and E). Digital pictures were taken with a Coolsnap ES camera *using* MetaVue software following visualization with an Olympus *BX51* microscope. Scale bars represent 20 µm (100x magnification). Intensity of laminin α4 staining (G and H) represent data obtained from MCAO followed by 48 hours (n=3) or 6 days (n=2) reperfusion, respectively, was measured using ImageJ software. Data obtained from different brains after MCAO followed by 48 hours reperfusion were statistically analysed using Prism version 5 and are shown as mean ± SD. Student t-test was applied to compare ipsilateral with contralateral data. All analysed data were considered statistically significant when $p<0.05$ (*).

Figure 4.2 Immunohistochemical detection of laminin α4 chain in mouse brain following middle cerebral artery occlusion

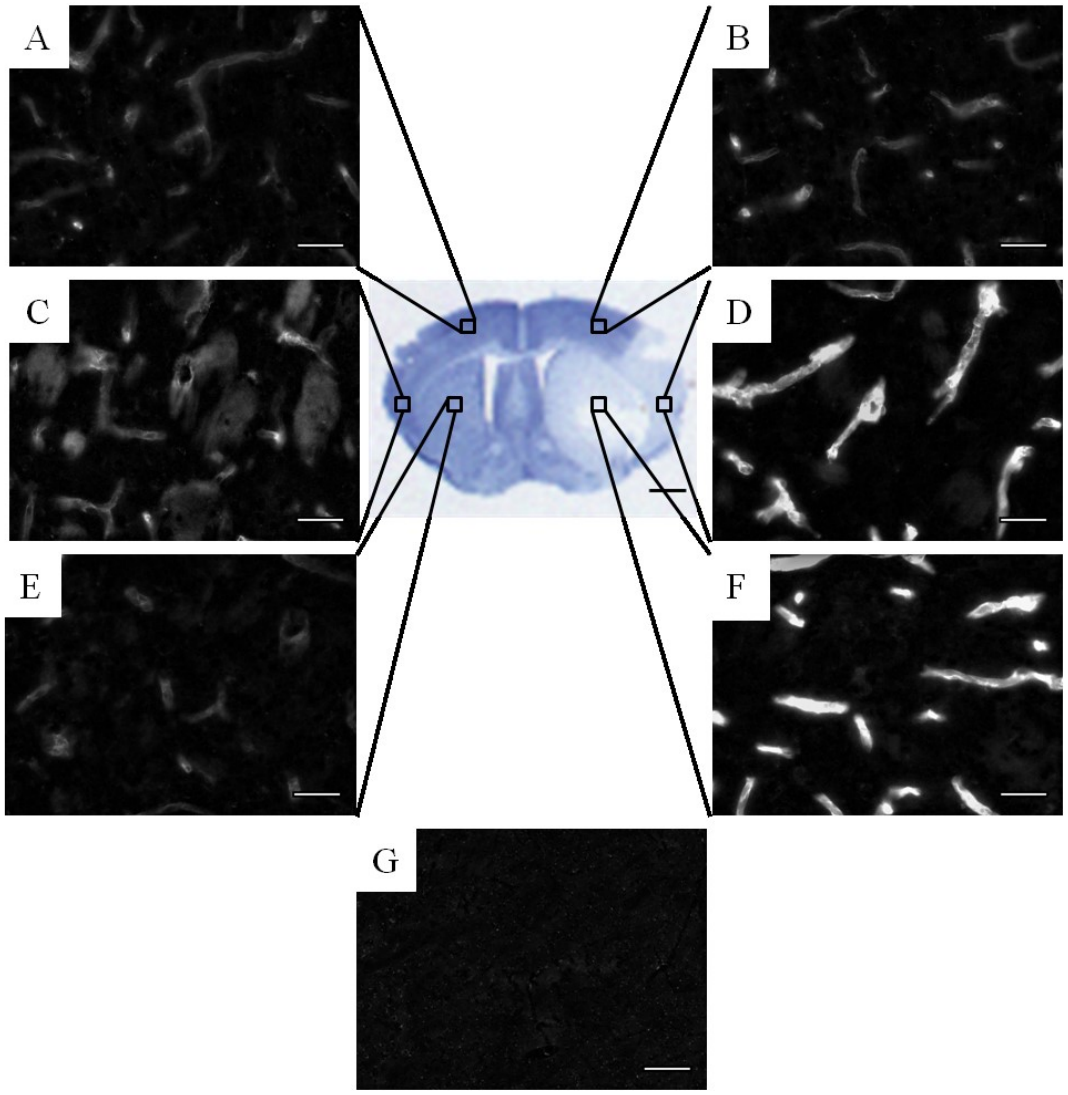

Mice underwent 45 minutes of MCAO followed by 48 hours reperfusion. Coronal brain sections were stained for laminin α4 chain. Panels A, C and E are images of the contralateral side of the brain whilst panels B, D and F are images of the ipsilateral side of the brain section. Fluorescent images were taken from the boxed areas indicated in the cresyl violet-stained panel. Image G is a negative control in which primary antibody was excluded and only secondary antibody used. Digital pictures were taken with a Coolsnap ES camera through MetaVue software following visualization with an Olympus BX51 microscope. Scale bars represent 20 μm (100x magnification).

Figure 4.3 Immunohistochemical detection of fibronectin in mouse brain following middle cerebral artery occlusion

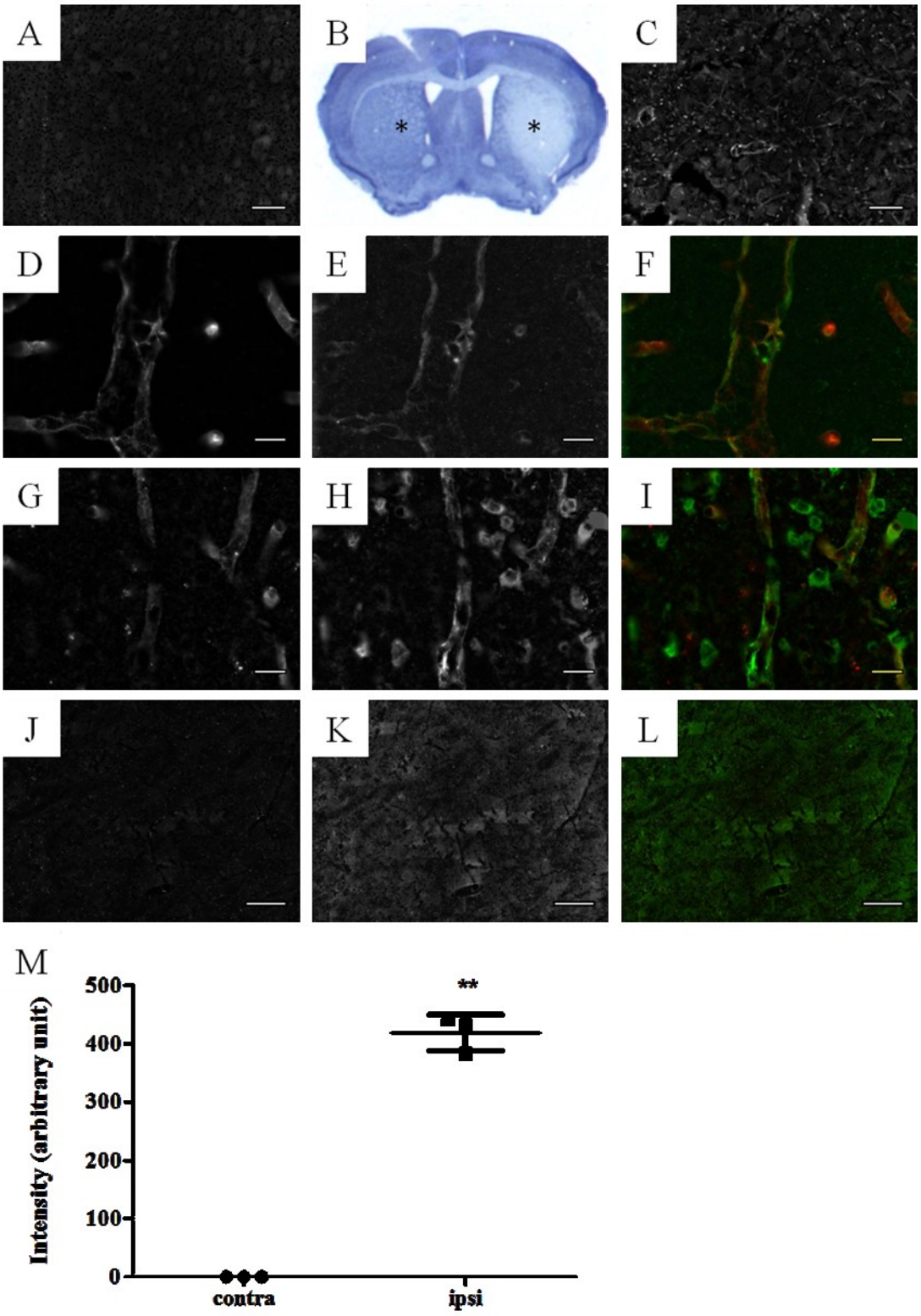

Mice underwent 45 minutes of MCAO followed by 48 hours reperfusion (n=2) (panels A-C). Coronal brain sections were probed for fibronectin. Panel A is the image of the contralateral side of the brain whilst panel C is the image of the ipsilateral side of the brain section. Fluorescent images were taken from the areas of the brain sections indicated by the area asterisked in the photograph of cresyl violet staining (panel B). Brain sections were probed for PECAM (D), fibronectin (E and H) and laminin α 4 (G). Image F is the composites of D (PECAM, red) and E (fibronectin, green). Image I is the composite of G (laminin α 4, red) and H (fibronectin, green). Image J and K is a negative control in which primary antibody was excluded and only secondary antibody used. L is the composite of J and K.

Digital pictures were taken with a Coolsnap ES camera through MetaVue software following visualization with an Olympus BX51 microscope. Scale bars represent 20 μm for A, B and the negative control (100x magnification) and 100 μm for the rest (40x magnification). Intensity of fibronectin staining (D) represent data obtained from MCAO followed by 48 hours reperfusion was measured using ImageJ software. Data obtained from different brains of mice subjected to MCAO followed by 48 hours reperfusion are shown as mean ± SD. Student t-test was applied to compare ipsilateral with contralateral data. All analysed data were considered statistically significant when $p<0.05$ (**=p<0.01).

4.3.2 Expression of extracellular matrix proteins by rBECs in culture

Extracellular matrix proteins are actually synthesised by endolthelial cells and subsequently secreted into the extracellular space. The expression profile of ECM proteins varies throughout the body but laminin-411, laminin-511, fibronectin and type IV collagen are found in the basement membrane of brain capillaries, immediately adjacent to brain endothelial cells. In the previous chapter we showed that pBECs maintained *in vitro* produced cellular fibronectin. Also, rBECs in culture have been demonstrated to produce laminin (Abbott et al., 1992). Here, we investigate if our *in vitro* BBB model comprising rBECs produces ECM proteins in a manner consistent with what is observed *in vivo*. We applied two methods including western blotting and immunocytochemistry. Western blotting is the method to determine the presence of ECM protein and can be further applied for semi-quantitative purpose which can be very useful for future experiments. Immunocytochemistry allow us to determine the presence of the ECM proteins of interest and also to observe the localisation of the proteins. Cellular fibronectin has been reported to be expressed by the brain endothelial cells and localised in the basal lamina as a fibrous-like layer underlying the endothelial cells. Therefore, we expect to find a production of cellular fibronectin which should localised thoroughly underneath the rBEC culture in a fibrous-like pattern.

The initial studies carried out were to determine whether rBECs grown on type I collagen were able to produce cellular fibronectin, which is a component of the basal lamina *in vivo.* Analysis of primary rat brain endothelial cell lysate by western blotting revealed two very faint bands of cross reactivity at 250 kDa and >250kDa proteins which had the same size to the bands obtained from fibroblast positive control (Figure 4.4A). Immunocytochemical images showed that rBEC produced cellular fibronectin (Figure 4.4B). Cellular fibronectin produced by rBEC culture displayed a reticulated fibrous structure covering the area on which rBECs were grown. The intensity of cellular fibronectin staining was low, although a faint fibrous meshwork can be seen in rBECs at DAPI positive areas.

Figure 4.4 Cellular fibronectin produced by rat brain endothelial cell monolayers

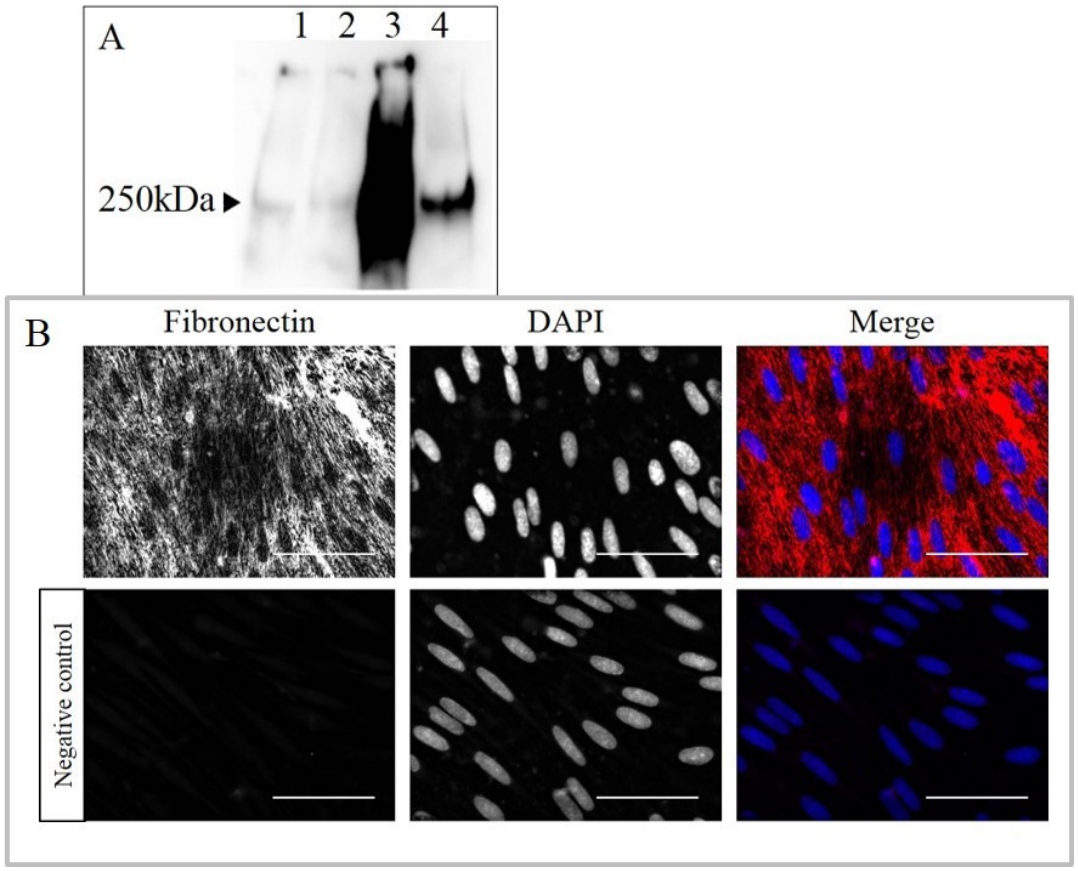

Western blotting (Panel A) of rBEC lysate (lane 1, 25 μg protein) and ECM produced by rBECs in culture (lane 2, 5 μg protein). Primary rat fibroblast lysate (lane 3, 50 μg protein) and ECM produced by fibroblasts in culture (lane 4, 5 μg protein) were used as positive controls. Samples were loaded onto a 10% SDS-PAGE gel and electrophoresis and transfer to PVDF membrane were carried out as described in section 4.2.5). PVDF membranes were then probed for cellular fibronectin and visualised for 1 minute using GE health care ImageQuant™.: Primary rat brain endothelial cells were grown on type I collagen-coated Transwell® inserts for 4 days prior to fixation and staining for cellular fibronectin (red) and DAPI (blue). Images in the last row represent negative control for fibronectin staining; IgG (red) and DAPI (blue). Digital pictures were taken with a Coolsnap ES camera through MetaVue software following visualization with an Olympus BX51 microscope. The image shown in Figure 4.4B is typical of three independent cultures. Scale bar represents 50 μm (Magnification 600x).

4.3.3 Effects of oxygen glucose deprivation and interleukin-1β on the expression of extracellular matrix in the *in vitro* blood-brain barrier model

In the previous chapters of this thesis we have shown that our *in vitro* model of the BBB produces laminin α4 and fibrinectin ECM proteins and that under pathological conditions associated brain injury (e.g. stroke, trauma), there are changes in the expression of ECM proteins. Here we subsequently investigated whether rBECs in culture were capable of expressing several other ECM protein components of the basal lamina and also the effects on ECM protein expression when rBECs were subjected to OGD and IL-1β treatment (*in vitro* equivalent of brain injury).

We investigated the expression of laminin alpha-4 gene, *LAMA4* (Figure 4.5), laminin beta-1 gene, *LAMB1* (Figure 4.6), laminin gamma-1 gene, *LAMC1* (Figure 4.7), fibronectin gene, *FN* (Figure 4.8) and type IV collagen alpha-1 gene, *COL4A1* (Figure 4.9) immediately following 2.5 hours normoxia or OGD, following 2.5 hours normoxia or OGD and 2 hours reperfusion ± IL-1β and following 2.5 hours normoxia or OGD and 18 hours reperfusion ± IL-1β. 60S ribosomal protein L13a or *RPL13A,* whose expression is considered to be unchanged in hypoxic conditions *in vitro* (Curtis et al., 2010, Gubern et al., 2009) was used as a house keeping gene.

Laminins are composed of three subunits, namely α, β and γ chains. The laminin subunits are encoded by different genes located on different chormosomes. In general, the basal lamina of the vasculature contains two forms of laminins: laminin-411 and laminin-511, although the expression of laminins may change in pathological conditions. For example, the expression of vascular laminins is modulated greatly by proinflammatory cytokines. Laminin α4 is one of the main laminin α chains (along with laminin α5) specifically localised in the brain endothelial cell basal lamina and not in brain parenchyma. Human laminin α4 is encoded by the *LAMA4* gene. In this thesis we investigated the expression of the *LAMA4* gene under normal, non-inflammatory conditions in rBECs maintained *in vitro*. We expected a positive signal for *LAMA4* expression, which would be consistent with expression of the gene *in vivo*. As the expression of vascular laminins could be modulated in pathological conditions and by inflammation, we also investigated if OGD and IL-1β affected the expression of the *LAMA4* gene in our rat *in vitro* BBB model.

The expression of *LAMA4* was two-fold increased in rBECs subjected to 2.5 hours of OGD compared to that underwent normoxia (Figure 4.5B). Expression of *LAMA4* by rBECs following 2.5 hours of OGD followed by 2 hours of reperfusion, 2.5 hours of normoxia and 2 hours treatment with IL-1β and 2.5 hours OGD and 2 hours of IL-1β treatment was significantly upregulated compared to control cells subjected to normoxia (Figure 4.5C).

The upregulation of *LAMA4* was prolonged up until 18 hours following IL-1β treatment and the combination of OGD and IL-1β treatment (Figure 4.5D). However, the expression of laminin alpha-5 gene (*LAMA5*), another main laminin isoform expressed by endothelial cells of healthy brain capillaries *in vivo,* by rBECs in culture was undetectable by RT-PCR at any time points tested (data not shown).

Figure 4.5 Effect of oxygen glucose deprivation and interleukin-1β treatment on *LAMA4* expression by rat brain endothelial cells.

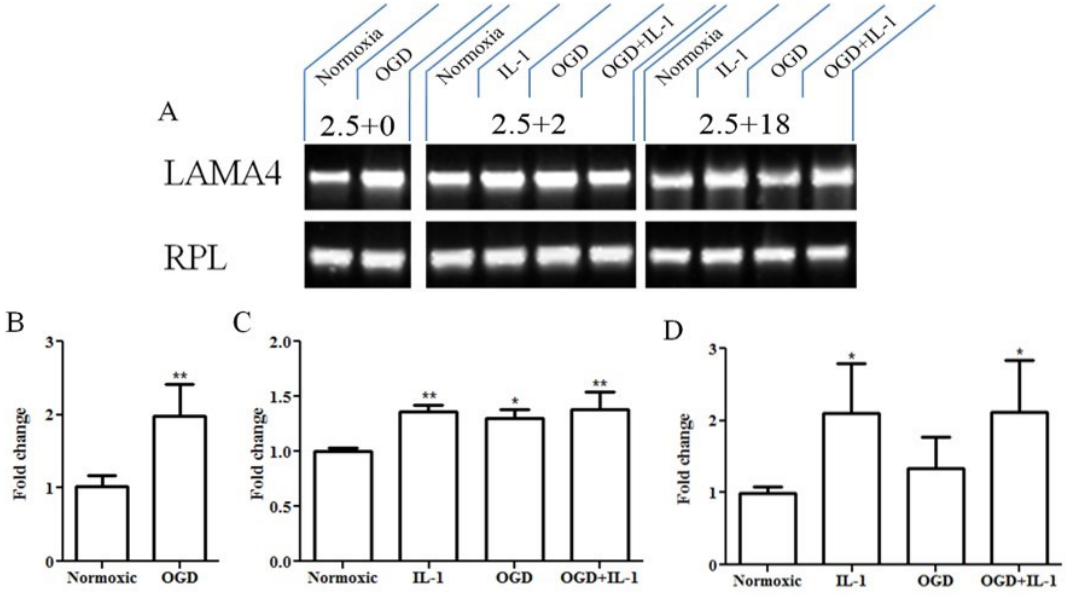

RT-PCR was carried out and amplification products were analysed by 1.2% (w/v) agarose gel electrophoresis as described in Section 4.2.4. Panel A: The expression of *LAMA4* and *RPL13A* (RPL) in rBECs subjected to normoxia, IL-1β**,** OGD and OGD+IL-1β at 2.5+0, 2.5+4 and 2.5+18 time points. The gel was visualised and photographed under UV using GE Healthcare ImageQuant™. The band intensity was measured with ImageJ software. Band intensity of PCR products obtained from: rBECs subjected to 2.5 hours normoxia or OGD (Panel B), 2.5 hours normoxia or OGD and 2 hours reperfusion ± IL-1β (Panel C) and following 2.5 hours normoxia or OGD and 18 hours reperfusion ± IL-1β (Panel D). Intensity data were statistically analysed using GraphPad Prism version 5 and are shown as mean ± SD. One-way ANOVA and Bonferroni post-hoc tests were applied to compare all data obtained from at least 3 independent cultures. All analysed data were considered statistically significant when $p<0.05$ (*p<0.05, **p<0.01).

Laminin β1, encoded by the *LAMB1* gene, is expressed in most basement membranes throughout the body. In the brain, laminin β1 is the laminin isoform expressed specifically within the endothelial basal lamina and, in conjunction with one laminin α chain and one laminin γ chain, assembles to form a complete heterotrimeric glycoprotein. Laminin β1 is also the only laminin β chain expressed in the endothelial cell basal lamina (laminin β2 being localised only at the smooth muscle layer of large vessels). In this thesis we therefore investigated the impact of OGD and inflammation on expression of laminin β1 chain by rat brain endothelial cell in culture.

Our studies revealed that *LAMB1* is constitutionally expressed in rBECs. The expression of *LAMB1* was modulated by 2.5 hours of OGD ± 10 ng/ml IL-1β treatment. Exposure to OGD for 2.5 hours was found to significantly induce upregulation of *LAMB1* mRNA in rBECs compared to that of rBECs subjected to normoxia (Figure 4.6B). Following treatment with IL-1β, we observed an initial decrease in *LAMB1* mRNA expression following 2 hours reperfusion (Figure 4.6C). Following 2.5 hours OGD and 2 hours reperfusion (without IL-1β), expression of *LAMB1* was comparable to rBECs subjected to normoxia. A subsequent increase in mRNA expression was observed following 2.5 hours OGD and 18 hours of IL-1β treatment but not 18 hours of IL-1β treatment and 2.5 hours OGD and 18 hours reperfusion (Figure 4.6D).

Figure 4.6 Effect of oxygen glucose deprivation and interleukin-1β treatment on *LAMB1* expression in rat brain endothelial cells

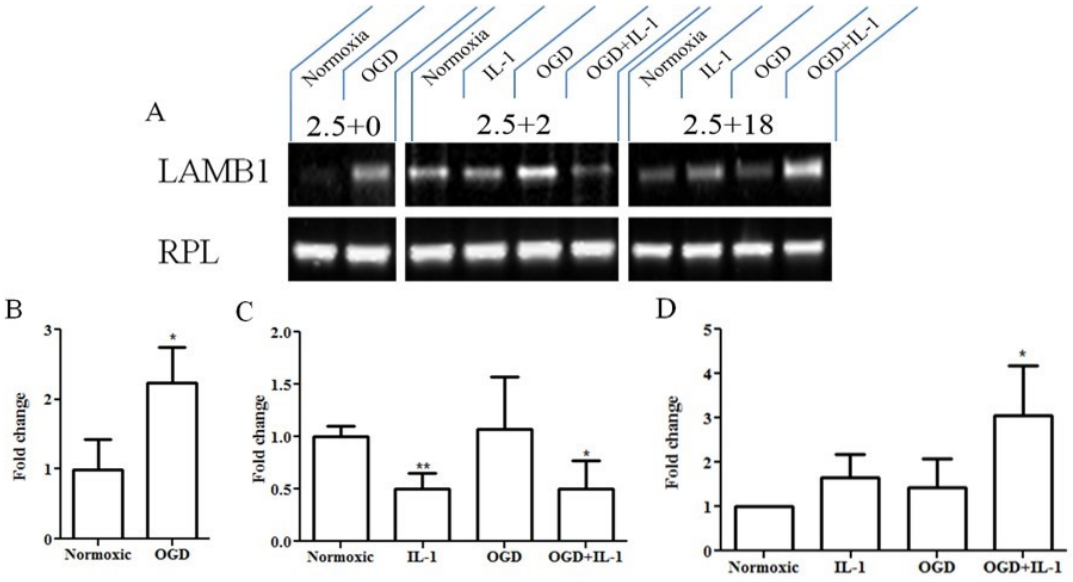

RT-PCR was carried out and amplification products were analysed by 1.2% (w/v) agarose gel electrophoresis as described in Section 4.2.4. Panel A: The expression of *LAMB1* and *RPL13A* (RPL) in rBECs subjected to normoxia, IL-1β**,** OGD and OGD+IL-1β at 2.5+0, 2.5+4 and 2.5+18 time points. The gel was visualised and photographed under UV using GE Healthcare ImageQuant™. The band intensity was measured with ImageJ software. Band intensity of PCR products obtained from: rBECs subjected to 2.5 hours normoxia or OGD (Panel B), 2.5 hours normoxia or OGD and 2 hours reperfusion ± IL-1β (Panel C) and following 2.5 hours normoxia or OGD and 18 hours reperfusion ± IL-1β (Panel D). Intensity data were statistically analysed using GraphPad Prism version 5 and are shown as mean ± SD. One-way ANOVA and Bonferroni post-hoc tests were applied to compare all data obtained from at least 3 independent cultures. All analysed data were considered statistically significant when $p<0.05$ (*p<0.05, **p<0.01).

The laminin γ chain is one component (along with α and β chains) of the laminin multidomain glycoprotein. Three isoforms of human laminin γ, laminin γ1, γ2 and γ3, have been discovered so far (Kallunki et al., 1992; Koch et al., 1999). The laminin γ1 chain, encoded by the *LAMC1* gene, was the first laminin γ chain identified and it is expressed by various cell types and is specifically incorporated into the basement membrane, including that of the brain vasculature. Importantly, laminin γ1 is a component of the main laminin isotypes, i.e. laminin-411 and -511, expressed by brain endothelial cells, thus changes in the expression of this molecule may significantly affect endothelial cell behaviour and the integrity of the BBB. Here we investigate the effect of OGD and IL-1β (representative of *in vitro* acute brain injury) on endothelial cell expression of LAMC1.

Immediately following 2.5 hours OGD, there was upregulation of *LAMC1* expression compared to normoxic control (Figure 4.7B). Exposure to 10 ng/ml IL-1β for 2 hours, but not 2.5 hours OGD and 2 hours of reperfusion in the absence of IL-1β and 2.5 hours OGD followed by 2 hours of IL-1β treatment, resulted in a significant increase in the expression of *LAMC1* mRNA compared to normoxic control (Figure 4.7C). Expression of *LAMC1* in rBECs subjected to either normoxic or 2.5 hours OGD followed by 18 hours of 10 ng/ml IL-1β (Figure 4.7D) was significantly upregulated compared to normoxic control. There was no change in *LAMC1* expression in cells subjected to 2.5 hours OGD and 18 hours of reperfusion observed compared to normoxic control.

Figure 4.7 Effect of oxygen glucose deprivation and interleukin-1β treatment on *LAMC1* expression in rat brain endothelial cells.

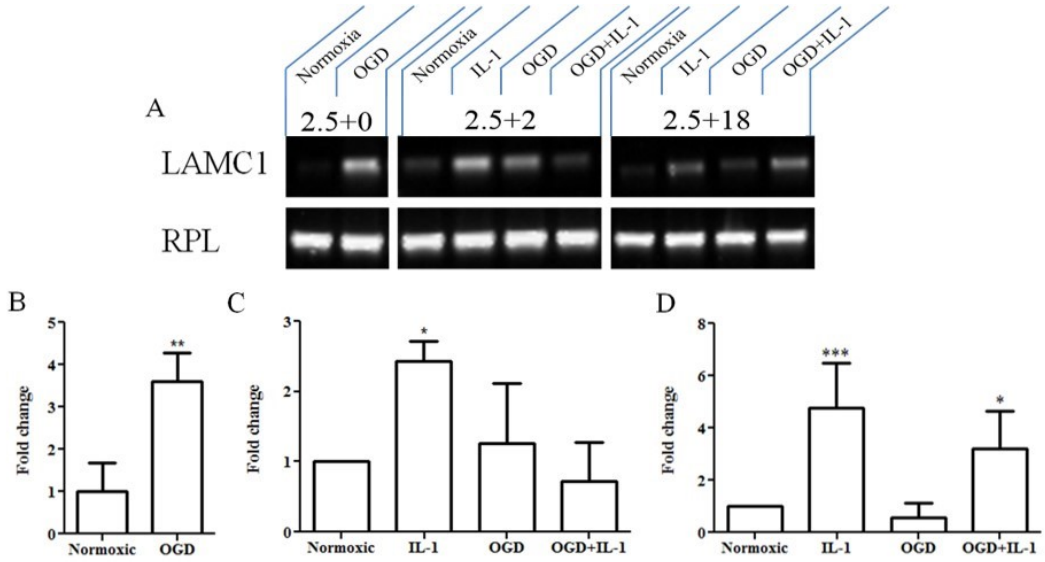

RT-PCR was carried out and amplification products were analysed by 1.2% (w/v) agarose gel electrophoresis as described in Section 4.2.4. Panel A: The expression of *LAMC1* and *RPL13A* (RPL) in rBECs subjected to normoxia, IL-1β**,** OGD and OGD+IL-1β at 2.5+0, 2.5+4 and 2.5+18 time points. The gel was visualised and photographed under UV using GE Healthcare ImageQuant™. The band intensity was measured with ImageJ software. Band intensity of PCR products obtained from: rBECs subjected to 2.5 hours normoxia or OGD (Panel B), 2.5 hours normoxia or OGD and 2 hours reperfusion ± IL-1β (Panel C) and following 2.5 hours normoxia or OGD and 18 hours reperfusion ± IL-1β (Panel D). Intensity data were statistically analysed using GraphPad Prism version 5 and are shown as mean ± SD. One-way ANOVA and Bonferroni post-hoc tests were applied to compare all data obtained from at least 3 independent cultures. All analysed data were considered statistically significant when $p<0.05$ (*=p<0.05, **=p<0.01, ***=p<0.001).

Fibronectin is a major extracellular matrix glycoprotein expression specifically in the vascular basement membrane in both physiological and disease conditions. In the brain, fibronectin is localised both in the basal lamina of the vessels and the parenchyma. It has been shown that fibronectin modulates cell adhesion, proliferation and migration and that changes in fibronectin expression have been reported in injured brain tissues (Muellner et al., 2003). Here we investigate whether conditions associated with brain injury, namely OGD and IL-1β treatment, influence fibronectin expression using the rat *in vitro* BBB model.

As was observed with *LAMC1*, expression of the fibronectin gene or *FN* was significantly increased (4-fold) following 2.5 hours OGD compared to normoxic control (Figure 4.8B) and there was a significant upregulation of fibronectin mRNA following 2.5 hours of IL-1β treatment (Figure 4.8C). However, there was no change in FN expression in rBECs subjected to 2.5 hours OGD and 2 hours reperfusion ± IL-1β. (Figure 4.8C). Exposure to 2.5 hours OGD and 18 hours reperfusion, 18 hours of IL-1β treatment or 2.5 hours of OGD and 18 hours of IL-1β treatment did not induce the expression of *FN* in rBECs compared to the normoxic control (Figure 4.8D).

Figure 4.8 Effect of oxygen glucose deprivation and interleukin-1β treatment on fibronectin expression in rat brain endothelial cells

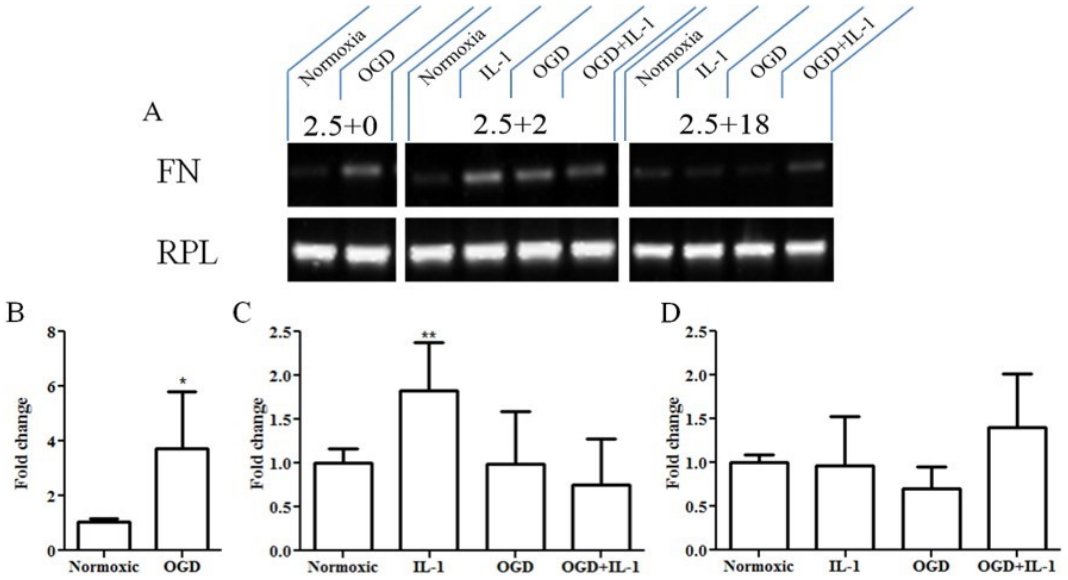

RT-PCR was carried out and amplification products were analysed by 1.2% (w/v) agarose gel electrophoresis as described in Section 4.2.4. Panel A: The expression of *FN* and *RPL13A* (RPL) in rBECs subjected to normoxia, IL-1β**,** OGD and OGD+IL-1β at 2.5+0, 2.5+4 and 2.5+18 time points. The gel was visualised and photographed under UV using GE Healthcare ImageQuant™. The band intensity was measured with ImageJ software. Band intensity of PCR products obtained from: rBECs subjected to 2.5 hours normoxia or OGD (Panel B), 2.5 hours normoxia or OGD and 2 hours reperfusion ± IL-1β (Panel C) and following 2.5 hours normoxia or OGD and 18 hours reperfusion ± IL-1β (Panel D). Intensity data were statistically analysed using GraphPad Prism version 5 and are shown as mean ± SD. One-way ANOVA and Bonferroni post-hoc tests were applied to compare all data obtained from at least 3 independent cultures. All analysed data were considered statistically significant when $p<0.05$ (*p<0.05, **p<0.01).

Type IV collagen is primarily localised in the basal lamina of endothelial cells. The major form of type IV collagen in the basement membrane, including that of brain endothelial cells, is a triple helix comprising two collagen alpha 1 chains and one collagen alpha 2 chain. These collagen alpha 1 and 2 chains are encoded by separate genes. The collagen alpha 1 is encoded by *COL4A1* gene and the collagen alpha 2 chain is encoded by *COL4A2* gene, both located on chromosome 13q34. Type IV collagen is involved in cell adhesion, migration and differentiation. It has been reported that microvascular endothelial cells express and produce type IV collagen *in vitro* (Tilling et al., 2002, Webersinke et al., 1992). Changes in type IV collagen expression have been observed following brain injury *in vivo* (Hamann et al., 1995). Therefore, our initial RT-PCR studies investigated whether rBECs in culture expressed the *COL4A1* gene under normoxic conditions. If the latter was expressed, subsequent studies would establish the effects of injury (OGD or IL-1β treatment) on the expression of type IV collagen alpha 1 chain in brain endothelial cells.

Expression of the type IV collagen alpha 1 encoding gene or *COL4A1* was undetectable in rBECs subjected to normoxia but became detectable in rBECs following exposure to OGD/IL-1β (Figure 4.9). OGD, 2.5 hours, followed by 2 hours of reperfusion, incubation for 2 hours with IL-1β or 2.5 hours OGD followed by 2 hours IL-1β treatment induced *COL4A1* expression. Rat brain endothelial cells subjected to 2.5 hours OGD and 18 hours reperfusion, 18 hours IL-1β treatment or 2.5 hours OGD and 18 hours IL-1β treatment showed positive expression of *COL4A1* whereas the *COL4A1* expression of cells undergone normoxia was still undetectable.

Figure 4.9 Effect of oxygen glucose deprivation and interleukin-1β treatment on *COL4A1* expression in rat brain endothelial cells

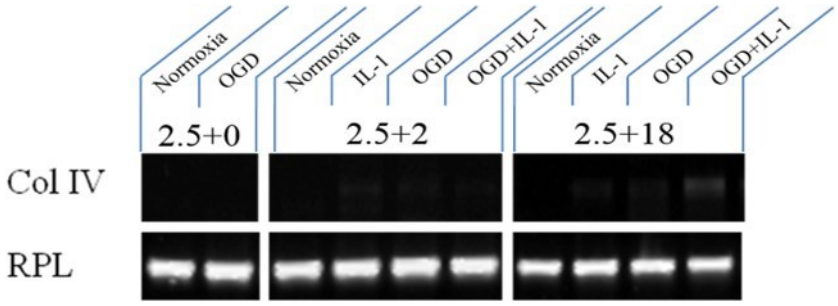

RT-PCR was carried out and amplification products were analysed by 1.2% (w/v) agarose gel electrophoresis as described in Section 4.2.4. Panel A: The expression of *COL41A* (Col IV) and *RPL13A* (RPL) in rBECs subjected to normoxia, IL-1β**,** OGD and OGD+IL-1β at 2.5+0, 2.5+4 and 2.5+18 time points. The gel was visualised and photographed under UV using GE Healthcare ImageQuant™.

4.4 Discussion

The basal lamina of normal brain vasculature is mainly composed of laminins, type IV collagen and fibronectin (Giordana et al., 1985, Kühn, 1995, Tilling et al., 2002, Sixt et al., 2001). Laminin-411 and laminin-511 are the main isoforms expressed where the ECM is in direct contact with brain endothelial cells, whereas laminin α1 and α2 chain are expressed in the parenchymal domain of the brain vasculature (Sixt et al., 2001, Gonzalez et al., 2002). Type IV collagen expressed in the brain basal lamina consists of two α1(IV) chains and one α2(IV) chain forming trimers (Tilling et al., 2002). In this study we investigated the expression of ECM proteins following acute brain injury and inflammation. Many studies have reported changes in ECM proteins during a pathological state of the brain (Hamann et al., 1995, Muellner et al., 2003, Trinkl et al., 2006, Scholler et al., 2007, Sixt et al., 2001). Several of the above studies showed disappearance of ECM proteins in the basal lamina of the brain. Significant loss of laminin and fibronectin in the basal lamina of the brain vasculature was observed in the brains of primates after being subjected to 2 hours of MCAO and 1, 4 and 24 hours of reperfusion (Hallmann et al., 2005). The disappearance of type IV collagen was also demonstrated in the brain of rats that underwent 3 hours of focal ischemia followed by 3 and 24 hours of reperfusion (Trinkl et al., 2006). Early loss of ECM components in the basal lamina might be caused by proteolytic degradation of the ECM proteins by enzymes released early following brain injury. For example, the plasminogen-plasmin system (Liotta et al., 1981, Ahn et al., 1999, Yepes et al., 2003, Hosomi et al., 2001) and MMPs (Gasche et al., 1999, Heo et al., 1999, Cunningham et al., 2005) are rapidly released following brain injury and are able to degrade the basal lamina.

In contrast to the studies above which reported loss of the basal lamina ECM following injury, our study revealed upregulation of both laminin α4 chain mRNA and fibronectin mRNA following MCAO and reperfusion in the area of brain damage. Moreover, the increase in laminin α4 mRNA expression observed in our study was prolonged for up to 6 days following MCAO. A number of studies have also demonstrated upregulation of the ECM component in the brain basal lamina following brain injury. Increases in fibronectin protein expression in the basal lamina

were demonstrated in an animal model of brain hypoxia (Milner et al., 2008, Li et al., 2010), the increase in fibronectin expression probably being the result of angiogenic activity. A study of mice that underwent MCAO found that components of the brain basal lamina including laminin, fibronectin and type IV collagen were significantly upregulated after 6 hours of MCAO (Ji and Tsirka, 2012). In the latter study, it has also been indicated that upregulation of laminin in the basal lamina was mediated by the inflammatory component, cyclooxygenase-2 (Ji and Tsirka, 2012). A study, using peripheral endothelial cells, reported the increase in laminin expression by endothelial cells in culture was also regulated by inflammation (Frieser et al., 1997). Studies by Sarkar et al. demonstrated that laminin proteins were undetectable by immunohistochemistry in intact brains (Sarkar et al., 2012, Sarkar and Schmued, 2010). Following neurotoxin injection into the brain, laminin expression was found to be upregulated as early as 8 hours and prolonged up to 2 months. The increase in laminin expression was restricted to the area of neurodegeneration, thus suggesting association between laminin expression and neuronal degeneration (Sarkar et al., 2012). Upregulation of laminin expression in the brain vasculature, presumably due to angiogenesis, has also been demonstrated in a hypoperfusion rat model (Wappler et al., 2011). In other conditions resulting in brain injury, such as in an animal model of status epilepticus (Gualtieri et al., 2012) and stab wound (Szabo and Kalman, 2008) upregulation of laminin in the basal lamina has also been reported.

It is noteworthy that reports suggest that the accessibility of ECM molecules in the basal lamina by the antibodies or tracers may affect the staining and detection of antigens. Brain injury may increase the staining as the antibodies can easily pass through the BBB (Krum et al., 1991, Szabo and Kalman, 2004). Incubation of the brain slide with collagenase (Giordana et al., 1985) or pepsin (Krum et al., 1991) prior to antibody application provided more consistent results. Therefore, the expression of ECM components in the brains of animals subjected to MCAO should be reconfirmed by other protein probing methods or by immunohistochemistry with enzyme treatment prior to staining.

In our *in vitro* studies it was reassuring that rat brain endothelial cells in culture expressed and produced the same ECM proteins expressed *in vivo*. Using immunocytochemistry, we demonstrated that rBECs produced a network of cellular

fibronectin. By RT-PCR, we showed that rBECs constitutively expressed laminin α4 laminin β1, laminin γ1, fibronectin and type IV collagen α1 encoding genes.

Immunocytochemistry studies have shown that rBECs grown on type I collagen produced laminin, with positive staining along the cell margin when the tight junction were opened and the basal lamina was revealed (Abbott et al., 1992). Several studies have investigated the expression of pan-laminin in the brain vasculature in pathological conditions, however not many studies separately determined the protein expression of each specific laminin isoform. For example, the study by Sixt et al. (2001) examined the expression of laminin α chains, including laminin α4 and α5, proteins in the brains of EAE mice. In control animals they demonstrated the basal lamina has two distinct layers, the endothelial layer containing laminin α4 and 5, and the parenchymal layer containing laminin α1 (Sixt et al., 2001). A change in protein expression in the endothelial basal lamina of EAE brain was observed. Laminin α5 protein was undetectable whilst laminin α4 remained in the basal lamina of inflamed vessels (Sixt et al., 2001). Modulation of ECM protein expression has also been demonstrated *in vitro* following OGD and inflammation. Inflammatory cytokines, including IL-1β and interferon-γ, regulated ECM protein mRNA expression in many cell types (Maheshwari et al., 1991, Raghunath et al., 1993, Richardson et al., 1995, O'Neill et al., 1997, Rinaldi et al., 2001, Armbrust et al., 2004, Baumert et al., 2009). Upregulation of laminin α2, β3 and γ1 mRNA expression was shown in immortalised human brain endothelial cells in culture following OGD (Ji and Tsirka, 2012). This corresponds with our finding showing modulation of ECM-gene mRNA by OGD and the proinflammatory cytokine, IL-1β. It has also been shown that laminin α5 mRNA was constitutively expressed (Ji and Tsirka, 2012) whereas LAMA5 mRNA was undetectable in our study. This probably was due to differences in the cell culture system (use of immortalised human cells compared to primary rat cells in our studies). Moreover, a study by Stratman et al. (2009) on ECM protein expression in human umbilical vein endothelial cells (HUVECs) showed that the expression of laminin α4 mRNA was constitutive and strong from day 1-5 in culture. However, laminin α5 mRNA was only expressed on the early day of culture (day 1) and the expression was lost later (day 3 and 5 in culture). In the case of type IV collagen alpha 1 chain, the mRNA

expression by HUVECs was also low (Stratman et al., 2009). This suggested that the number of days in culture might be a factor affecting ECM protein expression in the endothelial cells. Stratman, Malotte et al. 2009 also demonstrated that co-culturing HUVECs with pericytes significantly induced endothelial cell expression of fibronectin and laminin α5 (Stratman et al., 2009). This suggested that cellular components of the culture system also have an effect on ECM protein expression. Further experiments should be carried out to determine the effects of days in culture and cellular components on the expression of ECM genes.

Basal lamina ECM proteins including laminin, fibronectin and collagen IV play a role in vessel maintenance (Grant and Kleinman, 1997), the angiogenic process (Form et al., 1986, Wang and Milner, 2006, Li et al., 2010), regulating expression of tight junction proteins (Savettieri et al., 2000), barrier function (Tilling et al., 1998) and brain endothelial cell adhesion (Tilling et al., 2002). Therefore, changes in the expression of these ECM molecules following brain injury may affect brain endothelial cell behaviour and functions. In the next chapter, we have determined the effects of ECM proteins on brain endothelial cell behaviour and barrier function.

.

Chapter 5 Effects of the extracellular matrix on rat brain endothelial cell behaviour

5.1 Introduction

Cells in contact with ECM initially adhere and form filopodia and lamellipodia. These events are immediately followed by spreading of cells. The binding between cells and ECM components is mainly mediated by specific transmembrane receptors, integrins (Clyman et al., 1990, Wilson et al., 2003). Different cell types express different sets of integrins under different conditions. Integrins recognise specific binding sites on corresponding matrix molecules, for example, the RGD motif which is a three amino acid sequence Arg-Gly-Asp found in fibronectin. Upon binding to ECM, integrin activation triggers the assembly of a large number of adaptor molecules such as talin, α-actinin, filamin and vinculin that link the actin cytoskeleton and ECM proteins together. The sites are called "focal adhesions". Besides serving as mechanical linkages to the ECM, focal adhesions are also comprised of several signalling proteins and one of the most important tyrosine kinase is focal adhesion kinase (Schaller et al., 1992, Hanks et al., 1992, Guan and Shalloway, 1992, Kornberg et al., 1992) which is essential for cell proliferation, migration and survival (Slack et al., 2001, Wang et al., 2000, Hungerford et al., 1996). Initial adhesion (via filopodia and lamellipodia) of cells to matrix proteins is regulated by Rac and cdc42 (Nobes and Hall, 1995) and mature focal adhesions are regulated by Rho (Barry and Critchley, 1994, Ridley and Hall, 1992, Chrzanowska-Wodnicka and Burridge, 1996, Hotchin and Hall, 1995).

Following adhesion and spreading, cells are able to proliferate. The mechanism of ECM-integrin binding that promotes cell proliferation is generally the activation of MAP kinase (Wilson et al., 2003, Cybulsky and McTavish, 1997, Renshaw et al., 1997, Frost et al., 1997) which, in turn, increases the activity of cyclins (Schwartz and Assoian, 2001). Many laboratories have reported the regulatory role of ECM proteins on tight junction formation of epithelial and endothelial barriers (Jaeger et al., 1997, Weeks and Friedman, 1997)

The importance of ECM molecules has been emphasised by the evidence that the ECM molecules in the basal lamina are modified during many acute and chronic

pathological conditions in the brain (Sixt et al., 2001, Wu et al., 2009). We have demonstrated in the previous chapter that OGD and/or exposure to IL-1β can induce changes in the expression of genes encoding laminin α4, laminin β1, laminin γ1 and fibronectin in rBECs in culture. Also, studies reveal ECM in the basal lamina of the brain changed in many animal models of pathological conditions, such as loss of laminin α5 protein in inflamed vessels in the EAE animal model (Sixt et al., 2001), upregulation of fibronectin in brains of mice subjected to MCAO (Li et al., 2012). Cell-matrix adhesion via focal adhesions is also extremely important since it regulates cell behaviour, for example, cell adhesion, proliferation, migration. Specific cells produce and bind to specific ECM molecules. Moreover, it has been showed that the main vascular laminins underlying the brain endothelial cells *in vivo* is laminin-411 and laminin-511. However, brain endothelial cell behaviours on those laminins has still not been clarified. Therefore, in this chapter, we investigated the level of adhesion of rBECs to ECM proteins including type IV collagen, cellular fibronectin, laminin-411 and laminin-511 and whether these ECM proteins were able to influence cell morphology, cell proliferation and TEER.

5.2 Materials and Methods

5.2.1 Cell culture

Rat brain endothelial cells were isolated from two to three month-old Sprague-Dawley rats as described in Section 2.2.1. Cells were trypsinised, counted and prepared to a required concentration with either growth medium or serum-free medium depending on the experiment.

5.2.2 Plate coating

To investigate the effects of ECM on rBECs, tissue culture plates were coated with ECM proteins as described in Section 2.1.

5.2.3 Cell attachment and spreading assay

The cell attachment and spreading assay was carried out as previously reported (Humphries, 2001) First, primary rBECs were isolated from brains of adult male Sprague-Dawley rats as described in Section 2.2.1. Fragments of brain capillaries acquired were maintained for four days in T25 tissue-culture treated flasks. Cells were detached from the flasks by rinsing with 1 ml of 0.25% (w/v) trypsin in PBS for a few seconds and adding another 1 ml of 0.25% (w/v) trypsin in PBS for a few minutes until most of the cells detached from the surface. Serum-containing growth medium (DMEM supplemented with 16.7% (v/v) PDS, 2 mM glutamine, 80 μg/ml heparin, 100 units/ml penicillin, 0.1 mg/ml streptomycin and 1% (v/v) rBEC supplement, see Section 2.2.1 for details), 2 ml, was added to neutralise trypsin activity. Cells were then counted using a haemocytometer and the cell suspension were centrifuged at 400 xg for 5 min. Medium was removed from the cell pellet and the pellet was resuspended in the DMEM without serum. To measure cell attachment, 100 μl rBEC suspension was seeded in triplicate onto uncoated, BSA-treated and ECM-coated 96-well plates at 1 x 10^6 cells/ml (i.e. 1 x 10^5 cells/well). Cells were incubated at 37 °C for either 30 or 90 min.

To identify the adhesion molecules involved in cellular attachment to ECM, armenian hamster LEAF™ purified anti-mouse/rat CD29 (integrin β1) blocking antibody, specific integrin blocking peptides Gly-Arg-Gly-Asp-Asn-Pro (G**RGD**NP or RGD) and RAD control peptides Gly-Arg-Ala-Asp-Asn-Pro (G**RAD**NP) were

used at a concentration of 10 μg/ml. These blocking reagents were added to the cell suspension and cells incubated at 37 °C for 30 minutes prior to cell seeding for the cell adhesion assay.

Following incubation with the above reagents, the culture medium was gently aspirated and wells were washed once with PBS before fixing cells with 100 μl of 5% (v/v) glutaldehyde in dH_2O for 30 minutes. A standard curve was established by plating 1 x 10^5 cells/well, 0.5 x 10^5 cells/well and 0.25 x 10^5 cells/well onto uncoated or BSA treated wells, and fixing cells with 5 μl of 25% (v/v) glutaldehyde without washing.

The glutaldehyde solution was gently aspirated and wells were washed twice with dH_2O. Plates were blotted briefly on absorbent paper, 100 μl of 0.1% (w/v) crystal violet in PBS was added onto each well, and plates were incubated at room temperature for 1 hour. Wells were washed three times with 400 μL dH_2O before addition of 10% (v/v) acetic acid to dissolve intracellular crystal violet. Plates were shaken on a rocker at 100 rpm for 5 min at room temperature and the optical density was measured at 570 nm using Biotek plate reader (UK).

To measure cell spreading, 100 μl cell suspension, with a cell density of 1 x 10^5 cells/ml, was added to each well of a 96-well plate, and the plate incubated for 2 hour in a 37 °C humidified incubator. Cells were fixed (without removal of culture medium) with 20 μl 25% (v/v) glutaldehyde in dH_2O for 30 min at room temperature, washed three times with dH_2O, and plates were blotted briefly on absorbent paper. 100 μl of 0.1% (w/v) crystal violet in PBS was added to each well and plates incubated at room temperature for 1 hour. Cells were washed three times with 400 μl dH_2O and were maintained in PBS containing 0.05% (w/v) sodium azide. Cells were visualised by phase contrast microscopy. Rounded cells were counted as unspread, whilst spread cells appeared flat and phase dark.

5.2.4 Cell proliferation assay

The Bromodeoxyuridine (BrdU) cell proliferation assay kit was purchased from Calbiochem (UK). 96-well tissue culture plates were coated with appropriate ECM as described in section 2.1, and 100 μl rBEC suspension, (1 x 10^6 cells/ml) was added to each well. Cells were allowed to attach for 2 hours. BrdU reagent, 20 μl,

was added to each well, cells incubated for 18 hours, and the plate was inverted over the sink and gently blotted onto absorbent paper. Fixative/denaturing solution, 200 µl, was added to each well, cells incubated for 30 min at room temperature and the excess fixative/denaturing solution was removed. Anti-BrdU antibody in antibody diluent, 100 µl, was added to each well and plates incubated for 1 hour at room temperature. Cells were washed three times with 0.1% (w/v) chloroacetamide in PBS, and blotted gently onto absorbent paper. Peroxidase-conjugated goat anti-mouse IgG in conjugate diluents, 100 µl, was added to each well for 30 minutes. Wells were then washed with 0.1% (w/v) chloroacetamide in PBS and blotted gently onto absorbent paper. Wells were washed with 400 µl H_2O, and 100 µl tetra-methylbenzidine solution was added to each well after which plates were incubated for 15 min in the dark. A hundred microlitres of 2.5 N sulphuric acid was added to each well and the optical density of the samples measured using a Biotek plate reader (UK) (the optical density at 450 nm was subtracted from the optical density at 540 nm). Two control conditions were included in the cell proliferation assay: (i) no BrdU labeling reagent added to cells (ii) no cell monolayer but all reagents added.

5.2.5 Immunocytochemistry

To investigate focal adhesion formed by rBECs, cell suspension, 500 µl, were seeded at the density of 1 x 10^4 cells/ml onto ECM-coated glass coverslips, coverslips placed in a 24-well plate and incubated for 18 hours at 37 °C. Cells were then double immunostained for vinculin and phalloidin (actin) as described in Section 2.4.

5.2.6 Transendothelial electrical resistance measurement

rBECs were isolated, maintained, transferred to Transwell® inserts and co-cultured with astrocytes as described in Section 2.2.3. Following cell seeding onto ECM-coated Transwell® inserts, TEER was measured as described in Section 2.3 for four consecutive days.

5.3 Results

5.3.1 The effect of extracellular matrix proteins on adhesion of rat brain endothelial cells

Cell adhesion is the initial step before other cell activities such as cell differentiation, cell migration, cell growth and cell survival. Measuring the extent of cell adhesion can also help further elucidate rBEC-integrin interactions *in vitro*. Therefore, initially we investigated the effect of various ECM molecules on rBEC adhesion. The results showed that rBECs adhered to wells coated with type I collagen, type IV collagen, fibronectin, laminin-511 and the combination of laminin-411 and laminin-511 (1:1), with the extent of adhesion influenced by the amount of ECM protein used to coat the well (Figure 5.1). Adhesion of rBECs to ECM increased in response to an increasing amount of ECM used to coat plates. Cells did not adhere to uncoated tissue-culture plastic. Cells adhered to laminin-511, a combination of laminin-411 and laminin-511 (1:1), type I collagen and type IV collagen 30 min after seeding (Figure 5.1A). The extent of cell adhesion to those ECM proteins ranged from 76.8% to 92.8% when plates were coated with 2.5 pmol/cm^2 ECM protein. However, 56.7 ± 17.2% rBECs attached to surfaces treated with 2.5 pmol/cm^2 cellular fibronectin with 82.9 ± 20.6% attached at 10 pmol/cm^2. Whilst the majority of cells adhered onto 10 pmol/cm^2 type I collagen (92.4 ± 13.3%) and type IV collagen (84.3 ± 17.6%), cellular fibronectin (82.9 ± 20.6%), the combination of laminin-411 and 511 (94.1 ± 12.1%) and laminin-511 (98.4 ± 18.6%), only 19.3 ± 3.1% of cells adhered to 10 pmol/cm^2 laminin-411 coated wells at this 30 minutes time point. It is worth noting that cell attachment on 1.25 mol/cm^2 laminin-511 at 30-min time point was approximately 2-fold higher than that on the combination of laminin-411 and laminin-511 (1:1) (Figure 5.1A).

Ninety minutes following seeding, rBECs adhered very well to all ECM tested except laminin-411 (Figure 5.1B). Cell adhesion to type I collagen, type IV collagen, cellular fibronectin, laminin-511 and a combination of laminin-411 and laminin-511 (1:1) after 90 min incubation reached a plateau when 2.5 pmol/cm^2 ECM used (Figure 5.1B). At this plateau, between 60-80% of the total cells plated adhered to each ECM protein, with the exception of laminin-411 to which less that 7% of cells

adhered. Rat brain endothelial cells did not adhere to tissue culture plastic after 90 minutes incubation.

Figure 5.1 Attachment of rat brain endothelial cells to extracellular matrix proteins

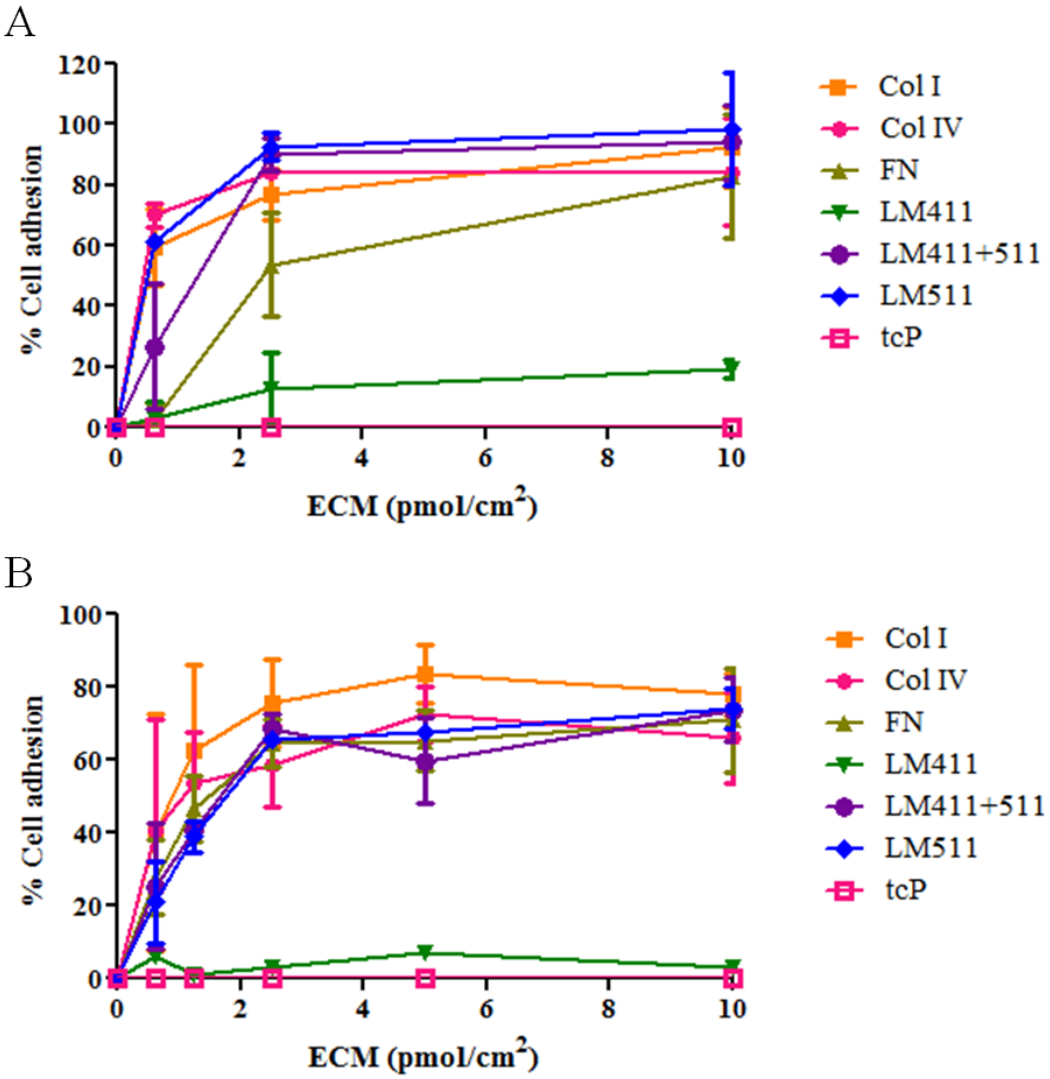

Plates were coated with ECM molecules from 6.25 to 100 pmol/cm^2 prior to cell seeding. Cells suspended in serum free medium were then seeded (1 x 10^5 cells/well) into 96-well plates coated with type I collagen (Col I), type IV collagen (Col IV), cellular fibronectin (FN), laminin-411 (LM411), combination of laminin-411 and laminin-511 (LM411+511), laminin-511 (LM511), or seeded onto tissue culture plastic (tcP) for 30 min (A) or 90 min (B) prior to measurement of cell adhesion. Data shown are the mean ± SD of three individual experiments.

5.3.2 The effect of extracellular matrix proteins on spreading of rat brain endothelial cell

Cell adhesion is usually followed by spreading of cells across the matrix surface. Rat brain endothelial cells were seeded onto ECM-coated 96-well plates for 2 hours. Cells were then fixed and stained with crystal violet. Images of cells under phase contrast microscopy were taken (Figure 5.2). Cells with a small, rounded compact morphology that were stained dark purple were classed as non-adherent or non-spreading cells whilst cells that displayed an expanded, flat morphology with faint staining were classed as spreading cells. Schematic illustrations of cell shapes are shown in Figure 5.3.

Most of the cells plated on type I collagen displayed a flat and round shape indicating cell spreading. Similarly, cells plated on type IV collagen were predominantly round and flat in morphology with lighter staining at the cell periphery and darker staining at the cell centre. A minority of the cells were fan-shaped and elongated. Cells plated on cellular fibronectin possessed a mainly round and flat morphology. Some of them clearly showed light staining at the cell periphery and dark staining at the cell centre. Fan-shaped cells were rarely seen. Cells plated onto laminin-511 and the combination of laminin-411 and laminin-511 (1:1) mainly displayed a round and fan-shaped morphology with light staining at the periphery and dark staining at the cell centre. Some of the cells had an elongated shape.

The percentage of spreading cells was also calculated. Type I collagen, type IV collagen, cellular fibronectin, the combination of laminin-411 and -511 (1:1) and laminin-511 promoted rBEC spreading compared to BSA-treated culture surface whereas cell spreading on laminin-411 and uncoated tissue culture plastic was not significantly different from that of BSA (Figure 5.2). Whilst there was no statistically significant difference in the extent of cell spreading for cells plated on type IV collagen compared to cells plated on type I collagen-coated wells, significantly higher cell spreading was observed for rBECs seeded onto laminin-511 and the combination of laminin-411 and laminin-511 (1:1) coated plates compared to cells on type I collagen-coated control wells. The extent of cells spreading observed for cells plated on laminin-411 coated wells was significantly less compared to cells

plated on type I collagen coated control wells. The extent of spreading of cells plated on cellular fibronectin did not differ significantly from the extent of spreading obderved for cell plated on type I collagen (control).

Figure 5.2 Cell spreading of rat brain endothelial cell culture

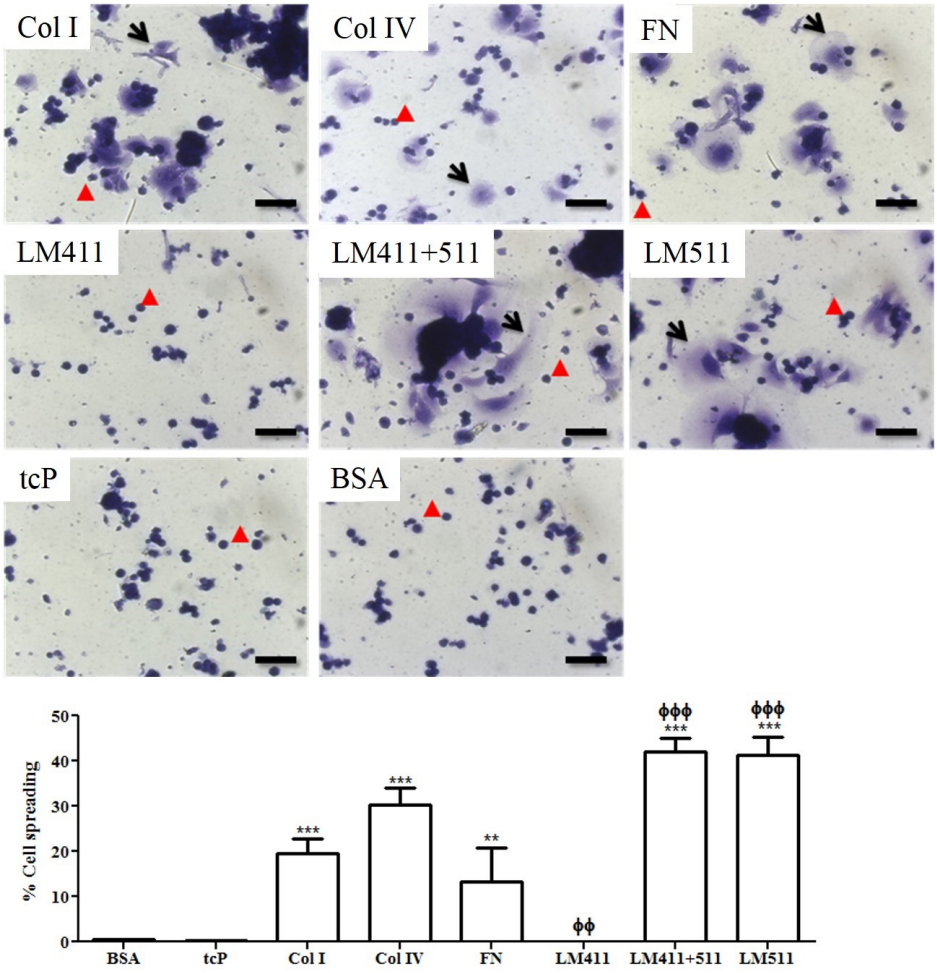

Cells were plated onto 96-well tissue culture plates coated with either type I collagen (Col I), type IV collagen (Col IV), cellular fibronectin (FN), laminin-411 (LM411), combination of laminin-411 and -511 (1:1) (LM411+511), laminin-511 (LM511), or onto uncoated wells (tcP). Cells on BSA-coated wells (BSA) were used as a control. Cells were allowed to adhere and spread for 2 hours before fixation and staining. Cells were visualised using a phase-contrast microscope. Three photos were randomly taken and spread (black arrows) and non-spread (red arrowhead) cells were quantified manually. Data were analysed using one-way ANOVA with Bonferroni post-hoc tests to compare treatment against percent cell spreading on BSA-treated surface, where $p<0.01$ ** and $p<0.001$ *** and to compare treatment against percent cell spreading on Col I where $p<0.01$ ϕϕ and $p<0.001$ ϕϕϕ. Data are the mean ± SD of three independent experiments. Scale bar represents 50 µm (100x magnification).

Figure 5.3 Schematic diagrams of spreading cell shapes

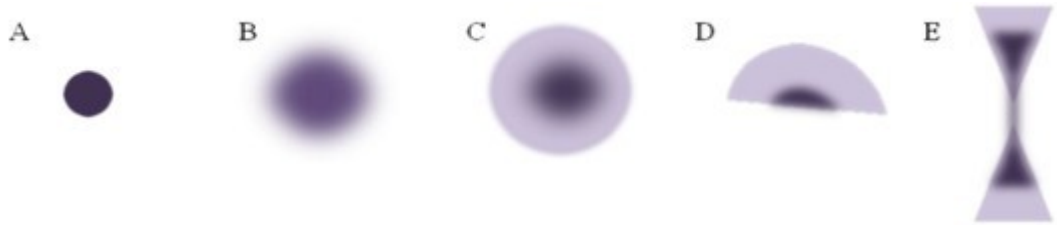

A: Non-spreading cells had round compact morphology with dark crystal violet staining.

B: Spreading cells had a round and flat morphology with the same shade of crystal violet staining at the cell periphery and the cell centre.

C: Spreading cells displayed round and flat morphology with light staining at the cell periphery and dark staining at the cell centre.

D: Fan-shaped cell with light staining at the cell periphery and dark staining at the cell centre.

E: Elongated cell shape.

5.3.3 Rat brain endothelial cells form focal adhesions with extracellular matrix proteins

To investigate whether rBECs formed focal adhesions in response to cell adhesion onto ECM proteins, rBECs were grown on ECM-coated coverslips. Cells were fixed and stained for actin and vinculin (section 2.4). Vinculin is a linker protein in the intracellular focal adhesion complex which connects ECM to the actin cytoskeleton. Due to its presence in both the initial state (dot) and mature state (dash) of focal contacts, vinculin is a suitable marker for investigating focal adhesion formation in cell cultures (Owen et al. 2005). Rat brain endothelial cells grown on all ECM proteins tested, except laminin-411, showed a spreading morphology (section 5.3.2). Rat brain endothelial cells did not adhere at all on uncoated glass coverslip. Thus focal adhesion of cells on laminin-411 and uncoated coverslip were not investigated in this section.

Focal adhesions were observed in cells with actin stress fibres visible by phalliodin staining (red) and positive immunoreactivity for vinculin (green) (Figure 5.4). Bright and punctate vinculin staining was evident in and around the nucleus area with dot, dash and plaque patterns throughout the cell cytoplasm, especially at the cell periphery. Phalloid-stained actin appeared as very fine fibres throughout cells. These could be observed on cells grown on every ECM tested. Actin bundles ended at the plaques of focal adhesions which appeared as yellow colouration in the composite images. Dash-like vinculin staining associated with actin fibres was mainly located at the edge of the cells.

Figure 5.4 Immunofluorescence microscopy of rat brain endothelial cells grown on extracellular matrix proteins

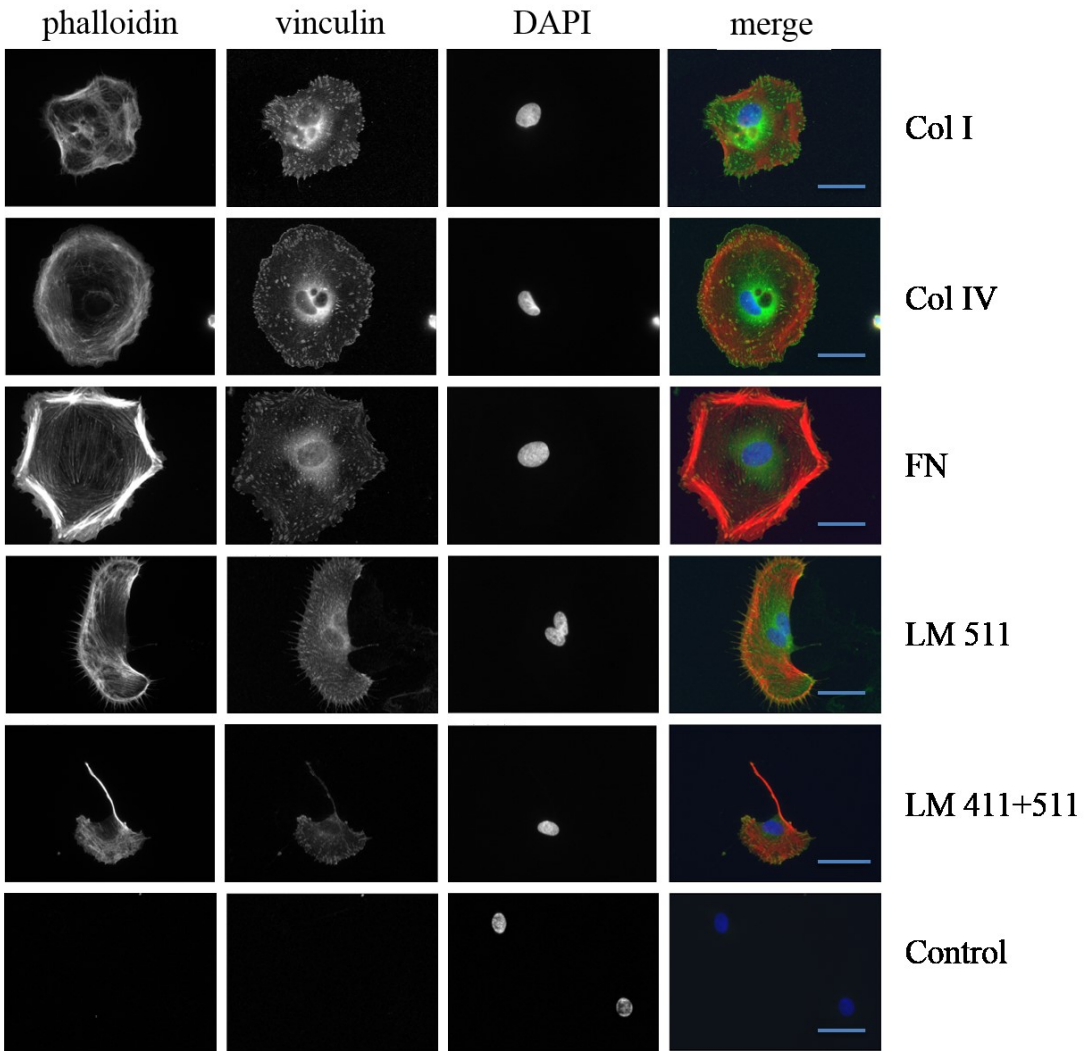

Primary cultures of rBECs on type I collagen (Col I), type IV collagen (Col IV), Cellular fibronectin (FN), laminin-511 (LM511) and the combination of laminin-411 and -511 (1:1) (LM 411+511)-coated coverslips were double labelled with phallodin to identify actin stress fibre (1st column), vinculin to identify focal adhesion (2nd column), and DAPI nuclei stain (3rd column). Images of the fourth column represent the composites of actin (red), vinculin (green) and DAPI (blue). Image U-X are the negative control. Inset windows show 2.5x zoom image of the area in thewhite box white box. Cells displayed stress fibres connected with vinculin (arrows). Scale bars represent 50 μm (600x magnification)

.

5.3.5 Integrin β1 and RGD peptide-mediated interactions between rat brain endothelial cells and the extracellular matrix

Binding between cells and ECM proteins is largely mediated by integrins. It has been reported that the subtype of integrin-mediated endothelium-ECM interaction is mainly integrin β1 (Kramer et al., 1990, Languino et al., 1989). ECM proteins such as fibronectin contain a short peptide sequence "RGD" which is important for ECM-integrin interaction. Here we have investigated whether integrin β1 is involved in cell-ECM binding using blocking antibody and peptide.

rBEC attachment to type I collagen, type IV collagen, cellular fibronectin, laminin-511 and the combination of laminin-411 and laminin-511 (1:1) was assessed in the presence of GRGDSP peptide (cell recognition site of fibronectin), GRADSP control peptide or anti-integrin β1 blocking antibody.

Attachment of rBECs to type I collagen was significantly inhibited by anti-integrin β1 blocking antibody (51.0 ± 1.7% compared to 100% adhesion with PBS control, Figure 5.5A). On the other hand, the GRGDSP peptide had no significant effect on rBEC attachment to type I collagen compared to the GRADSP control peptide (Figure 5.5A).

Adhesion of rBECs to type IV collagen was significantly inhibited by anti-integrin β1 blocking antibody by 74.2 ± 1.7% compared to 100% PBS control, whereas GRGDSP peptide had no significant effect on cell adhesion (Figure 5.5B).

As expected, addition of GRGDSP blocking peptide at 10 μg/ml significantly inhibited rBEC adhesion to cellular fibronectin by 62.2% (i.e. 33.8 ± 11.2% adhesion compared to 100% adhesion with PBS) (Figure 5.5C). GRADSP peptide, which was used as a control peptide, had no effect on rBEC adhesion to fibronectin (Figure 5.5C). Likewise, anti-integrin β1 blocking antibody at 10 μg/ml significantly inhibited cell adhesion to cellular fibronectin by 20.8% compared to control (i.e. 79.3 ± 8.6% adhesion compared to 100% adhesion with PBS (Figure 5.5C).

Adhesion of rBECs to laminin-511-coated wells was not inhibited by either anti-integrin β1 blocking antibody or GRGDSP peptide (Figure 5.5D). Neither anti-integrin β1 blocking antibody, GRGDSP blocking peptide nor GRADSP control peptide significantly affected cell attachment onto the combination of laminin-411 and laminin-511 (1:1) (Figure 5.5E).

Figure 5.5 Effect of functional blocking antibody, GRADSP and GRGDSP on adhesion of rat brain endothelial cells to extracellular matrix proteins

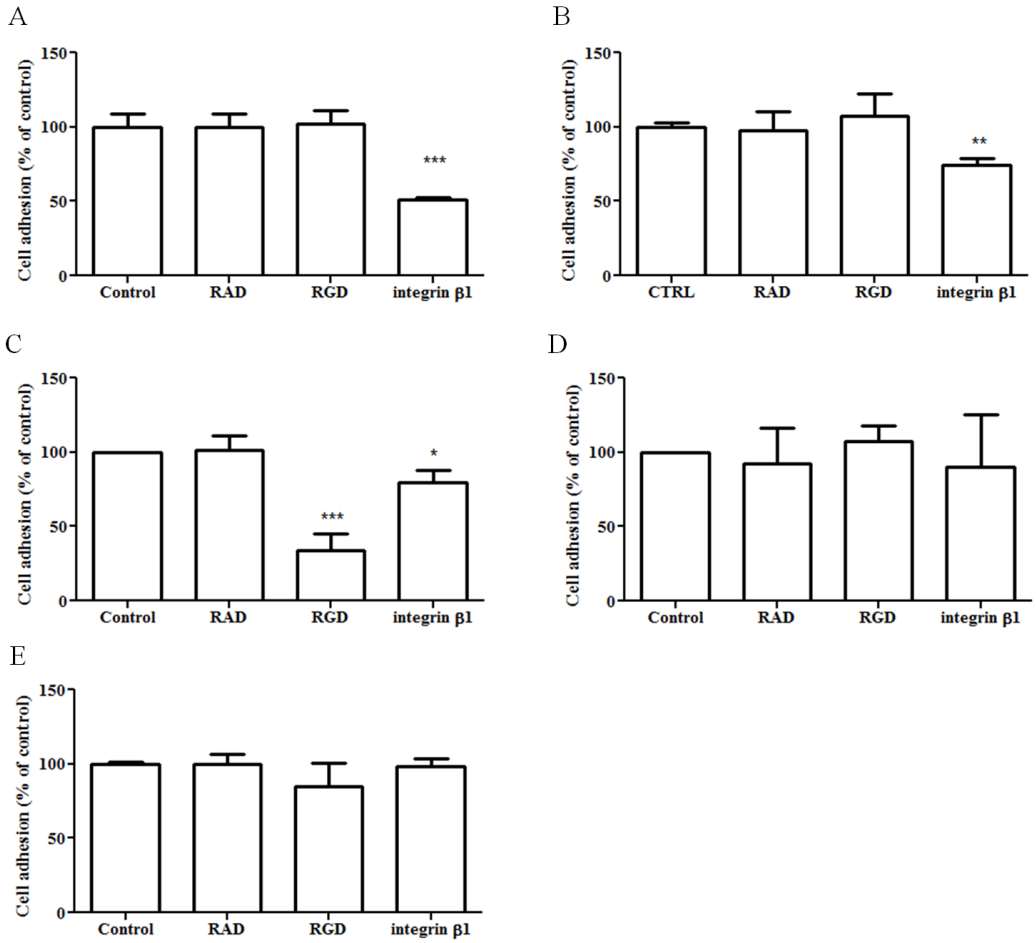

Rat brain endothelial cells in DMEM were incubated with either PBS (control), or PBS-containing integrin blocking antibodies (integrin β1, 10 µg/ml), GRGDSP blocking peptide (RGD, 10 µg/ml) or GRADSP control peptide (RAD, 10 µg/ml) for 30 minutes prior to cell seeding onto type I collagen (A), type IV collagen (B), cellular fibronectin (C), laminin-511 (D) and the combination of laminin-411 and laminin-511 (E) coated 96-well plates. Data were analysed using one-way ANOVA with Bonferroni's post-hoc tests to compare data with percentage cell adhesion of the control where *= $p<0.05$ and ***= $p<0.001$. The data of three individual experiments are shown as mean ± SD.

5.3.4 Extracellular matrix proteins affect proliferation of rat brain endothelial cells

Endothelial cell proliferation is a crucial step of angiogenesis which generally occurs during the tissue repair process after injury and inflammation. Defective proliferation of endothelial cells may therefore interfere the wound healing process. It is known that the ECM can positively or negatively affect endothelial cell proliferation. Our *in vitro* BBB model may therefore prove a useful system to investigate the effects of ECM components on endothelial cell profileration and establish whether the effects observed *in vitro* reflect reported changes in endothelial cell proliferation *in vivo*.

To evaluate the effect of vascular matrix proteins on rBEC proliferation *in vitro*, we investigated the proliferation rate of rBECs grown on ECM proteins using a BrdU ELISA kit (section 5.2.2). There was no significant difference in proliferation rate between cells grown on type I collagen, type IV collagen and cellular fibronectin (Figure 5.6). The proliferation rate of rBECs plated onto laminin-411 coated wells was significantly lower ($p < 0.001$) compared to cells grown on type I collagen (Figure 5.6). On the contrary, rBEC adhesion to laminin-511 and the combination of laminin-411 and laminin-511 (1:1) significantly ($p < 0.001$) increased cell proliferation compared to rBECs grown on type I collagen (Figure 5.6).

Figure 5.6 The effect of extracellular matrix on rat brain endothelial cell proliferation

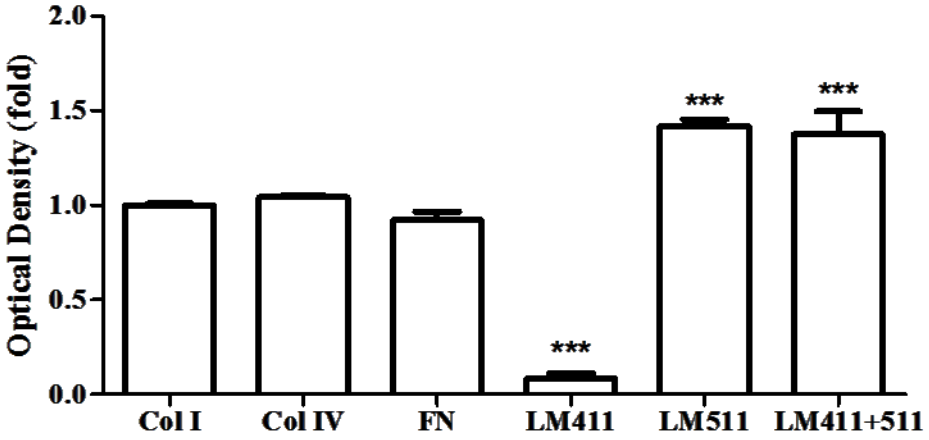

Cells were seeded (1 x 10^5 cells/well) onto ECM-coated 96-well plates and incubated overnight at 37ºC. Proliferation of rBEC was measured by BrdU ELISA. Data were analysed using one-way ANOVA with Bonferroni's post-hoc tests to compare data against optical density of the cells seeded onto collagen I. Data show the mean ± SD fold change in cell proliferation of cells on type IV collagen (Col IV), cellular fibronectin (FN), laminin-411 (LM411), laminin-511 (LM511) and laminin-411 and -511 (LM411+511) compared to that of cells on type 1 collagen (Col I) (*** = $p<0.001$).

5.3.5 Laminin-511 increased transendothelial electrical resistance of rat brain endothelial cell monolayers

The ECM components in the basal lamina provide structural support for the cellular component of the BBB. Formation of restrictive tight junctions is essential for a viable BBB and we hypothesised that the ECM proteins play an important role in BBB integrity by providing archoring sites and in helping regulate the actin cytoskeleton. It has been demonstrated that the TEER of brain endothelial cells was modulated by ECM proteins (Tilling et al., 1998). However, the effects of laminin-411 and laminin-511, the main vascular laminin isoforms, on the TEER of brain endothelial cell monolayers has not been reported. We investigated whether ECM proteins had an effect on barrier properties of rBECs in culture. Rat brain endothelial cells were plated onto type I collagen, type IV collagen, a combination of laminin-411 and laminin-511 (1:1), laminin-511 and fibronectin-coated Transwell® inserts (section 5.2.2). The transendothelial electrical resistance (TEER), a reflection of the barrier property of the monolayers, was assessed daily for four consecutive days.

The TEER of cell monolayers increased over time from approximately 30-45 $\Omega \cdot cm^2$ on the first day to approximately 69-108 $\Omega \cdot cm^2$ on the fourth day of culture (Figure 5.7). On Day 1, TEER values of the cell monolayers grown on type I collagen, type IV collagen, cellular fibronectin, a combination of laminin-411 and laminin-511 (1:1)and laminin-511 were 33, 35, 30, 43 and 45 $\Omega \cdot cm^2$, respectively. There was no significant difference between the electrical resistances of the rBEC monolayers grown on different ECM proteins at this time point. On day 2 of culture, rBEC monolayers grown on laminin-511-coated Transwell® inserts had significantly higher TEER compared to the TEER of the monolayers grown on type I collagen coated Transwell® (78 and 51 $\Omega \cdot cm^2$, respectively), Figure 5.7. The TEER of the monolayers grown on type IV collagen and cellular fibronectin did not differ significantly from the TEER of cells grown on type I collagen (57, 46 and 51 $\Omega \cdot cm^2$, respectively), Figure 5.7. The TEER of cells grown on a combination of laminin-411 and laminin-511 (1:1) was similar to the TEER of cells grown on laminin-511 alone (74 and 78 $\Omega \cdot cm^2$ respectively). However, the TEER of cells grown on a combination of laminin-411 and laminin-511 (1:1) was not statistically significantly different from the TEER of cells grown on type I collagen (Figure 5.7).

Likewise, on the third and the fourth days of culture, monolayers grown on laminin-511-coated Transwell® inserts had a significantly higher TEER compared to that of monolayers grown on type I collagen-coated Transwell® inserts (100 and 72 $\Omega \cdot cm^2$ on the third day, and 108 and 75 $\Omega \cdot cm^2$ on the fourth day) while TEER of monolayers grown on type IV collagen and cellular fibronectin did not differ significantly from the control cell monolayers grown on type I collagen.

Again, cell monolayers grown on a combination of laminin-411 and laminin-511 (1:1) had a similar TEER to monolayers grown on laminin-511 alone (91 and 100 $\Omega \cdot cm^2$ on the third day, and 96 and 108 $\Omega \cdot cm^2$ on the fourth day) however these were not statistically different from the TEER of monolayers grown on type I collagen (Figure 5.7).

Figure 5.7 Transendothelial electrical resistance of rat brain endothelial cell monolayers grown on extracellular-coated Transwell® inserts

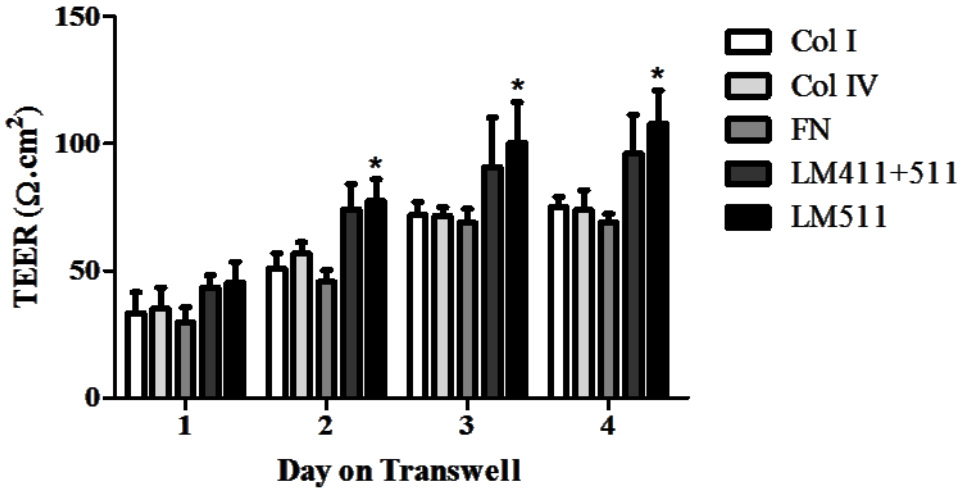

Cells were seeded on to ECM-coated Transwell® inserts. TEER measurements were performed daily using EVOM Epithelium Voltohmmeter electrodes for 4 days. TEER of cell monolayers grown on type IV collagen (Col IV), cellular fibronectin (FN), laminin-511 (LM511) and the combination of laminin-411 and laminin-511 (1:1) (LM411+511) were compared to control cell monolayers grown on type I collagen (Col I) and analysed using one-way ANOVA with Bonferroni's post-hoc tests. *=$p<0.05$. Data shown are the mean ± SD of five independent experiments.

5.3.6 Modulation of cell organisation by extracellular matrix proteins

Rat brain endothelial cells in culture largely displayed a spindle-shaped morphology and were tightly apposed to each other. Interestingly, cellular adhesion to different ECM proteins triggered marked differences in rBEC cellular organisation at confluency. Cells grown on laminin-511 and the combination of laminin-411 and laminin-511 (1:1) demonstrated neat cell alignment and formed classical monolayers (Figure 5.8). On the other hand, cell monolayers grown on type I collagen type IV collagen and fibronectin sometimes displayed multilayer-like organisation. Around the cell margin, cells formed crooked tight junctions and they had a small cobblestone-like morphology. Nuclei also appeared clumped, reflecting either overlapping or tightly apposed cells. Further studies of confluent cell monolayers grown on type I collagen (Figure 5.8: Col I, 6 days) revealed large areas of crooked tight junctions, multilayer-like structures and tube-like structures formed by spindle shaped cells.

Figure 5.8 Immunocytochemical detection of ZO-1 in rat brain endothelial cells

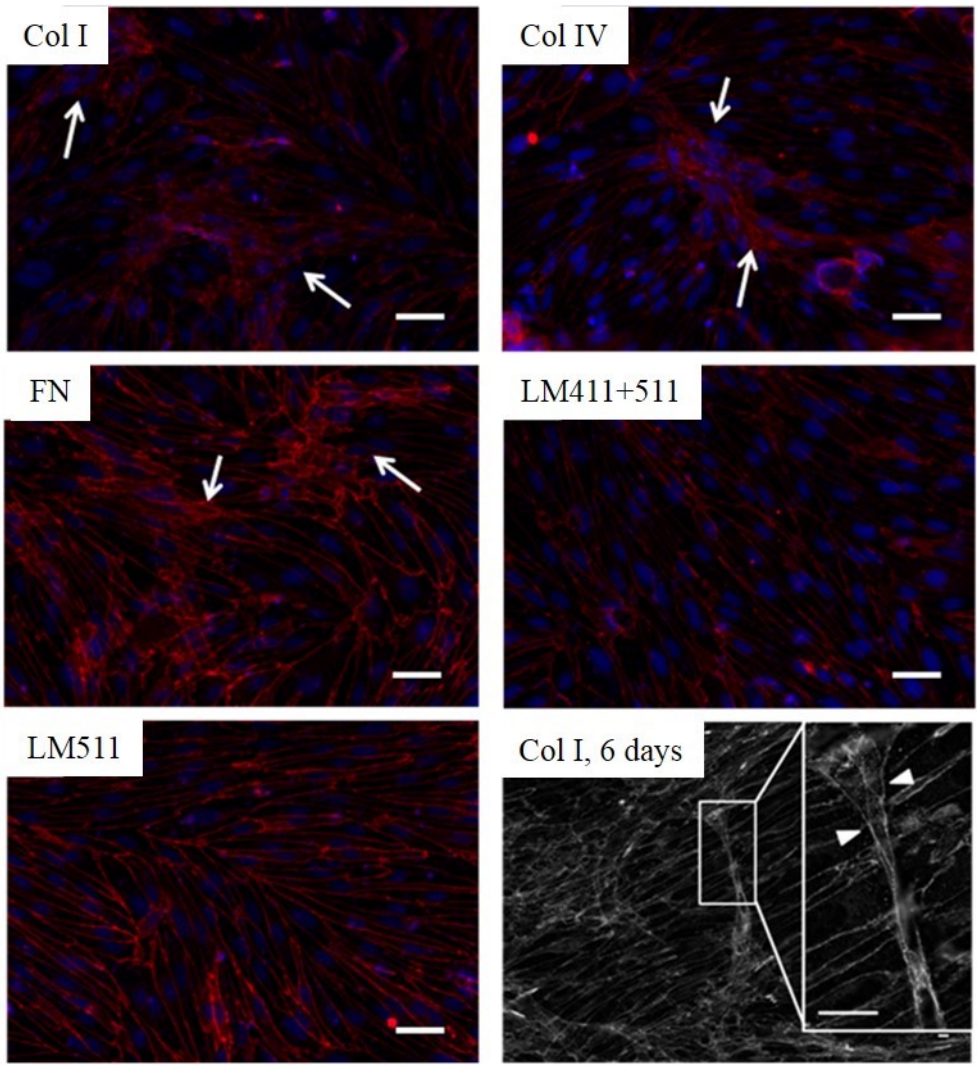

Rat brain endothelial cell monolayers were grown on type I collagen (Col I), type IV collagen (Col IV) cellular fibronectin (FN), laminin-411 and laminin-511 (1:1) (LM411+511) and laminin-511 (LM511) coated Transwell® inserts for 4 or 6 days. Cells were fixed with 4% (w/v) paraformaldehyde and 4% (w/v) sucrose in PBS and incubated with rabbit anti-ZO-1 antibody (red) and DAPI (blue) in images A-E. Image F, cells were probed for ZO-1. Digital pictures were taken with a Coolsnap ES camera through MetaVue software following visualization with an Olympus BX51 microscope. Cell multilayers are indicated by arrows; tube-like structure is indicated by arrowheads. Images shown are representative of three independent experiments. Scale bar = 50 µm (200x magnification).

5.4 Discussion

Brain endothelial cells require attachment to appropriate ECM proteins in order to correctly express their phenotype and maintain their normal functions. In this study, we investigated the effects of ECM on rBEC behaviour including cell morphology, cell adhesion, proliferation, barrier properties and cell organisation by growing cells on a variety of vascular ECM proteins including laminin-411, laminin-511, type IV collagen and fibronectin. Firstly, we investigated the ability of cells to adhere to vascular ECM proteins. It was observed that rBECs attached rapidly to some vascular ECM tested namely type IV collagen, cellular fibronectin, laminin-511 and the combination of laminin-411 and laminin-511 (1:1) as compared to plastic. This confirms that vascular ECM proteins including type IV collagen, fibronectin and laminin-511 promote cell adhesion (suggesting rBECs expressed ECM receptors that are specific to the vascular ECM tested). Unexpectedly, the extent of adhesion of rBECs to laminin-411 coated surface was comparable to that of uncoated plastic.

Quantitation of cell spreading on ECM proteins is another method to assess cell-substrate adhesion. While adhesion of rBECs to type I collagen, type IV collagen, cellular fibronectin, laminin-511 and the combination of laminin-411 and laminin-511 (1:1) was at a similar level, the extent of cell spreading was ECM protein-dependent. We demonstrated that laminin-511 and the combination of laminin-411 and laminin-511 (1:1) promote greater rBEC spreading compared to type I collagen whereas cell spreading on type IV collagen and cellular fibronectin induced comparable cell spreading compared to cell spreading on type I collagen. This indicates that cells demonstrated a greater interaction with laminin-511 and the combination of laminin-411 and laminin-511 (1:1) compared to other ECM tested. Cells plated on laminin-411 did not adhere, thus did not spread.

Laminin-411 and laminin-511 are the main ECM components in the central and peripheral basal lamina (Sixt et al, 2001; Wu et al., 2009). However, a number of previous studies have investigated the effects of laminin acquired from Engelbreth-Holm-Swarm or laminin-111 on endothelial cell behaviour. The lack of studies using laminin-411 and laminin-511 is probably because the purified human recombinant laminin-411 and laminin-511 with correct protein conformation, has only recently

become commercially available (Doi et al., 2002, Kortesmaa et al., 2000). Increasing evidence suggests distinctive interactions between cells and different isoforms of laminins. For example, cells of a T cell line adhered to laminin-411 and laminin-511, but not to laminin-111 and laminin-211 (Sixt et al., 2001). Laminin-111 and laminin-511 promoted mouse DRG neuronal growth *in vitro* whereas cells rarely grew on laminin-211 and laminin-411 (Plantman et al., 2008). In this study, we demonstrated the very distinctive effect of laminin-411 and laminin-511 on rBEC adhesion, and our findings are consistent with the reports of others as mentioned above. Laminin-411 and laminin-511 share the β and γ chains. The laminin α4 chain has a truncated N-terminal whereas the laminin α5 chain possesses a full-length N-terminal domain. The domains at the N-terminal of laminin chains are involved in self-polymerisation (Odenthal et al., 2004) and also serve as integrin binding sites (Nielsen and Yamada, 2000). Preferential adhesion of cells to laminin-511 compared to laminin-411 may be due to tight interconnection of laminin molecules (Sorokin, 2010) or that rBEC integrins mainly bind to the N-terminal domains of alpha chains (Nielsen and Yamada, 2000).

A study by Tilling et al. (2002) demonstrated that type IV collagen, plasma fibronectin and laminin-111 induced comparable adhesion of pBECs. However, they have shown that fibronectin had a superior effect on cell spreading compared to type IV collagen and laminin-111. Another study on adhesion of rBECs *in vitro* by Wang and Milner (2006) showed that fibronectin promoted the highest cell adhesion compared to type IV collagen and laminin-111 following one to three day incubations. We however, did not find fibronectin to promote increased cell adhesion compared to type I collagen. This may be due to the plate coating method. We coated plates with equal molar ratios of ECM proteins whereas other studies coated surfaces with equal weight of ECM proteins. Molecular weights of type I collagen, type IV collagen, cellular fibronectin, laminin-411 and laminin-511 are approximately 400, 500, 440, 640 and 820 kDa, respectively. Therefore, in our studies laminin-511 was coated to the surface at a higher amount by weight compared to other ECM proteins. As with previous studies, we also found that rBEC attachment was depended on the amount of ECM used to coat plates.

The study by Ingber and Folkman (1989) reported capillary endothelial cells adhered well to surfaces coated with 500 ng/cm^2 fibronectin, but cells remained detached when surfaces were coated with less than 100 ng/cm^2 (Ingber and Folkman, 1989). These findings suggest that the amount of ECM can greatly affect cell adhesion. Moreover, our studies showed that rBECs seeded onto plastic adhered and spread following an 8-hour incubation whereas rBECs seeded onto laminin-411 did not adhere, even after 2 days of incubation. From the previous chapter, we have demonstrated that rBECs were able to produce and secrete cellular fibronectin. Therefore, cells plated onto plastic may initially adhere loosely and then later produce adhesive ECM proteins.

Rat brain endothelial cells were not able to attach to laminin-411 thus were not able to secrete basal lamina ECM proteins. In addition, rBEC adhesion on 12.5 pmol/cm^2 laminin-511 was double that observed on a combination of 6.25 pmol/cm^2 laminin-411 and 6.25 pmol/cm^2 laminin-511 after 30 min incubation, but there was no significant difference in the extent of adhesion in the two conditions after 90 min of incubation.

Brain endothelial cells anchor to ECM proteins via cellular matrix receptors, integrins. Expression of integrin subunits in brain endothelial cells is shown in Table 1.2. Brain endothelial cells *in vivo* are found to express a set of integrins including integrin α1 (Tagaya et al., 2001, Sixt et al., 2001), α2, α3, α5, α6 (Paulus et al., 1993), β1 (Paulus et al., 1993, Tagaya et al., 2001), β3 and β4 (Paulus et al., 1993). It has been clearly demonstrated that integrin β1 is expressed by brain endothelial cells and astrocytes throughout normal brain vasculature (Paulus et al., 1993, Milner and Campbell, 2002, Haring et al., 1996, Grooms et al., 1993). Also, integrin α1 and α6 have been shown to localise in brain endothelial cells in a similar pattern to integrin β1, indicating that the main integrin expression pattern in endothelial cells is α1β1 and α6β1 (Milner and Campbell, 2006). Other integrins including α3β1, α5β1 and αvβ3 are also expressed in basal lamina underlining endothelial cells (Wang and Milner, 2006). In addition to integrins, Sixt et al. (2001) has also showed by immunohistochemistry that cerebral endothelial cells *in vivo* abundantly expressed β-dystroglycan. Integrin β1 is expressed by the endothelium in all cerebral vasculature (Sixt et al., 2001) and can interact with all key vascular ECM proteins including

laminins, collagens and fibronectin (Haring et al., 1996, Tagaya et al., 2001). Moreover, studies show a loss of endothelial integrin β1 expression in the ischemic brain, especially in the area of the ischemic core, of the primate MCAO model. These findings may suggest an important role of this integrin in the pathological state of the CNS (Tagaya et al., 2001). The majority of ECM proteins contain an RGD sequence as a key integrin recognition site (Ruoslahti, 1996). Therefore, we hypothesised that rBEC adhesion to vascular ECM proteins is mainly mediated by the RGD motif.

Cell binding to type IV collagen is generally mediated by integrin α1β1, α2β1, α10β1 and α11β1 (Vandenberg et al., 1991, Kramer and Marks, 1989, Leitinger and Hohenester, 2007, Kern et al., 1993). Our results showed that attachment of rBECs to type I collagen and type IV collagen was mediated by integrin β1. However, rBEC adhesion to type IV collagen was not inhibited with blocking RGD peptide. Although type IV collagen contains several RGD sequences, many studies have demonstrated that cellular adhesion to type IV collagen is not mediated by an RGD sequence (Herbst et al., 1988, Vandenberg et al., 1991, Kramer and Marks, 1989, Kim et al., 1994). It has been report that blocking RGD did not inhibit cell adhesion to type IV collagen (Vandenberg et al., 1991). One possible hypothesis is RGD sequences are located internally in the type IV collagen molecule, making it inaccessible to cellular receptors (Aumailley and Timpl, 1986, Santoro, 1986, Perris et al., 1993).

We have also investigated cell adhesion to cellular fibronectin. Many integrins mediate cell-fibronectin adhesion including α3β1, α4β1, α5β1, α8β1, αvβ1, αvβ3, αvβ6, αvβ1, αvβ3, αvβ6 and α4β7 (Johansson et al., 1997). Most of them recognise the RGD peptide in the cell-binding domain of fibronectin. Some of the integrins such as α4β1 and α4β7 can interact with the Leu-Asp-Val (LDV) sequence in the V region of fibronectin (Leiss et al., 2008, Humphries et al., 2006). Wang and Milner (2006) clearly demonstrated that brain endothelial cell adhesion to fibronectin was mediated by the RGD sequence, integrin α5β1 and integrin αvβ3 (Wang and Milner, 2006). Combined blocking of integrin β1 and β3 inhibits almost all rBEC adhesion to fibronectin. Accordingly, we showed that cell attachment to fibronectin was inhibited by both anti-integrin β1 antibody and blocking RGD peptide.

Most rBECs adhere strongly to laminin-511. They also spread very well on laminin-511 compared to type I collagen. Cell adhesion to laminin-511 is reported to be mediated by integrin α2β1, α3β1, α6β1, α6β4 and αvβ3 (Doi et al., 2002, Pouliot et al., 2000, Nigatu et al., 2006, Chia et al., 2007, Kawataki et al., 2007, Genersch et al., 2003b, Sasaki and Timpl, 2001). It is also reported that dystroglycan (Ferletta and Ekblom, 1999) and Lutheran blood group/basal cell adhesion molecule (Lu/BCAM) (Mankelow et al., 2007, Kikkawa et al., 2011) can recognise laminin-511. It has been reported that cerebral endothelial cells express potential laminin-411 and laminin-511 receptors including integrin α6β1 (Sixt et al., 2001), integrin α3β1 (Doi et al., 2002) and αvβ3 (Li et al., 2012). Brain endothelial cells also abundantly express Lutheran blood group antigen (Boado et al., 2000). A study by Kortesmaa et al. (2000) demonstrated that immortalised brain endothelial cell adhesion to laminin-411 was mediated by integrin α6 (Kortesmaa et al., 2000). Cell adhesion to laminin-511 is potentially mediated by α3β1 according to a study by Doi et al. (2001), which reported that adhesion of many types of endothelial cells, including HT-1080 and human saphenous vein endothelial cells, to laminin-511 were mainly mediated by integrin α2β1 and α3β1. Doi et al also investigated the role of RGD peptide in endothelial cell adhesion. Neither RGD nor cyclic RGD peptide had any inhibitory effect on cell adhesion (Doi et al., 2002). This is consistent with our study in which although the laminin α5 chain contains an available RGD sequence for cell binding, RGD blocking peptide did not inhibit cell adhesion. However, our studies show rBEC adhesion to laminin-511 was not blocked by anti-β1 integrin.

Determination of which integrins mediate rBEC adhesion to laminin-511 will require further investigation, perhaps using flow cytometry to identify integrin expression on rBECs or the use of additional integrin-blocking antibodies. Also, the use of a combination of two integrin subtype blocking antibodies may help elucidate the mechanism of rBEC- laminin-511 interaction.

Cell anchorage to ECM has been long known to have a crucial regulatory role in cell proliferation. The cell cycle is mainly regulated by cyclin-dependent kinase complexes. Cellular adhesion to ECM has been found to affect many functional components of cell cycle progression including cyclins (Zhu et al., 1996), cyclin-dependent kinases (Zhu et al., 1996, Orend et al., 2003) and cyclin-dependent kinase

inhibitor proteins (Orend et al., 2003). We found that rBECs proliferate more when plated onto laminin-511 and a 1:1 combination of laminin-411 and laminin-511-coated surfaces compared to type I collagen. This effect was not found in cells seeded onto cellular fibronectin and type IV collagen.

Cell shape is one of the main factors reflecting cell proliferation (Huang and Ingber, 2000, Kulesh and Greene, 1986, Folkman and Moscona, 1978). It has been demonstrated that anchorage-dependent cells with a flat spreading morphology, rather than adhered round cells, are designated to proliferate (Folkman and Moscona, 1978, Kulesh and Greene, 1986). Since laminin-511 and the combination of laminin-411 and laminin-511 (1:1) induced, rBECs spreading, it is possible that these ECM proteins stimulate cell proliferation. Many *in vitro* studies have demonstrated ECM-dependent proliferation of endothelial cells and other cell types (Ingber and Folkman, 1989, McIntosh et al., 1988, Ingber, 1992). A study by Wang and Milner (2006) showed that fibronectin, but not type I collagen, type IV collagen or laminin-111, significantly promoted primary rBEC proliferation compared to uncoated glass (Wang and Milner, 2006). However, in our studies, fibronectin did not seem to promote proliferative effect over collagen and laminins. In our study, we compared proliferation of rBECs plated onto vascular ECM with proliferation of cells on control matrix, namely type I collagen (in our studies tissue-culture plastic not glass was coated with ECM protein).

Both tight junction formation and cell-to-ECM adhesion affect blood-brain barrier integrity. Evidence suggests a role of ECM proteins in regulation of tight junction function. For example, cell grown on collagen (compared to cell grown on uncoated surface) enhanced TEER and the level of ZO-1 phosphorylation in the A6 epithelial cell line (Jaeger et al., 1997). Cell growth on laminin was found to reduce the passage of [^{3}H]inulin through a human keratinocyte cell line, reflecting promotion of tight junction formation (Weeks and Friedman, 1997). We have demonstrated that the TEER of the rat *in vitro* BBB model was modulated by some of the vascular ECM proteins investigated. Cell monolayers grown on laminin-511 demonstrated significantly higher TEER (108.0 ± 28.9 $\Omega \cdot cm^2$) compared to cell monolayers grown on type I (74.02 ± 17.1 $\Omega \cdot cm^2$). The TEER of cell monolayers grown on a 1:1 mixture of laminin-411 and laminin-511, 96.18 ± 33.8 $\Omega \cdot cm^2$, was similar to cells

grown on laminin-511 but was not significantly higher than the TEER of cell monolayers grown on type I collagen control. Rat brain endothelial cell monolayers grown on type IV collagen and on cellular fibronectin demonstrated comparable TEER to cell monolayers grown on the non-vascular ECM protein type I collagen (74.02 ± 17.1 $\Omega \cdot cm^2$, 69.01 ± 7.59 $\Omega \cdot cm^2$, 75.2 ± 8.73 $\Omega \cdot cm^2$ respectively). Rat brain endothelial cells did not adhere to uncoated Transwell® insert at all. Type I collagen is used as reference substrate in the study to aid cell adhesion because it is absent from the brain basement membrane. From the results we can conclude that vascular ECM proteins are an important factor effecting barrier formation *in vitro*.

A study by Tilling et al. (1998) found that pBEC monolayers grown on ECM proteins including fibronectin, laminin-111 and type IV collagen demonstrated significantly higher TEER compared to monolayers grown on type I collagen. These findings clearly demonstrate the important role of vascular ECM proteins in the development BBB phenotype of the brain endothelial cells (Tilling et al., 1998).

However, in the study of Tilling et al. (1998), the effect of ECM protein on TEER appeared to be dependent on initial TEER of cell monolayers (Tilling et al., 1998). In cell monolayers demonstrating relatively low TEER (approximately 350 $\Omega \cdot cm^2$) vascular ECM proteins increased TEER 2-3 fold whilst in cell monolayers with high TEER (approximately 1000 $\Omega \cdot cm^2$) the effect was much less pronounced, with an approximate 1.1-fold change in TEER. The authors hypothesised that endothelial culture with high TEER had reached a maximal TEER (equal to the TEER obtained *in vivo*) thus vascular ECM proteins did not further increase the TEER of the cell monolayers. The authors concluded that growing cerebral endothelial cells on vascular endothelial ECM proteins produced a more consistent *in vitro* barrier compared to plating cells onto a non-vascular basement membrane.

In our studies, we have developed an *in vitro* model with TEER values consistently at approximately 100 $\Omega \cdot cm^2$. Initially, the TEER of our model was quite low (66.2 ± 4.0 $\Omega \cdot cm^2$) but with hydrocortisone supplementation, the TEER of our model grown on type I collagen ranged from approximately 99.2 ± 8.2 $\Omega \cdot cm^2$.

When cells reached confluency, we noticed that rBECs grown on type I collagen, type IV collagen and cellular fibronectin displayed distinctive features including multilayering, a cobblestone shape, crooked tight junction and clumped nuclei. This

appearance could be seen in small areas of approximately 10-15 cells throughout the culture. However, cells grown on laminin-511 and the combination of laminin-411 and laminin-511 (1:1) grew as monolayers with spindle-like morphology and no clumping of nuclei nor crooked tight junctions.

We also noted that when post-confluent, cells grown on type I collagen organised into a capillary-like structure overlaying the cell monolayer. Generally, endothelial cells in culture grow until confluent and then cell division is inhibited by cellular contact (D'Amore, 1992, Gimbrone et al., 1974, Heimark and Schwartz, 1985). However, many studies have demonstrated tube formation by endothelial cells in culture. The first study to demonstrate angiogenesis *in vitro* is by Folkman and Haudenschild (1980) (Folkman and Haudenschild, 1980). They showed that pure human endothelial cells after growing in culture for a while in tumour conditioning medium could develop a tube-like structure overlaying the confluent endothelial monolayer. Another study by Montesano et al. (1983) demonstrated rapid tube formation of an adrenal cortical endothelial cell line grown on collagen matrix (Montesano et al., 1986). However, in this case, the capillary-like structures did not overlay on top of confluent cells as we found in our study.

Angiogenesis can be divided into three main steps. Initiation of angiogenesis usually involves vasodilation and matrix degradation. Then secondly, endothelial cells migrate and proliferate. The last step is maturation of the vessels. Therefore, tube formation by cells in culture could be caused by factors involved in angiogenesis, such as the activity of matrix proteases including plasminogen activator and collagenase (for review see (Folkman and Haudenschild, 1980)), VEGF (Berthod et al., 2006) and interaction of integrins with ECM molecules (Dixelius et al., 2004, Gamble et al., 1999, Gamble et al., 1993). It is possible that laminin-411 and laminin-511 promote proliferation in the angiogenic state and when cells become confluent these ECM molecules provide appropriate conditions for the vessel to mature. Although ZO-1 immunofluorescent images of post-confluent rBEC in culture suggest tube-like formation, this still requires further investigations such as confirmation of lumen formation using electron microscopy. In addition, identification of the factors responsible for inducing tube formation in the culture would be extremely interesting.

Chapter 6 Effects of extracellular matrix molecules on rat brain endothelial cell monolayer following interleukin-1β treatment

6.1 Introduction

Neuroinflammation has been implicated in acute and chronic neurodegeneration. A proinflammatory cytokine, IL-1 greatly contributes to brain damage following many brain pathological conditions. The role of IL-1 in stroke models has been clearly demonstrated. IL-1 gene expression and IL-1 protein (Zhang et al., 1998) is found in the ischemic area as early as minutes following the insult. IL-1 protein was expressed for 24 hours in the penumbra (Zhang et al., 1998) but in the ischemic area it was expressed for days (Liu et al., 1993a, Minami et al., 1992). Injection of IL-1β exacerbated damage from ischemic stroke in animal models whereas blocking IL-1 activity showed a reduction in brain damage (Touzani et al., 1999, Loddick and Rothwell, 1996, Relton and Rothwell, 1992, Stroemer and Rothwell, 1998, Yamasaki et al., 1995).

Brain vasculature is one of the most important units of the brain. The brain requires oxygen and nutrients to be delivered by the microvessels, thus changes in BBB integrity could affect overall function of the brain. An increase in vascular permeability and endothelial cell activation *in vitro* are observed following inflammation or hypoxia (Wong and Dorovini-Zis, 1992, Lindsberg et al., 1996, Arroyo and Iruela-Arispe, 2010, Didier et al., 2003). BBB breakdown and brain endothelial cell activation have been demonstrated after acute brain injury *in vivo* (Stanimirovic et al., 1997, Hess et al., 1994b, An and Xue, 2009, Lindsberg et al., 1996, Blamire et al., 2000, Zhang et al., 1995, Sandoval and Witt, 2008).

Moreover, ECM in the basal lamina of the brain vasculature has been shown to be affected by brain injuries (Hamann et al., 1995, Milner et al., 2008, Muellner et al., 2003, Sarkar et al., 2012). Studies have demonstrated that ECM proteins regulate NF-kB (Orr et al., 2005, Qin et al., 2000) and MAPK signalling pathway (Lu et al., 2013). ECM proteins have also shown to regulate inflammatory responses of cells. For example, fibronectin and inflammation have synergistic effect on nitric oxide induction via JNK in neutrophils (Ghosh et al., 2008). ECM can modulate neutrophil inflammatory responses to IL-8 and platelet-activating factor (Borgquist et al., 2002).

Overall, neuroinflammation, changes in ECM proteins in the basal lamina and cerebral endothelial activation occur during pathological condition of the brain and evidence suggests a close relationship between each incident. In this study, we investigated whether ECM proteins modulate IL-1β-induced brain endothelial cell activation (CINC-1 release) and change in BBB function (expression and localisation of tight junction proteins and TEER).

6.2 Materials and Methods

6.2.1 Plate coating

Transwell® inserts or tissue-culture plastic plates were coated at 2.5 pmol/cm^2 as described in Section 2.1.

6.2.2 Cell culture

Rat brain endothelial cells were isolated from rat brains as described in Section 2.2.1 and maintained in 180 ng/ml hydrocortisone supplemented growth medium. Following cell detachment, rBECs were transferred to 24-well fitted ECM-coated Transwell® inserts. The method of primary rat astrocytes isolation and culture were described in Section 2.2.2. Primary rat astrocytes were grown on PDL-coated tissue-culture 24-well plate for three days. Transwell® inserts containing rBECs were then transferred to 24-well plate which the astrocytes were grown. Plates were maintained in a 5% CO_2 humidified incubator at 37 ˚C for 4 days before IL-1β treatment.

6.2.3 Immunocytochemical detection of protein expression

rBECs grown on Transwell® inserts for four days prior to IL-1β treatment. Culture media were completely aspirated. Cells were then fixed, stained and analysed as described in Section 2.4. Three images, 200x magnification (222.72 x 166.40 μm), were taken and the number of DAPI positive staining was counted. The data were statistically analysed using one-way ANOVA by Prism version 5 software.

6.2.4 Interleukin-1β treatment

The primary rat BBB model was obtained as described in Section 3.2.2. The model was then exposed to 10 ng/ml IL-1β treatment as described in Section 2.5.

6.2.5 Enzyme-linked immunosorbent assay

Following IL-1β treatment, cell culture medium was collected on ice and kept in Eppendorf tubes at -20°C until use. Samples were thawed on ice for approximately an hour and were briefly mixed before ELISA. See section 2.6 for ELISA protocol.

6.3 Results

6.3.1 The effect of extracellular matrix proteins on interleukin-1β-induced Cytokine-Induced Neutrophil Chemoattractant-1 release by rat brain endothelial cells

Inflammation is a physiological event that follows brain injury which causes further damage of brain tissue. Endothelial cells are activated in response to injury and inflammation and it has been demonstrated that ECM protein expression is modulated during the course of injury (Fukuda et al., 2004, Hamann et al., 1995, Milner et al., 2008, Sixt et al., 2001, Tian et al., 2007). Although cerebromicrovascular endothelial cells are closely associated with the extracellular matrix in the basal lamina, the effect of the extracellular matrix on brain endothelial cell activation has not been reported. To improve understanding of the mechanism and the role of endothelial cell activation in acute brain injury, it is important to investigate whether ECM proteins can modulate endothelial cell activation.

Firstly, the effect of ECM proteins on IL-1β-induced CINC-1 release was determined. Rat brain endothelial cells were grown onto type IV collagen, cellular fibronectin, laminin-511 and the combination of laminin-411 and laminin-511 (1:1). Since cells did not attach at all to uncoated Transwell® insert, rBECs grown on type I collagen served as a control. The *in vitro* BBB model was treated with either vehicle or 10 ng/ml IL-1β. Following 4 hours IL-1β treatment, the media from apical and basolateral sides of the Transwell® insert were collected and for the CINC-1 concentration measured. The results (Figure 6.1A) showed CINC-1 release was significantly increased in response to 10 ng/ml IL-1β compared to vehicle-treated control for rBECs grown on all ECM proteins (type I collagen 765.6 pg/ml vs. 73.28 pg/ml; type IV collagen 984.3 pg/ml vs. 92.70 pg/ml; FN 1069 pg/ml vs. 83.84 pg/ml; combination of laminin-411 and -511 1312 pg/ml vs. 85.18 pg/ml and LM511 2101 pg/ml vs. 100.2 pg/ml). Rat brain endothelial cells grown on laminin-511 released more CINC-1 compared to rBECs grown on type I collagen (2101 ± 882.3 vs. 765.6 ± 126.9). The release of CINC-1 by rBECs grown on cellular fibronectin, type IV collagen and the combination of laminin-411 and laminin-511 (1:1) was comparable to that of cells grown on type I collagen. In the previous chapter, it was

demonstrated that laminin-511 and the combination of laminin-411 and -511 (1:1) induced rBECs proliferation compared to type I collagen. In order to determine whether there were more cells grown on laminin-511 and the combination of laminin-411 and -511 (1:1) compared to other ECM proteins, cell number per field (222.72 μm x 166.40 μm) were counted. The data showed no significantly difference in cell number between ECM proteins (Figure 6.1B).

Figure 6.1 Cytokine-induced neutrophil chemoattractant-1 release by the *in vitro* blood-brain barrier model following 4 hours interleukin-1β treatment and cell number per field of rat brain endothelial cell culture grown on varied extracellular matrix proteins

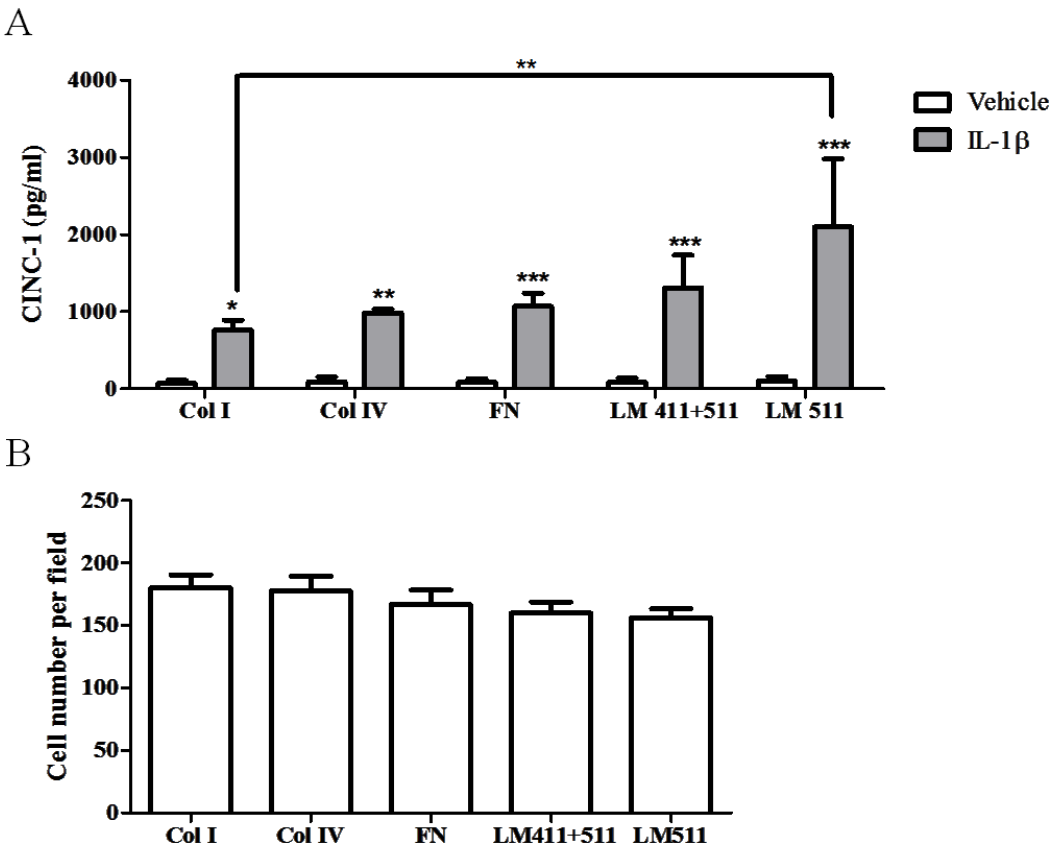

Rat brain endothelial cells were grown on Transwell® insert for four days until cells reached confluency. Cells were incubated with IL-1β at 10 ng/ml for 4 hours. A) The concentration of CINC-1 in cell culture medium was measured using ELISA. B) rBECs were fixed and nuclei stained with DAPI. Nuclei of rBECs grown on ECM proteins were counted. Data were statistically analysed using GraphPad Prism version 5 and are shown as mean ± SD. Two-way ANOVA (A) or one-way ANOVA (B) with Bonferroni post-hoc tests were applied to compare all data obtained from four independent experiments. All analysed data were considered statistically significant when $p<0.05$ (* = $p<0.05$; **=$p<0.01$; ***=$p<0.001$).

6.3.2 The effect of extracellular matrix proteins on transendothelial electrical resistance of rat blood-brain barrier model following interleukin-1β treatment

Blood-brain barrier integrity is vital for the brain to maintain its normal function. Breakdown of the BBB has observed shortly following brain injury. In the previous chapter of this thesis we have shown that ECM proteins modulated the TEER of the rat *in vitro* BBB model. However, the influence of those ECM proteins on TEER following inflammation was not studied. Here we investigated if the ECM proteins had any effect on the TEER of the *in vitro* BBB model under inflammatory conditions.

The TEER of rat BBB model composed of rBECs grown on varied ECM proteins including type I collagen (control), type IV collagen, cellular fibronectin, laminin-511 and the combination of laminin-411 and -511 (1:1) was measured before and after treatment with either vehicle or 10 ng/ml IL-1β. The results are presented as a percentage of the initial value (Figure 6.2). TEER of the vehicle-treated BBB model did not change from the TEER measured before vehicle was added (~100%). However, adding 10 ng/ml IL-1β to the *in vitro* BBB system resulted in a significant reduction of TEER regardless of the ECM proteins the rBECs were grown on. However, there was no significantly difference between the reductions of TEER of cells grown on different ECM proteins.

Figure 6.2 Transendothelial electrical resistance measurement of the in vitro blood-brain barrier model following interleukin-1β treatment

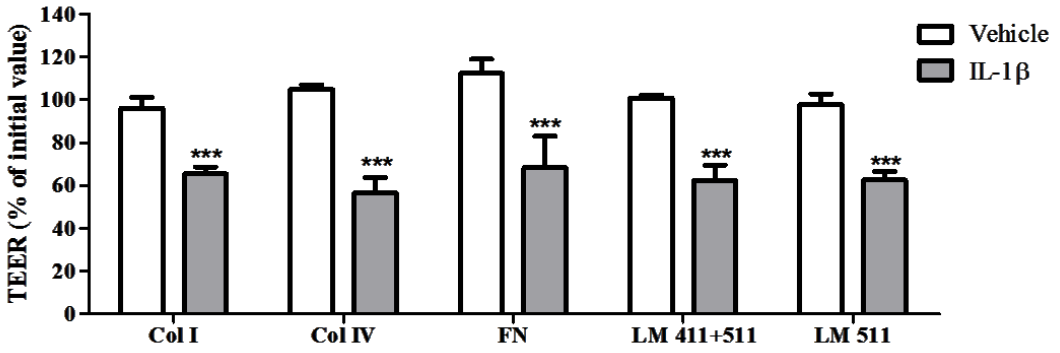

rBECs were grown on type I collagen (Col I, control), type IV collagen (Col IV), cellular fibronectin (FN), laminin-511 (LM 511) and the combination of laminin-411 and -511 (LM 411+511) coated Transwell® inserts for four days until they reached confluency. The TEER of the rat BBB model was initially measured immediately prior to treatment. Either vehicle or 10 ng/ml IL-1β was added to the luminal compartment. TEER was measured again following 4 hours of incubation. The result are showed as the percentage of the value measured prior to treatment. Data are shown as mean ± SD. Two-way ANOVA and Bonferroni post-hoc tests were applied to compare all data obtained from three independent experiments. All analysed data were considered statistically significant when $p<0.05$ (***=p<0.001).

6.3.3 The effect of extracellular matrix on expression of occludin and ZO-1

Tight junction proteins are highly expressed at the apical cell-cell contact zone of brain endothelial cells. Tight junction proteins in one cell bind to tight junction proteins of adjacent cells via extracellular domains and help produce a highly restrictive structure. Tight junction protein complexes are therefore useful indicators of the functional and structural integrity of the BBB. A decrease in tight junction protein expression associated with the disruption of the BBB following injury has been demonstrated (Bolton et al., 1998, Chen et al., 2012, Liu et al., 2012a). Consequently, changes in the ECM components of the basal lamina in the brain vasculature following injury may play an important role in regulation of expression of tight junction proteins.

Expression and localisation of tight junction proteins, occludin and ZO-1 in rBECs grown on ECM-coated Transwell® inserts following either vehicle or IL-1β treatment were determined using immunocytochemistry. Regardless of the ECM protein the rBECs were grown on, vehicle-treated rBECs displayed a spindle-shaped morphology and strongly expressed both occludin and ZO-1 (Figure 6.3). Both tight junction proteins were mainly localised in the cell membrane where cell contact occurred. There was very low or no cytoplasmic staining observed. In cells treated with IL-1β occludin was observed throughout cell cytoplasm. Discontinuous distribution or disappearance of occludin at the cell-cell contacts could also be observed in the cells grown on type I collagen, type IV collagen and cellular fibronectin. Rat brain endothelial cells grown on laminin-511 and the combination of laminin-411 and -511 (1:1) exposed to IL-1β mostly displayed continuous membranous occludin staining with punctate staining of cytoplasmic occludin. The intensity of occludin fluorescence (Figure 6.4A) and ZO-1 (Figure 6.4B) were also determined.

Treatment of rBECs grown on laminin-511 and the combination of laminin-411 and -511 (1:1) with IL-1β resulted in a significant increase in occludin fluorescence intensity (Figure 6.4A). No such increase in occludin fluorescence intensity was observed following IL-1β treatment in cells grown on type IV collagen and cellular

fibronectin. The intensity of ZO-1 fluorescence was also determined. Treatment of cells with IL-1β did not significantly affect the fluorescence intensity of ZO-1 in rBECs grown on all ECM proteins (Figure 6.4B). In term of morphology, cells grown on type I collagen, type IV collagen and cellular fibronectin became significantly rounder when treated with IL-1β-treated compared to vehicle-treated control cells (Figure 6.4C). There was no significant change in circularity when cells grown on laminin-511 and the combination of laminin-411 and -511 (1:1) were treated with IL-1β (Figure 6.4C).

To determine the distribution of staining of tight junction proteins, c/m of occludin fluorescence (Figure 6.4D) and ZO-1 fluorescence (Figure 6.4E) in rBEC monolayers were determined. The data showed that IL-1β slightly but not significantly, increased the c/m of occludin protein in rBECs grown on laminin-511 and the combination of laminin-411 and -511 (1:1) whereas IL-1β had a significant effect on the c/m of occludin protein in rBECs grown on type I collagen, type IV collagen and cellular fibronectin. The c/m ratio of ZO-1 was increased following IL-1β treatment regardless of which ECM molecules rBECs were grown on.

Figure 6.3 Localisation of occludin in rat brain endothelial cell monolayer following 4 hours of vehicle or interleukin-1β treatment

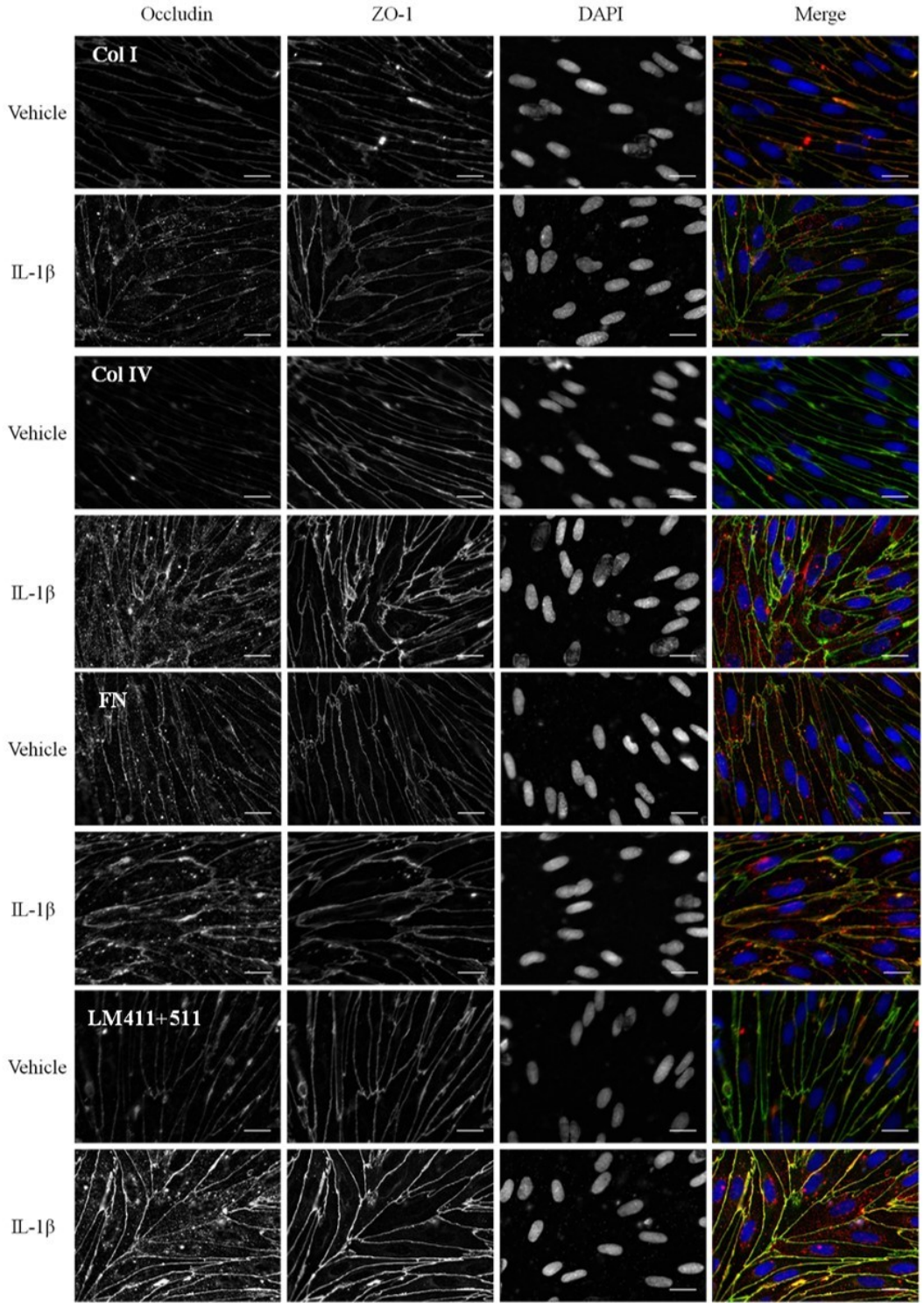

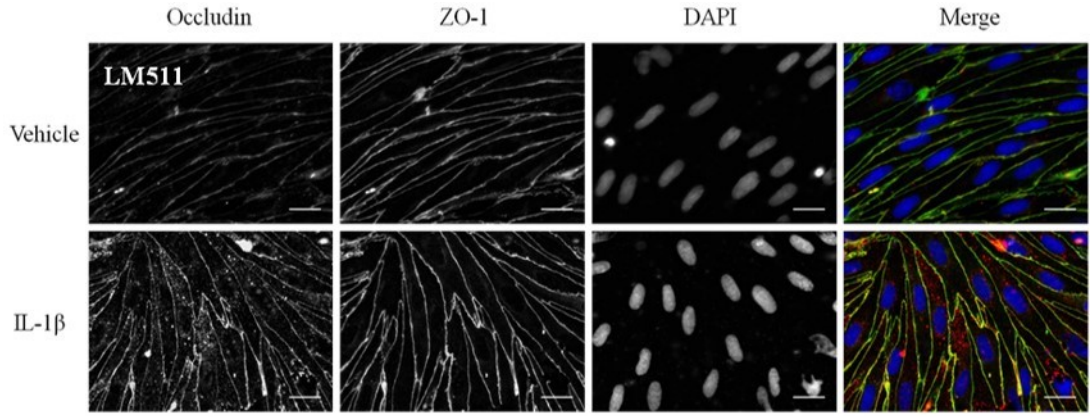

Primary culture of rBECs on type I collagen (Col I), type IV collagen (Col IV), cellular fibronectin (FN), the combination of laminin-411 and -511 (LM 411+511) and laminin-511 (LM511)-coated Transwell® was used after 4 hours of incubation with either vehicle or IL-1β treatment. Immunofluorescence microscopy images showed occludin staining in red, ZO-1 staining in green and DAPI (nuclei) staining in blue. Digital pictures were taken with a Coolsnap ES camera through MetaVue software following visualization with an Olympus BX51 microscope. Scale bar represents 10 μm (600x magnification).

Figure 6.4 Intensity of occludin and ZO-1 fluorescence in rat brain endothelial cell monolayers following interleukin-1β treatment

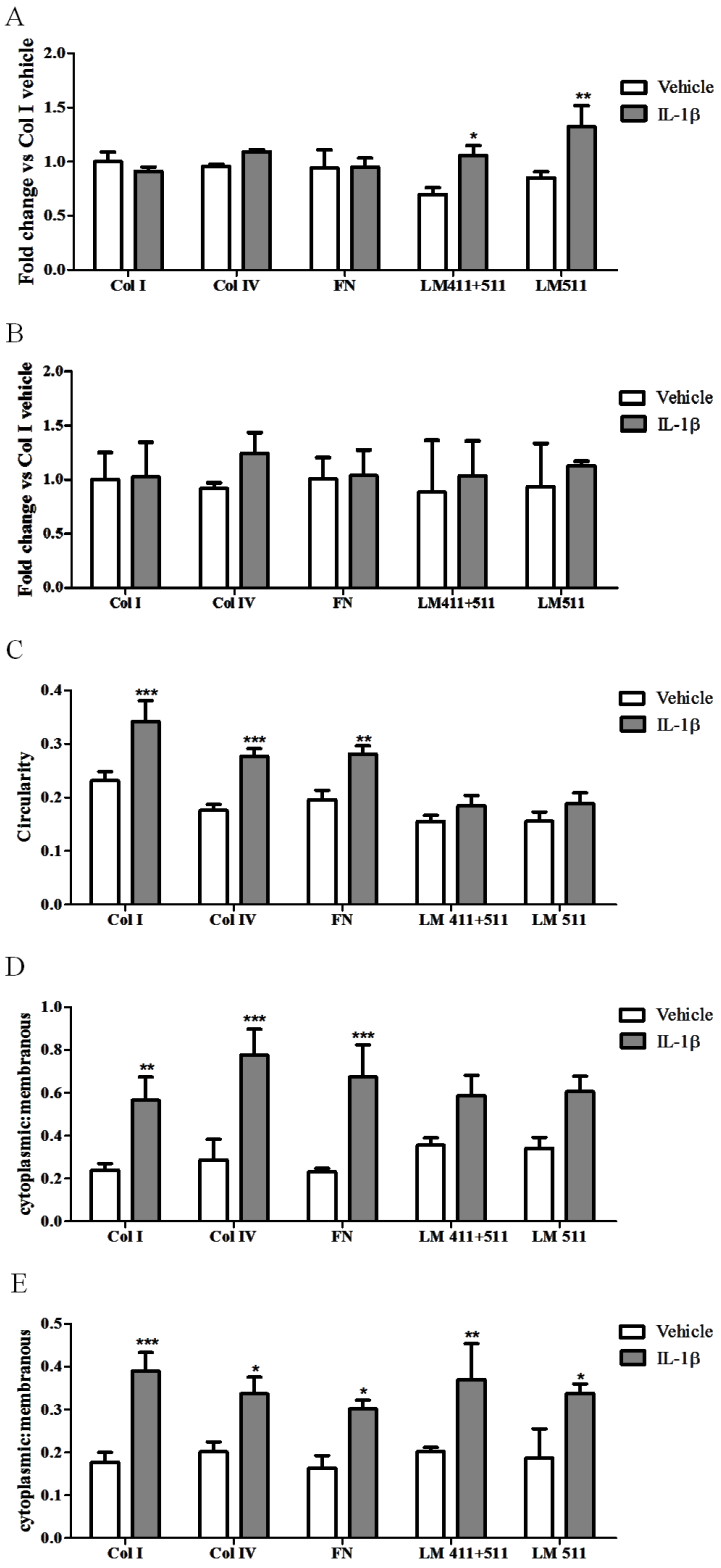

Primary rBECs were grown on type I collagen (Col I), type IV collagen (Col IV), cellular fibronectin (FN), the combination of laminin-411 and -511 (LM 411+511) and laminin-511 (LM511)-coated Transwell® insert. Following 4 hours of incubation with either vehicle or IL-1β, cells were fixed and incubated with anti-occludin antibody and anti-ZO-1 antibody. Digital pictures were taken with a Coolsnap ES camera through MetaVue software following visualization with an Olympus BX51 microscope. Immunocytochemical images for tight junction proteins were analysed with ImageJ software. Intensity of occludin fluorescence (A), intensity of ZO-1 fluorescence (B) circularity (C), c/m of occludin (D) and ZO-1 (E) are shown as mean ± SD. Data were obtained from three independent experiments. All analysed data were considered statistically significant when $p<0.05$ compare to vehicle treated cells (* = $p<0.05$; **=$p<0.01$; ***=$p<0.001$).

6.4 Discussion

Binding of IL-1β to its receptor on the cell membrane activates two main signalling pathways involving NF-κB and JNK and p38 MAPK which, in turn, induce the expression of target genes including chemokines (O'Neill and Greene, 1998). Studies showed that IL-1β and the inflammatory cytokine, TNF-α regulated barrier integrity through NF-κB and MAPK signalling pathway (Al-Sadi et al., 2011, Wu et al., 2011, Kimura et al., 2009, Aveleira et al., 2010). ECM proteins have been reported to modulate NF- κB activation (Hammar et al., 2005, Orr et al., 2005) and MAPK activity (Cybulsky and McTavish, 1997, Finlay et al., 2000). Some studies showed that ECM proteins and inflammation induced synergistic/antagonistic cellular response (Ghosh et al., 2008, Ribaux et al., 2007, Vaday et al., 2001).

Exposure to inflammatory cytokines activates brain endothelial cells to express chemokines and cell adhesion molecules. In the previous chapter, we showed that IL-1β induced CINC-1 release by the rat BBB model. From our results, it appears that ECM proteins have an effect on rBEC response to IL-1β. Laminin-511 and the combination of laminin-411 and laminin-511 (1:1) increase CINC-1 release by rBECs in response to IL-1β compared to type I collagen. CINC-1 is a chemokine which is highly upregulated early during MCAO (Liu et al., 1993b, Yamagami et al., 1999, Losy et al., 2005). It plays a crucial role in neutrophil recruitment and activation. ECM regulation of CINC-1 release by brain endothelial cells may affect leukocyte recruitment which is an initial step of leukocyte transmigration during stroke. Leukocyte extravasation is a multistep process including tethering, firm adhesion and transmigration across the endothelium. The expression of molecules involving extravasation of immune cells such as the selectins which induces leukocyte tethering and rolling and the cellular adhesion molecules (such as ICAM and VCAM) which mediate firm adhesion of leukocyte to the endothelium is also induced by IL-1β (Barkalow et al., 1996, Hess et al., 1994a, Sibson et al., 2004, Hess et al., 1996). Therefore, whether the basal lamina influences the production of these molecules is attractive to investigate.

ECM molecules have an effect on transmigration of leukocytes across the endothelium. Recently, T-cell transmigration across an empty (without endothelial

cells) Transwell® insert coated with laminin-411 has been demonstrated, however laminin-511 inhibited migration (Wu et al., 2009). The finding that ECM proteins also modulate endothelial cell activation and cell extravasation, it is very interesting to determine the effect of ECM proteins on leukocyte transmigration across the brain endothelium *in vitro* using our rat BBB model. In the previous chapter, it has been demonstrated that ECM molecules had an effect on rBEC proliferation. In order to confirm whether difference in CINC-1 release were due to the difference in cell numbers, the DAPI staining was counted. The result showed that although laminin-511 and the combination of laminin-411 and laminin-511 (1:1) significantly induced rBEC proliferation, the numbers of cells on ECM protein coated Transwell® inserts were not significantly different from cells grown on type I collagen. The reason why the number of rBECs grown on laminins was not more than those on other ECM protein even though the proliferation rate is significantly different is probably because endothelial cell-cell contact effectively stops cell proliferation when confluency reached (Vinals and Pouyssegur, 1999, D'Amore, 1992).

In this study, we also determine the effect of ECM proteins on barrier function following IL-1β treatment. Inflammatory cytokines modulate TEER (Skinner et al., 2009), barrier permeability (Argaw et al., 2006, Blamire et al., 2000, Didier et al., 2003) and organisation of tight junction proteins (Forster et al., 2008, McColl et al., 2008). It was demonstrated that IL-1β caused a reduction in TEER regardless of which ECM proteins rBECs were grown on. However, an increase in occludin expression following IL-1β treatment was found only in rBECs grown on laminin-511 and the combination of laminin-411 and -511 (1:1) coated Transwell® inserts. Moreover, a shift in occludin localisation from cell membrane to cell cytoplasm was observed in IL-1β-treated rBECs. Interestingly, cells grown on type I collagen, type IV collagen and cellular fibronectin displayed intracellular punctate staining of occludin with a disappearance or discontinuity of membranous occludin whilst IL-1β-treated cells grown on laminin-511 and the combination of laminin-411 and -511 (1:1) displayed punctate occludin staining in the cytoplasm without loss of membranous occludin. This suggests that ECM proteins regulate occludin internalisation and/or turnover of membranous occludin.

Occludin is a key integral membrane tight junction protein of epithelial and endothelial including the brain endothelial cells (Hirase et al., 1997, Lippoldt et al., 2000, Hawkins et al., 2004, Van Itallie et al., 2010). Correct expression and localisation of occludin are associated with BBB physiological function. In normal brain, occludin is highly and continuously expressed along the cell margins in the endothelium (Hawkins et al., 2004, Lippoldt et al., 2000). In pathological conditions, downregulation or dislocation of occludin was observed (Schubert-Unkmeir et al., 2010, Xu et al., 2012, Bolton et al., 1998, Lippoldt et al., 2000, Lochhead et al., 2010, Liu et al., 2012a). It has been reported that a change in localisation of occludin proteins is mediated by endocytosis. Punctate staining of occludin found in the cytoplasm of IL-1-treated rBECs was probably occludin internalised in vesicles. Three mechanisms of occludin redistribution have been identified: macropinocytosis (Bruewer et al., 2005), clathrin (Fletcher et al., 2012, Ivanov et al., 2004) and caveolar-mediated endocytosis (Van Itallie et al., 2010, Stamatovic et al., 2009, Shen and Turner, 2005, Schwarz et al., 2007, Marchiando et al., 2010). Relocalisation of occludin in brain endothelial cells is mediated by caveolae-mediated endocytosis (Stamatovic et al., 2009). Recently, it has been reported that TNF-α induced occludin internalisation in the intestinal epithelium *in vivo* which was found to be mediated by caveolar-mediated endocytosis (Marchiando et al., 2010). These findings suggest that redistribution of occludin in rBECs is likely to occur via caveolae-mediated endocytosis.

Degradation of occludin in ischemic brain is reported to be mediated by MMPs. Occludin is a substrate of MMPs (Liu et al., 2009, Yang et al., 2007). One of those is MMP-9 (Liu et al., 2009). It has been reported that activation of MMPs leads to degradation of tight junction proteins including claudin-5 and occludin and an increase in BBB permeability. Inhibition of MMPs prevented tight junction cleavage and BBB disruption (Yang et al., 2007, Liu et al., 2012a). MMPs are produced by both cellular components of the brain (Asahi et al., 2001, Lee et al., 2004) and blood-borne immune cells (Justicia et al., 2003, Jeffrey et al., 2005). The endothelium is one of the main sources of MMPs (Liu et al., 2009, Asahi et al., 2001). Inflammatory cytokines induce expression of MMPs in varied cell types (Kusano et al., 1998, Rawdanowicz et al., 1994, Liang et al., 2007). IL-1-induced MMP-9 expression by

tracheal smooth muscle cells involved NF-κB, p42/p44 MAPK, p38 MAPK, and JNK (Liang et al., 2007). The finding that cells grown on laminin-511 and the combination of laminin-411 and -511 showed upregulation of occludin expression and intact membranous occludin staining perhaps reflects alteration of the protein degradation process. Therefore, it would be very interesting to investigate production of MMPs by the BBB model and whether ECM proteins play a role on MMP production and function.

Claudin-5 is another key tight junction protein abundantly expressed in brain endothelial cells. Rat brain endothelial cells grown on laminin-511 and the combination of laminin-411 and -511 (1:1) following IL-1β treatment showed a significant reduction in TEER but disappearance of occludin at the cell membrane was not observed. Therefore, it would be interesting to investigate the effect of ECM on claudin-5 expression in the BBB model following IL-1β treatment and determine whether it is modulated by ECM proteins under this condition.

7. General discussion

First we characterised the *in vitro* BBB model comprising pBECs and an astrocytic cell line in a non-contact co-culture. We found that pBECs displayed endothelial morphology and possessed TEER comparable to TEER of the porcine BBB model previously reported by other laboratories (Rubin et al., 1991, Franke et al., 2000, Jeliazkova-Mecheva and Bobilya, 2003). ECM protein production of pBECs analysed by mass spectrometry and western blot revealed the production of fibronectin, an ECM component expressed by brain endothelial cells *in vivo* (Hamann et al., 1995, Krum et al., 1991). These results suggested that the porcine BBB model maintained some key *in vivo* BBB properties. Due to high similarity to human BBB and the high cell yield, the porcine BBB model has great potential for investigating changes in ECM production following ischemic injury. However, the method of ECM extraction and protein detection required further development and modification.

We also validated a rat *in vitro* BBB model composed of primary rBECs and primary rat astrocytes in a non-contact co-culture system. Rat brain endothelial cells displayed spindle-shaped morphology and expressed vWF, occludin and ZO-1 indicating cerebral endothelial characteristics. Exposure to OGD/IL-1β resulted in morphological changes, disruption of both occludin and ZO-1 proteins and CINC-1 release which corresponds to what is reported in acute pathological conditions of the brain *in vivo* (Liu et al., 2012a, Liu et al., 2009, Yang et al., 2007, Bolton et al., 1998, Keep et al., 2005, Campbell et al., 2003, Zehendner et al., 2012) and what reported *in vitro* following acute hypoxic injury (Liu et al., 2012a, An and Xue, 2009, Zehendner et al., 2012). Therefore, we conclude that the rat BBB model retained the key *in vivo* BBB properties and was a suitable model for investigating the cellular responses following OGD/IL-1β treatment in the latter experiments.

The effect of OGD and reperfusion on the expression of ECM proteins associated with the brain vasculature was determined using the MCAO mouse model, and the rat *in vitro* BBB model subjected to OGD/IL-1β. By Immunohistochemical analyses revealed upregulation of laminin α4 chain and fibronectin proteins in the ischemic core area of the MCAO brain sections. Our finding is in contrast to the majority of

studies which found downregulation of ECM proteins following ischemic brain injury *in vivo* (Heo et al., 1999, Hamann et al., 1995, Liu et al., 2012b, Fukuda et al., 2004) However, similarly to our finding, a study by Ji and Tsirka revealed upregulation of laminin protein in the brain of MCAO model (Ji and Tsirka, 2012). Our findings indicated that rBEC adhesion depends on type and amount of ECM proteins. Collagen I, collagen IV, cellular fibronectin, laminin-511 and the combination of laminin-411 and -511 (1:1) promoted rBEC adhesion whereas rBECs hardly adhered to laminin-411 coated plates. Upregulation of laminin α4 protein in MCAO brains may reduce endothelial cell adhesion to the basal lamina leading to disruption of the BBB.

Ji and Tsirka also found changes in laminin gene expression in brain endothelial cells in culture following OGD (Ji and Tsirka, 2012). Corresponding to their study, we found that expression of ECM genes including *LAMA4, LAMB1 and LAMC1* was modified following OGD/IL-1β. Many studies, both *in vitro* and *in vivo*, indicate loss of ECM proteins associated with brain vasculature was caused by protease activity especially MMPs (Fukuda et al., 2004, Heo et al., 1999, Gasche et al., 1999, Gu et al., 2005, Jeffrey et al., 2005, Monaco et al., 2006, Lee and Lo, 2004). Therefore, it is possible that ECM expression is upregulated during injury but, at the same time, there is also upregulation of proteolytic enzymes which cleave ECM proteins. Further study should focuses on ECM protein production and degradation in rBECs in culture following OGD/IL-1β.

Changes in ECM expression of proteins associated with brain endothelial cells were observed in the brain vasculature following brain injury, therefore we investigated the regulatory role of vascular ECM proteins on rBEC behaviours (in *in vitro* studies). Corresponding with what has previously been reported (Form et al., 1986, Tilling et al., 1998, Gonzalez et al., 2002, Wang and Milner, 2006, Tilling et al., 2002), ECM proteins may promote cell adhesion, spreading and proliferation. We also found that laminin-511 and the mixture of laminin-411 and -511 (1:1) induced the most spreading and proliferation of rBECs. Laminin-411 and -511 are the main cerebral endothelial ECM proteins expressed *in vivo* (Sixt et al., 2001). Our rBEC adhesion and proliferation results reflected that these laminins play a very important role as endothelial cell anchorage sites and potentially in tissue repair mechamisms.

The disappearance of these molecules following injury may affect BBB integrity. Distinct effects of laminin-411 and laminin-511 on rBEC behaviour, including adhesion and proliferation, were observed. Laminin-411 and laminin-511 were previously reported to be involved in leukocyte transmigration across the endothelium (Fujiwara et al., 2001, Pedraza et al., 2000, Sixt et al., 2001). The difference in the extent of rBEC adhesion to laminin-411 and laminin-511 compared to other ECM proteins is probably a key factor regulating leukocyte transmigration across the brain endothelium. The effect of ECM proteins especially laminin-411 and laminin-511 on leukocyte transmigration across the BBB model following ischemic injury is still unknown and it would be very interesting to investigate using our rat BBB model. Cells grown on type I collagen, type IV collagen and cellular fibronectin sometimes displayed multilayer-like organisation which probably developed further into a tube-like structure. Cells grown on laminin-511 and the combination of laminin-411 and -511 displayed classical spindle-like morphology and did not induce cell multi-layering or tube formation. A change in rBEC organisation induced by ECM proteins suggests a potential angiogenic role of ECM proteins. Laminin-511, but not type IV collagen, cellular fibronectin, and the combination of laminin-411 and -511, increased TEER of the rat BBB model compared to type I collagen. Brain endothelial cell binding to ECM proteins is mostly mediated by integrins. We found that rBEC binding to type IV collagen and fibronectin is mediated by integrin β1 and integrin β1 and RGD sequence, respectively. Corresponding to reports in the literature (Gehlsen et al., 1989, Pfaff et al., 1994, Knight et al., 2000, Hall et al., 1990, Nishiuchi et al., 2003, Li et al., 2012), cell binding to collagen IV is mainly mediated by integrin β1 but not RGD sequence and cell-fibronectin interaction is mediated by integrin β1 and RGD. Brain endothelial cell-laminin interaction is reported to be mainly mediated by integrin α6β1 (Nishiuchi et al., 2003, Kikkawa et al., 2000). However, rBEC adhesion to laminin-511 and the combination of laminin-411 and -511 was not inhibited by either anti-integrin β1 blocking antibody or GRGDSP peptide. Other cellular laminin receptors such as dystroglycans (Szabo and Kalman, 2008, Baeten and Akassoglou, 2011, del Zoppo and Milner, 2006), integrin β3 and β4 (Paulus et al., 1993, Li et al., 2012) are expressed by brain endothelial cells and these receptors may be involved

in rBEC-laminin binding *in vitro*. Rat brain endothelial cells grown on laminin-511 and the combination of laminin-411 and -511 displayed more spindle shape (circularity value closer to 0.0) compared to the shape of cells grown on type I collagen. As it has been reported that morphology of brain endothelial cells is associated with BBB properties (Weidenfeller et al., 2005), the spindle morphology of rBECs grown on laminin-511 may be associated with the higher TEER of the BBB model compare to cells grown on type I collagen which displayed a rounder morphology.

The effect of ECM proteins on brain endothelial cell activation in response to IL-1β treatment was also investigated. ECM proteins regulated rBEC activation in response to IL-1β treatment. Laminin-511 and the combination of laminin-411 and -511, but not type IV collagen, induced higher CINC-1 release by rBECs in culture in response to IL-1β treatment compared to type I collagen. IL-1β exerts its activity via MAPK and NF-κB (Summers et al., 2010, Al-Sadi et al., 2011, Parker et al., 2002, Al-Sadi et al., 2010, Liang et al., 2007, O'Neill and Greene, 1998) and thus cell binding to particular ECM proteins may regulate intracellular signalling, MAPK and NF-κB. Laminin-511 and the combination of laminin-411 and -511 upregulated occludin protein expression following IL-1β treatment whereas type IV collagen and cellular fibronectin did not increase occludin expression compared to collagen I. The mechanisms of upregulation of occludin expression in our model following IL-1β treatment are unknown. We hypothesise that cell binding to laminin-511 and the combination of laminin-411 and -511 may alter occludin production or occludin degradation in the rBECs following IL-1β treatment.

Our study has shown the effects of vascular ECM proteins on brain endothelial cell behaviours in non-inflammatory condition and in activated rBEC in which represent an inflammatory state. ECM proteins may serve as anchoring sites, promote proliferation, contribute to TEER and regulate tube formation of rBECs in culture. Changes in ECM protein expression and components in the basal lamina of the brain vasculature may affect normal behaviour and barrier function of the BBB. We also showed that ECM proteins can modulate rBEC responses to IL-1β treatment, suggesting that changes in ECM composition following injury is a critical regulator of IL-1-induced endothelial cell activation.

8. Conclusion

In this study we investigated whether expression of endothelial associated ECM molecules was modulated by OGD/IL-1β and whether ECM molecules had any effects on brain endothelial cell activation following injury. The *in vitro* BBB model comprising brain endothelial cells grown on ECM-coated Transwell® insert and astrocytes in a non-contact co-culture was established. This model displayed BBB phenotype. Treatment of rBECs with OGD and reperfusion or both induced changes in cell morphology, dislocalisation of occludin and ZO-1 and CINC-1 release. These changes suggested that OGD/IL-1β could activate endothelial cells and alter the barrier properties of this model. Changes in the expression of ECM proteins in the MCAO mouse model and changes in ECM mRNA levels in the rat BBB model following OGD/IL-1β confirmed our hypothesis that inflammation and ischemic insult alter ECM proteins expression. ECM proteins regulate rBEC behaviour including adhesion, proliferation, TEER and cell organisation. ECM proteins modulated CINC-1 release, occludin expression and distribution in rBEC monolayer following IL-1β treatment. These results indicate that changes in ECM composition following acute brain injury are a critical regulator of IL-1-induced endothelial cell activation. Future work should investigate further the mechanisms (intracellular signalling, the associated ECM receptors and role of MMPs) behind ECM-regulation of endothelial cell activation and barrier functions. Therefore, changes in ECM composition following injury is a critical regulator of IL-1-induced endothelial cell activation.

References

ABBOTT, N. J., DOLMAN, D. E., DRNDARSKI, S. & FREDRIKSSON, S. M. 2012. An improved in vitro blood-brain barrier model: rat brain endothelial cells co-cultured with astrocytes. *Methods Mol Biol,* 814**,** 415-30.

ABBOTT, N. J., HUGHES, C. C., REVEST, P. A. & GREENWOOD, J. 1992. Development and characterisation of a rat brain capillary endothelial culture: towards an in vitro blood-brain barrier. *J Cell Sci,* 103 (Pt 1)**,** 23-37.

ABBOTT, N. J., PATABENDIGE, A. A., DOLMAN, D. E., YUSOF, S. R. & BEGLEY, D. J. 2010. Structure and function of the blood-brain barrier. *Neurobiol Dis,* 37**,** 13-25.

ADIBHATLA, R. M. & HATCHER, J. F. 2008. Tissue plasminogen activator (tPA) and matrix metalloproteinases in the pathogenesis of stroke: therapeutic strategies. *CNS Neurol Disord Drug Targets,* 7**,** 243-53.

AHN, M. Y., ZHANG, Z. G., TSANG, W. & CHOPP, M. 1999. Endogenous plasminogen activator expression after embolic focal cerebral ischemia in mice. *Brain Res,* 837**,** 169-76.

AL-SADI, R., YE, D., SAID, H. M. & MA, T. Y. 2010. IL-1beta-induced increase in intestinal epithelial tight junction permeability is mediated by MEKK-1 activation of canonical NF-kappaB pathway. *Am J Pathol,* 177**,** 2310-22.

AL-SADI, R., YE, D., SAID, H. M. & MA, T. Y. 2011. Cellular and molecular mechanism of interleukin-1beta modulation of Caco-2 intestinal epithelial tight junction barrier. *J Cell Mol Med,* 15**,** 970-82.

ALBELDA, S. M., MULLER, W. A., BUCK, C. A. & NEWMAN, P. J. 1991. Molecular and cellular properties of PECAM-1 (endoCAM/CD31): a novel vascular cell-cell adhesion molecule. *J Cell Biol,* 114**,** 1059-68.

AMANTEA, D., NAPPI, G., BERNARDI, G., BAGETTA, G. & CORASANITI, M. T. 2009. Post-ischemic brain damage: pathophysiology and role of inflammatory mediators. *FEBS J,* 276**,** 13-26.

AN, P. & XUE, Y. X. 2009. Effects of preconditioning on tight junction and cell adhesion of cerebral endothelial cells. *Brain Res,* 1272**,** 81-8.

ANDRAS, I. E., PU, H., TIAN, J., DELI, M. A., NATH, A., HENNIG, B. & TOBOREK, M. 2005. Signaling mechanisms of HIV-1 Tat-induced alterations of claudin-5 expression in brain endothelial cells. *J Cereb Blood Flow Metab,* 25**,** 1159-70.

ARGAW, A. T., ZHANG, Y., SNYDER, B. J., ZHAO, M. L., KOPP, N., LEE, S. C., RAINE, C. S., BROSNAN, C. F. & JOHN, G. R. 2006. IL-1beta regulates blood-brain barrier permeability via reactivation of the hypoxia-angiogenesis program. *J Immunol,* 177**,** 5574-84.

ARMBRUST, T., KREISSIG, M., TRON, K. & RAMADORI, G. 2004. Modulation of fibronectin gene expression in inflammatory mononuclear phagocytes of rat liver after acute liver injury. *J Hepatol,* 40**,** 638-45.

ARROYO, A. G. & IRUELA-ARISPE, M. L. 2010. Extracellular matrix, inflammation, and the angiogenic response. *Cardiovasc Res,* 86**,** 226-35.

ARTHUR, F. E., SHIVERS, R. R. & BOWMAN, P. D. 1987. Astrocyte-mediated induction of tight junctions in brain capillary endothelium: an efficient in vitro model. *Brain Res,* 433**,** 155-9.

ASAHI, M., WANG, X., MORI, T., SUMII, T., JUNG, J. C., MOSKOWITZ, M. A., FINI, M. E. & LO, E. H. 2001. Effects of matrix metalloproteinase-9 gene knock-out on the proteolysis of blood-brain barrier and white matter components after cerebral ischemia. *J Neurosci,* 21**,** 7724-32.

AUMAILLEY, M. & TIMPL, R. 1986. Attachment of cells to basement membrane collagen type IV. *J Cell Biol,* 103**,** 1569-75.

AVELEIRA, C. A., LIN, C. M., ABCOUWER, S. F., AMBROSIO, A. F. & ANTONETTI, D. A. 2010. TNF-alpha signals through PKCzeta/NF-kappaB to alter the tight junction complex and increase retinal endothelial cell permeability. *Diabetes,* 59**,** 2872-82.

BAETEN, K. M. & AKASSOGLOU, K. 2011. Extracellular matrix and matrix receptors in blood-brain barrier formation and stroke. *Dev Neurobiol,* 71**,** 1018-39.

BALDA, M. S., GARRETT, M. D. & MATTER, K. 2003. The ZO-1-associated Y-box factor ZONAB regulates epithelial cell proliferation and cell density. *J Cell Biol,* 160**,** 423-32.

BALDA, M. S. & MATTER, K. 2000. The tight junction protein ZO-1 and an interacting transcription factor regulate ErbB-2 expression. *EMBO J,* 19**,** 2024-33.

BARKALOW, F. J., GOODMAN, M. J., GERRITSEN, M. E. & MAYADAS, T. N. 1996. Brain endothelium lack one of two pathways of P-selectin-mediated neutrophil adhesion. *Blood,* 88**,** 4585-93.

BARKSBY, H. E., LEA, S. R., PRESHAW, P. M. & TAYLOR, J. J. 2007. The expanding family of interleukin-1 cytokines and their role in destructive inflammatory disorders. *Clin Exp Immunol,* 149**,** 217-25.

BARRY, S. T. & CRITCHLEY, D. R. 1994. The RhoA-dependent assembly of focal adhesions in Swiss 3T3 cells is associated with increased tyrosine phosphorylation and the recruitment of both pp125FAK and protein kinase C-delta to focal adhesions. *J Cell Sci,* 107 (Pt 7)**,** 2033-45.

BAUMERT, J., SCHMIDT, K. H., EITNER, A., STRAUBE, E. & RODEL, J. 2009. Host cell cytokines induced by Chlamydia pneumoniae decrease the expression of interstitial collagens and fibronectin in fibroblasts. *Infect Immun,* 77**,** 867-76.

BAX, D. V., BERNARD, S. E., LOMAS, A., MORGAN, A., HUMPHRIES, J., SHUTTLEWORTH, C. A., HUMPHRIES, M. J. & KIELTY, C. M. 2003. Cell adhesion to fibrillin-1 molecules and microfibrils is mediated by alpha 5 beta 1 and alpha v beta 3 integrins. *J Biol Chem,* 278**,** 34605-16.

BEAULIEU, E., DEMEULE, M., GHITESCU, L. & BELIVEAU, R. 1997. P-glycoprotein is strongly expressed in the luminal membranes of the endothelium of blood vessels in the brain. *Biochem J,* 326 (Pt 2)**,** 539-44.

BECK, K., HUNTER, I. & ENGEL, J. 1990. Structure and function of laminin: anatomy of a multidomain glycoprotein. *Faseb J,* 4**,** 148-60.

BERTHOD, F., GERMAIN, L., TREMBLAY, N. & AUGER, F. A. 2006. Extracellular matrix deposition by fibroblasts is necessary to promote capillary-like tube formation in vitro.

BLAMIRE, A. M., ANTHONY, D. C., RAJAGOPALAN, B., SIBSON, N. R., PERRY, V. H. & STYLES, P. 2000. Interleukin-1beta -induced changes in blood-brain barrier permeability, apparent diffusion coefficient, and cerebral blood volume in the rat brain: a magnetic resonance study. *J Neurosci,* 20**,** 8153-9.

BOADO, R. J., LI, J. Y. & PARDRIDGE, W. M. 2000. Selective Lutheran glycoprotein gene expression at the blood-brain barrier in normal brain and in human brain tumors. *J Cereb Blood Flow Metab,* 20**,** 1096-102.

BOIS, P. R., O'HARA, B. P., NIETLISPACH, D., KIRKPATRICK, J. & IZARD, T. 2006. The vinculin binding sites of talin and alpha-actinin are sufficient to activate vinculin. *J Biol Chem,* 281**,** 7228-36.

BOLTON, S. J., ANTHONY, D. C. & PERRY, V. H. 1998. Loss of the tight junction proteins occludin and zonula occludens-1 from cerebral vascular endothelium during neutrophil-induced blood-brain barrier breakdown in vivo. *Neuroscience,* 86**,** 1245-57.

BOOMS, P., PREGLA, R., NEY, A., BARTHEL, F., REINHARDT, D. P., PLETSCHACHER, A., MUNDLOS, S. & ROBINSON, P. N. 2005. RGD-containing fibrillin-1 fragments upregulate matrix metalloproteinase expression in cell culture: a potential factor in the pathogenesis of the Marfan syndrome. *Hum Genet,* 116**,** 51-61.

BORGQUIST, J. D., QUINN, M. T. & SWAIN, S. D. 2002. Adhesion to extracellular matrix proteins modulates bovine neutrophil responses to inflammatory mediators. *J Leukoc Biol,* 71**,** 764-74.

BOUTIN, H., LEFEUVRE, R. A., HORAI, R., ASANO, M., IWAKURA, Y. & ROTHWELL, N. J. 2001. Role of IL-1alpha and IL-1beta in ischemic brain damage. *J Neurosci,* 21**,** 5528-34.

BOWMAN, P. D., ENNIS, S. R., RAREY, K. E., BETZ, A. L. & GOLDSTEIN, G. W. 1983. Brain microvessel endothelial cells in tissue culture: a model for study of blood-brain barrier permeability. *Ann Neurol,* 14**,** 396-402.

BRUEWER, M., UTECH, M., IVANOV, A. I., HOPKINS, A. M., PARKOS, C. A. & NUSRAT, A. 2005. Interferon-gamma induces internalization of epithelial tight junction proteins via a macropinocytosis-like process. *Faseb J,* 19**,** 923-33.

CAEP 2001. Thrombolytic therapy for acute ischemic stroke. *CJEM,* 3**,** 8-12.

CALABRIA, A. R., WEIDENFELLER, C., JONES, A. R., DE VRIES, H. E. & SHUSTA, E. V. 2006. Puromycin-purified rat brain microvascular endothelial cell cultures exhibit improved barrier properties in response to glucocorticoid induction. *J Neurochem,* 97**,** 922-33.

CAMPBELL, S. J., HUGHES, P. M., IREDALE, J. P., WILCOCKSON, D. C., WATERS, S., DOCAGNE, F., PERRY, V. H. & ANTHONY, D. C. 2003. CINC-1 is an acute-phase protein induced by focal brain injury causing leukocyte mobilization and liver injury. *Faseb J,* 17**,** 1168-70.

CANTRILL, C. A., SKINNER, R. A., ROTHWELL, N. J. & PENNY, J. I. 2012. An immortalised astrocyte cell line maintains the in vivo phenotype of a primary porcine in vitro blood-brain barrier model. *Brain Res,* 1479**,** 17-30.

CHAITANYA, G. V., CROMER, W., WELLS, S., JENNINGS, M., MATHIS, J. M., MINAGAR, A. & ALEXANDER, J. S. 2012. Metabolic modulation of cytokine-induced brain endothelial adhesion molecule expression. *Microcirculation,* 19**,** 155-65.

CHANA, R. S., MARTIN, J., RAHMAN, E. U. & WHEELER, D. C. 2003. Monocyte adhesion to mesangial matrix modulates cytokine and metalloproteinase production. *Kidney Int,* 63**,** 889-98.

CHANG, A. C., SALOMON, D. R., WADSWORTH, S., HONG, M. J., MOJCIK, C. F., OTTO, S., SHEVACH, E. M. & COLIGAN, J. E. 1995. Alpha 3 beta 1 and alpha 6 beta 1 integrins mediate laminin/merosin binding and function as costimulatory molecules for human thymocyte proliferation. *J Immunol,* 154**,** 500-10.

CHEN, H. C., APPEDDU, P. A., PARSONS, J. T., HILDEBRAND, J. D., SCHALLER, M. D. & GUAN, J. L. 1995. Interaction of focal adhesion kinase with cytoskeletal protein talin. *J Biol Chem,* 270**,** 16995-9.

CHEN, M., MARINKOVICH, M. P., JONES, J. C. R., O'TOOLE, E. A., LI, Y.-Y. & WOODLEY, D. T. 1999. NC1 Domain of Type VII Collagen Binds to the [beta]3 Chain of Laminin 5 Via a Unique Subdomain Within the Fibronectin-Like Repeats. 112**,** 177-183.

CHEN, X., THRELKELD, S. W., CUMMINGS, E. E., JUAN, I., MAKEYEV, O., BESIO, W. G., GAITANIS, J., BANKS, W. A., SADOWSKA, G. B. & STONESTREET, B. S. 2012. Ischemia-reperfusion impairs blood-brain barrier function and alters tight junction protein expression in the ovine fetus. *Neuroscience,* 226**,** 89-100.

CHIA, J., KUSUMA, N., ANDERSON, R., PARKER, B., BIDWELL, B., ZAMURS, L., NICE, E. & POULIOT, N. 2007. Evidence for a role of tumor-derived laminin-511 in the metastatic progression of breast cancer. *Am J Pathol,* 170**,** 2135-48.

CHRZANOWSKA-WODNICKA, M. & BURRIDGE, K. 1996. Rho-stimulated contractility drives the formation of stress fibers and focal adhesions. *J Cell Biol,* 133**,** 1403-15.

CLYMAN, R. I., MCDONALD, K. A. & KRAMER, R. H. 1990. Integrin receptors on aortic smooth muscle cells mediate adhesion to fibronectin, laminin, and collagen. *Circ Res,* 67**,** 175-86.

COLOGNATO-PYKE, H., O'REAR, J. J., YAMADA, Y., CARBONETTO, S., CHENG, Y. S. & YURCHENCO, P. D. 1995. Mapping of network-forming, heparin-binding, and alpha 1 beta 1 integrin-recognition sites within the alpha-chain short arm of laminin-1. *J Biol Chem,* 270**,** 9398-406.

COLOGNATO, H., MACCARRICK, M., O'REAR, J. J. & YURCHENCO, P. D. 1997. The laminin alpha2-chain short arm mediates cell adhesion through both the alpha1beta1 and alpha2beta1 integrins. *J Biol Chem,* 272**,** 29330-6.

COLOGNATO, H. & YURCHENCO, P. D. 2000. Form and function: the laminin family of heterotrimers. *Dev Dyn,* 218**,** 213-34.

CORDON-CARDO, C., O'BRIEN, J. P., CASALS, D., RITTMAN-GRAUER, L., BIEDLER, J. L., MELAMED, M. R. & BERTINO, J. R. 1989. Multidrug-resistance gene (P-glycoprotein) is expressed by endothelial cells at blood-brain barrier sites. *Proc Natl Acad Sci U S A,* 86**,** 695-8.

CORSON, G. M., CHARBONNEAU, N. L., KEENE, D. R. & SAKAI, L. Y. 2004. Differential expression of fibrillin-3 adds to microfibril variety in human and avian, but not rodent, connective tissues. *Genomics,* 83**,** 461-72.

CRITCHLEY, D. R. & GINGRAS, A. R. 2008. Talin at a glance. *J Cell Sci,* 121**,** 1345-7.

CUNNINGHAM, L. A., WETZEL, M. & ROSENBERG, G. A. 2005. Multiple roles for MMPs and TIMPs in cerebral ischemia. *Glia,* 50**,** 329-39.

CURTIS, K. M., GOMEZ, L. A., RIOS, C., GARBAYO, E., RAVAL, A. P., PEREZ-PINZON, M. A. & SCHILLER, P. C. 2010. EF1alpha and RPL13a represent normalization genes suitable for RT-qPCR analysis of bone marrow derived mesenchymal stem cells. *BMC Mol Biol,* 11**,** 61.

CYBULSKY, A. V. & MCTAVISH, A. J. 1997. Extracellular matrix is required for MAP kinase activation and proliferation of rat glomerular epithelial cells. *Biochem Biophys Res Commun,* 231**,** 160-6.

D'AMORE, P. A. 1992. Mechanisms of endothelial growth control. *American journal of respiratory cell and molecular biology,* 6**,** 1-8.

DE-CARVALHO, M. C., CHIMELLI, L. M. & QUIRICO-SANTOS, T. 1999. Modulation of fibronectin expression in the central nervous system of Lewis rats with experimental autoimmune encephalomyelitis. *Braz J Med Biol Res,* 32**,** 583-92.

DE BOER, A. G. & GAILLARD, P. J. 2006. Blood-brain barrier dysfunction and recovery. *J Neural Transm,* 113**,** 455-62.

DEAKIN, N. O. & TURNER, C. E. 2008. Paxillin comes of age. *J Cell Sci,* 121**,** 2435-44.

DEFILIPPI, P., SILENGO, L. & TARONE, G. 1992. Alpha 6.beta 1 integrin (laminin receptor) is down-regulated by tumor necrosis factor alpha and interleukin-1 beta in human endothelial cells. *J Biol Chem,* 267**,** 18303-7.

DEL ZOPPO, G. J. & MILNER, R. 2006. Integrin-matrix interactions in the cerebral microvasculature. *Arterioscler Thromb Vasc Biol,* 26**,** 1966-75.

DELI, M. A., DEHOUCK, M. P., ABRAHAM, C. S., CECCHELLI, R. & JOO, F. 1995. Penetration of small molecular weight substances through cultured bovine brain capillary endothelial cell monolayers: the early effects of cyclic adenosine 3',5'-monophosphate. *Exp Physiol,* 80**,** 675-8.

DELWEL, G. O., DE MELKER, A. A., HOGERVORST, F., JASPARS, L. H., FLES, D. L., KUIKMAN, I., LINDBLOM, A., PAULSSON, M., TIMPL, R. & SONNENBERG, A. 1994. Distinct and overlapping ligand specificities of the alpha 3A beta 1 and alpha 6A beta 1 integrins: recognition of laminin isoforms. *Mol Biol Cell,* 5**,** 203-15.

DESBAN, N., LISSITZKY, J. C., ROUSSELLE, P. & DUBAND, J. L. 2006. alpha1beta1-integrin engagement to distinct laminin-1 domains orchestrates spreading, migration and survival of neural crest cells through independent signaling pathways. *J Cell Sci,* 119**,** 3206-18.

DIAMOND, M. S., ALON, R., PARKOS, C. A., QUINN, M. T. & SPRINGER, T. A. 1995. Heparin is an adhesive ligand for the leukocyte integrin Mac-1 (CD11b/CD1). *J Cell Biol,* 130**,** 1473-82.

DIDIER, N., ROMERO, I. A., CREMINON, C., WIJKHUISEN, A., GRASSI, J. & MABONDZO, A. 2003. Secretion of interleukin-1beta by astrocytes mediates endothelin-1 and tumour necrosis factor-alpha effects on human brain microvascular endothelial cell permeability. *J Neurochem,* 86**,** 246-54.

DINARELLO, C. A. 1994. The interleukin-1 family: 10 years of discovery. *FASEB J,* 8**,** 1314-25.

DINARELLO, C. A. 2000. Proinflammatory cytokines. *Chest,* 118**,** 503-8.

DIXELIUS, J., JAKOBSSON, L., GENERSCH, E., BOHMAN, S., EKBLOM, P. & CLAESSON-WELSH, L. 2004. Laminin-1 promotes angiogenesis in synergy with fibroblast growth factor by distinct regulation of the gene and protein expression profile in endothelial cells. *J Biol Chem,* 279**,** 23766-72.

DOI, M., THYBOLL, J., KORTESMAA, J., JANSSON, K., IIVANAINEN, A., PARVARDEH, M., TIMPL, R., HEDIN, U., SWEDENBORG, J. & TRYGGVASON, K. 2002. Recombinant Human Laminin-10 (α5β1γ1): PRODUCTION, PURIFICATION, AND MIGRATION-PROMOTING ACTIVITY ON VASCULAR ENDOTHELIAL CELLS. *Journal of Biological Chemistry,* 277**,** 12741-12748.

EBNET, K., SCHULZ, C. U., MEYER ZU BRICKWEDDE, M. K., PENDL, G. G. & VESTWEBER, D. 2000. Junctional adhesion molecule interacts with the PDZ domain-containing proteins AF-6 and ZO-1. *J Biol Chem,* 275**,** 27979-88.

ELICES, M. J. & HEMLER, M. E. 1989. The human integrin VLA-2 is a collagen receptor on some cells and a collagen/laminin receptor on others. *Proc Natl Acad Sci U S A,* 86**,** 9906-10.

FABRY, Z., FITZSIMMONS, K. M., HERLEIN, J. A., MONINGER, T. O., DOBBS, M. B. & HART, M. N. 1993. Production of the cytokines interleukin 1 and 6 by murine brain microvessel endothelium and smooth muscle pericytes. *J Neuroimmunol,* 47**,** 23-34.

FAWCETT, J., BUCKLEY, C., HOLNESS, C. L., BIRD, I. N., SPRAGG, J. H., SAUNDERS, J., HARRIS, A. & SIMMONS, D. L. 1995. Mapping the homotypic binding sites in CD31 and the role of CD31 adhesion in the formation of interendothelial cell contacts. *J Cell Biol,* 128**,** 1229-41.

FERLETTA, M. & EKBLOM, P. 1999. Identification of laminin-10/11 as a strong cell adhesive complex for a normal and a malignant human epithelial cell line. *J Cell Sci,* 112 (Pt 1)**,** 1-10.

FINLAY, D., HEALY, V., FURLONG, F., O'CONNELL, F. C., KEON, N. K. & MARTIN, F. 2000. MAP kinase pathway signalling is essential for extracellular matrix determined mammary epithelial cell survival. *Cell Death Differ,* 7**,** 302-13.

FISCHER, S., WOBBEN, M., MARTI, H. H., RENZ, D. & SCHAPER, W. 2002. Hypoxia-induced hyperpermeability in brain microvessel endothelial cells involves VEGF-mediated changes in the expression of zonula occludens-1. *Microvasc Res,* 63**,** 70-80.

FLETCHER, S. J., POULTER, N. S., HAINING, E. J. & RAPPOPORT, J. Z. 2012. Clathrin-mediated endocytosis regulates occludin, and not focal adhesion, distribution during epithelial wound healing. *Biol Cell,* 104**,** 238-56.

FLORIS, S., VAN DEN BORN, J., VAN DER POL, S., DIJKSTRA, C. & DE VRIES, H. 2003. Heparan sulfate proteoglycans modulate monocyte migration across cerebral endothelium. *J neuropathol Exp Neurol,* 62**,** 780-90.

FOLKMAN, J. & HAUDENSCHILD, C. 1980. Angiogenesis in vitro. *Nature,* 288**,** 551-6.

FOLKMAN, J. & MOSCONA, A. 1978. Role of cell shape in growth control. *Nature,* 273**,** 345-9.

FORM, D. M., PRATT, B. M. & MADRI, J. A. 1986. Endothelial cell proliferation during angiogenesis. In vitro modulation by basement membrane components. *Lab Invest,* 55**,** 521-30.

FORSTER, C., BUREK, M., ROMERO, I. A., WEKSLER, B., COURAUD, P. O. & DRENCKHAHN, D. 2008. Differential effects of hydrocortisone and TNFalpha on tight junction proteins in an in vitro model of the human blood-brain barrier. *J Physiol,* 586**,** 1937-49.

FORSTER, C., SILWEDEL, C., GOLENHOFEN, N., BUREK, M., KIETZ, S., MANKERTZ, J. & DRENCKHAHN, D. 2005. Occludin as direct target for glucocorticoid-induced improvement of blood-brain barrier properties in a murine in vitro system. *J Physiol,* 565**,** 475-86.

FRANCOEUR, C., ESCAFFIT, F., VACHON, P. H. & BEAULIEU, J. F. 2004. Proinflammatory cytokines TNF-alpha and IFN-gamma alter laminin expression under an apoptosis-independent mechanism in human intestinal epithelial cells. *Am J Physiol Gastrointest Liver Physiol,* 287**,** G592-8.

FRANKE, H., GALLA, H.-J. & BEUCKMANN, C. T. 2000. Primary cultures of brain microvessel endothelial cells: a valid and flexible model to study drug transport through the blood-brain barrier in vitro. *Brain Research Protocols,* 5**,** 248-256.

FRIESER, M., NOCKEL, H., PAUSCH, F., RODER, C., HAHN, A., DEUTZMANN, R. & SOROKIN, L. M. 1997. Cloning of the mouse laminin alpha 4 cDNA. Expression in a subset of endothelium. *Eur J Biochem,* 246**,** 727-35.

FRIJNS, C. J. & KAPPELLE, L. J. 2002. Inflammatory cell adhesion molecules in ischemic cerebrovascular disease. *Stroke,* 33**,** 2115-22.

FROST, J. A., STEEN, H., SHAPIRO, P., LEWIS, T., AHN, N., SHAW, P. E. & COBB, M. H. 1997. Cross-cascade activation of ERKs and ternary complex factors by Rho family proteins. *Embo J,* 16**,** 6426-38.

FUJIWARA, H., KIKKAWA, Y., SANZEN, N. & SEKIGUCHI, K. 2001. Purification and characterization of human laminin-8. Laminin-8 stimulates cell adhesion and migration through alpha3beta1 and alpha6beta1 integrins. *J Biol Chem,* 276**,** 17550-8.

FUKUDA, K., GUPTA, S., CHEN, K., WU, C. & QIN, J. 2009. The pseudoactive site of ILK is essential for its binding to alpha-Parvin and localization to focal adhesions. *Mol Cell,* 36**,** 819-30.

FUKUDA, S., FINI, C. A., MABUCHI, T., KOZIOL, J. A., EGGLESTON, L. L., JR. & DEL ZOPPO, G. J. 2004. Focal cerebral ischemia induces active proteases that degrade microvascular matrix. *Stroke,* 35**,** 998-1004.

FURUSE, M., HIRASE, T., ITOH, M., NAGAFUCHI, A., YONEMURA, S. & TSUKITA, S. 1993. Occludin: a novel integral membrane protein localizing at tight junctions. *J Cell Biol,* 123**,** 1777-88.

FURUSE, M., ITOH, M., HIRASE, T., NAGAFUCHI, A., YONEMURA, S., TSUKITA, S. & TSUKITA, S. 1994. Direct association of occludin with ZO-1 and its possible involvement in the localization of occludin at tight junctions. *J Cell Biol,* 127**,** 1617-26.

GAILLARD, P. J., VOORWINDEN, L. H., NIELSEN, J. L., IVANOV, A., ATSUMI, R., ENGMAN, H., RINGBOM, C., DE BOER, A. G. & BREIMER, D. D. 2001. Establishment and functional characterization of an in vitro model of the blood-brain barrier, comprising a co-culture of brain capillary endothelial cells and astrocytes. *Eur J Pharm Sci,* 12**,** 215-22.

GAMBLE, J., MEYER, G., NOACK, L., FURZE, J., MATTHIAS, L., KOVACH, N., HARLANT, J. & VADAS, M. 1999. B1 integrin activation inhibits in vitro tube formation: effects on cell migration, vacuole coalescence and lumen formation. *Endothelium,* 7**,** 23-34.

GAMBLE, J. R., MATTHIAS, L. J., MEYER, G., KAUR, P., RUSS, G., FAULL, R., BERNDT, M. C. & VADAS, M. A. 1993. Regulation of in vitro capillary tube formation by anti-integrin antibodies. *The Journal of Cell Biology,* 121**,** 931-943.

GARCIA DE YEBENES, E., HO, A., DAMANI, T., FILLIT, H. & BLUM, M. 1999. Regulation of the heparan sulfate proteoglycan, perlecan, by injury and interleukin-1alpha. *J Neurochem,* 73**,** 812-20.

GASCHE, Y., FUJIMURA, M., MORITA-FUJIMURA, Y., COPIN, J. C., KAWASE, M., MASSENGALE, J. & CHAN, P. H. 1999. Early appearance of activated matrix metalloproteinase-9 after focal cerebral ischemia in mice: a possible role in blood-brain barrier dysfunction. *J Cereb Blood Flow Metab,* 19**,** 1020-8.

GEHLSEN, K. R., DICKERSON, K., ARGRAVES, W. S., ENGVALL, E. & RUOSLAHTI, E. 1989. Subunit structure of a laminin-binding integrin and localization of its binding site on laminin. *J Biol Chem,* 264**,** 19034-8.

GENERSCH, E., FERLETTA, M., VIRTANEN, I., HALLER, H. & EKBLOM, P. 2003a. Integrin alphavbeta3 binding to human alpha5-laminins facilitates FGF-2- and VEGF-induced proliferation of human ECV304 carcinoma cells. *European Journal of Cell Biology,* 82**,** 105-117.

GENERSCH, E., FERLETTA, M., VIRTANEN, I., HALLER, H. & EKBLOM, P. 2003b. Integrin αvβ3 binding to human α5-laminins facilitates FGF-2- and VEGF-induced proliferation of human ECV304 carcinoma cells. *European Journal of Cell Biology,* 82**,** 105-117.

GERSDORFF, N., KOHFELDT, E., SASAKI, T., TIMPL, R. & MIOSGE, N. 2005a. Laminin gamma3 chain binds to nidogen and is located in murine basement membranes. *J Biol Chem,* 280**,** 22146-53.

GERSDORFF, N., KOHFELDT, E., SASAKI, T., TIMPL, R. & MIOSGE, N. 2005b. Laminin γ3 Chain Binds to Nidogen and Is Located in Murine Basement Membranes. *Journal of Biological Chemistry,* 280**,** 22146-22153.

GHOSH, A., PARK, J. Y., FENNO, C. & KAPILA, Y. L. 2008. Porphyromonas gingivalis, gamma interferon, and a proapoptotic fibronectin matrix form a synergistic trio that induces c-Jun N-terminal kinase 1-mediated nitric oxide generation and cell death. *Infect Immun,* 76**,** 5514-23.

GIANNONE, G. & SHEETZ, M. P. 2006. Substrate rigidity and force define form through tyrosine phosphatase and kinase pathways. *Trends Cell Biol,* 16**,** 213-23.

GIMBRONE, M. A., JR., COTRAN, R. S. & FOLKMAN, J. 1974. Human vascular endothelial cells in culture. Growth and DNA synthesis. *J Cell Biol,* 60**,** 673-84.

GINSBERG, M. H., PARTRIDGE, A. & SHATTIL, S. J. 2005. Integrin regulation. *Curr Opin Cell Biol,* 17**,** 509-16.

GIORDANA, M. T., GERMANO, I., GIACCONE, G., MAURO, A., MIGHELI, A. & SCHIFFER, D. 1985. The distribution of laminin in human brain tumors: an immunohistochemical study. *Acta Neuropathol,* 67**,** 51-7.

GONZALEZ, A. M., GONZALES, M., HERRON, G. S., NAGAVARAPU, U., HOPKINSON, S. B., TSURUTA, D. & JONES, J. C. 2002. Complex interactions between the laminin alpha 4 subunit and integrins regulate endothelial cell behavior in vitro and angiogenesis in vivo. *Proc Natl Acad Sci U S A,* 99**,** 16075-80.

GRANT, D. S. & KLEINMAN, H. K. 1997. Regulation of capillary formation by laminin and other components of the extracellular matrix. *Exs,* 79**,** 317-33.

GRAVES, K. L. & ROMAN, J. 1996. Fibronectin modulates expression of interleukin-1 beta and its receptor antagonist in human mononuclear cells. *Am J Physiol,* 271**,** L61-9.

GREVE, M. W. & ZINK, B. J. 2009. Pathophysiology of traumatic brain injury. *Mt Sinai J Med,* 76**,** 97-104.

GROOMS, S. Y., TERRACIO, L. & JONES, L. S. 1993. Anatomical localization of beta 1 integrin-like immunoreactivity in rat brain. *Exp Neurol,* 122**,** 253-9.

GU, Z., CUI, J., BROWN, S., FRIDMAN, R., MOBASHERY, S., STRONGIN, A. Y. & LIPTON, S. A. 2005. A highly specific inhibitor of matrix metalloproteinase-9 rescues laminin from proteolysis and neurons from apoptosis in transient focal cerebral ischemia. *J Neurosci,* 25**,** 6401-8.

GUALTIERI, F., CURIA, G., MARINELLI, C. & BIAGINI, G. 2012. Increased perivascular laminin predicts damage to astrocytes in CA3 and piriform cortex following chemoconvulsive treatments. *Neuroscience,* 218**,** 278-94.

GUAN, J.-L. & SHALLOWAY, D. 1992. Regulation of focal adhesion-associated protein tyrosine kinase by both cellular adhesion and oncogenic transformation. *Nature,* 358**,** 690-692.

GUBERN, C., HURTADO, O., RODRIGUEZ, R., MORALES, J. R., ROMERA, V. G., MORO, M. A., LIZASOAIN, I., SERENA, J. & MALLOLAS, J. 2009. Validation of housekeeping genes for quantitative real-time PCR in in-vivo and in-vitro models of cerebral ischaemia. *BMC Mol Biol,* 10**,** 57.

HALL, D. E., REICHARDT, L. F., CROWLEY, E., HOLLEY, B., MOEZZI, H., SONNENBERG, A. & DAMSKY, C. H. 1990. The alpha 1/beta 1 and alpha 6/beta 1 integrin heterodimers mediate cell attachment to distinct sites on laminin. *J Cell Biol,* 110**,** 2175-84.

HALLMANN, R., HORN, N., SELG, M., WENDLER, O., PAUSCH, F. & SOROKIN, L. M. 2005. Expression and function of laminins in the embryonic and mature vasculature. *Physiol Rev,* 85**,** 979-1000.

HAMANN, G. F., OKADA, Y., FITRIDGE, R. & DEL ZOPPO, G. J. 1995. Microvascular basal lamina antigens disappear during cerebral ischemia and reperfusion. *Stroke,* 26**,** 2120-6.

HAMMAR, E. B., IRMINGER, J. C., RICKENBACH, K., PARNAUD, G., RIBAUX, P., BOSCO, D., ROUILLER, D. G. & HALBAN, P. A. 2005. Activation of NF-kappaB by extracellular matrix is involved in spreading and glucose-stimulated insulin secretion of pancreatic beta cells. *J Biol Chem,* 280**,** 30630-7.

HANKS, S. K., CALALB, M. B., HARPER, M. C. & PATEL, S. K. 1992. Focal adhesion protein-tyrosine kinase phosphorylated in response to cell attachment to fibronectin. *Proc Natl Acad Sci U S A,* 89**,** 8487-91.

HAORAH, J., RAMIREZ, S. H., SCHALL, K., SMITH, D., PANDYA, R. & PERSIDSKY, Y. 2007. Oxidative stress activates protein tyrosine kinase and matrix metalloproteinases leading to blood-brain barrier dysfunction. *J Neurochem,* 101**,** 566-76.

HARING, H. P., BERG, E. L., TSURUSHITA, N., TAGAYA, M. & DEL ZOPPO, G. J. 1996. E-selectin appears in nonischemic tissue during experimental focal cerebral ischemia. *Stroke,* 27**,** 1386-91; discussion 1391-2.

HARVEY, R. A. & FERRIER, D. R. 2011. *Lippincott's Illustrated Reviews: Biochemistry* Wolters Kluwer.

HASELOFF, R. F., BLASIG, I. E., BAUER, H. C. & BAUER, H. 2005. In search of the astrocytic factor(s) modulating blood-brain barrier functions in brain capillary endothelial cells in vitro. *Cell Mol Neurobiol,* 25**,** 25-39.

HASKINS, J., GU, L., WITTCHEN, E. S., HIBBARD, J. & STEVENSON, B. R. 1998. ZO-3, a novel member of the MAGUK protein family found at the tight junction, interacts with ZO-1 and occludin. *J Cell Biol,* 141**,** 199-208.

HAWKINS, B. T., ABBRUSCATO, T. J., EGLETON, R. D., BROWN, R. C., HUBER, J. D., CAMPOS, C. R. & DAVIS, T. P. 2004. Nicotine increases in vivo blood-brain barrier permeability and alters cerebral microvascular tight junction protein distribution. *Brain Res,* 1027**,** 48-58.

HEIMARK, R. L. & SCHWARTZ, S. M. 1985. The role of membrane-membrane interactions in the regulation of endothelial cell growth. *J Cell Biol,* 100**,** 1934-40.

HEO, J. H., LUCERO, J., ABUMIYA, T., KOZIOL, J. A., COPELAND, B. R. & DEL ZOPPO, G. J. 1999. Matrix metalloproteinases increase very early during experimental focal cerebral ischemia. *J Cereb Blood Flow Metab,* 19**,** 624-33.

HERBST, T. J., MCCARTHY, J. B., TSILIBARY, E. C. & FURCHT, L. T. 1988. Differential effects of laminin, intact type IV collagen, and specific domains of type IV collagen on endothelial cell adhesion and migration. *J Cell Biol,* 106**,** 1365-73.

HESS, D. C., BHUTWALA, T., SHEPPARD, J. C., ZHAO, W. & SMITH, J. 1994a. ICAM-1 expression on human brain microvascular endothelial cells. *Neurosci Lett,* 168**,** 201-4.

HESS, D. C., THOMPSON, Y., SPRINKLE, A., CARROLL, J. & SMITH, J. 1996. E-selectin expression on human brain microvascular endothelial cells. *Neurosci Lett,* 213**,** 37-40.

HESS, D. C., ZHAO, W., CARROLL, J., MCEACHIN, M. & BUCHANAN, K. 1994b. Increased expression of ICAM-1 during reoxygenation in brain endothelial cells. *Stroke,* 25**,** 1463-7; discussion 1468.

HIMI, T., YOSHIOKA, I. & KATAURA, A. 1997. Production and gene expression of IL-8-like cytokine GRO/CINC-1 in rat nasal mucosa. *Acta Otolaryngol,* 117**,** 123-7.

HIRASE, T., STADDON, J. M., SAITOU, M., ANDO-AKATSUKA, Y., ITOH, M., FURUSE, M., FUJIMOTO, K., TSUKITA, S. & RUBIN, L. L. 1997. Occludin as a possible determinant of tight junction permeability in endothelial cells. *J Cell Sci,* 110 (Pt 14)**,** 1603-13.

HOHEISEL, D., NITZ, T., FRANKE, H., WEGENER, J., HAKVOORT, A., TILLING, T. & GALLA, H.-J. 1998. Hydrocortisone Reinforces the Blood-Brain Barrier Properties in a Serum Free Cell Culture System. *Biochemical and Biophysical Research Communications,* 244**,** 312-316.

HOSOMI, N., LUCERO, J., HEO, J. H., KOZIOL, J. A., COPELAND, B. R. & DEL ZOPPO, G. J. 2001. Rapid differential endogenous plasminogen activator expression after acute middle cerebral artery occlusion. *Stroke,* 32**,** 1341-8.

HOTCHIN, N. A. & HALL, A. 1995. The assembly of integrin adhesion complexes requires both extracellular matrix and intracellular rho/rac GTPases. *J Cell Biol,* 131**,** 1857-65.

HUANG, J., UPADHYAY, U. M. & TAMARGO, R. J. 2006. Inflammation in stroke and focal cerebral ischemia. *Surg Neurol,* 66**,** 232-45.

HUANG, S. & INGBER, D. E. 2000. Shape-dependent control of cell growth, differentiation, and apoptosis: switching between attractors in cell regulatory networks. *Exp Cell Res,* 261**,** 91-103.

HUMPHRIES, J. D., BYRON, A., BASS, M. D., CRAIG, S. E., PINNEY, J. W., KNIGHT, D. & HUMPHRIES, M. J. 2009. Proteomic analysis of integrin-associated complexes identifies RCC2 as a dual regulator of Rac1 and Arf6. *Sci Signal,* 2**,** ra51.

HUMPHRIES, J. D., BYRON, A. & HUMPHRIES, M. J. 2006. Integrin ligands at a glance. *Journal of Cell Science,* 119**,** 3901-3903.

HUMPHRIES, M. 2001. Cell adhesion assays. *Molecular Biotechnology,* 18**,** 57-61.

HUNGERFORD, J. E., COMPTON, M. T., MATTER, M. L., HOFFSTROM, B. G. & OTEY, C. A. 1996. Inhibition of pp125FAK in cultured fibroblasts results in apoptosis. *J Cell Biol,* 135**,** 1383-90.

HUSSAIN, S. A., CARAFOLI, F. & HOHENESTER, E. 2011. Determinants of laminin polymerization revealed by the structure of the alpha5 chain amino-terminal region. *EMBO Rep,* 12**,** 276-82.

IDO, H., HARADA, K., FUTAKI, S., HAYASHI, Y., NISHIUCHI, R., NATSUKA, Y., LI, S., WADA, Y., COMBS, A. C., ERVASTI, J. M. & SEKIGUCHI, K. 2004. Molecular dissection of the alpha-dystroglycan- and integrin-binding sites within the globular domain of human laminin-10. *J Biol Chem,* 279**,** 10946-54.

IGNATIUS, M. J., LARGE, T. H., HOUDE, M., TAWIL, J. W., BARTON, A., ESCH, F., CARBONETTO, S. & REICHARDT, L. F. 1990. Molecular cloning of the rat integrin alpha 1-subunit: a receptor for laminin and collagen. *J Cell Biol,* 111**,** 709-20.

IIVANAINEN, A., SAINIO, K., SARIOLA, H. & TRYGGVASON, K. 1995. Primary structure and expression of a novel human laminin α4 chain. *FEBS Letters,* 365**,** 183-188.

INGBER, D. E. 1992. Extracellular matrix as a solid-state regulator in angiogenesis: identification of new targets for anti-cancer therapy. *Semin Cancer Biol,* 3**,** 57-63.

INGBER, D. E. & FOLKMAN, J. 1989. Mechanochemical switching between growth and differentiation during fibroblast growth factor-stimulated angiogenesis in vitro: role of extracellular matrix. *J Cell Biol,* 109**,** 317-30.

ITOH, M., FURUSE, M., MORITA, K., KUBOTA, K., SAITOU, M. & TSUKITA, S. 1999. Direct binding of three tight junction-associated MAGUKs, ZO-1, ZO-2, and ZO-3, with the COOH termini of claudins. *J Cell Biol,* 147**,** 1351-63.

ITOH, M., NAGAFUCHI, A., MOROI, S. & TSUKITA, S. 1997. Involvement of ZO-1 in cadherin-based cell adhesion through its direct binding to alpha catenin and actin filaments. *J Cell Biol,* 138**,** 181-92.

IVANOV, A. I., NUSRAT, A. & PARKOS, C. A. 2004. Endocytosis of epithelial apical junctional proteins by a clathrin-mediated pathway into a unique storage compartment. *Mol Biol Cell,* 15**,** 176-88.

JAEGER, M. M., KALINEC, G., DODANE, V. & KACHAR, B. 1997. A collagen substrate enhances the sealing capacity of tight junctions of A6 cell monolayers. *J Membr Biol,* 159**,** 263-70.

JANEWAY, C. A., TRAVERS, P., WALPORT, M., SHLOMCHIK, M. 2001. *Immunobiology*, Garland Science.

JEFFREY, M. G., YVAN, G. G., JEAN, C. C., AARTI, R. S., RONALD, S. P., STEVEN, D. S., PAK, H. C. & PARK, T. S. 2005. Leukocyte-derived matrix metalloproteinase-9 mediates blood-brain barrier breakdown and is proinflammatory after transient focal cerebral ischemia. *American Journal of Physiology - Heart and Circulatory Physiology,* 289**,** H558-H568.

JELIAZKOVA-MECHEVA, V. V. & BOBILYA, D. J. 2003. A porcine astrocyte/endothelial cell co-culture model of the blood-brain barrier. *Brain Research Protocols,* 12**,** 91-98.

JETTE, L., TETU, B. & BELIVEAU, R. 1993. High levels of P-glycoprotein detected in isolated brain capillaries. *Biochim Biophys Acta,* 1150**,** 147-54.

JI, K. & TSIRKA, S. E. 2012. Inflammation modulates expression of laminin in the central nervous system following ischemic injury. *J Neuroinflammation,* 9.

JOHANSSON, S., SVINENG, G., WENNERBERG, K., ARMULIK, A. & LOHIKANGAS, L. 1997. Fibronectin-integrin interactions. *Front Biosci,* 2**,** d126-46.

JUSTICIA, C., PANES, J., SOLE, S., CERVERA, A., DEULOFEU, R., CHAMORRO, A. & PLANAS, A. M. 2003. Neutrophil infiltration increases matrix metalloproteinase-9 in the ischemic brain after occlusion/reperfusion of the middle cerebral artery in rats. *J Cereb Blood Flow Metab,* 23**,** 1430-40.

KATSUNO, T., UMEDA, K., MATSUI, T., HATA, M., TAMURA, A., ITOH, M., TAKEUCHI, K., FUJIMORI, T., NABESHIMA, Y., NODA, T., TSUKITA, S. & TSUKITA, S. 2008. Deficiency of zonula occludens-1 causes embryonic lethal phenotype associated with defected yolk sac angiogenesis and apoptosis of embryonic cells. *Mol Biol Cell,* 19**,** 2465-75.

KAWATAKI, T., YAMANE, T., NAGANUMA, H., ROUSSELLE, P., ANDUREN, I., TRYGGVASON, K. & PATARROYO, M. 2007. Laminin isoforms and their integrin receptors in glioma cell migration and invasiveness: Evidence for a role of alpha5-laminin(s) and alpha3beta1 integrin. *Exp Cell Res,* 313**,** 3819-31.

KEEP, R. F., ANDJELKOVIC, A. V., STAMATOVIC, S. M., SHAKUI, P. & ENNIS, S. R. 2005. Ischemia-induced endothelial cell dysfunction. *Acta Neurochir Suppl,* 95**,** 399-402.

KERN, A., EBLE, J., GOLBIK, R. & KÜHN, K. 1993. Interaction of type IV collagen with the isolated integrins α1β1 and α2β1. *European Journal of Biochemistry,* 215**,** 151-159.

KHOSHNOODI, J., PEDCHENKO, V. & HUDSON, B. G. 2008. Mammalian collagen IV. *Microsc Res Tech,* 71**,** 357-70.

KIELTY, C. M., SHERRATT, M. J., MARSON, A. & BALDOCK, C. 2005. Fibrillin microfibrils. *Adv Protein Chem,* 70**,** 405-36.

KIKKAWA, Y., MIWA, T., TOHARA, Y., HAMAKUBO, T. & NOMIZU, M. 2011. An antibody to the lutheran glycoprotein (Lu) recognizing the LU4 blood type variant inhibits cell adhesion to laminin alpha5. *PLoS ONE,* 6**,** e23329.

KIKKAWA, Y., SANZEN, N., FUJIWARA, H., SONNENBERG, A. & SEKIGUCHI, K. 2000. Integrin binding specificity of laminin-10/11: laminin-10/11 are recognized by alpha 3 beta 1, alpha 6 beta 1 and alpha 6 beta 4 integrins. *J Cell Sci,* 113 (Pt 5)**,** 869-76.

KIKKAWA, Y., SANZEN, N. & SEKIGUCHI, K. 1998. Isolation and characterization of laminin-10/11 secreted by human lung carcinoma cells. laminin-10/11 mediates cell adhesion through integrin alpha3 beta1. *J Biol Chem,* 273**,** 15854-9.

KIKKAWA, Y., YU, H., GENERSCH, E., SANZEN, N., SEKIGUCHI, K., FÃ¤SSLER, R., CAMPBELL, K. P., TALTS, J. F. & EKBLOM, P. 2004. Laminin isoforms differentially regulate adhesion, spreading, proliferation, and ERK activation of beta1 integrin-null cells. *Experimental cell research,* 300**,** 94-108.

KIM, J. P., CHEN, J. D., WILKE, M. S., SCHALL, T. J. & WOODLEY, D. T. 1994. Human keratinocyte migration on type IV collagen. Roles of heparin-binding site and alpha 2 beta 1 integrin. *Lab Invest,* 71**,** 401-8.

KIMURA, K., TERANISHI, S. & NISHIDA, T. 2009. Interleukin-1beta Induced Disruption of Barrier Function in Cultured Human Corneal Epithelial Cells. *Investigative Ophthalmology & Visual Science,* 50**,** 597-603.

KLEPPEL, M. M., SANTI, P. A., CAMERON, J. D., WIESLANDER, J. & MICHAEL, A. F. 1989. Human tissue distribution of novel basement membrane collagen. *Am J Pathol,* 134**,** 813-25.

KNIGHT, C. G., MORTON, L. F., PEACHEY, A. R., TUCKWELL, D. S., FARNDALE, R. W. & BARNES, M. J. 2000. The Collagen-binding A-domains of Integrins α1β1 and α2β1 Recognize the Same Specific Amino Acid Sequence, GFOGER, in Native (Triple-helical) Collagens. *Journal of Biological Chemistry,* 275**,** 35-40.

KORNBERG, L., EARP, H. S., PARSONS, J. T., SCHALLER, M. & JULIANO, R. L. 1992. Cell adhesion or integrin clustering increases phosphorylation of a focal adhesion-associated tyrosine kinase. *Journal of Biological Chemistry,* 267**,** 23439-42.

KORTESMAA, J., YURCHENCO, P. & TRYGGVASON, K. 2000. Recombinant laminin-8 (alpha(4)beta(1)gamma(1)). Production, purification,and interactions with integrins. *J Biol Chem,* 275**,** 14853-9.

KRAMER, R. H., CHENG, Y. F. & CLYMAN, R. 1990. Human microvascular endothelial cells use beta 1 and beta 3 integrin receptor complexes to attach to laminin. *J Cell Biol,* 111**,** 1233-43.

KRAMER, R. H. & MARKS, N. 1989. Identification of integrin collagen receptors on human melanoma cells. *Journal of Biological Chemistry,* 264**,** 4684-4688.

KRIZANAC-BENGEZ, L., KAPURAL, M., PARKINSON, F., CUCULLO, L., HOSSAIN, M., MAYBERG, M. R. & JANIGRO, D. 2003. Effects of transient loss of shear stress on blood-brain barrier endothelium: role of nitric oxide and IL-6. *Brain Res,* 977**,** 239-46.

KRUEGER, M., HARTIG, W., REICHENBACH, A., BECHMANN, I. & MICHALSKI, D. 2013. Blood-brain barrier breakdown after embolic stroke in rats occurs without ultrastructural evidence for disrupting tight junctions. *PLoS ONE,* 8**,** e56419.

KRUM, J. M., MORE, N. S. & ROSENSTEIN, J. M. 1991. Brain angiogenesis: variations in vascular basement membrane glycoprotein immunoreactivity. *Exp Neurol,* 111**,** 152-65.

KÜHN, K. 1995. Basement membrane (type IV) collagen. *Matrix Biology,* 14**,** 439-445.

KULESH, D. A. & GREENE, J. J. 1986. Shape-dependent regulation of proliferation in normal and malignant human cells and its alteration by interferon. *Cancer Res,* 46**,** 2793-7.

KUSANO, K., MIYAURA, C., INADA, M., TAMURA, T., ITO, A., NAGASE, H., KAMOI, K. & SUDA, T. 1998. Regulation of matrix metalloproteinases (MMP-2, -3, -9, and -13) by interleukin-1 and interleukin-6 in mouse calvaria: association of MMP induction with bone resorption. *Endocrinology,* 139**,** 1338-45.

LANGUINO, L. R., GEHLSEN, K. R., WAYNER, E., CARTER, W. G., ENGVALL, E. & RUOSLAHTI, E. 1989. Endothelial cells use alpha 2 beta 1 integrin as a laminin receptor. *J Cell Biol,* 109**,** 2455-62.

LEE, E. C., LOTZ, M. M., STEELE, G. D., JR. & MERCURIO, A. M. 1992. The integrin alpha 6 beta 4 is a laminin receptor. *J Cell Biol,* 117**,** 671-8.

LEE, J. H., LEE, J., SEO, G. H., KIM, C. H. & AHN, Y. S. 2007. Heparin inhibits NF-kappaB activation and increases cell death in cerebral endothelial cells after oxygen-glucose deprivation. *J Mol Neurosci,* 32**,** 145-54.

LEE, S. C., LIU, W., DICKSON, D. W., BROSNAN, C. F. & BERMAN, J. W. 1993. Cytokine production by human fetal microglia and astrocytes. Differential induction by lipopolysaccharide and IL-1 beta. *J Immunol,* 150**,** 2659-67.

LEE, S. R. & LO, E. H. 2004. Induction of caspase-mediated cell death by matrix metalloproteinases in cerebral endothelial cells after hypoxia-reoxygenation. *J Cereb Blood Flow Metab,* 24**,** 720-7.

LEE, S. R., TSUJI, K. & LO, E. H. 2004. Role of matrix metalloproteinases in delayed neuronal damage after transient global cerebral ischemia. *J Neurosci,* 24**,** 671-8.

LEGATE, K. R., MONTANEZ, E., KUDLACEK, O. & FASSLER, R. 2006. ILK, PINCH and parvin: the tIPP of integrin signalling. *Nat Rev Mol Cell Biol,* 7**,** 20-31.

LEGOS, J. J., WHITMORE, R. G., ERHARDT, J. A., PARSONS, A. A., TUMA, R. F. & BARONE, F. C. 2000. Quantitative changes in interleukin proteins following focal stroke in the rat. *Neurosci Lett,* 282**,** 189-92.

LEISS, M., BECKMANN, K., GIROS, A., COSTELL, M. & FASSLER, R. 2008. The role of integrin binding sites in fibronectin matrix assembly in vivo. *Curr Opin Cell Biol,* 20**,** 502-7.

LEITINGER, B. & HOHENESTER, E. 2007. Mammalian collagen receptors. *Matrix Biol,* 26**,** 146-55.

LEOW-DYKE, S. 2012. *Inflammatory activation of the cerebrovascular endothelium in response to oxygen-glucose deprivation.* PhD, University of Manchester.

LI, L., LIU, F., WELSER-ALVES, J. V., MCCULLOUGH, L. D. & MILNER, R. 2012. Upregulation of fibronectin and the alpha5beta1 and alphavbeta3 integrins on blood vessels within the cerebral ischemic penumbra. *Exp Neurol,* 233**,** 283-91.

LI, L., WELSER, J. V., DORE-DUFFY, P., DEL ZOPPO, G. J., LAMANNA, J. C. & MILNER, R. 2010. In the hypoxic central nervous system, endothelial cell proliferation is followed by astrocyte activation, proliferation, and increased expression of the alpha 6 beta 4 integrin and dystroglycan. *Glia,* 58**,** 1157-67.

LIANG, K. C., LEE, C. W., LIN, W. N., LIN, C. C., WU, C. B., LUO, S. F. & YANG, C. M. 2007. Interleukin-1beta induces MMP-9 expression via p42/p44 MAPK, p38 MAPK, JNK, and nuclear factor-kappaB signaling pathways in human tracheal smooth muscle cells. *J Cell Physiol,* 211**,** 759-70.

LIMA, W. R., PARREIRA, K. S., DEVUYST, O., CAPLANUSI, A., N'KULI, F., MARIEN, B., VAN DER SMISSEN, P., ALVES, P. M., VERROUST, P., CHRISTENSEN, E. I., TERZI, F., MATTER, K., BALDA, M. S., PIERREUX, C. E. & COURTOY, P. J. 2010. ZONAB promotes proliferation and represses differentiation of proximal tubule epithelial cells. *J Am Soc Nephrol,* 21**,** 478-88.

LINDSBERG, P. J., CARPEN, O., PAETAU, A., KARJALAINEN-LINDSBERG, M. L. & KASTE, M. 1996. Endothelial ICAM-1 expression associated with inflammatory cell response in human ischemic stroke. *Circulation,* 94**,** 939-45.

LIOTTA, L. A., GOLDFARB, R. H., BRUNDAGE, R., SIEGAL, G. P., TERRANOVA, V. & GARBISA, S. 1981. Effect of plasminogen activator (urokinase), plasmin, and thrombin on glycoprotein and collagenous components of basement membrane. *Cancer Res,* 41**,** 4629-36.

LIPPOLDT, A., KNIESEL, U., LIEBNER, S., KALBACHER, H., KIRSCH, T., WOLBURG, H. & HALLER, H. 2000. Structural alterations of tight junctions are associated with loss of polarity in stroke-prone spontaneously hypertensive rat blood-brain barrier endothelial cells. *Brain Res,* 885**,** 251-61.

LIU, J., JIN, X., LIU, K. J. & LIU, W. 2012a. Matrix metalloproteinase-2-mediated occludin degradation and caveolin-1-mediated claudin-5 redistribution contribute to blood-brain barrier damage in early ischemic stroke stage. *J Neurosci,* 32**,** 3044-57.

LIU, T., MCDONNELL, P. C., YOUNG, P. R., WHITE, R. F., SIREN, A. L., HALLENBECK, J. M., BARONE, F. C. & FEURESTEIN, G. Z. 1993a. Interleukin-1 beta mRNA expression in ischemic rat cortex. *Stroke,* 24**,** 1746-50; discussion 1750-1.

LIU, T., YOUNG, P. R., MCDONNELL, P. C., WHITE, R. F., BARONE, F. C. & FEUERSTEIN, G. Z. 1993b. Cytokine-induced neutrophil chemoattractant mRNA expressed in cerebral ischemia. *Neurosci Lett,* 164**,** 125-8.

LIU, W., HENDREN, J., QIN, X. J., SHEN, J. & LIU, K. J. 2009. Normobaric hyperoxia attenuates early blood-brain barrier disruption by inhibiting MMP-9-mediated occludin degradation in focal cerebral ischemia. *J Neurochem,* 108**,** 811-20.

LIU, X. R., LUO, M., YAN, F., ZHANG, C. C., LI, S. J., ZHAO, H. P., JI, X. M. & LUO, Y. M. 2012b. Ischemic postconditioning diminishes matrix metalloproteinase 9 expression and attenuates loss of the extracellular matrix proteins in rats following middle cerebral artery occlusion and reperfusion. *CNS Neurosci Ther,* 18**,** 855-63.

LOCHHEAD, J. J., MCCAFFREY, G., QUIGLEY, C. E., FINCH, J., DEMARCO, K. M., NAMETZ, N. & DAVIS, T. P. 2010. Oxidative stress increases blood-brain barrier permeability and induces alterations in occludin during hypoxia-reoxygenation. *J Cereb Blood Flow Metab,* 30**,** 1625-36.

LODDICK, S. A. & ROTHWELL, N. J. 1996. Neuroprotective effects of human recombinant interleukin-1 receptor antagonist in focal cerebral ischaemia in the rat. *J Cereb Blood Flow Metab,* 16**,** 932-40.

LOSY, J., ZAREMBA, J. & SKROBANSKI, P. 2005. CXCL1 (GRO-alpha) chemokine in acute ischaemic stroke patients. *Folia Neuropathol,* 43**,** 97-102.

LU, Y.-Y., CHEN, Y.-C., KAO, Y.-H., CHEN, S.-A. & CHEN, Y.-J. 2013. Extracellular matrix of collagen modulates arrhythmogenic activity of pulmonary veins through p38 MAPK activation. *Journal of Molecular and Cellular Cardiology,* 59**,** 159-166.

LUCAS, S. M., ROTHWELL, N. J. & GIBSON, R. M. 2006. The role of inflammation in CNS injury and disease. *Br J Pharmacol,* 147 Suppl 1**,** S232-40.

LUO, B. H., CARMAN, C. V. & SPRINGER, T. A. 2007. Structural basis of integrin regulation and signaling. *Annu Rev Immunol,* 25**,** 619-47.

MAHESHWARI, R. K., KEDAR, V. P., COON, H. C. & BHARTIYA, D. 1991. Regulation of laminin expression by interferon. *J Interferon Res,* 11**,** 75-80.

MANKELOW, T. J., BURTON, N., STEFANSDOTTIR, F. O., SPRING, F. A., PARSONS, S. F., PEDERSEN, J. S., OLIVEIRA, C. L., LAMMIE, D., WESS, T., MOHANDAS, N., CHASIS, J. A., BRADY, R. L. & ANSTEE, D. J. 2007. The Laminin 511/521-binding site on the Lutheran blood group glycoprotein is located at the flexible junction of Ig domains 2 and 3. *Blood,* 110**,** 3398-406.

MARCHIANDO, A. M., SHEN, L., GRAHAM, W. V., WEBER, C. R., SCHWARZ, B. T., AUSTIN, J. R., 2ND, RALEIGH, D. R., GUAN, Y., WATSON, A. J., MONTROSE, M. H. & TURNER, J. R. 2010. Caveolin-1-dependent occludin endocytosis is required for TNF-induced tight junction regulation in vivo. *J Cell Biol,* 189**,** 111-26.

MARTIN-PADURA, I., LOSTAGLIO, S., SCHNEEMANN, M., WILLIAMS, L., ROMANO, M., FRUSCELLA, P., PANZERI, C., STOPPACCIARO, A., RUCO, L., VILLA, A., SIMMONS, D. & DEJANA, E. 1998. Junctional adhesion molecule, a novel member of the

immunoglobulin superfamily that distributes at intercellular junctions and modulates monocyte transmigration. *J Cell Biol,* 142**,** 117-27.

MARTIN, S., MARUTA, K., BURKART, V., GILLIS, S. & KOLB, H. 1988. IL-1 and IFN-gamma increase vascular permeability. *Immunology,* 64**,** 301-5.

MCCOLL, B. W., ROTHWELL, N. J. & ALLAN, S. M. 2008. Systemic inflammation alters the kinetics of cerebrovascular tight junction disruption after experimental stroke in mice. *J Neurosci,* 28**,** 9451-62.

MCINTOSH, L. C., MUCKERSIE, L. & FORRESTER, J. V. 1988. Retinal capillary endothelial cells prefer different substrates for growth and migration. *Tissue and Cell,* 20**,** 193-209.

MCNEIL, E., CAPALDO, C. T. & MACARA, I. G. 2006. Zonula occludens-1 function in the assembly of tight junctions in Madin-Darby canine kidney epithelial cells. *Mol Biol Cell,* 17**,** 1922-32.

MILLER, F., FENART, L., LANDRY, V., COISNE, C., CECCHELLI, R., DEHOUCK, M. P. & BUEE-SCHERRER, V. 2005. The MAP kinase pathway mediates transcytosis induced by TNF-alpha in an in vitro blood-brain barrier model. *Eur J Neurosci,* 22**,** 835-44.

MILNER, R. & CAMPBELL, I. L. 2002. Developmental regulation of beta1 integrins during angiogenesis in the central nervous system. *Mol Cell Neurosci,* 20**,** 616-26.

MILNER, R. & CAMPBELL, I. L. 2003. The extracellular matrix and cytokines regulate microglial integrin expression and activation. *J Immunol,* 170**,** 3850-8.

MILNER, R. & CAMPBELL, I. L. 2006. Increased expression of the beta4 and alpha5 integrin subunits in cerebral blood vessels of transgenic mice chronically producing the pro-inflammatory cytokines IL-6 or IFN-alpha in the central nervous system. *Mol Cell Neurosci,* 33**,** 429-40.

MILNER, R., HUNG, S., EROKWU, B., DORE-DUFFY, P., LAMANNA, J. C. & DEL ZOPPO, G. J. 2008. Increased expression of fibronectin and the alpha 5 beta 1 integrin in angiogenic cerebral blood vessels of mice subject to hypobaric hypoxia. *Mol Cell Neurosci,* 38**,** 43-52.

MINAMI, M., KURAISHI, Y., YABUUCHI, K., YAMAZAKI, A. & SATOH, M. 1992. Induction of interleukin-1 beta mRNA in rat brain after transient forebrain ischemia. *J Neurochem,* 58**,** 390-2.

MINER, J. H., LEWIS, R. M. & SANES, J. R. 1995. Molecular cloning of a novel laminin chain, alpha 5, and widespread expression in adult mouse tissues. *J Biol Chem,* 270**,** 28523-6.

MONACO, S., SPARANO, V., GIOIA, M., SBARDELLA, D., DI PIERRO, D., MARINI, S. & COLETTA, M. 2006. Enzymatic processing of collagen IV by MMP-2 (gelatinase A) affects neutrophil migration and it is modulated by extracatalytic domains. *Protein Sci,* 15**,** 2805-15.

MONTANEZ, E., USSAR, S., SCHIFFERER, M., BOSL, M., ZENT, R., MOSER, M. & FASSLER, R. 2008. Kindlin-2 controls bidirectional signaling of integrins. *Genes Dev,* 22**,** 1325-30.

MONTESANO, R., VASSALLI, J. D., BAIRD, A., GUILLEMIN, R. & ORCI, L. 1986. Basic fibroblast growth factor induces angiogenesis in vitro. *Proceedings of the National Academy of Sciences,* 83**,** 7297-7301.

MORITA, K., SASAKI, H., FURUSE, M. & TSUKITA, S. 1999. Endothelial claudin: claudin-5/TMVCF constitutes tight junction strands in endothelial cells. *J Cell Biol,* 147**,** 185-94.

MUELLNER, A., BENZ, M., KLOSS, C. U., MAUTES, A., BURGGRAF, D. & HAMANN, G. F. 2003. Microvascular basal lamina antigen loss after traumatic brain injury in the rat. *J Neurotrauma,* 20**,** 745-54.

MULLER, S. L., PORTWICH, M., SCHMIDT, A., UTEPBERGENOV, D. I., HUBER, O., BLASIG, I. E. & KRAUSE, G. 2005. The tight junction protein occludin and the adherens junction protein alpha-catenin share a common interaction mechanism with ZO-1. *J Biol Chem,* 280**,** 3747-56.

MURAKAMI, T., FELINSKI, E. A. & ANTONETTI, D. A. 2009. Occludin phosphorylation and ubiquitination regulate tight junction trafficking and vascular endothelial growth factor-induced permeability. *J Biol Chem,* 284**,** 21036-46.

NAGASE, T., NAKAYAMA, M., NAKAJIMA, D., KIKUNO, R. & OHARA, O. 2001. Prediction of the coding sequences of unidentified human genes. XX. The complete sequences of 100 new cDNA clones from brain which code for large proteins in vitro. *DNA Res,* 8**,** 85-95.

NAKAGAWA, S., DELI, M. A., KAWAGUCHI, H., SHIMIZUDANI, T., SHIMONO, T., KITTEL, A., TANAKA, K. & NIWA, M. 2009. A new blood-brain barrier model using primary rat brain endothelial cells, pericytes and astrocytes. *Neurochem Int,* 54**,** 253-63.

NIGATU, A., SIME, W., GORFU, G., GEBERHIWOT, T., ANDUREN, I., INGERPUU, S., DOI, M., TRYGGVASON, K., HJEMDAHL, P. & PATARROYO, M. 2006. Megakaryocytic cells synthesize and platelets secrete alpha5-laminins, and the endothelial laminin isoform laminin 10 (alpha5beta1gamma1) strongly promotes adhesion but not activation of platelets. *Thromb Haemost,* 95**,** 85-93.

NIKOLOPOULOS, S. N. & TURNER, C. E. 2001. Integrin-linked kinase (ILK) binding to paxillin LD1 motif regulates ILK localization to focal adhesions. *J Biol Chem,* 276**,** 23499-505.

NINDS 1995. Tissue plasminogen activator for acute ischemic stroke. The National Institute of Neurological Disorders and Stroke rt-PA Stroke Study Group. *N Engl J Med,* 333**,** 1581-7.

NISHIUCHI, R., MURAYAMA, O., FUJIWARA, H., GU, J., KAWAKAMI, T., AIMOTO, S., WADA, Y. & SEKIGUCHI, K. 2003. Characterization of the Ligand-Binding Specificities of Integrin α3β1 and α6β1 Using a Panel of Purified Laminin Isoforms Containing Distinct α Chains. *Journal of Biochemistry,* 134**,** 497-504.

NITTA, T., HATA, M., GOTOH, S., SEO, Y., SASAKI, H., HASHIMOTO, N., FURUSE, M. & TSUKITA, S. 2003. Size-selective loosening of the blood-brain barrier in claudin-5-deficient mice. *J Cell Biol,* 161**,** 653-60.

NITZ, T., EISENBLATTER, T., PSATHAKI, K. & GALLA, H. J. 2003. Serum-derived factors weaken the barrier properties of cultured porcine brain capillary endothelial cells in vitro. *Brain Res,* 981**,** 30-40.

NOBES, C. D. & HALL, A. 1995. Rho, rac, and cdc42 GTPases regulate the assembly of multimolecular focal complexes associated with actin stress fibers, lamellipodia, and filopodia. *Cell,* 81**,** 53-62.

NOMIZU, M., KIM, W. H., YAMAMURA, K., UTANI, A., SONG, S. Y., OTAKA, A., ROLLER, P. P., KLEINMAN, H. K. & YAMADA, Y. 1995. Identification of cell binding sites in the laminin alpha 1 chain carboxyl-terminal globular domain by systematic screening of synthetic peptides. *J Biol Chem,* 270**,** 20583-90.

O'NEILL, B. C., SUZUKI, H., LOOMIS, W. P., DENISENKO, O. & BOMSZTYK, K. 1997. Cloning of rat laminin gamma 1-chain gene promoter reveals motifs for recognition of multiple transcription factors. *Am J Physiol,* 273**,** F411-20.

O'NEILL, L. A. & GREENE, C. 1998. Signal transduction pathways activated by the IL-1 receptor family: ancient signaling machinery in mammals, insects, and plants. *J Leukoc Biol,* 63**,** 650-7.

OHTSUKI, S., SATO, S., YAMAGUCHI, H., KAMOI, M., ASASHIMA, T. & TERASAKI, T. 2007. Exogenous expression of claudin-5 induces barrier properties in cultured rat brain capillary endothelial cells. *J Cell Physiol,* 210**,** 81-6.

OHTSUKI, S., YAMAGUCHI, H., KATSUKURA, Y., ASASHIMA, T. & TERASAKI, T. 2008. mRNA expression levels of tight junction protein genes in mouse brain capillary endothelial cells highly purified by magnetic cell sorting. *J Neurochem,* 104**,** 147-54.

OKADA, Y., COPELAND, B. R., MORI, E., TUNG, M. M., THOMAS, W. S. & DEL ZOPPO, G. J. 1994. P-selectin and intercellular adhesion molecule-1 expression after focal brain ischemia and reperfusion. *Stroke,* 25**,** 202-11.

OREND, G., HUANG, W., OLAYIOYE, M. A., HYNES, N. E. & CHIQUET-EHRISMANN, R. 2003. Tenascin-C blocks cell-cycle progression of anchorage-dependent fibroblasts on fibronectin through inhibition of syndecan-4. *Oncogene,* 22**,** 3917-3926.

ORR, A. W., SANDERS, J. M., BEVARD, M., COLEMAN, E., SAREMBOCK, I. J. & SCHWARTZ, M. A. 2005. The subendothelial extracellular matrix modulates NF-kappaB activation by flow: a potential role in atherosclerosis. *J Cell Biol,* 169**,** 191-202.

PANKOV, R. & YAMADA, K. M. 2002. Fibronectin at a glance. *J Cell Sci,* 115**,** 3861-3.

PANNEQUIN, J., DELAUNAY, N., DARIDO, C., MAURICE, T., CRESPY, P., FROHMAN, M. A., BALDA, M. S., MATTER, K., JOUBERT, D., BOURGAUX, J. F., BALI, J. P. & HOLLANDE, F. 2007. Phosphatidylethanol accumulation promotes intestinal hyperplasia by inducing ZONAB-mediated cell density increase in response to chronic ethanol exposure. *Mol Cancer Res,* 5**,** 1147-57.

PARDRIDGE, W. M., EISENBERG, J. & YANG, J. 1985. Human blood-brain barrier insulin receptor. *J Neurochem,* 44**,** 1771-8.

PARKER, L. C., LUHESHI, G. N., ROTHWELL, N. J. & PINTEAUX, E. 2002. IL-1 beta signalling in glial cells in wildtype and IL-1RI deficient mice. *Br J Pharmacol,* 136**,** 312-20.

PAULUS, W., BAUR, I., SCHUPPAN, D. & ROGGENDORF, W. 1993. Characterization of integrin receptors in normal and neoplastic human brain. *Am J Pathol,* 143**,** 154-63.

PEARSON, V. L., ROTHWELL, N. J. & TOULMOND, S. 1999. Excitotoxic brain damage in the rat induces interleukin-1beta protein in microglia and astrocytes: correlation with the progression of cell death. *Glia,* 25**,** 311-23.

PEDRAZA, C., GEBERHIWOT, T., INGERPUU, S., ASSEFA, D., WONDIMU, Z., KORTESMAA, J., TRYGGVASON, K., VIRTANEN, I. & PATARROYO, M. 2000. Monocytic cells synthesize, adhere to, and migrate on laminin-8 (alpha 4 beta 1 gamma 1). *J Immunol,* 165**,** 5831-8.

PERRIERE, N., DEMEUSE, P., GARCIA, E., REGINA, A., DEBRAY, M., ANDREUX, J. P., COUVREUR, P., SCHERRMANN, J. M., TEMSAMANI, J., COURAUD, P. O., DELI, M. A. & ROUX, F. 2005. Puromycin-based purification of rat brain capillary endothelial cell cultures. Effect on the expression of blood-brain barrier-specific properties. *J Neurochem,* 93**,** 279-89.

PERRIÈRE, N., YOUSIF, S., CAZAUBON, S., CHAVEROT, N., BOURASSET, F., CISTERNINO, S., DECLÃ¨VES, X., HORI, S., TERASAKI, T., DELI, M., SCHERRMANN, J.-M., TEMSAMANI, J., ROUX, F. O. & COURAUD, P.-O. 2007. A functional in vitro model of rat blood-brain barrier for molecular analysis of efflux transporters. *Brain Research,* 1150**,** 1-13.

PERRIS, R., SYFRIG, J., PAULSSON, M. & BRONNER-FRASER, M. 1993. Molecular mechanisms of neural crest cell attachment and migration on types I and IV collagen. *J Cell Sci,* 106 (Pt 4)**,** 1357-68.

PETTY, M. A. & LO, E. H. 2002. Junctional complexes of the blood-brain barrier: permeability changes in neuroinflammation. *Prog Neurobiol,* 68**,** 311-23.

PFAFF, M., GOHRING, W., BROWN, J. C. & TIMPL, R. 1994. Binding of purified collagen receptors (alpha 1 beta 1, alpha 2 beta 1) and RGD-dependent integrins to laminins and laminin fragments. *Eur J Biochem,* 225**,** 975-84.

PINTEAUX, E., PARKER, L. C., ROTHWELL, N. J. & LUHESHI, G. N. 2002. Expression of interleukin-1 receptors and their role in interleukin-1 actions in murine microglial cells. *J Neurochem,* 83**,** 754-63.

PINTEAUX, E., ROTHWELL, N. J. & BOUTIN, H. 2006. Neuroprotective actions of endogenous interleukin-1 receptor antagonist (IL-1ra) are mediated by glia. *Glia,* 53**,** 551-6.

PINTEAUX, E., TROTTER, P. & SIMI, A. 2009. Cell-specific and concentration-dependent actions of interleukin-1 in acute brain inflammation. *Cytokine,* 45**,** 1-7.

POULIOT, N., CONNOLLY, L. M., MORITZ, R. L., SIMPSON, R. J. & BURGESS, A. W. 2000. Colon cancer cells adhesion and spreading on autocrine laminin-10 is mediated by multiple integrin receptors and modulated by EGF receptor stimulation. *Exp Cell Res,* 261**,** 360-71.

QIN, H., ISHIWATA, T., WANG, R., KUDO, M., YOKOYAMA, M., NAITO, Z. & ASANO, G. 2000. Effects of extracellular matrix on phenotype modulation and MAPK transduction of rat aortic smooth muscle cells in vitro. *Exp Mol Pathol,* 69**,** 79-90.

RAGHUNATH, P. N., SIDHU, G. S., COON, H. C., LIU, K., SRIKANTAN, V. & MAHESHWARI, R. K. 1993. Interferons upregulate the expression of laminin and its receptor LBP-32 in cultured cells. *J Biol Regul Homeost Agents,* 7**,** 22-30.

RATNIKOV, B. I., PARTRIDGE, A. W. & GINSBERG, M. H. 2005. Integrin activation by talin. *J Thromb Haemost,* 3**,** 1783-90.

RAWDANOWICZ, T. J., HAMPTON, A. L., NAGASE, H., WOOLLEY, D. E. & SALAMONSEN, L. A. 1994. Matrix metalloproteinase production by cultured human endometrial stromal cells: identification of interstitial collagenase, gelatinase-A, gelatinase-B, and stromelysin-1 and their differential regulation by interleukin-1 alpha and tumor necrosis factor-alpha. *J Clin Endocrinol Metab,* 79**,** 530-6.

REICHARDT, L. F. & TOMASELLI, K. J. 1991. Extracellular matrix molecules and their receptors: functions in neural development. *Annu Rev Neurosci,* 14**,** 531-70.

RELTON, J. K. & ROTHWELL, N. J. 1992. Interleukin-1 receptor antagonist inhibits ischaemic and excitotoxic neuronal damage in the rat. *Brain Res Bull,* 29**,** 243-6.

RENSHAW, M. W., REN, X. D. & SCHWARTZ, M. A. 1997. Growth factor activation of MAP kinase requires cell adhesion. *Embo J,* 16**,** 5592-9.

RIBAUX, P., EHSES, J. A., LIN-MARQ, N., CARROZZINO, F., BONI-SCHNETZLER, M., HAMMAR, E., IRMINGER, J. C., DONATH, M. Y. & HALBAN, P. A. 2007. Induction of CXCL1 by extracellular matrix and autocrine enhancement by interleukin-1 in rat pancreatic beta-cells. *Endocrinology,* 148**,** 5582-90.

RICHARDSON, C. A., GORDON, K. L., COUSER, W. G. & BOMSZTYK, K. 1995. IL-1 beta increases laminin B2 chain mRNA levels and activates NF-kappa B in rat glomerular epithelial cells. *Am J Physiol,* 268**,** F273-8.

RIDLEY, A. J. & HALL, A. 1992. The small GTP-binding protein rho regulates the assembly of focal adhesions and actin stress fibers in response to growth factors. *Cell,* 70**,** 389-99.

RINALDI, N., WILLHAUCK, M., WEIS, D., BRADO, B., KERN, P., LUKOSCHEK, M., SCHWARZ-EYWILL, M. & BARTH, T. F. 2001. Loss of collagen type IV in rheumatoid synovia and cytokine effect on the collagen type-IV gene expression in fibroblast-like synoviocytes from rheumatoid arthritis. *Virchows Arch,* 439**,** 675-82.

ROGGENDORF, W., OPITZ, H. & SCHUPPAN, D. 1988. Altered expression of collagen type VI in brain vessels of patients with chronic hypertension. A comparison with the distribution of collagen IV and procollagen III. *Acta Neuropathol,* 77**,** 55-60.

ROSENBERG, G. A., ESTRADA, E. Y. & DENCOFF, J. E. 1998. Matrix metalloproteinases and TIMPs are associated with blood-brain barrier opening after reperfusion in rat brain. *Stroke,* 29**,** 2189-95.

ROUX, F. & COURAUD, P. O. 2005. Rat brain endothelial cell lines for the study of blood-brain barrier permeability and transport functions. *Cell Mol Neurobiol,* 25**,** 41-58.

ROYALL, J. A., BERKOW, R. L., BECKMAN, J. S., CUNNINGHAM, M. K., MATALON, S. & FREEMAN, B. A. 1989. Tumor necrosis factor and interleukin 1 alpha increase vascular endothelial permeability. *Am J Physiol,* 257**,** L399-410.

RUBIN, L. L., HALL, D. E., PORTER, S., BARBU, K., CANNON, C., HORNER, H. C., JANATPOUR, M., LIAW, C. W., MANNING, K., MORALES, J. & ET AL. 1991. A cell culture model of the blood-brain barrier. *J Cell Biol,* 115**,** 1725-35.

RUOSLAHTI, E. 1996. RGD and other recognition sequences for integrins. *Annu Rev Cell Dev Biol,* 12**,** 697-715.

SANDOVAL, K. E. & WITT, K. A. 2008. Blood-brain barrier tight junction permeability and ischemic stroke. *Neurobiol Dis,* 32**,** 200-19.

SANTORO, S. A. 1986. Identification of a 160,000 dalton platelet membrane protein that mediates the initial divalent cation-dependent adhesion of platelets to collagen. *Cell,* 46**,** 913-920.

SARKAR, S., RAYMICK, J. & SCHMUED, L. 2012. Temporal progression of kainic acid induced changes in vascular laminin expression in rat brain with neuronal and glial correlates. *Curr Neurovasc Res,* 9**,** 110-9.

SARKAR, S. & SCHMUED, L. 2010. Kainic acid and 3-Nitropropionic acid induced expression of laminin in vascular elements of the rat brain. *Brain Res,* 1352**,** 239-47.

SASAKI, T. & TIMPL, R. 2001. Domain IVa of laminin α5 chain is cell-adhesive and binds β1 and αVβ3 integrins through Arg-Gly-Asp. *FEBS Letters,* 509**,** 181-185.

SAVETTIERI, G., DI LIEGRO, I., CATANIA, C., LICATA, L., PITARRESI, G. L., D'AGOSTINO, S., SCHIERA, G., DE CARO, V., GIANDALIA, G., GIANNOLA, L. I. & CESTELLI, A. 2000. Neurons and ECM regulate occludin localization in brain endothelial cells. *Neuroreport,* 11**,** 1081-4.

SCHALLER, M. D. 2001. Paxillin: a focal adhesion-associated adaptor protein. *Oncogene,* 20**,** 6459-72.

SCHALLER, M. D., BORGMAN, C. A., COBB, B. S., VINES, R. R., REYNOLDS, A. B. & PARSONS, J. T. 1992. pp125FAK a structurally distinctive protein-tyrosine kinase associated with focal adhesions. *Proc Natl Acad Sci U S A,* 89**,** 5192-6.

SCHALLER, M. D., HILDEBRAND, J. D., SHANNON, J. D., FOX, J. W., VINES, R. R. & PARSONS, J. T. 1994. Autophosphorylation of the focal adhesion kinase, pp125FAK, directs SH2-dependent binding of pp60src. *Mol Cell Biol,* 14**,** 1680-8.

SCHIERA, G., BONO, E., RAFFA, M. P., GALLO, A., PITARRESI, G. L., DI LIEGRO, I. & SAVETTIERI, G. 2003. Synergistic effects of neurons and astrocytes on the differentiation of brain capillary endothelial cells in culture. *J Cell Mol Med,* 7**,** 165-70.

SCHITTNY, J. C. & YURCHENCO, P. D. 1989. Basement membranes: molecular organization and function in development and disease. *Curr Opin Cell Biol,* 1**,** 983-8.

SCHOLLER, K., TRINKL, A., KLOPOTOWSKI, M., THAL, S. C., PLESNILA, N., TRABOLD, R., HAMANN, G. F., SCHMID-ELSAESSER, R. & ZAUSINGER, S. 2007. Characterization of microvascular basal lamina damage and blood-brain barrier dysfunction following subarachnoid hemorrhage in rats. *Brain Res,* 1142**,** 237-46.

SCHUBERT-UNKMEIR, A., KONRAD, C., SLANINA, H., CZAPEK, F., HEBLING, S. & FROSCH, M. 2010. Neisseria meningitidis induces brain microvascular endothelial cell detachment from the matrix and cleavage of occludin: a role for MMP-8. *PLoS Pathog,* 6**,** e1000874.

SCHWARZ, B. T., WANG, F., SHEN, L., CLAYBURGH, D. R., SU, L., WANG, Y., FU, Y. X. & TURNER, J. R. 2007. LIGHT signals directly to intestinal epithelia to cause barrier dysfunction via cytoskeletal and endocytic mechanisms. *Gastroenterology,* 132**,** 2383-94.

SHEN, L. & TURNER, J. R. 2005. Actin depolymerization disrupts tight junctions via caveolae-mediated endocytosis. *Mol Biol Cell,* 16**,** 3919-36.

SIBSON, N. R., BLAMIRE, A. M., BERNADES-SILVA, M., LAURENT, S., BOUTRY, S., MULLER, R. N., STYLES, P. & ANTHONY, D. C. 2004. MRI detection of early endothelial activation in brain inflammation. *Magn Reson Med,* 51**,** 248-52.

SIDDHARTHAN, V., KIM, Y. V., LIU, S. & KIM, K. S. 2007. Human astrocytes/astrocyte-conditioned medium and shear stress enhance the barrier properties of human brain microvascular endothelial cells. *Brain Res,* 1147**,** 39-50.

SIMI, A., TSAKIRI, N., WANG, P. & ROTHWELL, N. J. 2007. Interleukin-1 and inflammatory neurodegeneration. *Biochem Soc Trans,* 35**,** 1122-6.

SIMS, J. E., GAYLE, M. A., SLACK, J. L., ALDERSON, M. R., BIRD, T. A., GIRI, J. G., COLOTTA, F., RE, F., MANTOVANI, A., SHANEBECK, K. & ET AL. 1993. Interleukin 1 signaling occurs exclusively via the type I receptor. *Proc Natl Acad Sci U S A,* 90**,** 6155-9.

SIXT, M., ENGELHARDT, B., PAUSCH, F., HALLMANN, R., WENDLER, O. & SOROKIN, L. M. 2001. Endothelial cell laminin isoforms, laminins 8 and 10, play decisive roles in T cell recruitment across the blood-brain barrier in experimental autoimmune encephalomyelitis. *J Cell Biol,* 153**,** 933-46.

SKINNER, R. A., GIBSON, R. M., ROTHWELL, N. J., PINTEAUX, E. & PENNY, J. I. 2009. Transport of interleukin-1 across cerebromicrovascular endothelial cells. *Br J Pharmacol,* 156**,** 1115-23.

SLACK, J. K., ADAMS, R. B., ROVIN, J. D., BISSONETTE, E. A., STOKER, C. E. & PARSONS, J. T. 2001. Alterations in the focal adhesion kinase/Src signal transduction pathway correlate with increased migratory capacity of prostate carcinoma cells. *Oncogene,* 20**,** 1152-63.

SOBEL, R. A., HINOJOZA, J. R., MAEDA, A. & CHEN, M. 1998. Endothelial cell integrin laminin receptor expression in multiple sclerosis lesions. *Am J Pathol,* 153**,** 405-15.

SONG, L. & PACHTER, J. S. 2003. Culture of murine brain microvascular endothelial cells that maintain expression and cytoskeletal association of tight junction-associated proteins. *In Vitro Cell Dev Biol Anim,* 39**,** 313-20.

SONNENBERG, A., LINDERS, C. J., MODDERMAN, P. W., DAMSKY, C. H., AUMAILLEY, M. & TIMPL, R. 1990. Integrin recognition of different cell-binding fragments of laminin (P1, E3, E8) and evidence that alpha 6 beta 1 but not alpha 6 beta 4 functions as a major receptor for fragment E8. *J Cell Biol,* 110**,** 2145-55.

SONNENBERG, A., MODDERMAN, P. W. & HOGERVORST, F. 1988. Laminin receptor on platelets is the integrin VLA-6. *Nature,* 336**,** 487-9.

STAMATOVIC, S. M., KEEP, R. F. & ANDJELKOVIC, A. V. 2008. Brain endothelial cell-cell junctions: how to "open" the blood brain barrier. *Curr Neuropharmacol,* 6**,** 179-92.

STAMATOVIC, S. M., KEEP, R. F., WANG, M. M., JANKOVIC, I. & ANDJELKOVIC, A. V. 2009. Caveolae-mediated internalization of occludin and claudin-5 during CCL2-induced tight junction remodeling in brain endothelial cells. *J Biol Chem,* 284**,** 19053-66.

STANIMIROVIC, D. & SATOH, K. 2000. Inflammatory mediators of cerebral endothelium: a role in ischemic brain inflammation. *Brain Pathol,* 10**,** 113-26.

STANIMIROVIC, D. B., WONG, J., SHAPIRO, A. & DURKIN, J. P. 1997. Increase in surface expression of ICAM-1, VCAM-1 and E-selectin in human cerebromicrovascular endothelial cells subjected to ischemia-like insults. *Acta Neurochir Suppl,* 70**,** 12-6.

STEVENSON, B. R., SILICIANO, J. D., MOOSEKER, M. S. & GOODENOUGH, D. A. 1986. Identification of ZO-1: a high molecular weight polypeptide associated with the tight junction (zonula occludens) in a variety of epithelia. *J Cell Biol,* 103**,** 755-66.

STINS, M. F., GILLES, F. & KIM, K. S. 1997. Selective expression of adhesion molecules on human brain microvascular endothelial cells. *J Neuroimmunol,* 76**,** 81-90.

STONE, D. M. & NIKOLICS, K. 1995. Tissue- and age-specific expression patterns of alternatively spliced agrin mRNA transcripts in embryonic rat suggest novel developmental roles. *J Neurosci,* 15**,** 6767-78.

STOWE, A. M., ADAIR-KIRK, T. L., GONZALES, E. R., PEREZ, R. S., SHAH, A. R., PARK, T. S. & GIDDAY, J. M. 2009. Neutrophil elastase and neurovascular injury following focal stroke and reperfusion. *Neurobiol Dis,* 35**,** 82-90.

STRATMAN, A. N., MALOTTE, K. M., MAHAN, R. D., DAVIS, M. J. & DAVIS, G. E. 2009. Pericyte recruitment during vasculogenic tube assembly stimulates endothelial basement membrane matrix formation. *Blood,* 114**,** 5091-101.

STROEMER, R. P. & ROTHWELL, N. J. 1998. Exacerbation of ischemic brain damage by localized striatal injection of interleukin-1beta in the rat. *J Cereb Blood Flow Metab,* 18**,** 833-9.

SUBRAMANIAM, S., STANSBERG, C. & CUNNINGHAM, C. 2004. The interleukin 1 receptor family. *Dev Comp Immunol,* 28**,** 415-28.

SUMMERS, L., KANGWANTAS, K., NGUYEN, L., KIELTY, C. & PINTEAUX, E. 2010. Adhesion to the extracellular matrix is required for interleukin-1 beta actions leading to reactive phenotype in rat astrocytes. *Mol Cell Neurosci,* 44**,** 272-81.

SUMMERS, L., KIELTY, C. & PINTEAUX, E. 2009. Adhesion to fibronectin regulates interleukin-1 beta expression in microglial cells. *Mol Cell Neurosci,* 41**,** 148-55.

SZABO, A. & KALMAN, M. 2004. Disappearance of the post-lesional laminin immunopositivity of brain vessels is parallel with the formation of gliovascular junctions and common basal lamina. A double-labelling immunohistochemical study. *Neuropathol Appl Neurobiol,* 30**,** 169-77.

SZABO, A. & KALMAN, M. 2008. Post traumatic lesion absence of beta-dystroglycan-immunopositivity in brain vessels coincides with the glial reaction and the immunoreactivity of vascular laminin. *Curr Neurovasc Res,* 5**,** 206-13.

TAGAYA, M., HARING, H. P., STUIVER, I., WAGNER, S., ABUMIYA, T., LUCERO, J., LEE, P., COPELAND, B. R., SEIFFERT, D. & DEL ZOPPO, G. J. 2001. Rapid loss of microvascular integrin expression during focal brain ischemia reflects neuron injury. *J Cereb Blood Flow Metab,* 21**,** 835-46.

TAIPALE, J. & KESKI-OJA, J. 1997. Growth factors in the extracellular matrix. *FASEB J,* 11**,** 51-59.

TANIGUCHI, Y., IDO, H., SANZEN, N., HAYASHI, M., SATO-NISHIUCHI, R., FUTAKI, S. & SEKIGUCHI, K. 2009. The C-terminal region of laminin beta chains modulates the integrin binding affinities of laminins. *J Biol Chem,* 284**,** 7820-31.

TIAN, H. L., CHEN, H., CUI, Y. H., XU, T. & ZHOU, L. F. 2007. Increased protein and mRNA expression of endostatin in the ischemic brain tissue of rabbits after middle cerebral artery occlusion. *Neurosci Bull,* 23**,** 35-40.

TILLING, T., ENGELBERTZ, C., DECKER, S., KORTE, D., HUWEL, S. & GALLA, H. J. 2002. Expression and adhesive properties of basement membrane proteins in cerebral capillary endothelial cell cultures. *Cell Tissue Res,* 310**,** 19-29.

TILLING, T., KORTE, D., HOHEISEL, D. & GALLA, H. J. 1998. Basement membrane proteins influence brain capillary endothelial barrier function in vitro. *J Neurochem,* 71**,** 1151-7.

TOUZANI, O., BOUTIN, H., CHUQUET, J. & ROTHWELL, N. 1999. Potential mechanisms of interleukin-1 involvement in cerebral ischaemia. *Journal of Neuroimmunology,* 100**,** 203-215.

TRINKL, A., VOSKO, M. R., WUNDERLICH, N., DICHGANS, M. & HAMANN, G. F. 2006. Pravastatin reduces microvascular basal lamina damage following focal cerebral ischemia and reperfusion. *Eur J Neurosci,* 24**,** 520-6.

TSUKITA, S., KATSUNO, T., YAMAZAKI, Y., UMEDA, K., TAMURA, A. & TSUKITA, S. 2009. Roles of ZO-1 and ZO-2 in establishment of the belt-like adherens and tight junctions with paracellular permselective barrier function. *Ann N Y Acad Sci,* 1165**,** 44-52.

TUROVEROVA, L. V., KHOTIN, M. G., IUDINTSEVA, N. M., MAGNUSSON, K. E., BLINOVA, M. I., PINAEV, G. P. & TENTLER, D. G. 2009. [Analysis of extracellular matrix proteins produced by cultured cells]. *Tsitologiia,* 51**,** 691-6.

UMEDA, K., IKENOUCHI, J., KATAHIRA-TAYAMA, S., FURUSE, K., SASAKI, H., NAKAYAMA, M., MATSUI, T., TSUKITA, S., FURUSE, M. & TSUKITA, S. 2006. ZO-1 and ZO-2 independently determine where claudins are polymerized in tight-junction strand formation. *Cell,* 126**,** 741-54.

UMEDA, K., MATSUI, T., NAKAYAMA, M., FURUSE, K., SASAKI, H., FURUSE, M. & TSUKITA, S. 2004. Establishment and characterization of cultured epithelial cells lacking expression of ZO-1. *J Biol Chem,* 279**,** 44785-94.

USPENSKAIA, O., LIEBETRAU, M., HERMS, J., DANEK, A. & HAMANN, G. F. 2004. Aging is associated with increased collagen type IV accumulation in the basal lamina of human cerebral microvessels. *BMC Neurosci,* 5**,** 37.

VADAY, G. G., FRANITZA, S., SCHOR, H., HECHT, I., BRILL, A., CAHALON, L., HERSHKOVIZ, R. & LIDER, O. 2001. Combinatorial signals by inflammatory cytokines and chemokines mediate leukocyte interactions with extracellular matrix. *J Leukoc Biol,* 69**,** 885-92.

VAN DAM, A. M., DE VRIES, H. E., KUIPER, J., ZIJLSTRA, F. J., DE BOER, A. G., TILDERS, F. J. & BERKENBOSCH, F. 1996. Interleukin-1 receptors on rat brain endothelial cells: a role in neuroimmune interaction? *Faseb J,* 10**,** 351-6.

VAN ITALLIE, C. M., FANNING, A. S., HOLMES, J. & ANDERSON, J. M. 2010. Occludin is required for cytokine-induced regulation of tight junction barriers. *J Cell Sci,* 123**,** 2844-52.

VANDENBERG, P., KERN, A., RIES, A., LUCKENBILL-EDDS, L., MANN, K. & KUHN, K. 1991. Characterization of a type IV collagen major cell binding site with affinity to the alpha 1 beta 1 and the alpha 2 beta 1 integrins. *J Cell Biol,* 113**,** 1475-83.

VENSTROM, K. A. & REICHARDT, L. F. 1993. Extracellular matrix. 2: Role of extracellular matrix molecules and their receptors in the nervous system. *FASEB J,* 7**,** 996-1003.

VINALS, F. & POUYSSEGUR, J. 1999. Confluence of vascular endothelial cells induces cell cycle exit by inhibiting p42/p44 mitogen-activated protein kinase activity. *Mol Cell Biol,* 19**,** 2763-72.

VOGT, C., HAILER, N. P., GHADBAN, C., KORF, H. W. & DEHGHANI, F. 2008. Successful inhibition of excitotoxic neuronal damage and microglial activation after delayed application of interleukin-1 receptor antagonist. *J Neurosci Res,* 86**,** 3314-21.

WANG, C. X. & SHUAIB, A. 2007. Critical role of microvasculature basal lamina in ischemic brain injury. *Prog Neurobiol,* 83**,** 140-8.

WANG, D., GRAMMER, J. R., COBBS, C. S., STEWART, J. E., JR., LIU, Z., RHODEN, R., HECKER, T. P., DING, Q. & GLADSON, C. L. 2000. p125 focal adhesion kinase promotes malignant astrocytoma cell proliferation in vivo. *J Cell Sci,* 113 Pt 23**,** 4221-30.

WANG, J. & MILNER, R. 2006. Fibronectin promotes brain capillary endothelial cell survival and proliferation through alpha5beta1 and alphavbeta3 integrins via MAP kinase signalling. *J Neurochem,* 96**,** 148-59.

WANG, X., SIREN, A. L., LIU, Y., YUE, T. L., BARONE, F. C. & FEUERSTEIN, G. Z. 1994. Upregulation of intercellular adhesion molecule 1 (ICAM-1) on brain microvascular endothelial cells in rat ischemic cortex. *Brain Res Mol Brain Res,* 26**,** 61-8.

WAPPLER, E. A., ADORJAN, I., GAL, A., GALGOCZY, P., BINDICS, K. & NAGY, Z. 2011. Dynamics of dystroglycan complex proteins and laminin changes due to angiogenesis in rat cerebral hypoperfusion. *Microvasc Res,* 81**,** 153-9.

WEBERSINKE, G., BAUER, H., AMBERGER, A., ZACH, O. & BAUER, H. C. 1992. Comparison of gene expression of extracellular matrix molecules in brain microvascular endothelial cells and astrocytes. *Biochem Biophys Res Commun,* 189**,** 877-84.

WEEKS, B. S. & FRIEDMAN, H. M. 1997. Laminin reduces HSV-1 spread from cell to cell in human keratinocyte cultures. *Biochem Biophys Res Commun,* 230**,** 466-9.

WEGENER, K. L., PARTRIDGE, A. W., HAN, J., PICKFORD, A. R., LIDDINGTON, R. C., GINSBERG, M. H. & CAMPBELL, I. D. 2007. Structural basis of integrin activation by talin. *Cell,* 128**,** 171-82.

WEIDENFELLER, C., SCHROT, S., ZOZULYA, A. & GALLA, H. J. 2005. Murine brain capillary endothelial cells exhibit improved barrier properties under the influence of hydrocortisone. *Brain Res,* 1053**,** 162-74.

WELSER-ALVES, J. V., BOROUJERDI, A., TIGGES, U., WRABETZ, L., FELTRI, M. L. & MILNER, R. 2013. Endothelial beta4 integrin is predominantly expressed in arterioles, where it promotes vascular remodeling in the hypoxic brain. *Arterioscler Thromb Vasc Biol,* 33**,** 943-53.

WESCHE, H., KORHERR, C., KRACHT, M., FALK, W., RESCH, K. & MARTIN, M. U. 1997. The interleukin-1 receptor accessory protein (IL-1RAcP) is essential for IL-1-induced activation of interleukin-1 receptor-associated kinase (IRAK) and stress-activated protein kinases (SAP kinases). *J Biol Chem,* 272**,** 7727-31.

WICKSTROM, S. A., LANGE, A., MONTANEZ, E. & FASSLER, R. 2010. The ILK/PINCH/parvin complex: the kinase is dead, long live the pseudokinase! *EMBO J,* 29**,** 281-91.

WILHELM, I., FAZAKAS, C. & KRIZBAI, I. A. In vitro models of the blood-brain barrier. *Acta Neurobiol Exp (Wars),* 71**,** 113-28.

WILSON, S. H., LJUBIMOV, A. V., MORLA, A. O., CABALLERO, S., SHAW, L. C., SPOERRI, P. E., TARNUZZER, R. W. & GRANT, M. B. 2003. Fibronectin fragments promote human retinal endothelial cell adhesion and proliferation and ERK activation through alpha5beta1 integrin and PI 3-kinase. *Invest Ophthalmol Vis Sci,* 44**,** 1704-15.

WOLBURG, H., NEUHAUS, J., KNIESEL, U., KRAUSS, B., SCHMID, E. M., OCALAN, M., FARRELL, C. & RISAU, W. 1994. Modulation of tight junction structure in blood-brain

barrier endothelial cells. Effects of tissue culture, second messengers and cocultured astrocytes. *J Cell Sci,* 107 (Pt 5)**,** 1347-57.

WOLBURG, H., NOELL, S., MACK, A., WOLBURG-BUCHHOLZ, K. & FALLIER-BECKER, P. 2009. Brain endothelial cells and the glio-vascular complex. *Cell Tissue Res,* 335**,** 75-96.

WONG, D. & DOROVINI-ZIS, K. 1992. Upregulation of intercellular adhesion molecule-1 (ICAM-1) expression in primary cultures of human brain microvessel endothelial cells by cytokines and lipopolysaccharide. *J Neuroimmunol,* 39**,** 11-21.

WU, C., IVARS, F., ANDERSON, P., HALLMANN, R., VESTWEBER, D., NILSSON, P., ROBENEK, H., TRYGGVASON, K., SONG, J., KORPOS, E., LOSER, K., BEISSERT, S., GEORGES-LABOUESSE, E. & SOROKIN, L. M. 2009. Endothelial basement membrane laminin alpha5 selectively inhibits T lymphocyte extravasation into the brain. *Nat Med,* 15**,** 519-27.

WU, W., HUANG, Q., HE, F., XIAO, M., PANG, S., GUO, X., BRUNK, U. T., ZHAO, K. & ZHAO, M. 2011. Roles of mitogen-activated protein kinases in the modulation of endothelial cell function following thermal injury. *Shock,* 35**,** 618-25.

XU, J., HE, L., AHMED, S. H., CHEN, S. W., GOLDBERG, M. P., BECKMAN, J. S. & HSU, C. Y. 2000. Oxygen-glucose deprivation induces inducible nitric oxide synthase and nitrotyrosine expression in cerebral endothelial cells. *Stroke,* 31**,** 1744-51.

XU, J., KAUSALYA, P. J., PHUA, D. C., ALI, S. M., HOSSAIN, Z. & HUNZIKER, W. 2008. Early embryonic lethality of mice lacking ZO-2, but Not ZO-3, reveals critical and nonredundant roles for individual zonula occludens proteins in mammalian development. *Mol Cell Biol,* 28**,** 1669-78.

XU, R., FENG, X., XIE, X., ZHANG, J., WU, D. & XU, L. 2012. HIV-1 Tat protein increases the permeability of brain endothelial cells by both inhibiting occludin expression and cleaving occludin via matrix metalloproteinase-9. *Brain Res,* 1436**,** 13-9.

YAMAGAMI, S., TAMURA, M., HAYASHI, M., ENDO, N., TANABE, H., KATSUURA, Y. & KOMORIYA, K. 1999. Differential production of MCP-1 and cytokine-induced neutrophil chemoattractant in the ischemic brain after transient focal ischemia in rats. *J Leukoc Biol,* 65**,** 744-9.

YAMAGATA, K., TAGAMI, M., TAKENAGA, F., YAMORI, Y. & ITOH, S. 2004. Hypoxia-induced changes in tight junction permeability of brain capillary endothelial cells are associated with IL-1beta and nitric oxide. *Neurobiology of Disease,* 17**,** 491-499.

YAMAMOTO, T., HARADA, N., KANO, K., TAYA, S., CANAANI, E., MATSUURA, Y., MIZOGUCHI, A., IDE, C. & KAIBUCHI, K. 1997. The Ras target AF-6 interacts with ZO-1 and serves as a peripheral component of tight junctions in epithelial cells. *J Cell Biol,* 139**,** 785-95.

YAMASAKI, Y., MATSUURA, N., SHOZUHARA, H., ONODERA, H., ITOYAMA, Y. & KOGURE, K. 1995. Interleukin-1 as a pathogenetic mediator of ischemic brain damage in rats. *Stroke,* 26**,** 676-80; discussion 681.

YANG, Y., ESTRADA, E. Y., THOMPSON, J. F., LIU, W. & ROSENBERG, G. A. 2007. Matrix metalloproteinase-mediated disruption of tight junction proteins in cerebral vessels is reversed by synthetic matrix metalloproteinase inhibitor in focal ischemia in rat. *J Cereb Blood Flow Metab,* 27**,** 697-709.

YANG, Y. & ROSENBERG, G. A. 2011. MMP-mediated disruption of claudin-5 in the blood-brain barrier of rat brain after cerebral ischemia. *Methods Mol Biol,* 762**,** 333-45.

YAO, C. C., ZIOBER, B. L., SQUILLACE, R. M. & KRAMER, R. H. 1996. Alpha7 integrin mediates cell adhesion and migration on specific laminin isoforms. *J Biol Chem,* 271**,** 25598-603.

YEPES, M., SANDKVIST, M., MOORE, E. G., BUGGE, T. H., STRICKLAND, D. K. & LAWRENCE, D. A. 2003. Tissue-type plasminogen activator induces opening of the blood-brain barrier via the LDL receptor-related protein. *J Clin Invest,* 112**,** 1533-40.

YIN, K.-J., CHEN, S.-D., LEE, J.-M., XU, J. & HSU, C. Y. 2002. ATM Gene Regulates Oxygen-Glucose Deprivationâ€“Induced Nuclear Factor-ÎºB DNA-Binding Activity and Downstream Apoptotic Cascade in Mouse Cerebrovascular Endothelial Cells. *Stroke,* 33**,** 2471-2477.

YU, H. & TALTS, J. F. 2003. Beta1 integrin and alpha-dystroglycan binding sites are localized to different laminin-G-domain-like (LG) modules within the laminin alpha5 chain G domain. *Biochem J,* 371**,** 289-99.

YURCHENCO, P. D., TSILIBARY, E. C., CHARONIS, A. S. & FURTHMAYR, H. 1985. Laminin polymerization in vitro. Evidence for a two-step assembly with domain specificity. *J Biol Chem,* 260**,** 7636-44.

ZEHENDNER, C. M., LIBRIZZI, L., DE CURTIS, M., KUHLMANN, C. R. & LUHMANN, H. J. 2012. Caspase-3 contributes to ZO-1 and Cl-5 tight-junction disruption in rapid anoxic neurovascular unit damage. *PLoS ONE,* 6**,** e16760.

ZHANG, R. L., CHOPP, M., ZALOGA, C., ZHANG, Z. G., JIANG, N., GAUTAM, S. C., TANG, W. X., TSANG, W., ANDERSON, D. C. & MANNING, A. M. 1995. The temporal profiles of ICAM-1 protein and mRNA expression after transient MCA occlusion in the rat. *Brain Res,* 682**,** 182-8.

ZHANG, W., SMITH, C., HOWLETT, C. & STANIMIROVIC, D. 2000. Inflammatory activation of human brain endothelial cells by hypoxic astrocytes in vitro is mediated by IL-1beta. *Journal of cerebral blood flow and metabolism : official journal of the International Society of Cerebral Blood Flow and Metabolism,* 20**,** 967-978.

ZHANG, W., SMITH, C., SHAPIRO, A., MONETTE, R., HUTCHISON, J. & STANIMIROVIC, D. 1999. Increased expression of bioactive chemokines in human cerebromicrovascular

endothelial cells and astrocytes subjected to simulated ischemia in vitro. *J Neuroimmunol,* 101**,** 148-60.

ZHANG, Z., CHOPP, M., GOUSSEV, A. & POWERS, C. 1998. Cerebral vessels express interleukin 1beta after focal cerebral ischemia. *Brain Res,* 784**,** 210-7.

ZHU, D., WANG, Y., SINGH, I., BELL, R. D., DEANE, R., ZHONG, Z., SAGARE, A., WINKLER, E. A. & ZLOKOVIC, B. V. 2010. Protein S controls hypoxic/ischemic blood-brain barrier disruption through the TAM receptor Tyro3 and sphingosine 1-phosphate receptor. *Blood,* 115**,** 4963-72.

ZHU, P., XIONG, W., RODGERS, G. & QWARNSTROM, E. E. 1998. Regulation of interleukin 1 signalling through integrin binding and actin reorganization: disparate effects on NF-kappaB and stress kinase pathways. *Biochem J,* 330 (Pt 2)**,** 975-81.

ZHU, X., OHTSUBO, M., BOHMER, R. M., ROBERTS, J. M. & ASSOIAN, R. K. 1996. Adhesion-dependent cell cycle progression linked to the expression of cyclin D1, activation of cyclin E-cdk2, and phosphorylation of the retinoblastoma protein. *J Cell Biol,* 133**,** 391-403.

ZOJA, C., BENIGNI, A., PICCININI, G., FIGLIUZZI, M., LONGARETTI, L. & REMUZZI, G. 1993. Interleukin-6 stimulates gene expression of extracellular matrix components in bovine mesangial cells in culture. *Mediators Inflamm,* 2**,** 429-33.